Predicting in-service performance of alternative pavement materials for New Zealand conditions

B.T. Vuong
ARRB Group

G. Arnold
PaveSpec Ltd

Land Transport New Zealand Research Report 304

ISBN 0-478-28716-X
ISSN 1177-0600

PO Box 2840, Waterloo Quay, Wellington, New Zealand
Telephone 64-4-931-8700; Facsimile 64-4 931 8701
Email: *research@landtransport.govt.nz*
Website: *www.landtransport.govt.nz*

Vuong, B.T.[1], Arnold, G.[2] 2006. Predicting in-service performance of alternative pavement materials for New Zealand conditions. *Land Transport New Zealand Research Report 304*. 179pp.

[1] ARRB Transport Research Ltd, 500 Burwood Hwy, Vermont South, VIC 3133, Australia. *binhv@arrb.com.au*
[2] formerly Transit New Zealand, PaveSpec Ltd, 26 Copeland St, Lower Hutt, New Zealand. *greg.arnold@pavespec.co.nz*

Keywords: aggregates, deformation, performance specifications, recycled materials, repeated load triaxial, rutting

An important note for the reader

Land Transport New Zealand is a Crown entity established under the Land Transport Management Act 2003. The objective of Land Transport New Zealand is to allocate resources and to undertake its functions in a way that contributes to an integrated, safe, responsive and sustainable land transport system. Each year, Land Transport New Zealand invests a portion of its funds on research that contributes to this objective.

The research detailed in this report was commissioned by Land Transport New Zealand.

While this report is believed to be correct at the time of its preparation, Land Transport New Zealand, and its employees and agents involved in its preparation and publication, cannot accept any liability for its contents or for any consequences arising from its use. People using the contents of the document, whether directly or indirectly, should apply and rely on their own skill and judgement. They should not rely on its contents in isolation from other sources of advice and information. If necessary, they should seek appropriate legal or other expert advice in relation to their own circumstances, and to the use of this report.

The material contained in this report is the output of research and should not be construed in any way as policy adopted by Land Transport New Zealand but may be used in the formulation of future policy.

Contents

Executive summary

A practical method for predicting the performance of unbound granular materials, including alternative, industrial by-products and recycled materials has been proposed. It is recommended that this method replace the existing laboratory repeated load triaxial (RLT) method adopted in the Transit New Zealand specification *TNZ M/22* (2000) to determine the suitability of the alternative road material for use as a base or sub-base material for thin-surfaced granular pavements in the New Zealand context.

The work, carried out in 2005, utilised available field performance data in New Zealand to calibrate/validate the following material assessment methods that were selected by laboratory RLT testing:

- a simple performance assessment method developed at ARRB to predict field performance (in terms of terminal deformation behaviour, deformation life and layer deformation) from a reduced set of permanent strain results obtained from the existing Austroads RLT test method for material specifications,
- a rut depth model developed in 2004 by Arnold at the University of Nottingham to predict field performance (in terms of incremental deformations of unbound granular pavements for various loading periods) using a full set of RLT permanent strain results at 12 different stress levels,
- a simplified Arnold rut depth model (by considering only the rate of deformation between 25–50 k-cycles and a reduced RLT data set representing only four different stress levels) to rank materials for use in material specifications.

The Austroads/ARRB method
In the Austroads/ARRB simple performance assessment method, a range of pavement cross sections were analysed using a 2-dimensional Finite Element Model (FEM) (VMOD-PAVE) under a design vehicle load of 40 kN on a single tyre to select representative pavement stresses at different depths (base, upper sub-base and lower sub-base). These representative stresses were applied in the Austroads RLT permanent strain test to determine permanent strains, which were then converted into simple indices such as terminal deformation behaviour, deformation life and layer deformation. In the validation of the Austroads/ARRB material assessment methods using pavements tested with Canterbury Accelerated Pavement Testing Indoor Facility (CAPTIF) 40 kN axle load in New Zealand, laboratory material rankings were found to be consistent with the rankings based on field performance. However, different laboratory compaction methods produced different predictions of deformation life and base deformation. Therefore, in the current form, the simple Austroads/ARRB method can be used only to rank the performance of granular bases. Further research on the effects of laboratory compaction is required to enable field deformation life and layer deformation to be accurately predicted for pavement design.

Arnold rut depth model
The Arnold rut depth model required a large RLT testing programme (full data set) to obtain permanent strain data at various stress levels in the pavement. The RLT testing

equipment and test procedures used in this method were different from those adopted in the Austroads RLT test method. It also used a simple two-dimensional FEM model (DEFPAV) to predict pavement stresses and a simple procedure to estimate incremental permanent strains for various loading periods from the RLT multi-stage permanent strain testing. In the calibration/validation of the Arnold rut depth model using 17 actual pavements (15 pavements tested with CAPTIF in New Zealand and 2 in-service pavements in Ireland), the model was found not to consistently and accurately predict field deformations, particularly for pavements with thick asphalt surfacing layers (> 40 mm). However, similar trends in rut depth progression (i.e. slope after 500 k-cycles) existed between the predicted and measured rut depth curves for some 11 out of 17 pavements studied.

Simplified Arnold rut depth model

To simplify the Arnold rut depth model, the total number of RLT stages (12 stages) as required by this model was reduced to 4 stress stages. There were some difficulties in fitting the 3-parameter incremental permanent strain model (as adopted in the Arnold rut depth model) using only four data points, but this was overcome by fixing one of the variables. Comparison of predicted incremental base deformations for the period 20–50 k-cycles and the field values measured in the above 17 actual pavements also indicated that they were significantly different (i.e. the predicted incremental deformations in the range of 2–110 mm/10^6 cycles as compared with filed values in the range of 0.6–6.0 mm/10^6 cycles).

Comparison of two FEM stress prediction models

DEFPAV (used in the Arnold rut depth model), and VMOD-PAVE (used in the ARRB/ Austroads simple performance prediction models), indicated that DEFPAV is too simple and is likely to produce large errors in the predicted stresses. Comparisons of predicted incremental base deformations for the period 20-50 k-cycles using the same RLT data set but different pavement stresses predicted with DEFPAV and VMOD-PAVE indicated that the effects of predicted stresses on the base deformation prediction were very significant. The use of pavement stresses predicted with VMOD-PAVE appeared to produce base incremental deformations closer to field values. By using the pavement stresses calculated with VMOD-PAVE, the simplified Arnold rut depth model was able to rank the material performance as found in the CAPTIF tests. Therefore, the use of VMOD-PAVE to predict stresses in base layers is recommended.

Comparison of equipment and methods

Comparison of RLT testing equipment and test methods used by ARRB and Nottingham University indicated that they had different requirements such as RLT testing equipment (triaxial cell, measurement devices, software), sample preparation methods (e.g. dynamic and vibratory compaction), and testing procedures (load pulse, stress levels, number of loading cycles, drained or undrained). It was difficult to quantify the effects of testing equipment, sample compaction method and testing procedure at this stage. However, based on experience gained in the development of both routine and research RLT test

methods at ARRB, it was possible to select a practical RLT test method for deformation prediction which meets the material requirements in New Zealand.

Recommendations

- a specimen of 150-mm diameter × 300-mm high be used for maximum particle size of up to 40 mm,
- vibratory compaction be used to prepare New Zealand materials,
- two linear variable displacement transducers (LVDTs) are mounted on the sample end caps to measure the average permanent strain for the whole sample for practical reasons,
- a higher loading speed can be used to reduce the testing time (say maximum 5 cycles per second) for long-term permanent strain testing (> 50,000 loading cycle per stress stage). However, an inter-laboratory study is required to check the performance of the loading equipment, control software, and measure equipment for standardisation purposes.

Based on the results of the validation of available methods of performance assessment for granular materials and further discussions on the effects of predicted pavement stresses and RLT testing equipment and test methods on deformation prediction, it is recommended that the Austroads/ARRB RLT test method for material specifications be tentatively incorporated into *TNZ M/22 Notes for the evaluation of unbound road base and sub-base aggregates* with the following modifications:

- A large triaxial specimen size of 150 mm diameter and 300 mm high should be used for 40 mm maximum particle size base materials.
- The triaxial specimen should be prepared using vibratory compaction to suit the material types use in New Zealand.

This test method was already subjected to inter-laboratory precision studies for the purpose of standardisation of testing equipment and test procedures for 20 mm maximum particle size base materials. It has also been demonstrated in this report that the methods can be extended to 40 mm maximum particle size base materials.

Testing conditions

Density and moisture conditions for RLT testing should be similar to field conditions and RLT testing should be conducted in a drained condition to enable field performance to be correctly predicted. An undrained condition may not be the same as long-term moisture conditions in conventional bases (with protection against moisture penetration), unless the bases were specifically designed to soak up moisture in very wet conditions. Further, because of the severe pore pressure effects on deformation at undrained, saturated conditions, the use of this condition is not recommended when the objective is to accurately model permanent deformation in the pavement. Given the difficulties in accurately measuring pore pressure in partially-saturated granular materials in both field and laboratory conditions, it is difficult to assess the differences in pore pressure between field and laboratory conditions and quantify the effects of pore pressure for various

material types. No inter-laboratory study has been done on undrained RLT testing to standardise the test equipment and testing procedures. Therefore, a need exists to improve the method for pore pressure measurement in partially saturated material as well as to standardise the test equipment and test procedures of the undrained RLT before the introduction of this test method for practical use.

Further research

Further research should be undertaken to improve deformation prediction models. A number of research issues need to be addressed in this area, particularly the quantification of errors produced by:

- different pavement stresses prediction models,
- different interpretation methods of test data obtained with the multi-stage permanent strain test,
- different laboratory compaction methods, which may arise in the use of different material types, different pavement configurations, different loading configurations and different moisture environments.

Abstract

This research proposes a new practical method for predicting the performance of unbound granular materials, including alternative, industrial by-products and recycled materials in New Zealand.

This investigation, carried out in 2005, utilised available field performance data in New Zealand to calibrate/validate available material assessment methods based on laboratory repeated load triaxial testing. The recommendation is that the simple ARRB performance assessment method, which is based on a reduced set of permanent strain results obtained from the existing Austroads repeated load triaxial test method, be used in material specification.

Further research should be undertaken to improve and simplify general deformation prediction models, which are based on a full set of permanent strain results at various tress levels, to make them suitable for practical use in pavement design.

1. Introduction

The principal aim of this project was to develop a practical method for predicting the performance of unbound granular materials, including alternative, industrial by-products and recycled materials. It is expected that this method will replace the existing laboratory repeated load triaxial (RLT) method adopted in the Transit New Zealand specification *TNZ M/22* (2000) to determine the suitability of alternative road material for use as a base or sub-base material for thin-surfaced granular pavements in the New Zealand context.

This project covers the following major investigations:

- validation of the Austroads existing RLT test method for performance-based material specifications (Vuong & Brimble 2000) on NZ granular materials tested at Canterbury Accelerated Pavement Testing Indoor Facility (CAPTIF),
- validation of the Arnold rut depth model developed by Arnold (2004) at the University of Nottingham for prediction of in-service rutting of unbound granular pavements,
- development of a simplified Arnold rut depth model which would allow the deformation performance of unbound materials to be more accurately predicted using laboratory permanent strain results,
- development of performance criteria for alternative base or sub-base materials that can be used in the performance-based material specifications (*TNZ M/22*) under New Zealand conditions.

This report details the above investigations and provides a draft material assessment method for alternative pavement materials.

2. Background

As road authorities are progressively moving towards minimisation of traditional pavement aggregates and utilising alternative aggregates (including industrial by-products, marginal and recycled materials) an increasing need exists for improved, more accurate methods to predict the performance of these alternative materials from laboratory tests.

Several methods for predicting performance of unbound base materials using laboratory testing have been proposed (Vuong 2003a). Among those, the repeated load triaxial (RLT) test is increasingly being used by Austroads member authorities including Transit New Zealand. It is worth mentioning that, in the past, laboratory RLT tests have been confined to resilient modulus testing as pavement design models (e.g. Austroads 1992, 2004) require only the resilient modulus of unbound materials as input. Recently, Austroads member authorities have extended laboratory RLT tests to permanent strain testing (e.g. 1995 Australian Standard RLT test method and the Austroads simplified RLT Test Method APRG 00/33 (Vuong & Brimble 2000). In some road authorities, these test methods have been used for material ranking and specification compliance in terms of permanent deformation and resilient modulus (Transport South Australia 2000, TNZ 2000).

Currently, Transit New Zealand specification *TNZ M/22* (2000) allows the use of RLT results to relax the existing standards for non-traditional aggregates (e.g. grading, sand equivalence and broken face). In this case, the 1995 Standards Australia RLT test method (AS 1289) is used to obtain permanent deformation data at the most critical compaction-moisture condition in the base for material assessment. A provision also exists which allows the RLT test conditions (in terms of stresses, moisture and density) to be modified to more accurately reflect representative 'in-service conditions'. However, no guidance is given as to how these 'in-service conditions' should be defined and, until these conditions can be more accurately defined, it will be difficult to use the results of laboratory RLT testing for the material specifications under New Zealand conditions.

Arnold (2004) has recently developed, at the University of Nottingham, a model for predicting the deformation of unbound granular materials using permanent strain results obtained from laboratory RLT testing. In this report, this model is referred to as the Arnold rut depth model. In this case, a research RLT test method was used to obtain a full material data set at various stresses for the study of material behaviour and pavement analysis. Under the direction of Transit NZ, the performance model has recently been investigated under accelerated loading using CAPTIF at a range of axle loads covering all possible loads that may be applied to in-service pavements (Arnold et al. 2005b). While initial results from the validation work are very promising, the model requires further validation and simplification if it is to obtain widespread and routine use in the development of performance-based specifications and for structural pavement design.

Vuong (2003b) has also recommended the use of a reduced set of RLT test results in developing performance based material specifications. In this case, the ARRB simple

assessment method (Vuong 2000, 2004) has been developed so that the reduced set of RLT permanent strain test results obtained with the 2000 Austroads simplified RLT test method can be used to predict in-service performance. While this method provides a practical and low-cost method, no work has been done to validate the relationships between the reduced set of RLT test results and field performance for pavement conditions in Australia and New Zealand.

It is intended that the above capabilities for laboratory testing and analytical modelling will be applied to the recent accelerated pavement testing field trials with Transit New Zealand's accelerated pavement testing facility, CAPTIF, to allow validation of any proposed method of material assessment utilising results from the RLT apparatus.

It is also intended to use the above methodology of material assessment and prediction of performance to develop a methodology to determine a design traffic loading limit for alternative unbound pavement materials used as either a base or sub-base material for use under New Zealand conditions.

These investigations will be part of a Land Transport New Zealand Research Report by Transit New Zealand: *Performance tests for road aggregates and alternative materials*, funded in 2005-2006, due to be published in 2007.

3. Material assessment methods using laboratory repeated load triaxial testing

Brief descriptions of the RLT testing methods adopted by Transit New Zealand, Austroads and Nottingham University are given in Appendices 1, 2, and 3, respectively. Some major requirements of the three RLT methods are also summarised in Table 3.1.

Table 3.1 Comparison of material assessment methods based on 1-D RLT testing.

Features	*TNZ M/22* (Appendix 1)	Austroads (Appendix 2)	Nottingham University (Appendix 3)
Material size	Maximum particle size in the range of 20–40 mm	Maximum particle size not exceeding 19 mm	Maximum particle size in the range of 20–40 mm
Sample size	150 mm diameter and 300 mm length	100 mm diameter and 200 mm length	150 mm diameter and 300 mm length
Sample preparation	Vibratory Hammer Compaction test (NZS 4402.4.1.3: 1986)	Dynamic compaction methods	Vibrating compaction test method (BS 1377-4: 1990)
Target density-	95% Vibratory MDD (TNZ B/2:1997)	Field dry density as specified by Austroads Members	Field dry density
Moisture condition	Fully saturated condition or optimum moisture content (OMC)	Field moisture content as specified by Austroads Members	Field moisture content
1-D RLT test apparatus (vertical loading pulse)	No specific specifications	Trapezoidal pulse with 0.2 second load and 1.8 second rest (pneumatic equipment)	Sinusoidal pulse at 5 times a second (5 hertz) (hydraulic equipment
Triaxial cell and instrumentation	No specific specifications	Strict specifications of loading friction and loading piston-top cap connections when using external load cell and external displacement transducers	Using internal load cell and on-sample displacement transducers
Drainage Condition	Undrained	Drained	Drained
Stress conditions for permanent strain testing	Single stage with a deviator stress of 425 kPa and a confining stress of 125 kPa	3 stages on one specimen with constant confining stress of 50 kPa and increasing deviator stresses being selected based on the vertical position of the material in the pavement (base, upper sub-base and lower sub-base)	21 stages using 3 specimens, viz. 7 stages per specimen with constant mean stresses and increasing shear stresses

Table 3.1 (continued):

Features	*TNZ M/22* (Appendix 1)	Austroads (Appendix 2)	Nottingham University (Appendix 3)
Stress conditions for resilient modulus testing	As above	64 stress stages to cover stress levels at various positions in the pavement	As above
Number of specimens required	1 specimen per target density and moisture condition	1 specimen per target density and moisture condition	3 specimens per target density and moisture condition
Number of loading cycles	50,000 cycles of a specified stress level	10,000 cycles per stress stage	50,000 cycles per specified stress level
Stress and strain measurement methods	No specific measurement requirements for stress, strain and pore pressure	External load cell (for non-friction triaxial cell) and whole-sample strain measured with 2 LVDTs* mounted between loading caps	Internal load cell and on-sample strain measured at sample mid-half using studs embedded in the specimen at two opposite locations
Interpretation of test results	Trend of permanent strain rate with loading cycles	Individualisation of data for each stress stage by taking into account permanent strain developed in previous loading stages using a load equivalency rule	Individualisation of data for each stress stage by ignoring permanent strain developed in previous loading stages
Assessment criteria	Use decreasing permanent strain rate as pass-fail criterion	Simple assessment methods based on material behaviour, deformation life and design base deformation	Compare predicted rut depth** with design rut depth
Other assessment methods required	Minimum soaked CBR^{+} requirement of 80%	–	–

* LVDT = linear variable displacement transducer

** Require models of permanent strain and resilient modulus to be fitted with experimental results and an analysis to be performed to predict rut depth

$^{+}$ California bearing ratio

Generally, the test methods have different requirements for key features such as:

- RLT testing equipment (triaxial cell, measurement devices, software),
- sample preparation methods (e.g. dynamic and vibratory compaction),
- testing procedures (load pulse, stress levels, number of loading cycles, drained or undrained).

In view of the great diversity of testing requirements for unbound granular materials, it is considered necessary to conduct inter-laboratory precision studies to assess the limitations of the testing method and standardise the testing requirements for practical use. Currently, only the Austroads RLT testing method has been subjected to inter-laboratory precision studies (Vuong et al. 1998) for standardisation purposes.

Different test methods also produce different test results and require different assessment methods as discussed below.

3.1 TNZ material assessment method (for material specification)

Typical test results for a standard granular base material obtained with the *TNZ M/22* RLT test method are given in Figure 3.1.

The basecourse is considered to have passed *TNZ M/22* if:

- the results of permanent strain RLT test shows the basecourse material exhibits stable behaviour. Stable behaviour is defined as a decreasing rate of permanent strain accumulation on a permanent strain v number of cycles graph,
- it satisfies a minimum soaked CBR requirement of 80%.

Effectively, the adoption of the RLT testing in the current TNZ performance-based specifications (TNZ 2000) is based on the assumption that the minimum design requirement of pavement performance will be achieved if the basecourse material exhibits stable deformational behaviour under a cyclic vertical deviator loading of 425 kPa and a constant confining stress of 125 kPa on a sample compacted to 95% vibratory compaction and a maximum moisture condition of 100% saturation under undrained conditions.

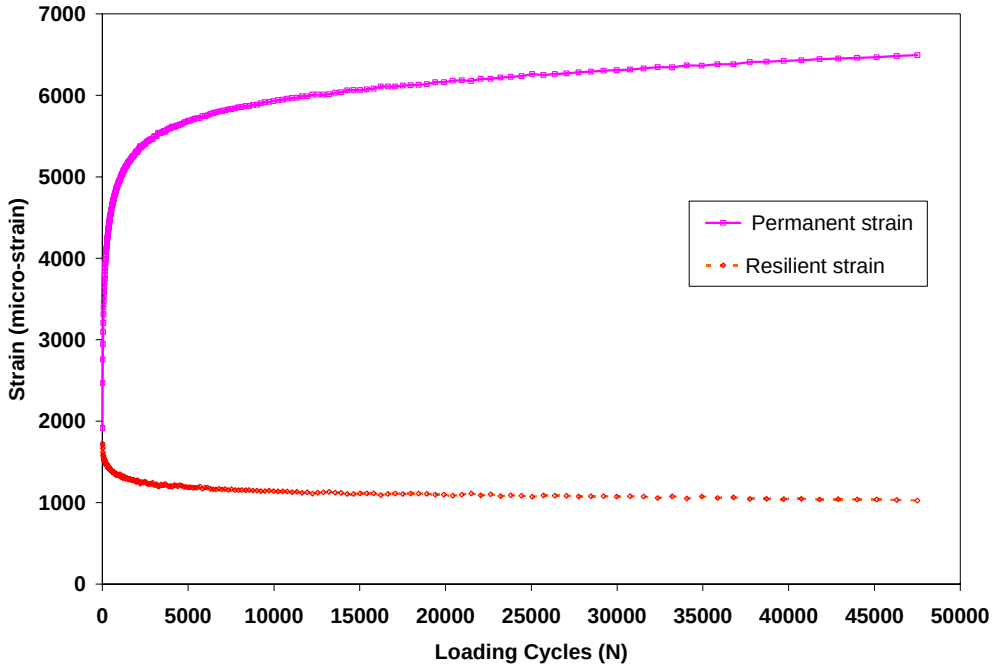

Figure 3.1 Typical results obtained from permanent deformation testing.

The above assumption was derived (Dodds et al. 1999) by testing aggregates that are routinely used in New Zealand pavements as complying with Transit New Zealand's specification for basecourse aggregate along with an aggregate being deliberately contaminated with 10% silty clay fines and thus not complying with *TNZ M/4* specification

(TNZ 1995) for basecourse aggregate. Dodds et al. (1999) reported that 100% saturation with undrained conditions resulted in early failure of the contaminated sample while the complying aggregates passed. In this study no attempt was made to determine the magnitude of rutting but simply to use the triaxial test as a pass-fail test.

Studies by both Vuong (2004) and Arnold (2004) found it is necessary to determine the deformation performance in the triaxial apparatus for a range of stress conditions to cover combinations of vertical and horizontal stresses present in a pavement under a wheel load. For example, Arnold (2004) found that the stress conditions at a depth of 150–200 mm, where the vertical loading is less than 250 kPa but the horizontal confining stress is nearly nil, caused the largest amount of deformation within the pavement. This is because a granular material has very little tensile strength and requires horizontal confinement to have the necessary strength to support the load. Thus the loading in the current *TNZ M/22* specification may not be the most severe loading that can occur in the pavement. However, the most severe loading is material-dependent and it can only be determine via multi-stage RLT tests at a range of stress conditions via modelling and interpretation of extrapolation. Hence, this project is aimed at developing the most appropriate set of test stress conditions to ensure confidence in the method of material assessment.

Note that *TNZ M/22 – Provisional Notes 1* also allows the contractor to change all the conditions of the RLT test from those stated above if the test conditions chosen can be demonstrated to be more accurate and more representative of the in-service conditions. However, no guidance is given for determination of in-service conditions (in terms of moisture content, density and stress levels).

Other concerns also exist with *TNZ M/22* associated with:

- the uncertainty as to whether the materials selected based on the current specifications (RLT test result and minimum soaked CBR requirement of 80%) may have the capacity to withstand the future higher stresses placed by emerging heavy vehicles,
- loosely defined specifications of loading equipment that may produce unreliable test results.

3.2 Austroads/ARRB material assessment method

Austroads/ARRB material assessment was developed at ARRB (Vuong 2000) in conjunction with the 2000 Austroads simplified RLT test method (Vuong & Brimble 2000) so that the RLT permanent strain test results obtained with this test method can be used to predict in-service performance. Although inter-laboratory testing has been conducted to standardise the testing equipment and test procedures of the Austroads RLT test method since 1998 (Vuong et al. 1998), note that little application of this RLT test has been made by state road authorities in their material specifications as well as little development of the material assessment method because of the scarcity of research and development funding. More details of the Austroads/ARRB material assessment method are given in Appendix 2.

In principle, the Austroads/ARRB material assessment method allows the following types of materials to be selected for use at different pavement depths:

- base materials (0–150 mm below the pavement surface),
- upper sub-base materials (150–250 mm below the pavement surface),
- lower sub-base materials (>250 mm below the pavement surface).

The method was developed by using an FEM computer program (VMOD-PAVE) to predict stresses in sprayed seal surfacing granular pavements under an axle load of 40 kN on a single wheel. This enabled selection of the representative stress levels (or design stresses) for base, upper sub-base and lower sub-base. The expectation is that the results of RLT permanent strain testing at this design stress level can be used to assess the deformation of a material to be used at a given depth. Two other stress levels, one below and one above the design stress level, were also selected to determine stress dependent permanent strain characteristics for the assessment of the base deformation caused by underloading or overloading. More details of the selection of RLT stresses are given in Appendix 2 (Section A2.7).

Table 3.1 lists the required values of dynamic deviator stress (σ_d) and static confining stress (σ_3) for the stress stages 1, 2 and 3 for RLT testing of base, upper sub-base and lower sub-base materials.

Table 3.2 Stress levels for permanent strain testing (material ranking and specifications).

Permanent deformation stress levels (kPa)						
Stress stage number	**Base**		**Upper Sub-base**		**Lower Sub-base**	
	σ_3	σ_d	σ_3	σ	σ_3	σ_d
1	50	350	50	250	50	150
2*	50	450	50	350	50	250
3	50	550	50	450	50	350

* Design stress level

Figure 3.2 shows typical results obtained from permanent strain testing using the Austroads standard RLT test method APRG 00/33 for a granular base material to be used at depth of 0-150 mm below the surface. Three loading stages were applied to the single specimen compacted to specified density and moisture condition, each involving 10,000 cycles at a stress condition of specified dynamic deviator stress and static confining stress as given in Table 3.2.

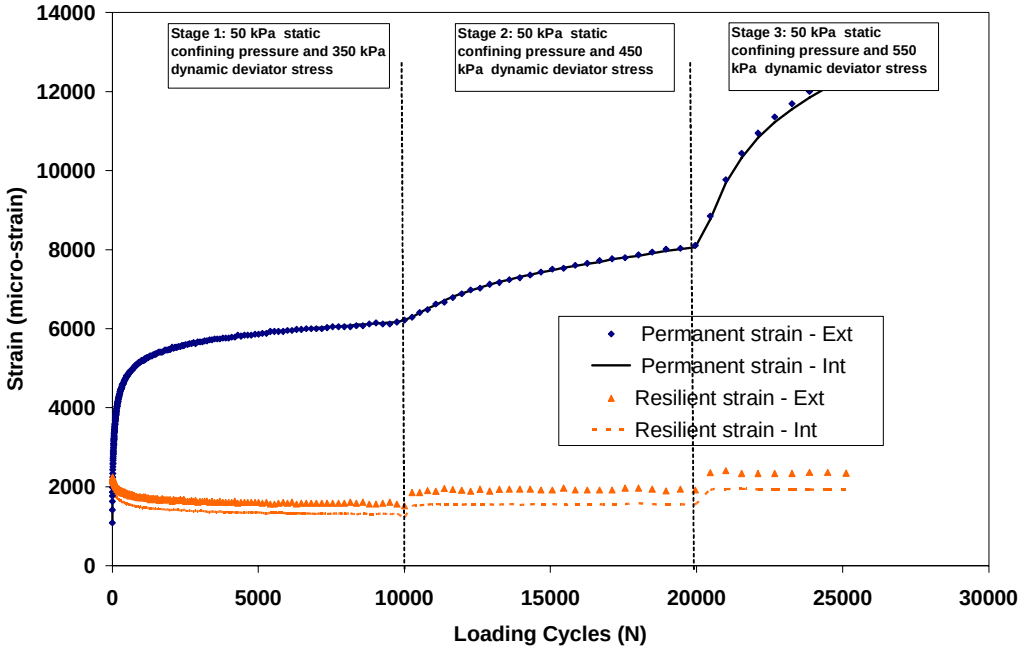

Figure 3.2 Typical results obtained from permanent deformation testing.

The results of the 3-stage permanent strain test as shown in Figure 3.2 can be used to derive the basic material behaviour, deformation life and design base deformation using three simple assessment methods (Vuong 2000) as briefly described below.

3.2.1 Performance assessment based on material behaviour

In principle, the material performance can be judged based on three basic material behaviour modes that can exhibit at a given loading stress as follows:

- Stable behaviour is defined as a decreasing permanent strain rate and decreasing to constant resilient strain with increasing loading cycles.
- Unstable behaviour is defined as a decreasing to constant permanent strain rate and constant to increasing resilient strain with increasing loading cycles.
- Failure behaviour is defined as a constant to increasing rate of permanent strain and increasing resilient strain with increasing loading cycles or when the total permanent strain reaches a nominal failure strain observed in static triaxial shear test (say in the range of 15,000-20,000 microstrain).

Table 3.3 summarises the proposed requirements of material behaviour exhibiting in the 3-stage permanent strain test, which can be used to select a base material for use in different pavement classes subjected to light, medium and heavy traffic.

- For pavements subjected to light traffic ($<10^6$ equivalent standard axles (ESA)), allowing a constant deformation rate in the base layer is considered appropriate at the design stress level in the base layer under a 40 kN wheel load (Stage 2). In this case, the basecourse is considered to have passed if the results of permanent strain RLT test show that the basecourse material exhibits stable behaviour in Stage 1 and unstable behaviour in Stage 2.

- For pavements subjected to medium traffic (10^6–10^7 ESA), where potential occurs for higher traffic loads, allowing a decreasing deformation rate in the base layer is considered appropriate at the critical stress level under a 40 kN wheel load (Stage 2). In this case, the base material is considered to have passed if the results of permanent strain RLT test show that the base material exhibits stable behaviour in Stage 2 and may exhibit failure in Stage 3.
- For pavements subjected to heavy traffic (>10^7 ESA), where potential occurs for stresses in the pavement to reach the stresses in Stage 3, allowing a decreasing deformation rate is considered appropriate in the base layer at the stress level in Stage 3. In this case, the base material is considered to have passed if the results of permanent strain RLT test show that the base material exhibits stable behaviour in Stage 2 and unstable behaviour in Stage 3.

Table 3.3 Requirements of material behaviour for granular bases (Vuong 2000).

Stage	Loading stress (kPa)		Behaviour requirements of granular bases		
	Static confining	Dynamic deviator	<10^6 ESA (light)	10^6–10^7 ESA (medium)	>10^7 ESA (heavy)
Stage 1	50	350	Stable	Stable	Stable
Stage 2*	50	450	Unstable	Unstable	Stable
Stage 3	50	550	Failure	Unstable to failure	Stable to unstable

*Design stress level

A similar procedure is used for the assessment of upper sub-base and lower sub-base materials. In addition, comparison of resilient modulus is also made for material ranking. This assessment method is simple and is suitable for the purpose of material ranking in specifications. However, the method requires validation with field performance data for pavement conditions in Australia and New Zealand.

3.2.2 Performance assessment based on deformation life

In principle, the material performance can be judged based on number of loading cycles at a given loading stress to reach failure condition or deformation life.

In this case, a curve-fitting procedure (see Appendix 2, Section A2.8) is used to determine the relationships between permanent strain and loading cycle for different stress levels applied in the 3-stage loading test. From these relationships, the number of loading cycles to reach a nominal failure strain (say 15,000 microstrain) can be calculated and plotted against the applied stress as shown in Figure 3.3. The loading cycles to failure at the design stress in Stage 2 (or design deformation life) and deformation lives for other stress levels outside the tested stress range (by means of extrapolation) can be used in material assessment.

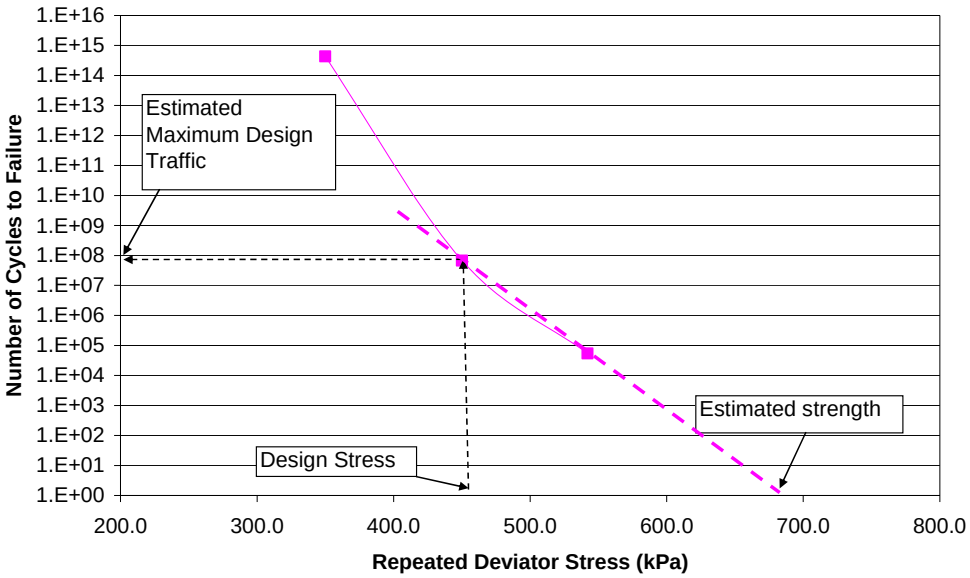

Figure 3.3 Example of the relationship between granular base deformation life and stress level.

Figure 3.4 also shows the proposed requirements of minimum deformation life (Vuong 2000), which can be used to select materials for use in different pavement classes subjected to different design lives. Each line of minimum deformation life is defined by the minimum design deformation life at the critical design stress in Stage 2 and strength limits (stress that cause failure in one cycle). It was considered appropriate to use:

- the minimum design deformation life at the critical design stress as the criterion for terminal rut depths,
- the minimum strength limit as the criterion for protection against overloading, viz. low-strength base materials (minimum strength of 600 kPa) being used in light-traffic local roads (10^5 ESA) and high-strength base materials (strengths >800 kPa) used in high class heavy-duty roads (>10^7 ESA).

In this case, the basecourse is considered to have passed for a specific pavement design life if the results of the permanent strain RLT test show that the basecourse material shows greater deformation lives for the three loading stages than the required minimum deformation lives (i.e. on the right hand side of each curve to be selected for design life concerned).

Examples of two materials, A and B, are also shown in Figure 3.4. Material A is considered to have a better performance than Material B as the results of the permanent strain RLT test show that the Material A produces higher deformation lives for all stress levels. In addition, based on the proposed requirements of minimum deformation life, Material A is considered suitable for pavements with a design traffic of <10^7 ESA; whereas Material B is be suitable for pavements with a design traffic of <10^6 ESA.

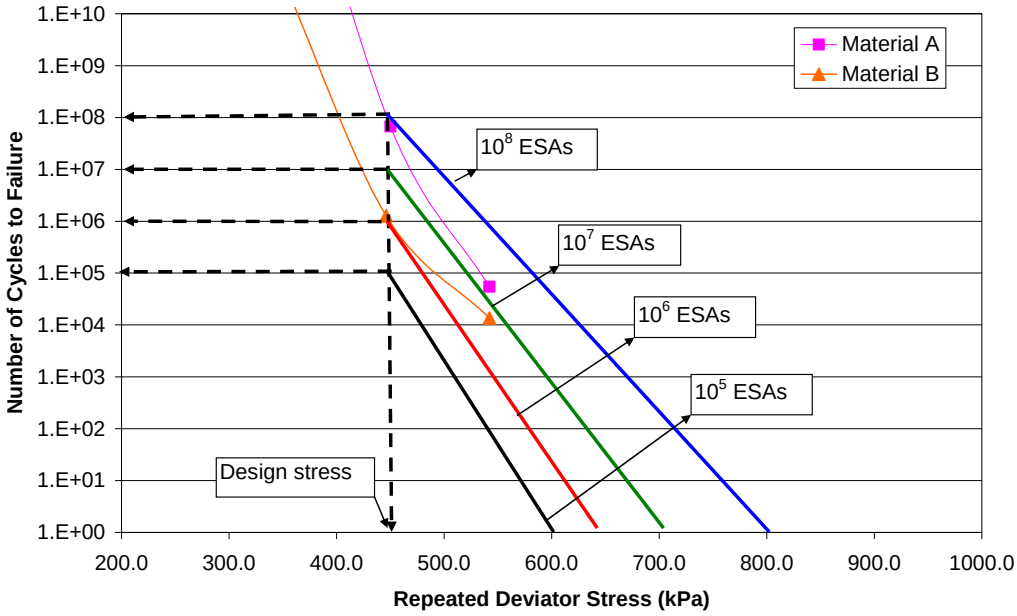

Figure 3.4 Boundaries of deformation life and strength for different pavement classes.

This method is more versatile than the assessment method based on material behaviour (see Section 3.2.1) as it can be used for a designated pavement design life. However, this assessment method has not been validated or applied in Australia or New Zealand.

3.2.3 Performance assessment based on estimated base deformation

Alternatively, the relationships between permanent strain and loading cycle for each stress level derived from the 3-stage permanent strain test can be used to predict deformations of a granular layer with sprayed seal at various loading cycles of standard axle loads using a simple rule, viz. deformation of the granular layer being the product of permanent strain at the design stress level ($\varepsilon_{p(Stage2)}$) and the thickness of the layer (ΔH) concerned.

$$\Delta d_{Base} = \varepsilon_{p(Stage2)Base} \times \Delta H_{Base} \quad \text{(Equation 3.1)}$$

$$\Delta d_{Upper\ Sub\text{-}base} = \varepsilon_{p(Stage2)Upper\ Sub\text{-}base} \times \Delta H_{Upper\ Sub\text{-}base} \quad \text{(Equation 3.2)}$$

$$\Delta d_{Lower\ Sub\text{-}base} = \varepsilon_{p(Stage2)Lower\ Sub\text{-}base} \times \Delta H_{Lower\ Sub\text{-}base} \quad \text{(Equation 3.3)}$$

As shown in Table 3.2, the RLT test stresses selected for each material at a given depth include a design stress (Stage 2), and two stress levels for the layers below and above this depth (Stage 1 and Stage 3). Therefore, deformation of a thick granular base layer can be estimated by sub-layering the layer and summing the deformation of the sub-layers; e.g.:

$$\Delta d_{Basetotal} = [\varepsilon_{p(Stage2)Base} \times \Delta H_{Base}] + [\varepsilon_{p(Stage1)Base} \times \Delta H_{Upper\ Sub\text{-}base}]$$

(Equation 3.4)

This method is more suitable for pavement design, where requirements of base deformation for different pavement classes are specified. However, it has not been validated for pavement conditions in New Zealand.

3.2.4 Comparison of models against Australian field performance data

A preliminary evaluation of the above ARRB assessment methods has been made using field performance obtained from limited accelerated pavement testing trials at ARRB (Vuong & Yeo 2004). The comparisons of laboratory and field performance in these accelerated loading facility (ALF) trials indicated that the three assessment methods can be used to rank material based on relative comparison of deformations rather than absolute deformations. This may be because stress conditions in actual granular pavement layers under rolling wheel loads are different from those in laboratory RLT testing condition. Therefore, if the absolute pavement deformation needs to be predicted, the laboratory-determined permanent strain may need to be corrected for the differences between the laboratory and field loading conditions, i.e. the model should be calibrated.

Currently, a deformation prediction model developed by ARRB (Vuong 2005a) has also been validated against ALF field trials to establish the correlations between laboratory RLT permanent strain results and field base deformations. It was also proposed (Vuong 2003b) that the above ARRB assessment methods should be further validated using:

- interim specification limits based on results of a testing programme of typical traditional base materials with known field conditions and performance,
- field performance obtained for various field conditions of density and moisture contents.

Chapter 6 will discuss further the validation of the above assessment methods using recent CAPTIF field trials as a precursor to a more extensive investigation on their suitability for practical use in New Zealand.

3.3 Material assessment using Arnold rut depth model for pavement design

The rut depth model proposed by Arnold (2004) is detailed in Appendix 3. Figure 3.5 shows Arnold's methodology to calculate rut depth and to validate his model.

In principle, the method requires the following major steps to predict the surface rut depth of a granular pavement:

- Step 1: Conduct permanent strain testing using the Nottingham RLT test method to collect full data set of permanent strain and resilient modulus data at various pavement stresses.
- Step 2: Develop material models of resilient modulus from the full data set for FEM pavement analysis to predict pavement stress.
- Step 3: Develop material models of permanent strain from the full data set for the calculation of surface rut depth from the FEM-predicted pavement stresses.

Step 4: Validate with field performance and make adjustments to assumptions of residual stress, and initial rut depth, if required.

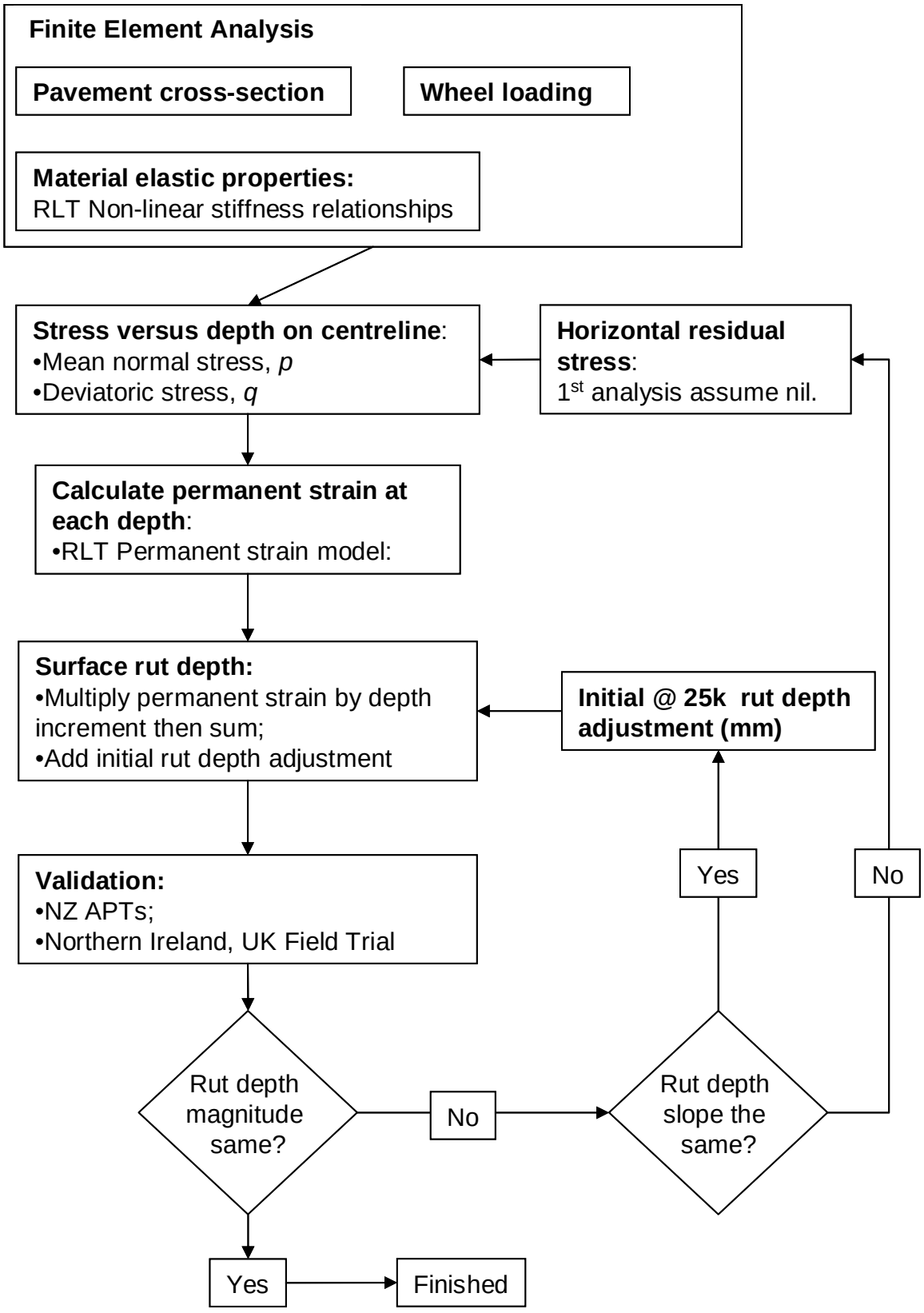

Figure 3.5 Methodology for calculation of rut depth and validation (Arnold 2004).

3.3.1 Permanent strain testing using the Nottingham RLT test method

The objective of the Nottingham laboratory RLT test method (Appendix 3) is to measure sufficient permanent strain data at various stress states (each being defined by a mean principal stress and a deviator stress) to obtain a model to calculate permanent strain for any given stress value. In the testing programme, testing stresses are varied to cover the full spectra of stresses expected in the pavement. To reduce testing effort, multi-stage RLT permanent strain tests using the Arnold (2004) RLT test method as described in Appendix 3 were used. Generally, three five-stage tests conducted on three different specimens are required to provide modulus and permanent strain data for 15 stress states (3 mean stresses x 5 deviator stresses). Figure 3.6 shows typical results obtained from a 5-stage RLT permanent strain test.

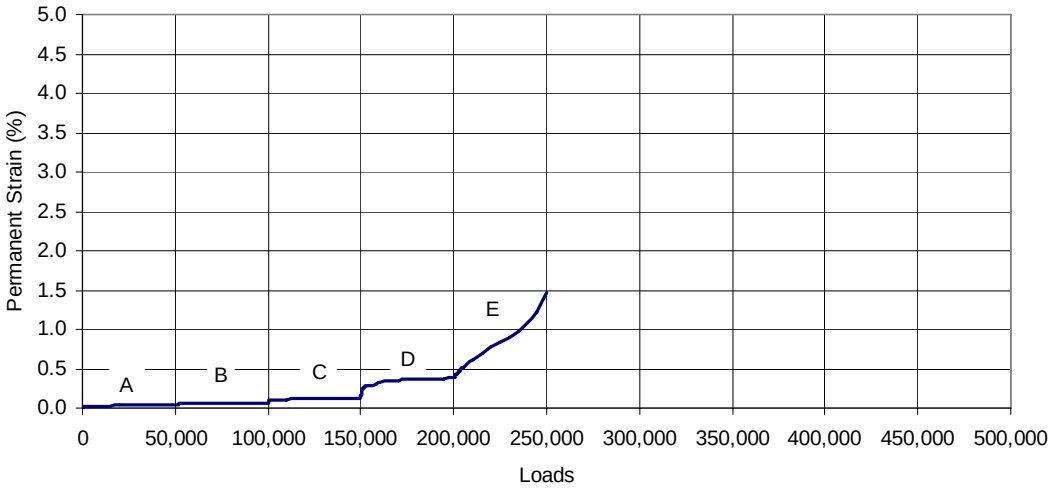

Figure 3.6 Typical RLT permanent strain result (CAPTIF 1 material, Test 1 – p = 75kPa) (Arnold 2004).

3.3.2 Resilient modulus model and FEM analysis to predict pavement stresses

A simple 2-D axi-symmetrical non-linear finite element model, DEFPAV (Snaith et al. 1980) was used to predict stresses within the pavement. DEFPAV was chosen because of its availability and ease of use in terms of obtaining the outputs and utilising the non-linear resilient characteristics of the granular and subgrade materials.

The following assumptions were considered (Arnold 2004) in a pavement analysis using this FEM model:

- A single circular load of uniform stress is used to approximate actual dual tyre wheel load.
- Modulus of unbound material is expressed in terms of K-θ model and Poisson's ratio is constant.

$$E = K_1 \times \theta^{K_2} \qquad \text{(Equation 3.5)}$$

where:

E = resilient modulus (MPa)

θ = total stress (MPa) = $(\sigma_1 + \sigma_2 + \sigma_3)$

K_1, K_2 = experimental test constants.

- Material is weightless.
- Zero horizontal residual confining stresses resulted after compaction of the pavement layers.
- Tensile stresses are allowed to be developed in granular elements.

Given that the above assumptions only approximated the non-linear characteristics of the granular and subgrade materials, there may be errors in the calculation of stresses from DEFPAV.

From the pavement stress analysis, the mean principal stress (p) and deviator stress (q) under the centre of the load are calculated for input into a spreadsheet along with depth for the calculation of rut depth.

3.3.3 Permanent strain model and calculation of rut depth

Arnold (2004) described permanent strain rate at any loading cycle (or incremental permanent strain at any loading period) as a function of mean principal stress (p) and deviator stress (q) using Equation 3.6:

$$\Delta\varepsilon_p = e^{(A)}\, e^{(Bp)}\, (e^{(Cq)} - 1) \qquad \text{(Equation 3.6)}$$

where:

e = 2.718282

$\Delta\varepsilon_{p(rate\ or\ magn)}$ = permanent strain rate

A, B & C = constants obtained by regression analysis fitted to the measured RLT data

p = mean principal stress (MPa)

q = deviator stress (MPa)

Four different relationships (Equations 3.7, 3.8, 3.9 and 3.10) were used to describe incremental strains at four loading periods, namely:

i. 0 – 25k loading cycles for early behaviour (compaction important),
ii. 25k – 100k loading cycles for mid-term behaviour,
iii. 100k – 1M loading cycles for late behaviour,
iv. 1M-2M loading cycles for long term behaviour.

$$\Delta\varepsilon_{p(0\text{-}25k)} = e^{(A1)}\, e^{(B1\ p)}\, (e^{(C1\ q)} - 1) \times 25k \qquad \text{(Equation 3.7)}$$

$$\Delta\varepsilon_{p(25\text{-}100k)} = e^{(A2)}\, e^{(B2\ p)}\, (e^{(C2\ q)} - 1) \times 75k \qquad \text{(Equation 3.8)}$$

$$\Delta\varepsilon_{p(100k\text{-}1M)} = e^{(A3)}\, e^{(B3\ p)}\, (e^{(C3\ q)} - 1) \times 900k \qquad \text{(Equation 3.9)}$$

$$\Delta\varepsilon_{p(1M\text{-}2M)} = e^{(A4)}\, e^{(B4\ p)}\, (e^{(C4\ q)} - 1) \times 1000k \qquad \text{(Equation 3.10)}$$

A simple procedure (Arnold 2004, see Appendix 3) was also used to estimate the incremental permanent strain data for different stresses, which are used to establish the equation for the loading period concerned (e.g. 25-50 k-cycles), from results obtained

from the Nottingham multi-stage permanent strain test method. In principle, the following major assumptions were made in this procedure:

- The permanent strain test for each stress stage in the multi-stage permanent strain test can be treated as an individual test on the virgin specimen by ignoring the permanent strain occurring in the previous loading stages.
- Given that test data for each stress level were limited to 50 k-cycles, extrapolation was required to estimate strain rates in the loading periods between 50 k-cycles and 2 M cycles.

Some errors were expected in the predicted incremental permanent strains using Equations 3.7, 3.8, 3.9 and 3.10 because:

- the first assumption may not be valid as permanent strain of granular material is known to be strongly influenced by previous loading histories and changes in both sample density and shear deformation in the specimen over the course of testing,
- further errors are caused by the extrapolation-measured permanent strain rates to predict strain rates after 50 k-cycles.

Equations 3.11, 3.12, 3.13, and 3.14 are used to calculate incremental surface permanent deformation at the centre of the single circular load for each loading period.

$$\Delta d_{(0\text{-}25k)} = \sum \Delta \varepsilon_{p(0\text{-}25k)}(I) \times \Delta H(I) \times \Delta N_{(0\text{-}25k)} \quad \text{(Equation 3.11)}$$

$$\Delta d_{(25\text{-}100k)} = \sum \Delta \varepsilon_{p(25\text{-}100k)}(I) \times \Delta H(I) \times \Delta N_{(25\text{-}100k)} \quad \text{(Equation 3.12)}$$

$$\Delta d_{(100k-1M)} = \sum \Delta \varepsilon_{p(100k-1M)}(I) \times \Delta H(I) \times \Delta N_{(100k-1M)} \quad \text{(Equation 3.13)}$$

$$\Delta d_{(1M\text{-}2M)} = \sum \Delta \varepsilon_{p(1M\text{-}2M)}(I) \times \Delta H(I) \times \Delta N_{(1M\text{-}2M)} \quad \text{(Equation 3.14)}$$

where:

Δd = incremental surface deformation

$\Delta \varepsilon_p(I)$ = incremental permanent strain for the stresses at depth I (or depth to middle of the sub-layer I)

$\Delta H(I)$ = associated depth increment (or thickness of the sub-layer I)

ΔN = applied number of loading cycles for the loading period concerned

The total surface permanent deformation at the centre of the single circular load at a specified loading cycle is the sum of incremental deformation in all previous loading periods.

$$d = \sum \Delta d \quad \text{(Equation 3.15)}$$

In this method, the predicted surface permanent deformation at the centre of the single circular load was assumed to be similar to the rut depth developed in actual pavements trafficked with actual heavy vehicles:

$$RD = d \quad \text{(Equation 3.16)}$$

3.3.4 Model validation and calibration

Arnold, as part of his PhD studies, validated the model using a larger data set of CAPTIF pavement trials, and the results are reported in Chapter 5.

As detailed in Figure 3.5, Arnold calibrated the model by comparing the predicted rut depth with the measured rut depth in the pavement trials. Based on comparison with actual pavement test results, an initial rut depth was added (or subtracted) to account for simplifying assumptions in the model.

Arnold used the following methods to adjust the predicted surface deformation during the calibration:

- For rut depth at 25 k, adjustment is directly based on the differences between measured and predicted rut depth. This is because the differences are caused by sample preparation and compaction which are very difficult to quantify because of the use of RLT multi-stage tests where prior loading affected the initial deformation that occurs at the start of a new loading stress.
- For rut depth increments at greater than 25 k-cycles, adjustment is made in terms of the magnitude of horizontal stress added. This parameter was found to significantly influence the predicted rut depth. In this case, an iterative process is required to determine the initial rut depth adjustment and the amount of horizontal residual stress to add in order that the calculated surface rut depth matches the measured values.

3.4 Material assessment using simplified Arnold rut depth model for material specification

The Arnold rut depth model (Arnold 2004), in its present state, was considered to be impractical for use in specification because of its complexity, non-linear finite element analysis and large number of RLT tests required. Therefore, this project also aims to simplify the Arnold rut depth model and develop a practical test and analysis procedure for routine use in specifications.

To reduce efforts in material testing and conducting the analyses, the proposal was that:

- The total number of stages (15 stages) in the Nottingham RLT test method (see Section 3.3) be reduced to 4 stress stages. The four stress stages will be selected so that similar relationships of permanent strain rate and stresses (see Equations 3.7, 3.8, 3.9 and 3.10) could be produced by the full data set (15 stress stages) and reduced data set (4 stress stages).
- Pavement analysis is limited to the prediction of incremental surface permanent deformation at the centre of the single circular load for the loading period of 25-50 k-cycles.

Chapter 7 of this report will describe the development of the reduced data set (4 stress stages) for the simplified rut depth model using existing full RLT data set for the CAPTIF aggregates (i.e. CAPTIF 1, 2, 3, and 4) and the validation of this simplified approach using field results obtained from CAPTIF pavement trials.

4. Field trials for validation and calibration of material assessment methods

Ten full-scaled pavements were selected for the validation of the rut depth models. They included:

- eight pavements tested with the accelerated pavement testing facility by Transit New Zealand,
- two in-service pavements in Northern Ireland, tests on which were conducted by Queens University Belfast, Northern Ireland.

4.1 Details of CAPTIF field trials

Details of the trials, including pavement construction, loading and monitoring of field performance, are given in Arnold (2004). They are briefly described below.

4.1.1 CAPTIF test facilities

CAPTIF is located in Christchurch, New Zealand, and is owned and operated by Transit New Zealand. It consists of a 58-m long (on the centre line) circular track contained within a 1.5-m deep x 4-m wide concrete tank (Figure 4.1). A centre platform carries the machinery and electronics needed to drive the system. Mounted on this platform is a sliding frame that can move horizontally by 1 m. This radial movement enables the wheel paths to be varied laterally and can be used to have the two 'vehicles' operating in independent wheel paths. An elevation view is shown in Figure 4.2.

At the ends of this frame, two radial arms connect to the Simulated Loading and Vehicle Emulator (SLAVE) units shown in Figure 4.3. These arms are hinged in the vertical plane so that the SLAVEs can be removed from the track during pavement construction, profile measurement etc., and in the horizontal plane to allow vehicle bounce.

CAPTIF is unique among accelerated pavement test (APT) facilities in that it was specifically designed to generate realistic dynamic wheel forces. Other accelerated pavement testing facility designs attempt to minimise dynamic loading. The SLAVE units at CAPTIF are designed to have sprung and unsprung mass values of similar magnitude to those on actual vehicles and utilise standard heavy vehicle suspension components. The net result of this is that the SLAVEs apply dynamic wheel loads to the test pavement that are similar in character and magnitude to those applied by real vehicles. A more detailed description of the CAPTIF and its systems is given by de Pont & Pidwerbesky (1995).

Figure 4.1 Transit New Zealand's pavement testing facility CAPTIF.

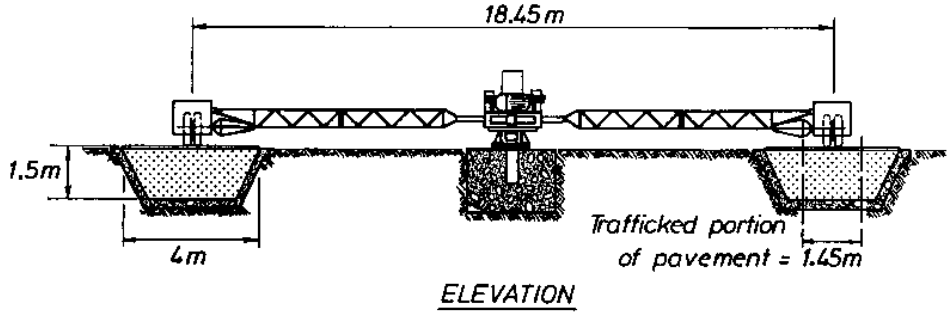

Figure 4.2 Elevation view of CAPTIF.

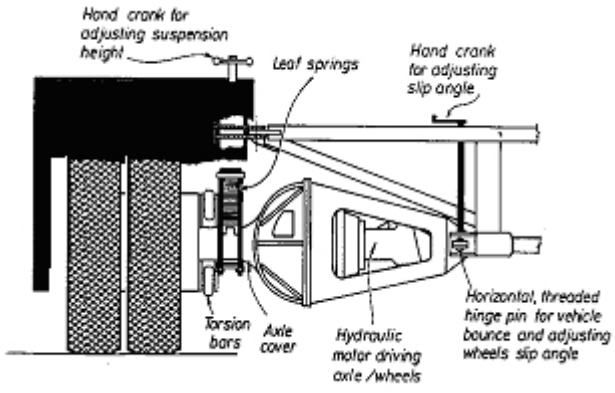

Figure 4.3 The CAPTIF SLAVE unit.

4.1.2 Pavement details

Eight CAPTIF pavement sections were constructed with four different granular bases and were given unique identifications as shown in Table 4.1.

- Pavement test sections having the same materials but different base thickness were placed in the same group.
- The granular materials used in these pavement sections are referred as CAPTIF 1, CAPTIF 2, CAPTIF 3, and CAPTIF 4. All CAPTIF pavements were constructed on the same subgrade. Brief descriptions of the granular materials and subgrade are given in Table 4.2.
- These pavement sections were tested in three CAPTIF tests, which have been defined by the year the first report was published, either 1997 (de Pont 1997, de Pont et al. 1996), 2001 (Arnold et al. 2001, de Pont et al. 2001) or 2003 (Arnold et al. 2005a, 2005b).
    - For the CAPTIF test in 2001 (Figure 4.4), the CAPTIF test track was divided into four segments. Three segments were used to accommodate the three different granular materials (CAPTIF 1, CAPTIF 2, and CAPTIF 3) constructed at same base thickness of 275 mm. The 4th segment was not used for research study, because of the extra compaction from construction traffic that this segment receives, which from experience affects the results. All segments had a thin asphalt surfacing of 25 mm.
    - For the CAPTIF test in 2003 (Figure 4.5*)*, the CAPTIF test track was also divided into five segments to accommodate two granular materials (CAPTIF 1 and CAPTIF 3) constructed at two thicknesses of 200 mm and 275 mm. All segments had an asphalt thickness of 25 mm.
    - The earlier CAPTIF test in 1997 was not split into small pavement sections and the same granular material (CAPTIF 4) was used for all four segments. The asphalt surface was 90 mm thick and the granular material layer was a 200 mm thick.

Table 4.1 CAPTIF pavement test sections.

ID	Granular Material	Granular Depth (mm)	CAPTIF Test	Asphalt Surface Depth (mm)
1	CAPTIF 1	275	2001	25
1a		275	2003	
1b		200	2003	
2	CAPTIF 2	275	2001	
3	CAPTIF 3	275	2001	
3a		275	2003	
3b		200	2003	
4	CAPTIF 4	200	1997	90

Table 4.2 Materials used in the CAPTIF pavement test sections.

Material Name	Description
NI* Good	Premium quality crushed rock - graded aggregate with a maximum particle size of 40 mm from Banbridge, Northern Ireland, UK
NI Poor	Low quality crushed quarry waste rock - graded aggregate (red in colour) with a maximum particle size of 40 mm from Banbridge, Northern Ireland, UK
CAPTIF 1	Premium quality crushed rock – graded aggregate with a maximum particle size of 40 mm from Christchurch, New Zealand
CAPTIF 2	Same as CAPTIF 1 but contaminated with 10% by mass of silty clay fines
CAPTIF 3	Australian class 2 premium crushed rock – graded aggregate with a maximum particle size of 20 mm from Montrose, Victoria, Australia
CAPTIF 4	Premium quality crushed rock – graded aggregate with a maximum particle size of 20 mm from Christchurch, New Zealand
CAPTIF Subgrade	Silty clay soil used as the subgrade for tests at CAPTIF from Christchurch, New Zealand

* NI = Northern Ireland

Figures 4.4 and 4.5 detail how the pavements were split for the two CAPTIF tests (2001 and 2003). A typical pavement cross section is shown in Figure 4.6.

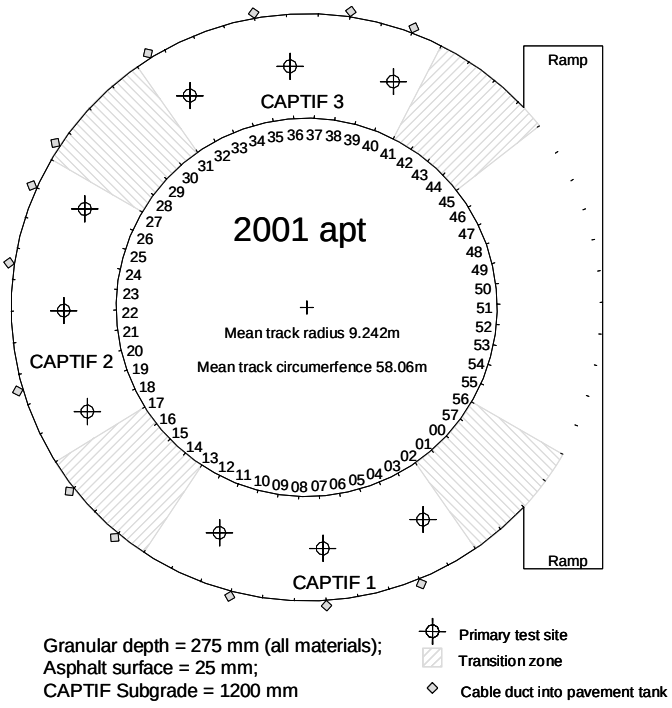

Figure 4.4 Layout of CAPTIF pavement test sections for the 2001 test.

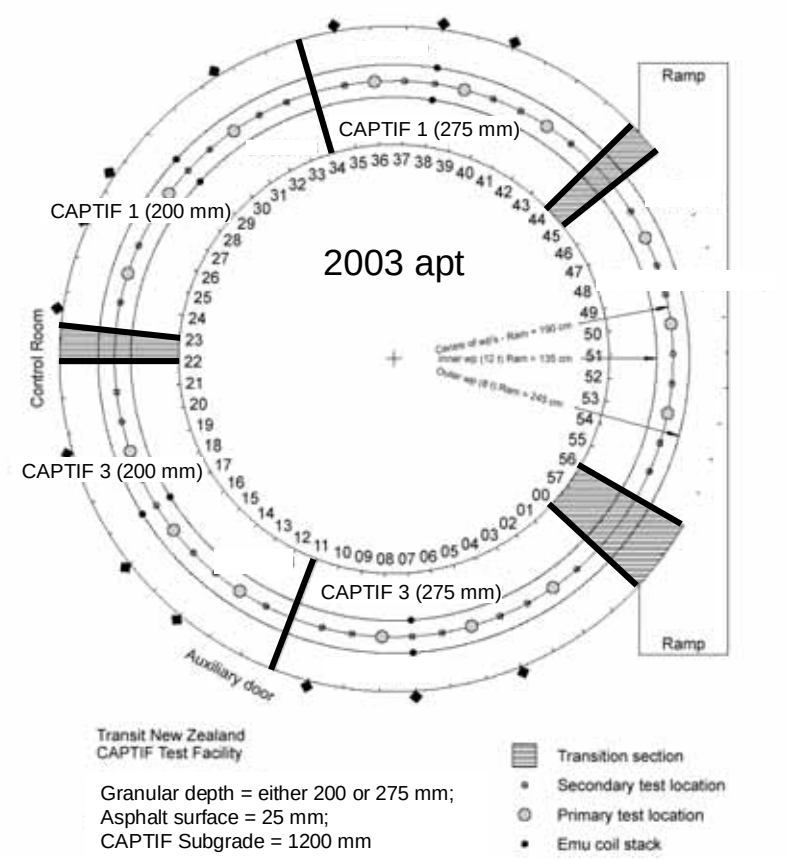

Figure 4.5 Layout of CAPTIF pavement test sections for the 2003 test.

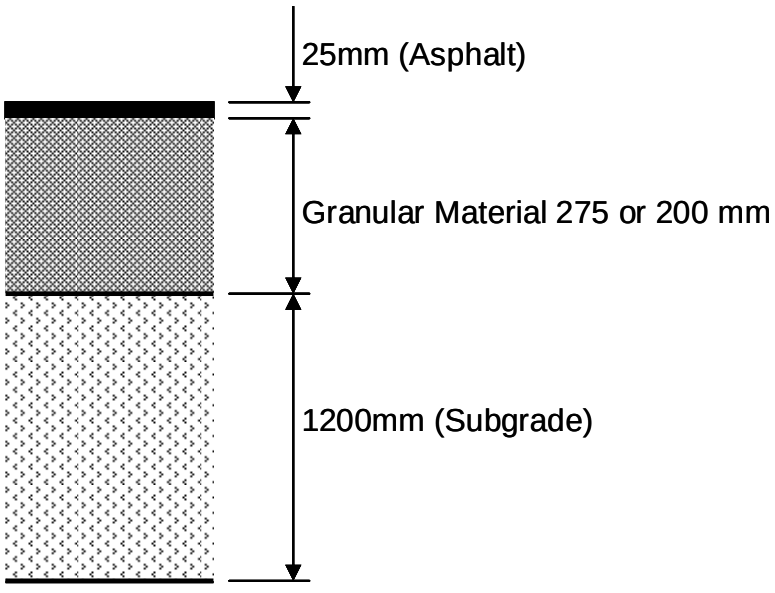

Figure 4.6 Pavement cross section for CAPTIF 1, 2, and 3 trials.

4.1.3 Loading details

For the three CAPTIF tests, the wheel paths of the two vehicles on the circular test track were separated for the purpose of assessing the relative damaging effect on the pavement caused by different suspension types and wheel loads.

For the 1997 CAPTIF tests steel and air-bag suspensions were used for each wheel path, while the wheel load was the same i.e. of 50 kN on a single tyre.

The two wheel paths for the 2001 CAPTIF tests were at different loads of 40 kN and 50 kN load on dual tyres, while steel suspension was used for both wheel loads.

For the 2003 CAPTIF tests 40 kN and 60 kN wheel loads were tested but with air-bag suspension systems being used.

Accelerated pavement loading was conducted at a speed of 45 km/h and a wheel wander of ±50 mm with a normal distribution. Testing was stopped periodically to undertake pavement testing. The axle load and number of wheel passes for each pavement test section are summarised in Table 4.3. The lighter wheel paths were tested with a load of 40 kN for 1 M passes and then the load increased to either 50 kN or 60 kN for the remainder of the test. A reason for this change was to determine the affect on an already trafficked road should legal mass limits of heavy vehicles increase (de Pont et al. 2001).

Table 4.3 Pavement loading for each test section of all CAPTIF tests.

Pavement ID	Load (kN) 0 –1 M passes	Load (kN) > 1 M passes	Wheel type & suspension	Tyre Inflation Pressure (kPa)	Axle load (tonnes)	Total wheel passes (M)
Lighter Wheel Path: 1, 2, 3	40	50	dual/steel	750	8 (<1M) 10 (>1M)	1.32
Heavier Wheel Path: 1, 2, 3	50	50	dual/steel	750	10	1.32
Lighter Wheel Path: 1a, 1b, 3a, 3b	40	60	dual/air-bag	750	8 (<1M) 12 (>1M)	1.4
Heavier Wheel Path: 1a, 1b, 3a, 3b	60	60	dual/air-bag	750	12	1.4
Inside Wheel Path: 4	50	50	single/air-bag	750	10	1.7
Outside Wheel Path: 4	50	50	single/steel	750	10	1.7

4.1.4 Measured performance

The following devices were used to monitor the surface deformation:

- the laser profiler to measure longitudinal profile in the wheel path centreline,
- the CAPTIF profilometer to measure transverse profile at each of the 58 stations around the track.

Surface deformations were measured before pavement loading and at the completion of 15, 25, 35, 50, 100, 150, 200, 250, 300, 400, 500, 600, 700, 800, 900 and 1000 k-cycles.

Vertical surface deformation (VSD) and straight-edge rut depth for each pavement section was calculated as the average value determined from approximately 10 measurements at 1 m stations for the 2001 and 2003 tests and from 52 measurements for the 1997 test. Results of the surface deformations were group in terms of the pavement types as shown in Figures 4.7 to 4.10.

4.2 Details of the Northern Ireland in-service pavements

Arnold (2004) reported two field trials using in-service pavements in Northern Ireland, which are summarised below.

4.2.1 Location

The field trial is located on a private access road into the landfill at Ballyclare, Northern Ireland.

4.2.2 Pavement details

Two pavement sections were built side by side in order to test the Northern Ireland (NI) 'Good' and NI 'Poor' aggregates. Asphalt cover thickness varied randomly from 80 to 120 mm and the aggregate depth ranged from 600 to 800 mm over a solid rock subgrade.

4.2.3 Loading details

A weigh bridge was used to record the weight of every vehicle that passed. The total number of passes per year for all axles combined was about 55,000.

Data of truck axles (number and type) and weights was also collected during a short period (while undertaking measurements of stress and strain). Most of the trucks were waste collection vehicles with a single-tyre front steering axle and two dual-tyre axles at the rear. Other axle configurations were either:

- one single-tyre front steering axle and only one dual-tyre rear axle,
- two single-tyre front steering axles (twin-steers) and two dual- tyre rear axles.

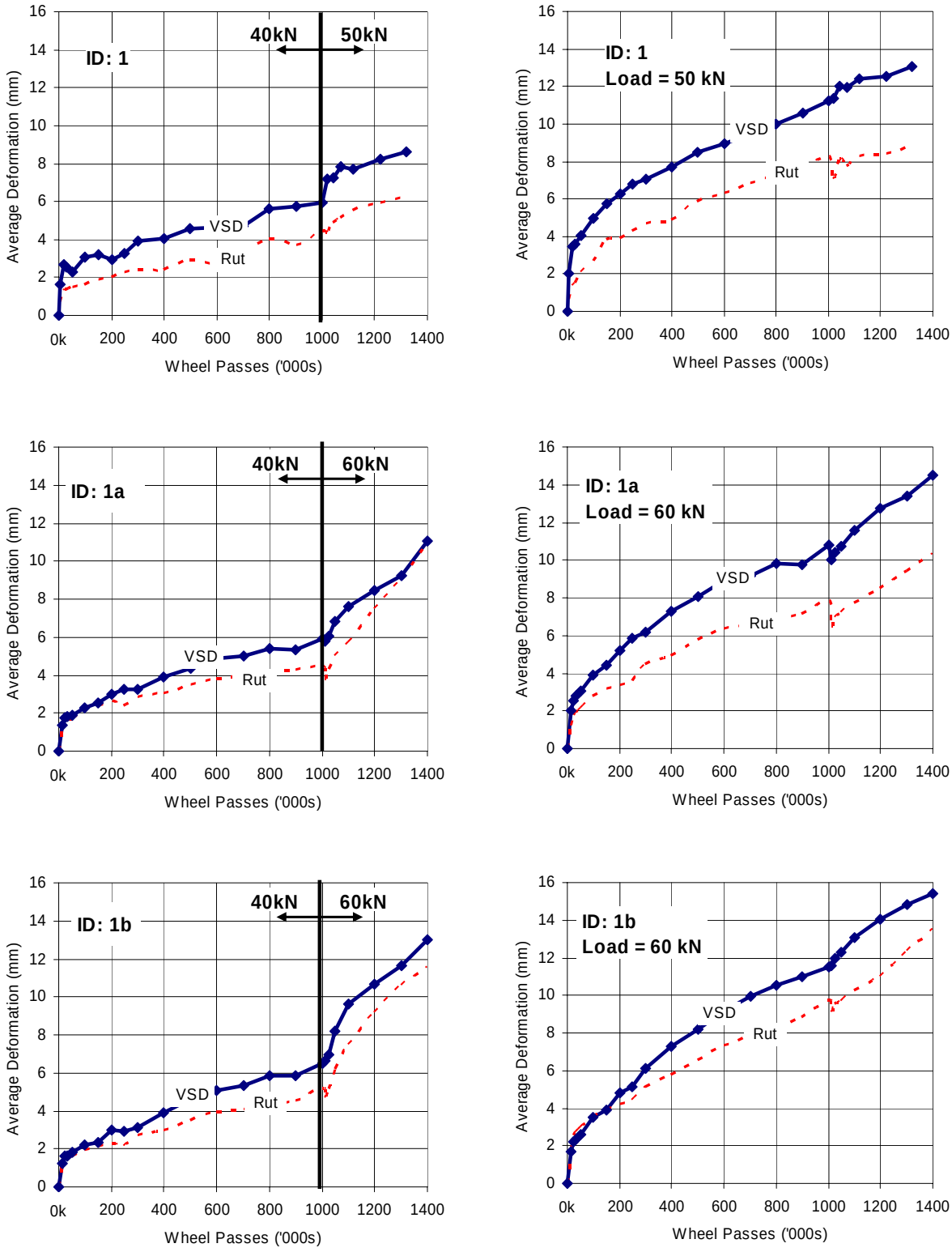

Figure 4.7 Measured maximum surface deformations of pavement sections 1, 1a, and 1b.

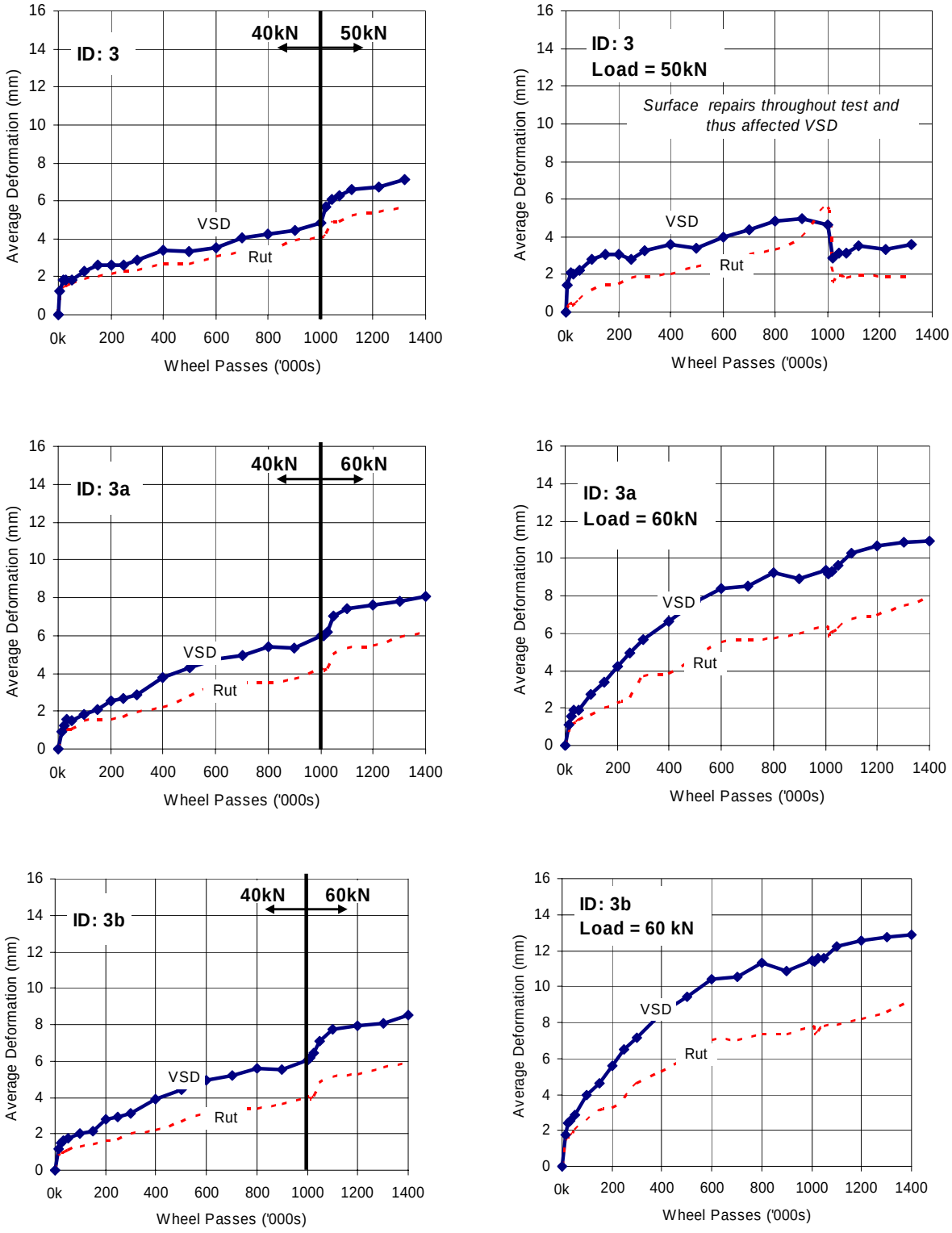

Figure 4.8 Measured maximum surface deformations of pavement sections 3, 3a, and 3b.

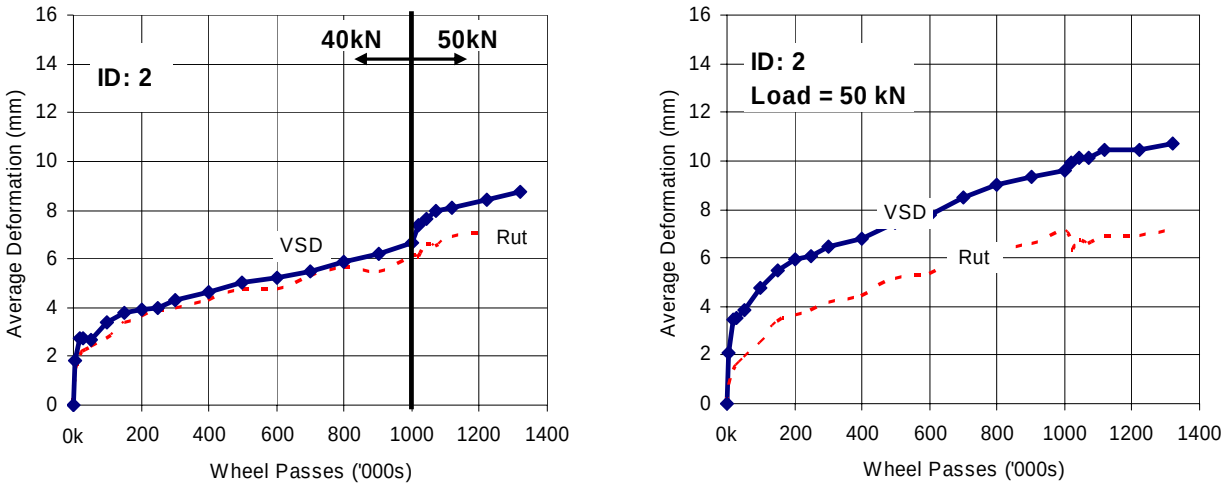

Figure 4.9 Measured maximum surface deformations of pavement section 2.

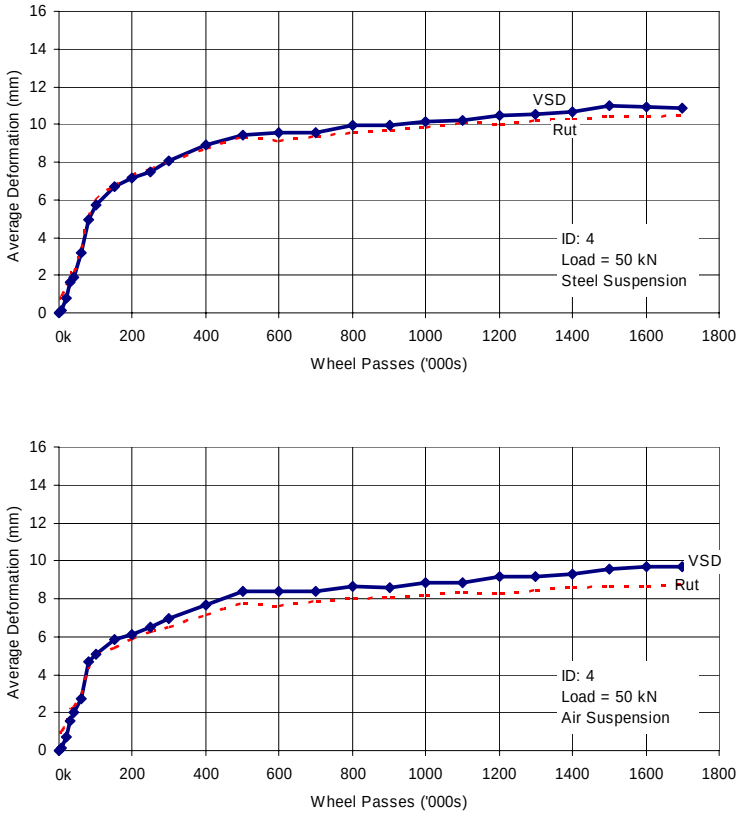

Figure 4.10 Measured maximum surface deformations of pavement section 4.

Figure 4.11 shows the estimates of the proportions of single- and dual-tyred axle load numbers.

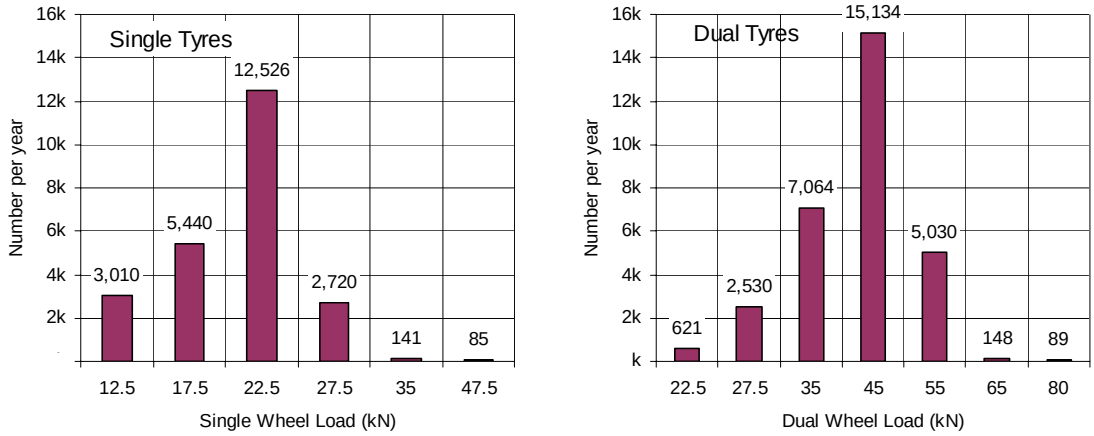

Figure 4.11 Half axle load distributions for single and dual tyres.

The most common axle groups are 22.5 kN (i.e. 20-25 kN) for the single wheel load and 45 kN (i.e. 40-50 kN) for the dual-tyre wheel load. The data were converted into equivalent standard axles (ESA) using the damage law equation (Equation 4.1) (Austroads 1992).

$$ESAs = Number\left[\frac{Axle\_load}{Std\_axle\_load}\right]^4 \qquad \text{(Equation 4.1)}$$

The annual traffic on the pavement test sections was estimated at about 88,200 ESA. Since pavement construction in November 2001 the total number of loads to the end of monitoring in August 2003 was estimated as 150,000 axles or 243,000 ESA.

4.2.4 Measured performance

The surface deformation was measured using the University of Nottingham profiler. This device was placed transversely at 2-m intervals on the field trial. Two measurements were required to cover the full lane width of the field trial. An example transverse profile with a 2-m straight-edge is shown in Figure 4.12.

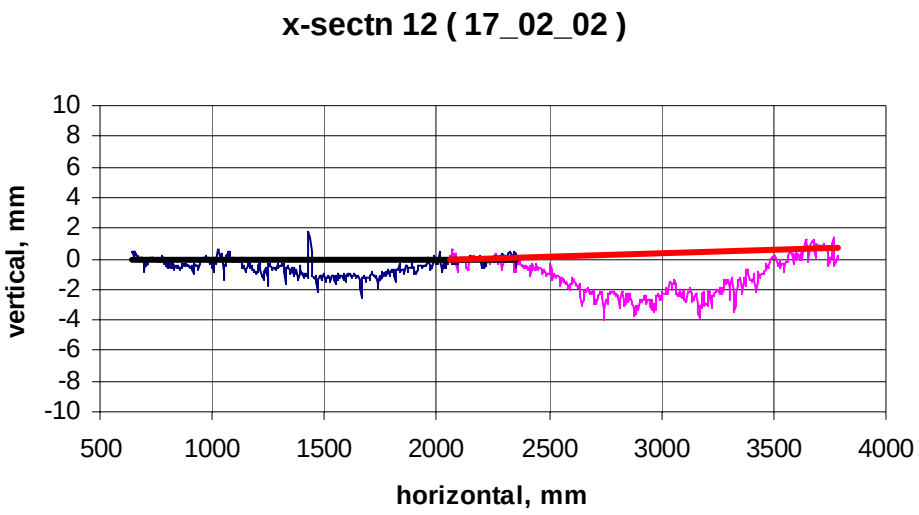

Figure 4.12 Transverse profile example with 2-m straight-edges to calculate rut depth.

Figure 4.13 shows the average rut depths for the NI good and NI poor aggregate sections. Results show that trends and magnitudes of rutting in all the cross sections were similar. The rate of rutting is low at approximately 1 mm per year (88k ESA) for both sections.

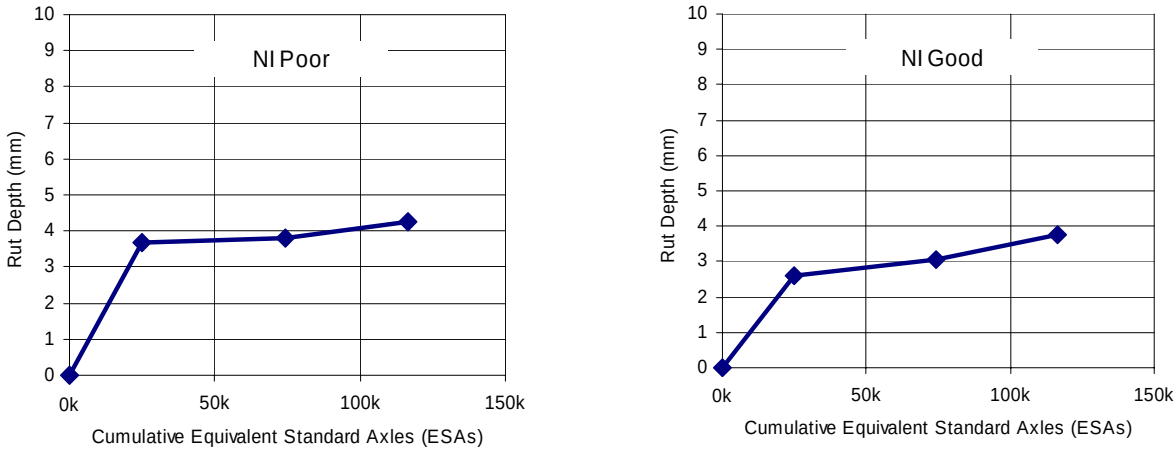

Figure 4.13 Measured rut depth of Northern Ireland in-service pavements.

5. Calibration of the Arnold (2004)rut depth model

5.1 Methodology

As discussed in Section 3.3, the following major steps were used to validate the Arnold rut depth model utilising pavement test results obtained at CAPTIF for the past 6 years and from Northern Ireland field data.

- Step 1: Conduct permanent strain testing using the Nottingham RLT test method to collect full data set of permanent strain and resilient modulus data at various pavement stresses.
- Step 2: Develop material models of resilient modulus from the full data set or FEM pavement analysis to predict pavement stress.
- Step 3: Develop material models of permanent strain from the full data set for the calculation of surface rut depth from the FEM predicted pavement stresses.
- Step 4: Validate with field performance and make adjustments to assumptions of residual stress and initial rut depth, if required.

They are briefly described below.

5.2 RLT test programme and test results

5.2.1 Test programme

A total of six unbound granular materials (UGMs) and one subgrade soil (a silty clay) were tested using the Nottingham RLT testing method (see Section 5.3). They included:

- Four UGMs (CAPTIF 1, 2, 3, and 4, Table 4.2) and the subgrade (CAPTIF subgrade) which were used in the CAPTIF trials in New Zealand.
- The other two UGMs (NI Good and NI Poor) which were used in the in-service field trials in Northern Ireland.

Details of the laboratory testing programme, including permanent strain data, are given in Arnold (2004).

5.2.2 Typical results of permanent strain

Figure 5.1 shows typical results obtained from a multi-stage RLT permanent strain test using the Arnold (2004) RLT test method as described in Section 5.3. Results of other tests are also given in Arnold (2004).

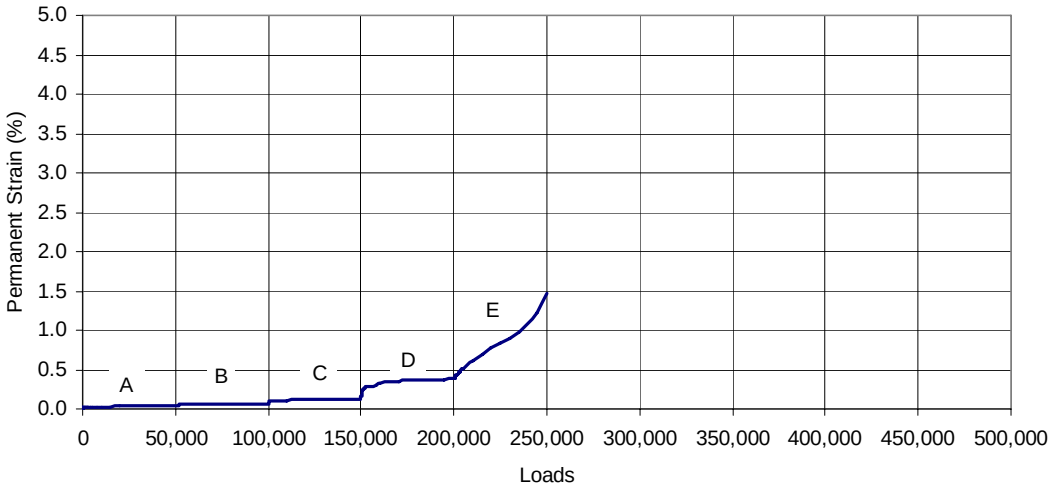

Figure 5.1 Typical RLT permanent strain result (CAPTIF 1 material, Test 1 - p=75 kPa).

5.3 Development of material models

5.3.1 Predicted models of incremental permanent strain

Figure 5.2 shows the permanent strain results for each stress stage used by Arnold to develop his model using the interpretation method as described in Section 5.4.

- For each stress stage, the incremental permanent strain for the period 0-25 k-cycles was estimated from the incremental permanent strain from each stage of a multi-stage RLT permanent strain test by ignoring the permanent strain which occurred in the previous loading stages.
- Similarly, by ignoring the cumulative loading cycles applied before the loading stage concerned, the permanent strains between 0-50 k-cycles for each stage were fitted with an equation of:

$$\varepsilon_p = A + BN^{\alpha} \qquad \text{(Equation 5.1)}$$

Results of curve fitting for permanent strain values of 0-50 k-cycles indicated that a mean error of less than 0.10% could be achieved. The fitted equation was then used to predict the incremental permanent strains for the three periods of 25-100 k-cycles, 100-1000 k-cycles, and 1000-2000 k-cycles for the stress stage concerned.

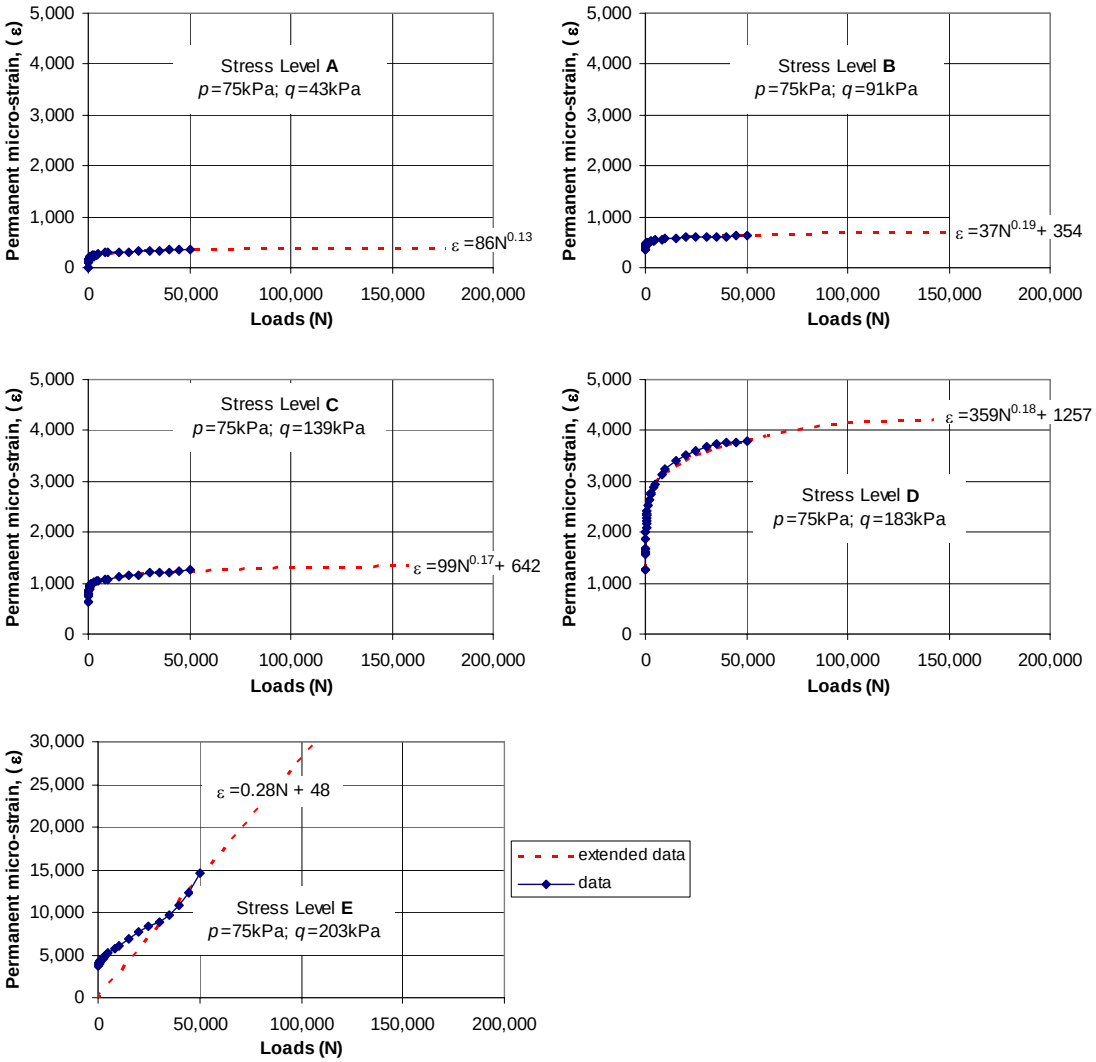

Figure 5.2 Permanent strain results for each individualised stress stage (CAPTIF 1 material Test 1 - p=75 kPa).

Figures 5.3 and 5.4 show typical results of the estimated incremental strains at 25 k-cycles and for loading periods after 25 k-cycles, which are plotted against deviator stresses (q). Parameters for Equations 3.8, 3.9 and 3.10, which are used to calculate the amount of permanent strain in the three periods of 25–50 k-cycles, 100–1000 k-cycles and 1000–2000 k-cycles, were then determined by fitting these equations with the estimated incremental strains. Results of other tests are given in Appendix 4.

The results in Figures 5.3 and 5.4 indicated that Equations 3.8, 3.9 and 3.10 could be used to fit the estimated incremental strains for the first period of 0–25 k-cycles. However, larger fitted errors may occur for other later periods after 25 k-cycles (see the results of NI Poor and NI Good in Figures 5.3 and 5.4). Large fitting errors were found at strain values greater than 1% and also at high values of mean stress (p = 0.250 MPa) and deviator stress (q>0.300 MPa).

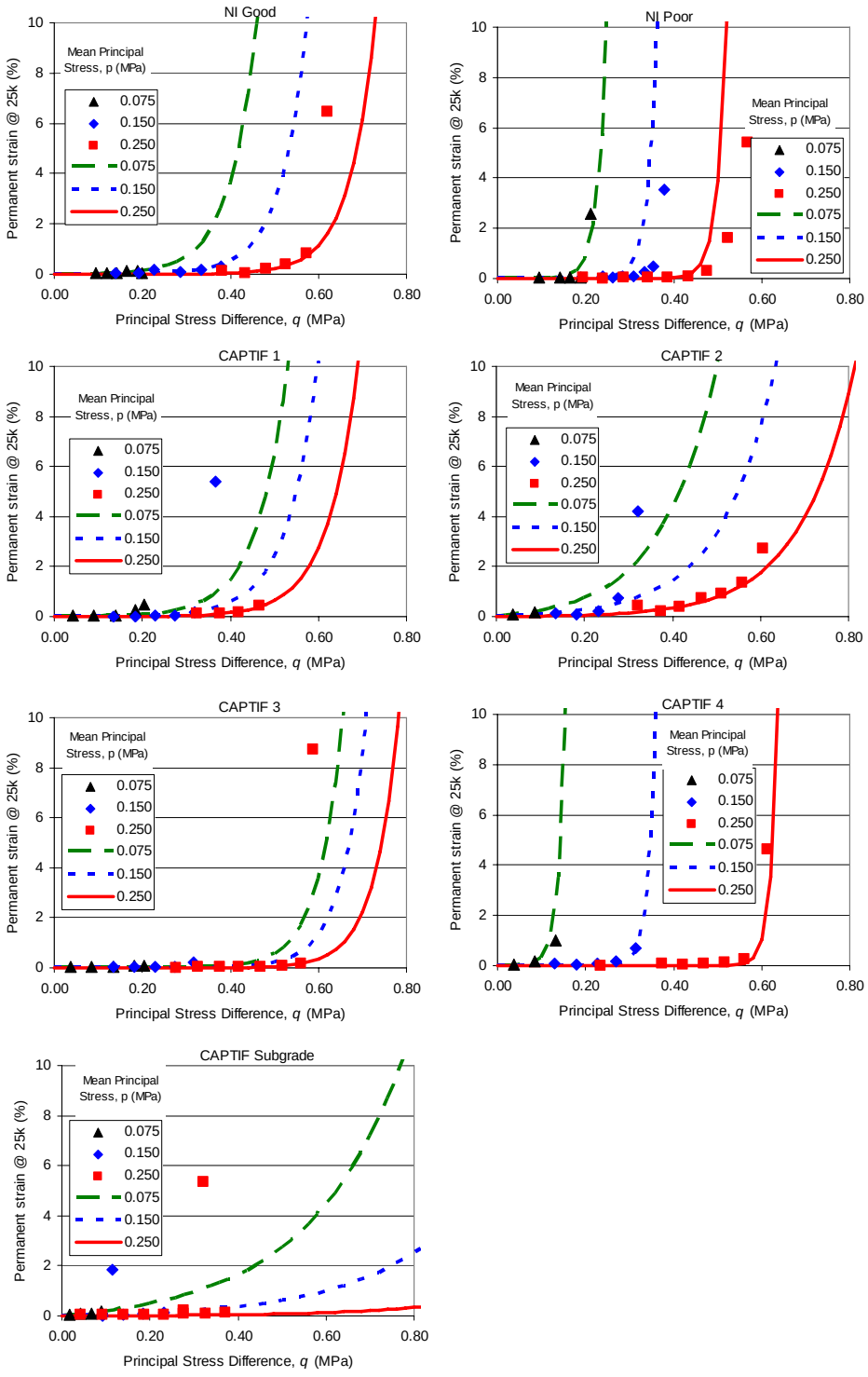

Figure 5.3 Comparison of measured permanent strains at 25 k-cycles and fitted curves using Equation 3.7.

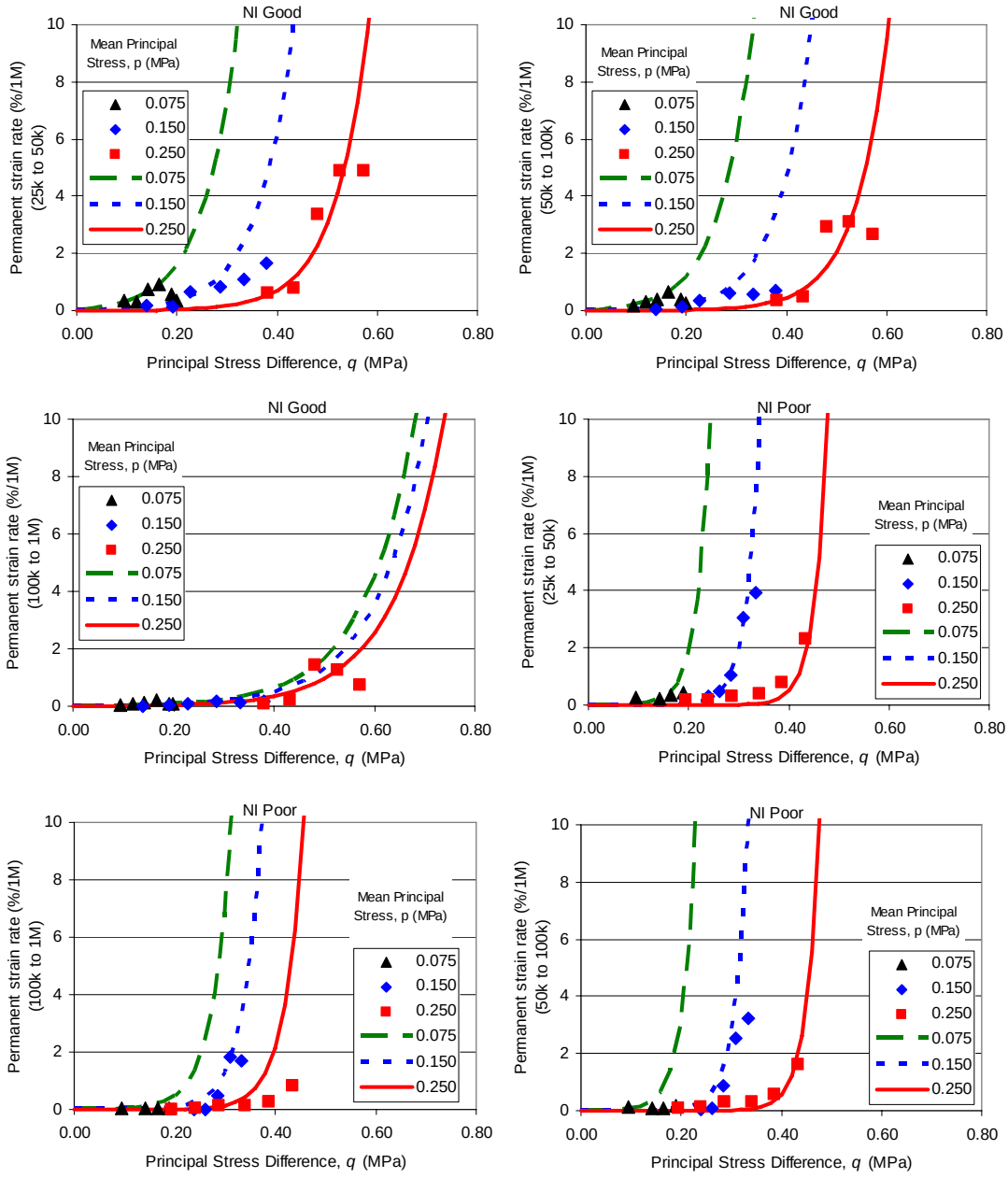

Figure 5.4 Comparison of measured incremental permanent strains for loading periods after 25 k-cycles and fitted curves using Equations 3.8, 3.9, and 3.10 for NI Good and NI Poor materials.

In summary, ignoring the cumulative permanent strain which occurred before the loading stage in a multi-stage test would result in errors in the predicted permanent strains. The expectation was that the incremental permanent strain values for stress stages after the first stage in a multi-stage test would be under-estimated as the sample has already received some additional compaction from the previous tests. The use of Equations 3.8, 3.9, and 3.10 also resulted in some fitting errors. However, the above effects of errors in the predicted incremental permanent strains on the predicted rut depth are not known at this stage.

5.3.2 Predicted model of resilient modulus

Figure 5.5 shows the results of resilient modulus for CAPTIF 1 material, which were fitted with the k-θ model (Equation 3.5). Results of other tests are given in Appendix 4.

Referring to Figure 5.5 and Appendix 4, the fitted R^2 values produced by the fitted curves are in the range of 0.03–0.96, indicating that the $k-\theta$ model may not be best suited to describe resilient modulus for various material types (including granular materials and subgrade). Errors in modulus could be up to ±40%. As discussed previously, the rut depth model utilises predicted pavement stress values, which in turn depend on the layer moduli. The effect of errors in modulus values on the predicted pavement stresses and hence layer deformation are not known at this stage.

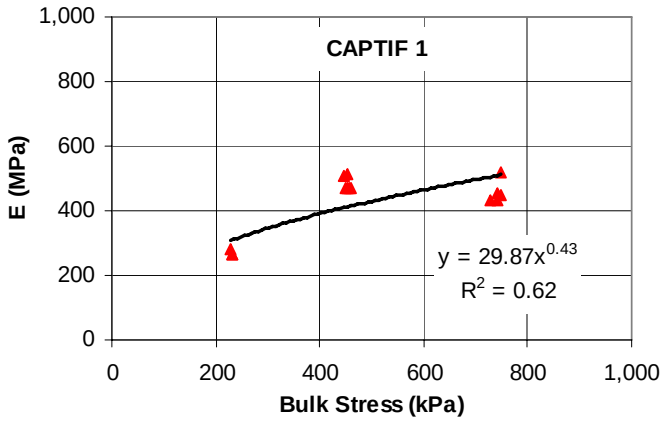

Figure 5.5 Example of elastic modulus versus bulk stress.

5.4 Predicted pavement stresses from FEM pavement analysis

Table 5.1 shows typical results of mean principal stresses, p, and deviator stresses, q, under the centre of the load at depth increments of 25 mm computed using DEFPAV for all loading and cross section combinations. Results of FEM predicted stresses in other pavement test sections are given in Appendix 4. It was assumed in this analysis that the residual horizontal stress from compaction is nil.

Table 5.1 Typical results of predicted stresses in Pavement 1a at various depth increments under a single wheel load calculated with DEFPAV.

Pavement ID and Load	Stress Parameter	Stress at various depth below surface (kPa)							
		Depth within granular base (mm)				Depth within subgrade (mm)			
		25	***59***	***106***	***184***	***300***	***483***	***1102***	***2569***
1: 40kN	***p***	445.6	170.5	62.1	4.6	26.1	0.7	−2.5	0.2
	q	723.2	535.7	322.9	152.4	61.2	11.4	−0.7	0.2
1: 50kN	***p***	471.1	181.5	75.2	7.3	34.3	1.6	−3.3	0.2
	q	715.0	540.8	349.8	183.5	79.9	15.2	−0.9	0.2
1a: 60kN	***p***	476.8	195.7	90.1	12.0	40.3	3.2	−4.1	0.2
	q	676.5	533.9	374.7	214.3	98.5	19.3	−1.2	0.2

5.5 Predicted incremental rut depths

5.5.1 Uncalibrated prediction

The surface rut depths were calculated using the uncalibrated rut depth model (using zero residual stress and no correction of initial rut depth after 25 k-cycles) as follows.

For each pavement section, incremental surface rut depths for various loading periods (being 0-25k, 25-50k, 50-100k, 100k-1M, 1-1.4M and 1.4-1.7M) were calculated using Equations 3.11, 3.12, 3.13 and 3.14 (see Section 3.3.3) and the total surface rut depths were calculated as the sum of the calculated incremental surface rut depths (see Equation 3.15).

Figures 5.6 to 5.11 compare the predicted rut depth (labelled as calculated–original) and measured rut depths for various pavement sections. The results indicated substantial differences between the predicted and measured rut depths for all pavement test sections:

- Referring to Figure 5.6 (p.49), for pavement sections 1, 1a, and 1b (with CAPTIF 1 base material), the predicted total rut depths were generally higher than the measured rut depths, being about 50–100% higher for all 40 kN loading tests, 5% lower for the 50 kN loading test, and 0–30% higher for 60 kN loading tests.
- Referring to Figure 5.7 (p.50), for pavement section 2 (with CAPTIF 2 base material), the predicted total rut depths were much higher than the measured rut depth for all 40 kN and 50 kN loading tests.
- Referring to Figure 5.8 (p.51), for pavement sections 3, 3a, and 3b (with CAPTIF 3 base material), the predicted total rut depths were generally lower than the measured rut depths, being about 20–40% lower than the measured rut depth for all 40 kN loading tests, 10% lower for the 50 kN loading test, and 30-50% lower for the 60 kN loading tests.
- Referring to Figure 5.9 (p.52), for pavement section 4 (with CAPTIF 3 base material), the predicted total rut depth was about 20–40% lower than the measured rut depth for the 50 kN loading tests.
- Referring to Figure 5.10 (p.52), for pavement section 5 (with NI Good base material), the predicted total rut depth was about 85% lower than the measured rut depth for the 50 kN loading tests.
- Referring to Figure 5.11 (p.53), for pavement sections 5 (with NI Good base material), the predicted total rut depth was about 85% lower than the measured rut depth for the 50 kN loading tests.

Referring to Figures 5.6 to 5.11, the following six pavement test sections produced similar slope after 100 k-cycles between the predicted and measured rut depth curves: 1:50 kN, 1:60 kN, 1b:60 kN, 3:40 kN, 3:50 kN and 6:45 kN. Five other pavement test sections produced similar slopes after 500 k-cycles between the predicted and measured rut depth curves: 3a:40 kN, 3a:60 kN, 3b:40 kN, 3b:60 kN and 4:50 kN.

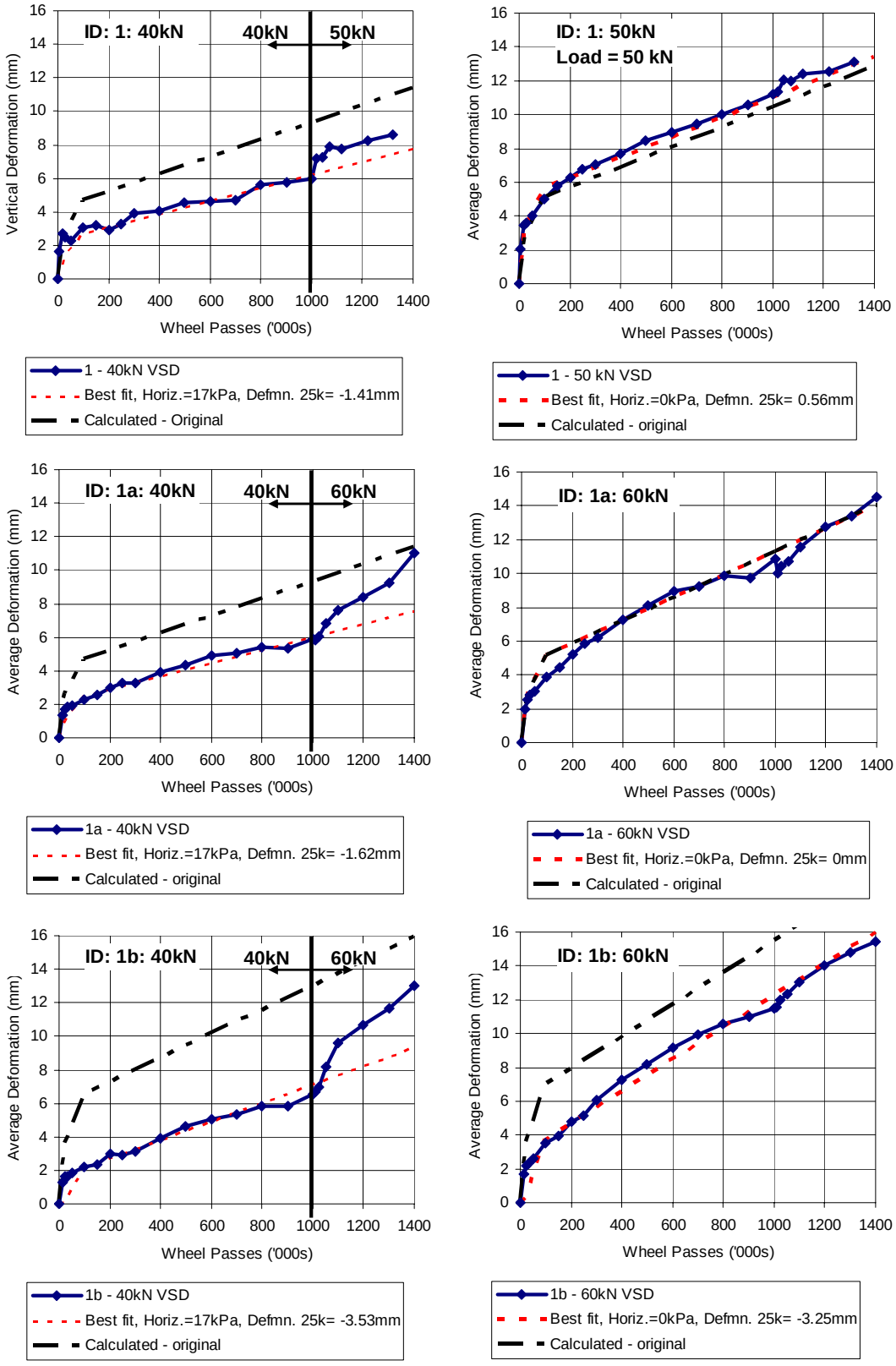

Figure 5.6 Predicted compared with measured rut depth for pavement test sections 1, 1a, and 1b (Arnold 2004).

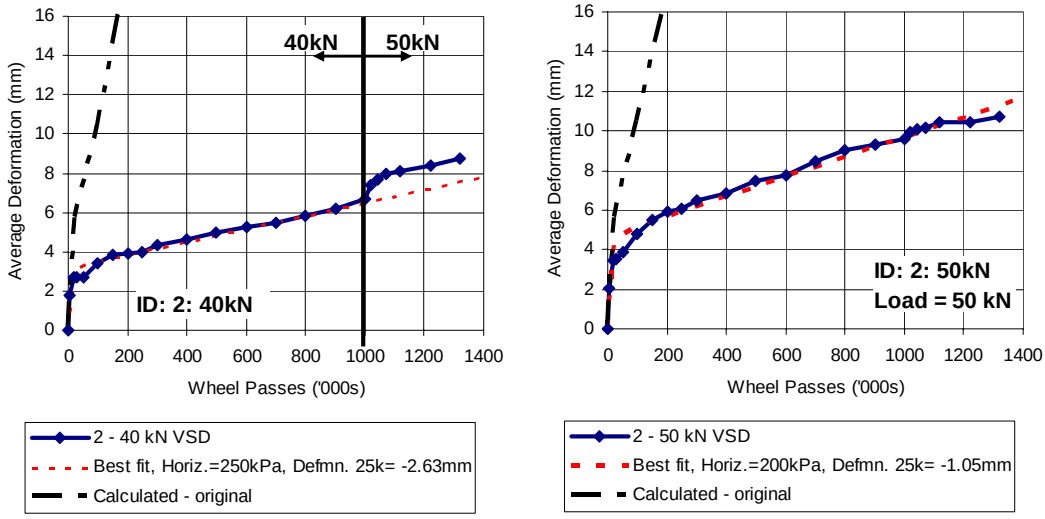

Figure 5.7 Predicted compared with measured rut depth for pavement test section 2 (Arnold 2004).

Table 5.2 Adjustments required to obtain best fit of calculated to measured rut depth.

Pavement Test Section ID	Asphalt / GR base thickness (mm)	Adjustments to obtain best fit to measured rut depth.		
		Rut depth added @ 25k (mm)	Horizontal residual stress (kPa)	Figure
1: 40kN	25/275	***–1.4***	***17***	5.6
1: 50kN		0.6	0	
1a: 40kN		***–1.6***	***17***	
1a: 60kN		0.0	0	
1b: 40kN	25/200	***–3.5***	***17***	
1b: 60kN		–3.3	0	
2: 40kN	25/275	***–2.6***	***250***	5.7
2: 50kN		***–1.1***	***200***	
3: 40kN		1.1	0	5.8
3: 50kN		0.9	0	
3a: 40kN		2.2	0	
3a: 60kN		4.3	0	
3b: 40kN	25/200	1.3	0	
3b: 60kN		5.9	0	
4: 50kN	90/200	***6.3***	***50***	5.9
5: 45kN	100/700*	1.9	0	5.10
6: 45kN	100/700*	0.9	0	5.11

* average values

Bold values are for experiments that required adjustments of both rut depths at 25 k-cycles and horizontal residual stress

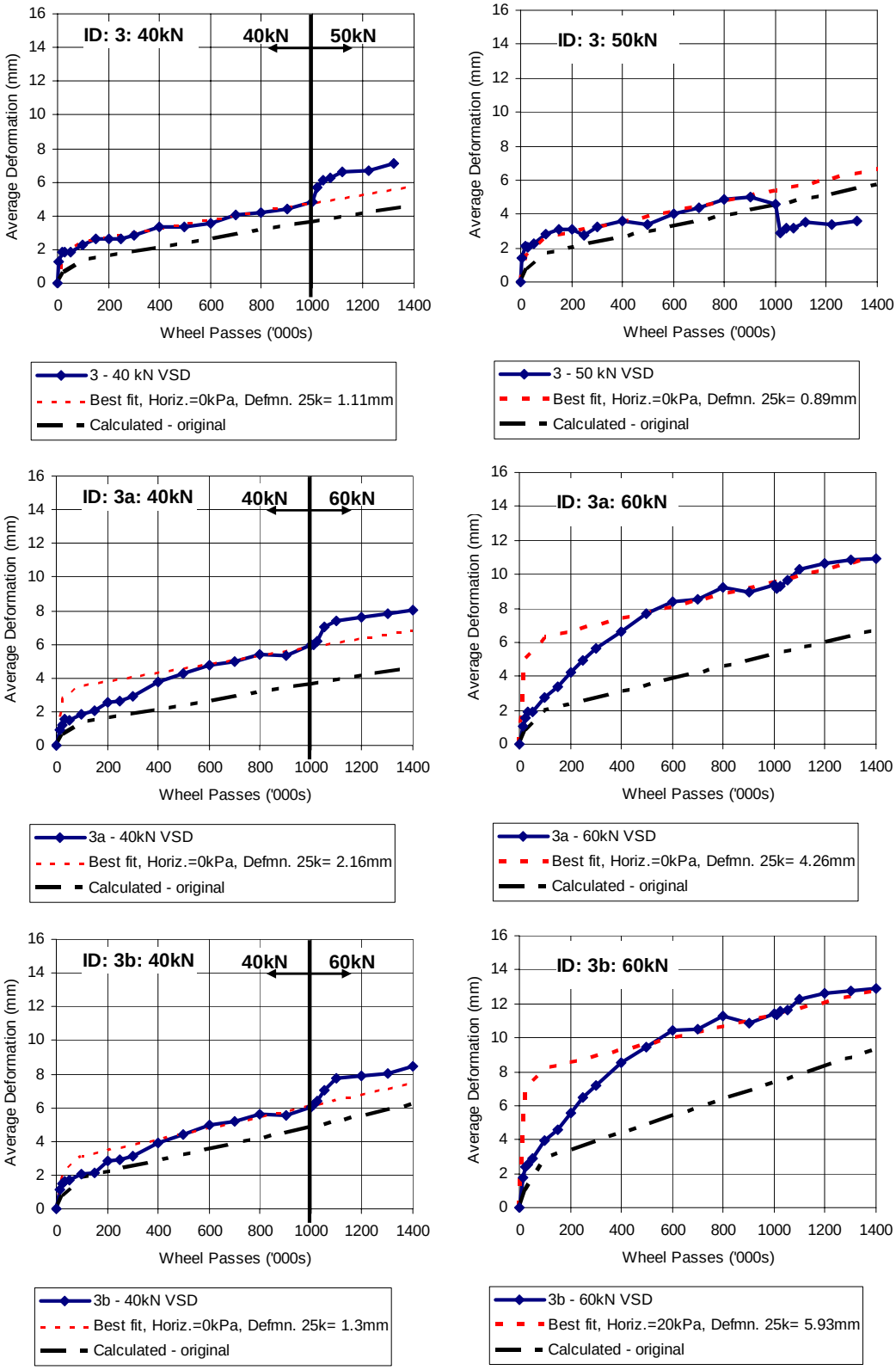

Figure 5.8 Predicted compared with measured rut depth for pavement test sections 3, 3a, and 3b (Arnold 2004).

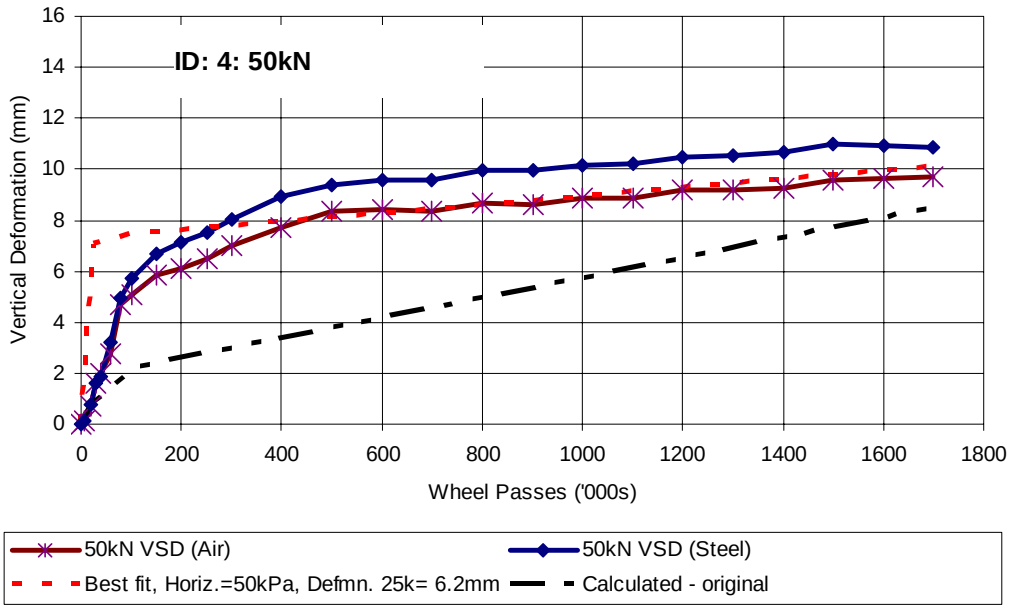

Figure 5.9 Predicted compared with measured rut depth for pavement test section 4 (Arnold 2004).

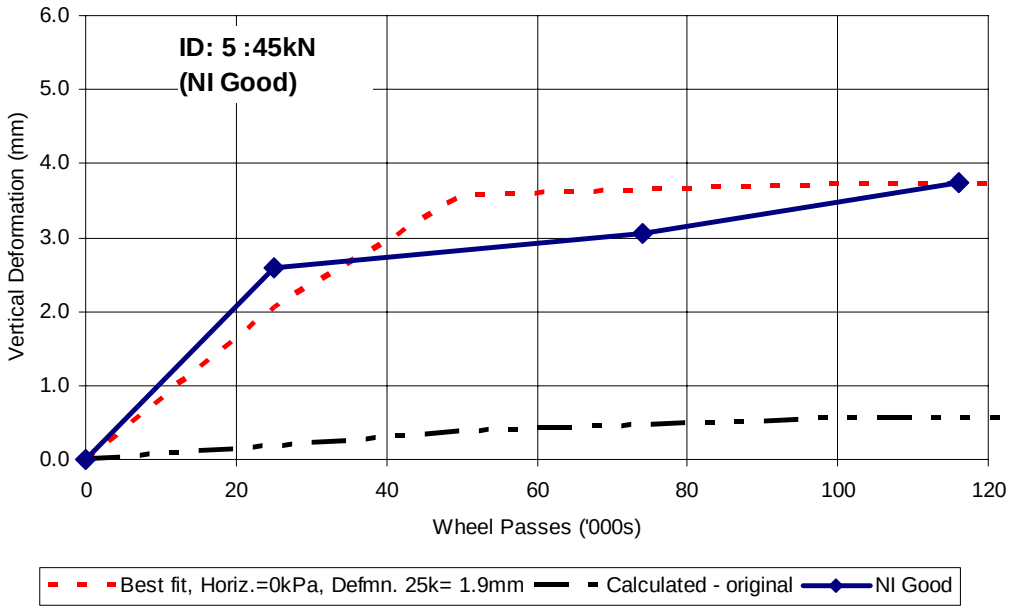

Figure 5.10 Predicted compared with measured rut depth for pavement test section 5 (NI Good material) (Arnold 2004).

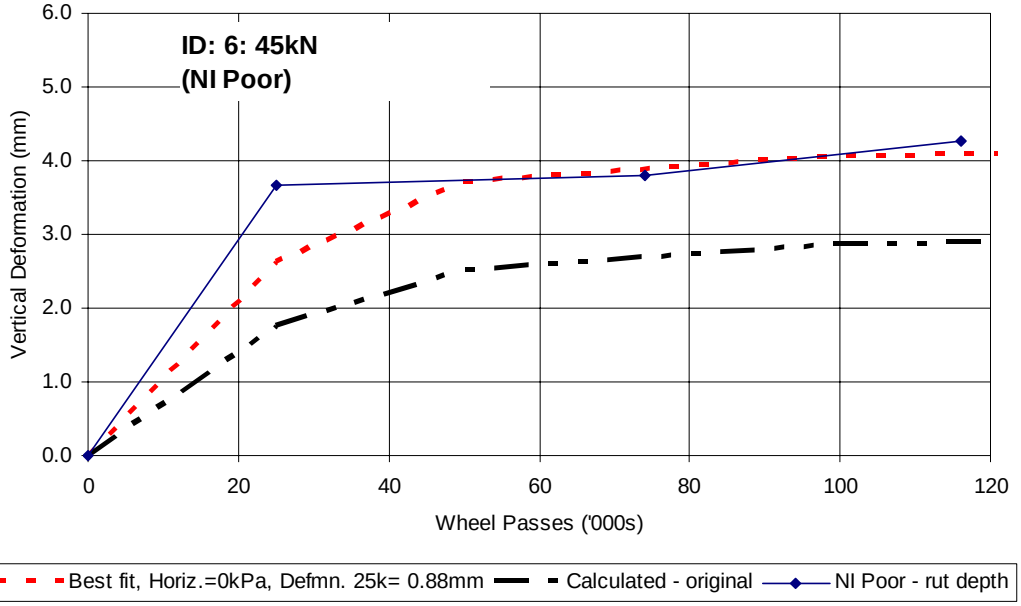

Figure 5.11 Predicted compared with measured rut depth for pavement test section 6 (NI Poor material) (Arnold 2004).

5.5.2 Required adjustments (from comparison with measured rut depth)

As discussed in Section 3.3, adjustments of predicted surface deformation, if they are found to be different from the field results, can be made in terms of:

- The differences between measured and predicted rut depth for rut depth at 25 k-cycles. This is because the differences may be caused by different conditions of laboratory sample preparation and field compaction, and inaccuracy of estimated value of incremental permanent strain after the first 25 k (as the permanent strain that occurred in the previous loading stages was ignored).
- The magnitude of residual stress added to the predicted pavement stresses for predicting rut depth increments at greater than 25 k-cycles. This parameter was found to significantly influence the predicted rut depth. In this case, an iterative process is required to determine the initial rut depth adjustment and the amount of horizontal residual stress to add in order that the calculated surface rut depth matches the measured values.

Values of the adjusted rut depths at 25 k-cycles and horizontal residual stress in order to obtain a near perfect match between predicted and measured rut depth are given in Table 5.2. Figures 5.6 to 5.11 also show the predicted rut depth curves after the adjustments (labelled as best fit) for the comparison with measured rut depths.

Referring to Table 5.2, out of 17 pavement sections studied:

- Only one pavement section: 1a: 60 kN did not require any adjustment.
- Eleven pavement sections required adjustments of rut depth at 25 k-cycles. Generally, the predicted rut depth at 25 k for these pavement sections required an additional value in the range between 0 mm and +6 mm to obtain an accurate

prediction of rut depth, with the exception of pavement section 1b:60kN that required an adjusted value of −3.3 mm.

- Another five sections required adjustments of both rut depth at 25 k-cycles and magnitude of horizontal stress. For these pavements, the adjustments of rut depth at 25 k-cycles varied from −3.5 mm to 6.3 mm, while the adjustments of horizontal stress varied in the range of 17-250 kPa.

Note that, for pavement test section 4, although deformation was measured with air and steel suspension (see Figure 5.9), adjustments were made based on results measured with air suspension.

5.6 Summary

As discussed in Chapter 3, numerous assumptions are applied in the Arnold rut depth model (Arnold 2004) which are associated with the use of:

- a simple 1-D RLT test with repeated deviator stress and constant confining stress,
- a simple method to estimate incremental permanent strains for various stresses from multi-stage permanent strain test results,
- a simple material model of resilient modulus for pavement analysis,
- simplification of load configurations and FEM techniques adopted in pavement analysis,
- a simple calculation method for rut depth.

These assumptions could significantly affect the magnitude of measured laboratory permanent strains and calculated pavement stresses and, hence, the predicted rut depth. Because of these potential errors, the original Arnold (2004) rut depth model could not accurately predict permanent deformations for 17 field pavements included in this study (including 15 different pavements tested with New Zealand Accelerated Pavement Tests and 2 in-service pavements in Northern Ireland).

Therefore, in the current form of the rut depth model, it was necessary to adjust the predicted rut depth to achieve a closer prediction to field performance. It was found that 10 pavements out of 17 pavements studied only needed adjustments of rut depth predicted at 25 k wheel passes (up to 6 mm); whereas other 6 pavements needed adjustments of both rut depth at 25 k-cycles (in the range from −3.5 mm to 6.0 mm) and additional horizontal stress (in the range of 17–250 kPa). Given that the adjustments of were not constant, but varied in large ranges, it was difficult to apply consistent adjustments for all pavement cases.

However, the trends were similar in rut depth progression (i.e. slope after 500 k-cycles) between the predicted (before adjustment) and measured rut depth curves for some 11 pavements out of 17 pavements studied (see Figures 5.6 to 5.11). Therefore, the Arnold (2004) rut depth model, in its current form, may be used only to predict the long-term trend in rut depth progression, rather than absolute deformations.

ARRB has also developed a general pavement deformation prediction model (Vuong 2005) for an Austroads research project using a similar approach. However, the ARRB general pavement deformation prediction model used a more comprehensive 2-dimensional FEM model VMOD-PAVE, and a 3-dimensional FEM model Strand7 that had improved non-linear material models to take into account the effects of residual horizontal stress from compaction, mean stress and shear stress, and stress limits for failure and no-tension. It is likely that these latter FEM models produce fewer errors in the predicted stresses than those predicted with DEFPAV, which used a simple K-θ model (dependent on total stress) for granular and subgrade modulus. This will be discussed further in Chapter 8.

6. Validation of Austroads/ARRB assessment methods

6.1 Methodology

The following major steps were used to validate the ARRB assessment methods (see Section 3.2) using pavement test results at CAPTIF (see Section 4.1).

- Step 1: Select field pavement tests from available CAPTIF trials (see Chapter 4) that had similar base thickness and subgrade type, to obtain field performance data for ranking of base performance.
- Step 2: Conduct RLT permanent strain testing on materials obtained from the CAPTIF pavement test sections (at field densities and moisture contents) using the Austroads multistage permanent strain testing method (see Appendix 2).
- Step 3: Determine relationship of permanent strain v loading cycle for each stress level used in the multistage testing (see Appendix 2, Section A2.8).
- Step 4: Rank the materials using laboratory performance criteria as specified by the ARRB simple assessment methods (see Section 3.2) and compare with the rankings based on field performance.

The results of each step are described below.

6.2 Material ranking based on field performance

6.2.1 Selected field pavement tests

In this study, the CAPTIF trials conducted in 2001 and 2003 on 7 pavement test sections: 1, 1a, 1b, 3, 3a, 3b, and 2 (see Table 6.1) were selected for the validation of the ARRB simple performance model. Pavement tests 1b and 3a had the same base thickness of 200 mm, whereas others (1, 1a, 3, 3b, and 2) had the same base thickness of 275 mm. They also had a similar subgrade type and were trafficked with over 1M cycles of a 40 kN dual-tyred half axle (equivalent to a full standard axle of 80 kN). Therefore, they are suitable for ranking the material based on field performance. Details of the base thickness, material type and performance data (surface permanent deformation) measured for each CAPTIF experiment with the 40 kN dual-tyred half axle are given in Table 6.1.

Table 6.1 Measured surface deformation under CAPTIF 40 kN half axle load.

ID	Base Material	Base Thickness (mm)	Maximum surface deformation at specified loading cycles (mm)								
			25k	50k	100k	150k	200k	300k	500k	700k	1000k
1b	CAPTIF 1	200	1.6	1.8	2.2	2.4	3.0	3.1	4.6	5.3	6.5
3b	CAPTIF 3	200	1.5	1.7	2.0	2.2	2.8	3.1	4.4	5.2	6.0
1	CAPTIF 1	275	2.6	2.3	3.1	2.6	2.9	3.9	4.5	4.7	6.0
1a		275	1.7	1.9	2.3	2.6	3.0	3.3	4.4	5.0	5.9
3	CAPTIF 3	275	1.8	1.8	2.3	1.8	2.6	2.8	3.3	4.0	4.8
3a		275	1.2	1.5	1.8	2.1	2.5	2.9	4.3	5.0	6.0
2	CAPTIF 2	275					4.0		5.0		6.5

6.2.2 Base performance ranking

6.2.2.1 Ranking based on total deformation

As discussed in Chapter 5, for all pavements with CAPTIF 1, CAPTIF 2 and CAPTIF 3 bases, surface deformation (rutting) resulted from gradual deformations within the seal, base layer and subgrade. There was no indication of shallow shear failure (shoving and heaving). Table 6.2 compares the total deformations produced by the pavement sections after 1M cycles of axle loads of 40 kN. Total deformations produced by the pavement sections after 1M cycles of axle loads of 50 kN and 60 kN are also given in Table 6.2 for comparison.

- For pavements having the same base thickness of 200 mm, all pavements with different base materials (namely CAPTIF 1 and CAPTIF 3) produced similar total deformations at 1M cycles of axle loads of 40 kN and 60 kN.
- For pavements having the same base thickness of 275 mm, all pavements with different base materials (CAPTIF 1, CAPTIF 2 and CAPTIF 3) also produced similar total deformations at 1M cycles of axle loads of 40 kN. However, pavements with CAPTIF 3 produced a slightly lower total deformation at 1M cycles of axle loads of 50 kN and 60 kN than CAPTIF 1.

Table 6.2 Material ranking based on observed field deformation at 1M cycles.

Pavement	Thickness (mm)	Material	Observed deformation at 1M cycles (mm)			Overall Ranking
			40 kN	50 kN	60 kN	
1b	200	CAPTIF 1	6.5		11.5	2
3b		CAPTIF 3	6.0		11.5	1
1 and 1a	275	CAPTIF 1	6.0	11.0	11.0	3
3 and 3a		CAPTIF 3	5.0–6.0	5.0	9.5	1
2		CAPTIF 2	6.5	9.5	–	2

Therefore, the conclusion is that all pavements produced similar performance under the axle loads of 40 kN. However, CAPTIF 3 may have a slightly better performance than CAPTIF 1 under higher axle loads of 50 kN and 60 kN, whereas CAPTIF 2 may have a

slightly better performance than CAPTIF 1 under the axle load of 50 kN. For the purpose of field performance ranking for the assessment of Austroads/ARRB assessment methods, CAPTIF 3 was ranked higher than CAPTIF 2 and CAPTIF 1.

6.2.2.2 Ranking based on deformation life

Results of surface deformation measured for each CAPTIF experiment with 40 kN dual-tyred half axle are also plotted against loading cycles in Figure 6.1. It was estimated, by extrapolation using a linear rate, that the pavements would have deformation lives (number of cycles to reach a total surface deformation of 20 mm) in the range of 5.2–5.9 M loading cycles of 40 kN dual tyred half axle (or 5.2–5.9 x 10^6 ESA). Based on the results in Figure 6.1, the ranking in order of highest deformation life would be CAPTIF 3, CAPTIF 1 and CAPTIF 2.

6.3 Laboratory testing programme and test results

6.3.1 RLT permanent strain testing programme

Two RLT test series were conducted using the Austroads RLT test methods by ARRB and the Transportation Laboratory at the University of Canterbury.

For the tests conducted at ARRB, the standard triaxial testing equipment was used to test standard specimens (100 mm diameter and 200 mm high) for materials of 20 mm nominal grain size, and the dynamic compaction method was used to prepare the specimen. In this case, two base materials: CAPTIF 1 (with particles of grain size >20 mm being replaced by particles of grain size 20 mm), and CAPTIF 3, were tested.

For the tests conducted at the Transportation Laboratory at the University of Canterbury, the larger triaxial testing equipment was used to test large specimens (150 mm diameter and 300 mm high) for materials of 40 mm nominal grain size, and the vibratory compaction method was used to prepare the specimen. In this case, two base materials: (CAPTIF 1 and CAPTIF 2), were tested. Details of the equipment and test results are given in Steven (2005).

Different compaction methods produced significantly different permanent strain results (Vuong 1998) and comparing the permanent strain results produced between the two compaction methods was difficult. Therefore, in this study, comparison of laboratory RLT permanent strain for material ranking was made for materials tested by each laboratory.

Table 6.3 summarises the results of laboratory dry density and moisture contents of the base materials (CAPTIF 1, CAPTIF 2 and CAPTIF 3) tested by ARRB and University of Canterbury. The results of field dry density and moisture contents of the base materials (Alabaster et al. 2002) are also included in Table 6.3 for comparison.

- The RLT specimen of CAPTIF 1 tested by ARRB had a similar moisture content to the field moisture content, but a slightly higher dry density than field density.
- The RLT specimen of CAPTIF 3 tested by ARRB had a similar dry density to the field density, but a higher moisture content than the field moisture content.

- The RLT specimen of CAPTIF 1 tested by University of Canterbury had a slightly lower dry density than field density and a lower moisture content than the field moisture content.
- The RLT specimen of CAPTIF 2 tested by University of Canterbury had a slightly lower dry density and slightly higher moisture content than field values.

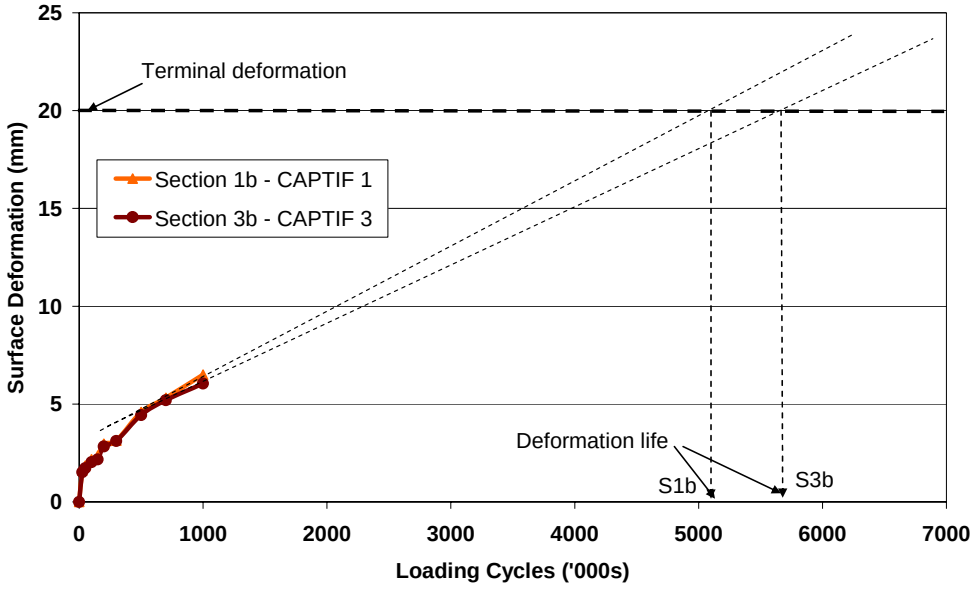

(a) Pavements having 200 mm granular bases.

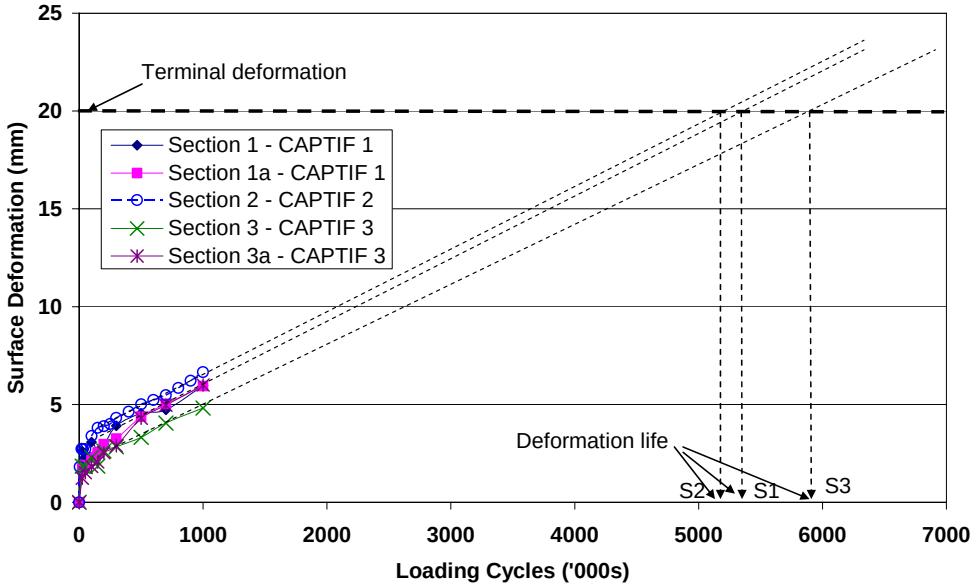

(b) Pavements having 275 mm granular bases.

Figure 6.1 Measured pavement deformation lives under a 40 kN axle load on dual tyres.

Table 6.3 Densities and moisture contents of RLT specimens tested by standard equipment.

Material	Max. grain size (mm)	Sample size	Compaction method	Sample No.	Lab. Dry Density (t/m^3)	Lab. Moisture Content (%)	Field Dry Density (t/m^3)	Field Moisture Content (%)
CAPTIF 1	20	Small*	Dynamic (ARRB)	NZ9726	2.172	2.7	2.163	2.7
CAPTIF 3				MO39546	2.168	4.6	2.166	3.9
CAPTIF 1	40	Large**	Vibratory (U of C)	CANT1	2.070	1.8	2.163	2.7
CAPTIF 2				CANT2	2.158	2.7	2.220	2.6

* 100 mm diameter and 200 mm high
** 150 mm diameter and 300 mm high

6.4 Test results

Figure 6.2 shows typical results of permanent strain obtained form a 3-stage permanent strain testing using the Austroads RLT test method. Results of other tests are given in Appendix 5.

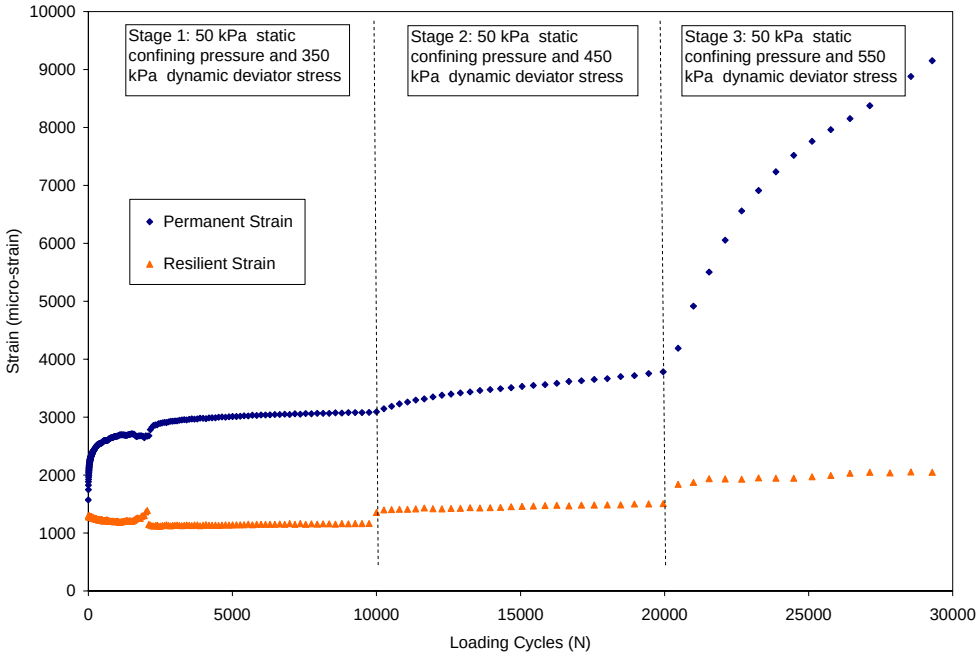

Figure 6.2 Permanent strain results for CAPTIF 1 (Sample No. CANT-1).

6.5 Relationships of permanent strain v loading cycle

The relationship between permanent strain and loading cycle for each stress stage can be expressed using a simple power law as given in Equation 6.1.

$$\varepsilon_p = [\mu.\varepsilon_r/\alpha].\ N^{\alpha} \qquad \text{(Equation 6.1)}$$

where:

ε_r = resilient strain for the stress level applied

α, μ = material constants

The procedures for back-calculation of permanent strain data as described in Section A2.8, Appendix 2 was used to determine the values of parameters α and μ for each stress stage in the multi-stage permanent strain test.

Figures 6.3 and 6.4 show typical results of curve fitting. Results of other tests are given in Appendix 5. The results in Figure 6.3 indicated that the curves produced by the procedure fitted closely with the test data, whereas the results in Figure 6.4 indicated that the trend for each parameter with increasing repeated deviator stresses, as applied in the three stress stages, was very consistent between stress stages. Therefore, the permanent strain models can be used to accurately predict either permanent strains at any loading cycles or number of cycles to failure strain for a specified loading stress.

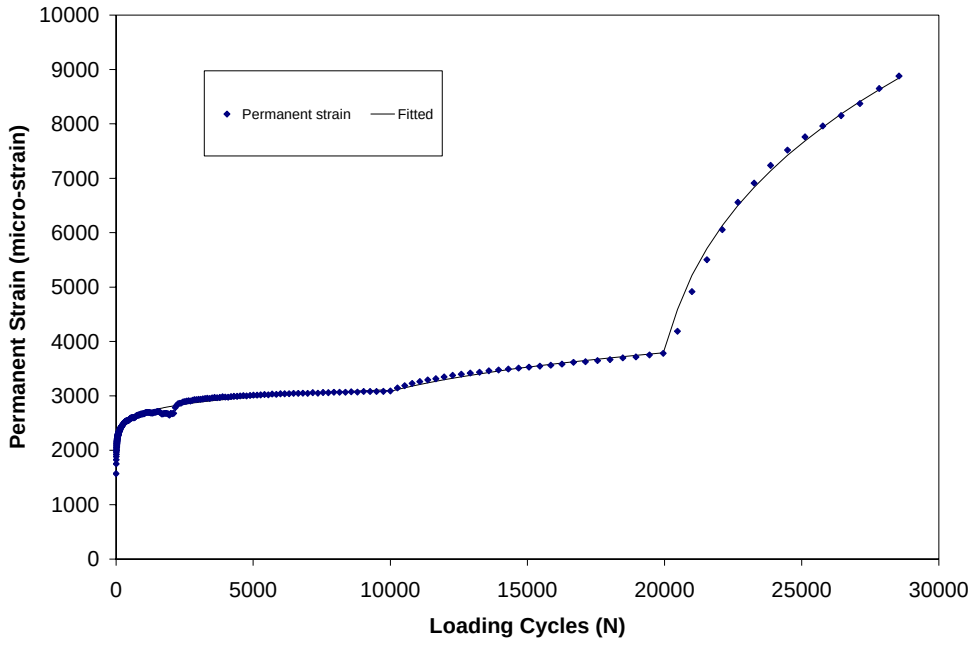

Figure 6.3 Results of fitted permanent strain results for CAPTIF 1 (Sample No. CANT-1).

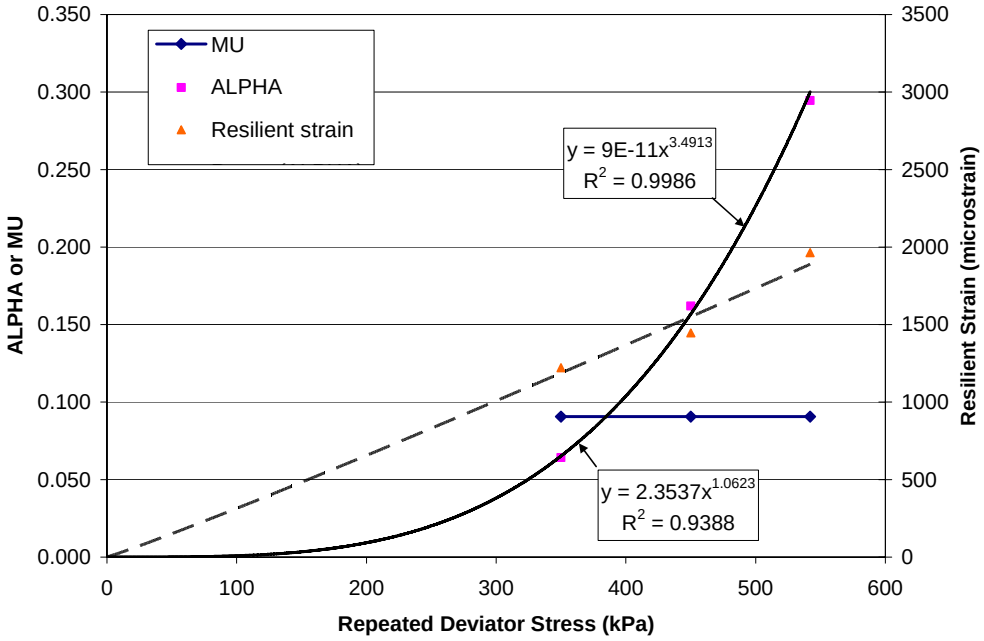

Figure 6.4 Results of parameters of Equation 6.1 for CAPTIF 1 (Sample No. CANT-1).

Tables 6.4 and 6.5 summarise values of parameters α, μ and ε_r for all specimens tested by ARRB and the University of Canterbury.

Table 6.4 Parameters of permanent strain model for all RLT specimens tested by ARRB.

Test No.	Confining Stress (kPa)	Deviator stress (kPa)	Mean stress (kPa)	Shear Stress (kPa)	α	ε_r	μ
NZ9726	50	350	167	165	0.167	1325	0.197
	50	450	200	212	0.252	1686	0.197
	50	550	233	259	0.317	2222	0.197
MO39546	50	350	167	165	0.117	1559	0.216
	50	450	200	212	0.209	1863	0.216
	50	550	233	259	0.301	2438	0.216

Table 6.5 Parameters of permanent strain model for all RLT specimens tested by the University of Canterbury.

Test No.	Confining Stress (kPa)	Deviator stress (kPa)	Mean stress (kPa)	Shear Stress (kPa)	α	ε_r	μ
CAN-1	54	350	171	165	0.064	1221	0.091
	55	450	205	212	0.162	1447	0.091
	54	542	235	255	0.295	1964	0.091
CAN-2	52	350	169	165	0.034	1329	0.057
	52	446	201	210	0.217	1567	0.057
	52	542	232	255	0.264	1950	0.057
CAN-3	52	350	169	165	0.173	1324	0.028
	52	446	201	210	0.330	1727	0.028
	51	542	232	256	0.500	2292	0.028

6.6 Method 1: Performance assessment based on material behaviour

As discussed in Section 3.2.1, material behaviour observed in the 3-stage permanent strain testing can be used to rank the material performance.

Based on the detailed results of the permanent strain for each loading stage as given in Appendix 5, the incremental permanent strain and behaviour for each loading stage of the materials tested by ARRB and the University of Canterbury were derived and summarised in Tables 6.6 and 6.7, respectively. Ranking of the material performance, in terms of most stable behaviour or lowest incremental permanent strain for the design stress in Stage 2 are also given in Tables 6.6 and 6.7.

- From Table 6.6, the two materials CAPTIF 1 and CAPTIF 3 produced similar behaviour, but the CAPTIF 3 produced a slightly lower incremental permanent strain in Stage 2 and, therefore, was ranked higher than CAPTIF 1. This is consistent with the ranking based on field performance (see Table 6.2).
- From Table 6.7, the two materials CAPTIF 1 and CAPTIF 2 produced similar behaviour, but the CAPTIF 2 produced a slightly lower incremental permanent strain in Stage 2, and therefore was ranked higher than CAPTIF 1. This is consistent with the ranking based on field performance (see Table 6.2).

Table 6.6 Comparison of material behaviour based on RLT test results produced by ARRB.

Pavement	Observed Behaviour (kPa)			Incremental Permanent Strain (kPa)			Ranking
	350	450	550	350	450	550	
CAPTIF 1-9726	Stable	Stable	Failure	7210	6154	Failed	2
CAPTIF 3-9546	Stable	Stable	Failure	8312	5100	Failed	1

Table 6.7 Comparison of material behaviour based on RLT test results produced by the University of Canterbury.

Pavement	Observed Behaviour(kPa)			Incremental Permanent Strain (kPa)			Ranking
	350	450	550	350	450	550	
CAPTIF 1-CAN1	Stable	Stable	Unstable	3083	698	5369	2
CAPTIF 2-CAN2	Stable	Stable	Unstable	3017	450	1417	1

Tables 6.8 and 6.9 summarise the results of pass or fail for the materials for different pavement classes subjected to light traffic ($<10^6$ ESA), medium traffic ($<10^6$–10^7 ESA) and heavy traffic ($>10^7$ ESA) using the behaviour limits as given in Table 3.1 (see Section 3.2).

- The results in Table 6.8 indicated that both materials CAPTIF 1 and CAPTIF 3 can be used in pavements subjected to light to medium traffic ($<10^7$ ESA). This assessment is consistent with field performance observed in the CAPTIF

experiments, viz. all CAPTIF pavement sections had a deformation life of about 5.5 x 10^6 ESA.

- The results in Table 6.9 indicated that both materials CAPTIF 1 and CAPTIF 2 can be used in pavements subjected to heavy traffic (>10^7 ESA). This assessment is not consistent with field performance as all CAPTIF pavement sections had a deformation life of about 5.5 x 10^6 ESA.

Table 6.8 Performance rating for different pavement classes based on RLT test results produced by ARRB.

Pavement	Performance Rating		
	<10^6 ESA	10^6-10^7 ESA	>10^7 ESA
CAPTIF 1-9726	Pass	Pass	Fail
CAPTIF 3-9546	Pass	Pass	Fail

Table 6.9 Performance rating for different pavement classes based on RLT test results produced by University of Canterbury.

Pavement	Performance Rating		
	<10^6 ESA	10^6-10^7 ESA	>10^7 ESA
CAPTIF 1-CANT-1	Pass	Pass	Pass
CAPTIF 2-CANT-2	Pass	Pass	Pass

6.7 Method 2: Performance assessment based on deformation life

As discussed in Section 3.2.2, deformation lives estimated for the 3-stage permanent strain testing can be used to rank the material performance.

In this case, a curve-fitting procedure (see Appendix 2, Section A2.8) is used to determine the relationships between permanent strain and loading cycle for different stress levels applied in the 3-stage loading test. From these relationships, the number of loading cycles to reach a nominal failure strain (say 15,000 microstrain) can be calculated. Figure 6.5 shows typical results of deformation life obtained from a 3-stage permanent strain test using the Austroads RLT test method. Results of other tests are given in Appendix 5.

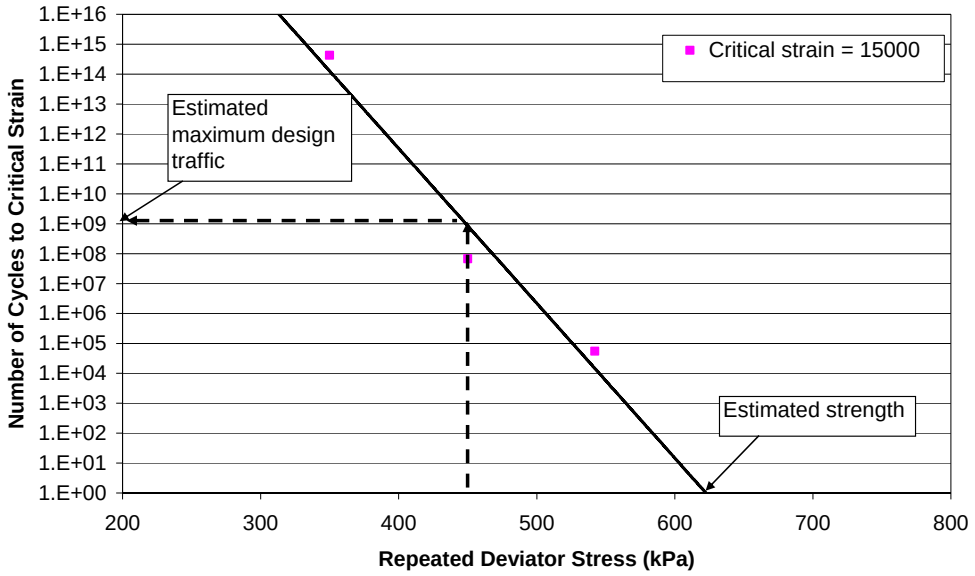

Figure 6.5 Results of parameters of Equation 6.1 for CAPTIF 1 (Sample No CANT-1).

Tables 6.10 and 6.11 summarise the deformation life at the design stress in Stage 2 and the shear strength (stress that produces failure in 1 cycle) for materials tested by ARRB and the University of Canterbury, respectively. As discussed previously, different laboratories used different compaction methods and, therefore, comparing the permanent strain results produced between the two laboratories was not possible for material ranking.

Table 6.10 Comparison of shear strength and design deformation life (based on tests conducted by ARRB).

Pavement	Nominal failure strain(%)	Shear strength (kPa)	Deformation life for design stress in Stage 2 (cycles)	Ranking
CAPTIF 1-9726	1.5	785	1.5E+04	2
CAPTIF 3-9546	1.5	745	1.8E+04	1

Table 6.11 Comparison of shear strength and design deformation life (based on tests conducted by University of Canterbury).

Pavement	Nominal failure strain(%)	Shear strength (kPa)	Deformation life for design stress in Stage 2 (cycles)	Ranking
CAPTIF 1-CANT-1	1.5	700	6.75E+07	1
CAPTIF 2-CANT-2	1.5	580	1.57E+07	2

- From Table 6.10, the two materials CAPTIF 1 and CAPTIF 3 produced very similar performance. Given that CAPTIF 3 produced a slightly higher deformation life in Stage 2, it was ranked higher than CAPTIF 1. This is consistent with the ranking based on field deformation life (see Figure 6.1a).
- From Table 6.11, CAPTIF 1 produced a higher deformation life and was ranked higher than CAPTIF 2. This is consistent with the ranking based on field deformation life (see Figure 6.1b).

6.8 Method 3: Performance assessment based on estimated base deformation

As discussed in Section 3.2.3, base deformation can be estimated as the product of the RLT permanent strain and base thickness.

For the pavement cases studied, the bases had a thickness in the range of 200-275 mm. For simplicity, only the total deformation of the top 200 mm base was predicted using permanent strain results for stress levels applied in both Stage 2 (for the layer at depth of 30-150 mm below surface) and Stage 1 (for the layer at depth 150–230 mm).

$$\Delta d_{Basetotal} = [\varepsilon_{p(Stage2)Base} \times \Delta H_{Base}] + [\varepsilon_{p(Stage1)Base} \times \Delta H_{Upper\ Sub\text{-}base}]$$

(Equation 6.2)

where:

$\varepsilon_{p(Stage2)Base}$ and $\varepsilon_{p(Stage1)Base}$ are permanent strains predicted for Stage 2 and Stage 1, respectively, using the relationships as derived in Section 6.4.

ΔH_{Base} = 120 mm

$\Delta H_{Upper\ Sub\text{-}base}$ = 80 mm

Figures 6.6 and 6.7 compare the predicted base deformation with the measured surface deformation for pavement test sections tested with 40 kN axle load using RLT permanent strain test results produced by ARRB and the University of Canterbury, respectively. As discussed previously, different laboratories used different compaction methods and therefore the predicted base deformations produced by the two compaction methods were expected to be substantially different.

- From Figures 6.6a and 6.6b, the RLT permanent strain data produced by the dynamic compaction method was used to predict base deformation. In this case, the predicted base deformations were found to be similar to field surface deformations for CAPTIF 1 and CAPTIF 3.
- From Figures 6.7a and 6.7b, the RLT permanent strain data produced by the vibratory compaction method was used to predict base deformation. In this case, the predicted base deformations were found to be about 25% of the field surface deformations for CAPTIF 1 and CAPTIF 2.

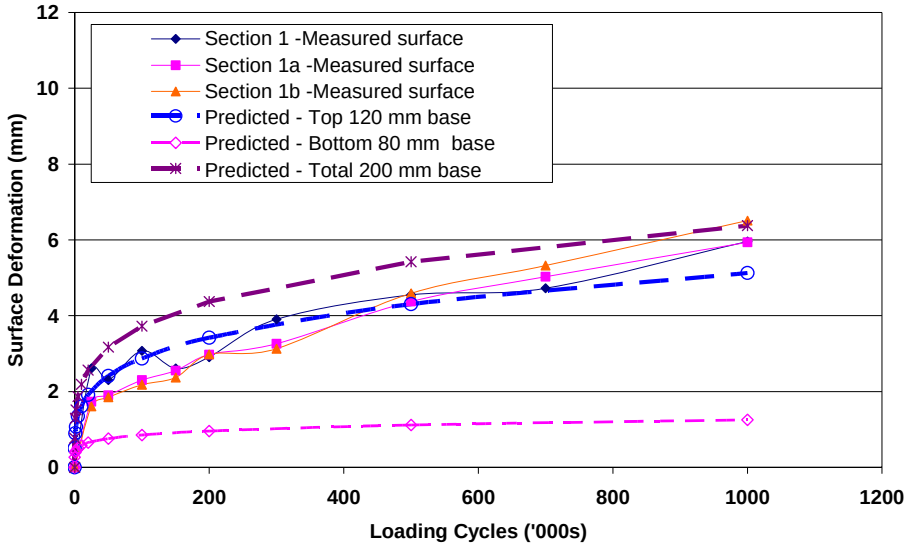

(a) Section 1 – CAPTIF 1

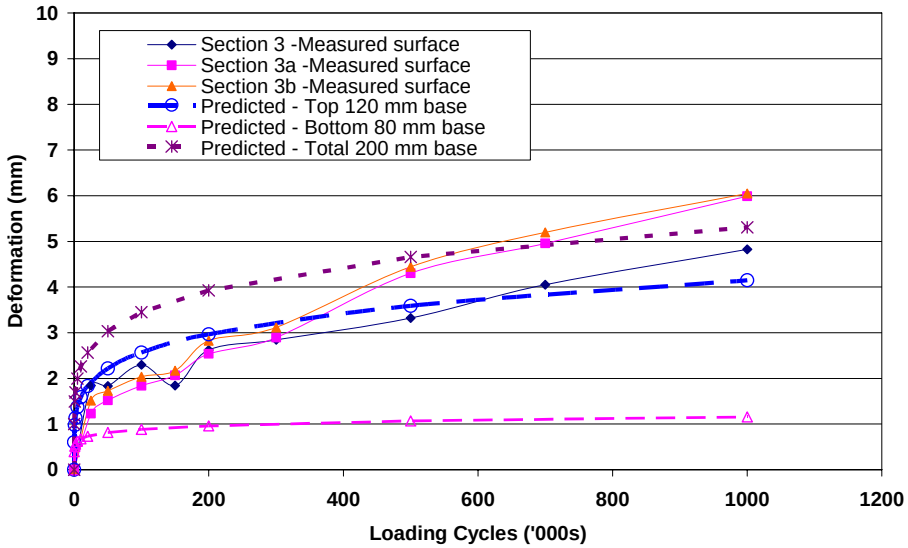

(b) Section 3 – CAPTIF 3

Figure 6.6 Comparison between measured surface deformation and predicted base deformation based on laboratory RLT tests conducted by ARRB.

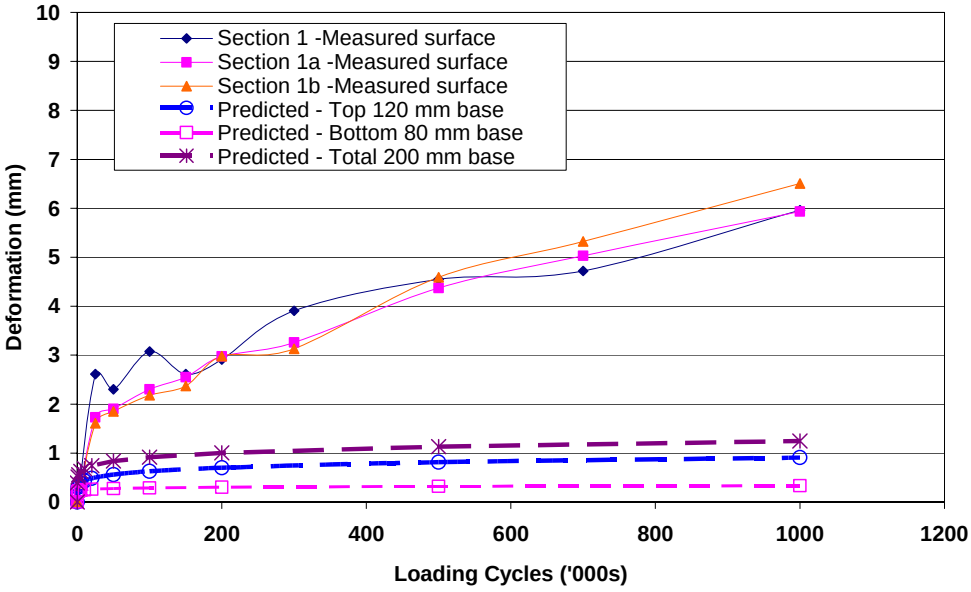

(a) Section 1 – CAPTIF 1

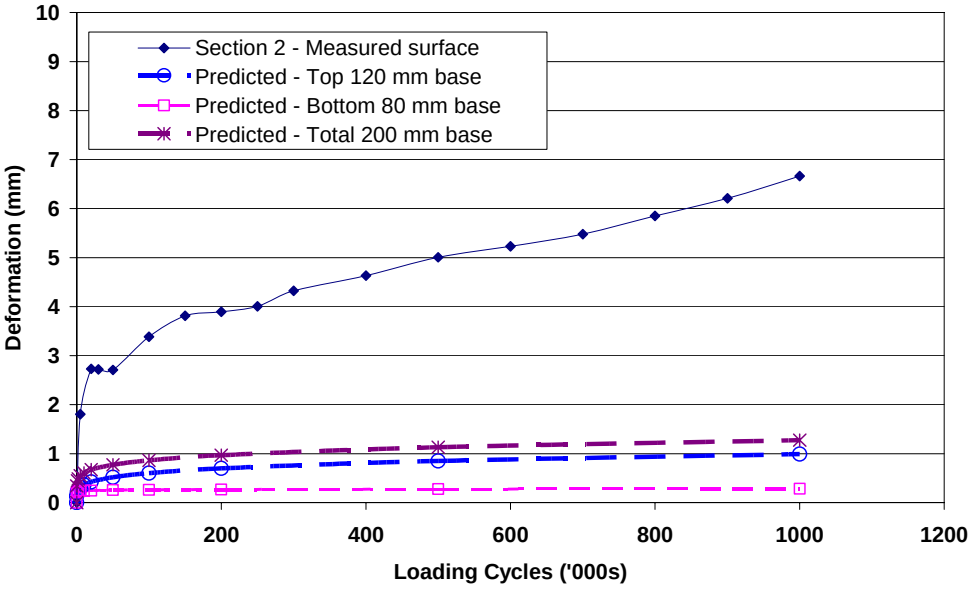

(a) Section 2 – CAPTIF 2

Figure 6.7 Comparison between measured surface deformation and predicted base deformation based on laboratory RLT tests conducted by the University of Canterbury.

Post-mortem-trenches in the New Zealand accelerated pavement tests also revealed over 50% of the surface rut depth was attributed to the granular bases. Therefore, the results in Figures 6.6 and 6.7 may indicate that the predicted base deformation produced by dynamic compaction is higher than the measured base deformation, possibly caused by higher bedding errors. However, the predicted base deformation produced by dynamic compaction is lower than the measured surface deformation.

Therefore, a concern existed that compaction in actual granular pavement layers under heavy compaction is different from that in the laboratory compaction RLT testing condition. Therefore, it may be desirable that the laboratory-determined permanent strain be corrected for the differences between the laboratory and field compaction methods. It should be noted that other factors such as rotating stresses may cause the differences between laboratory and field performance. However, these effects are not possible to quantify in this study.

6.9 Summary

In this study, two different laboratory compaction methods were used to compact laboratory specimens. They were found to produce different results of permanent deformation. Generally, the dynamic compaction method produced higher permanent deformations than those produced by the vibratory compaction method.

Comparison of laboratory and field performance data obtained from seven different pavements tested with CAPTIF indicated that:

- All the Austroads/ARRB simple assessment methods based on deformation behaviour, deformation life, and estimated base deformation, produced material rankings consistent with the rankings based on field performance.
- The estimated base deformations may not be similar to the field values. The vibratory compaction method produced lower estimated base deformation than field values, whereas the dynamic compaction method produced higher base deformation than field values.

Therefore, the Austroads/ARRB performance assessment method, in the current form, should be restricted to results produced by the same laboratory compaction method and could only be used for ranking and selecting base materials based on relative base performance. However, given that all field pavement tests produced low rut depths (<8 mm) at the end of testing, more field trials need to be conducted to validate the method.

Further research is also required to correct laboratory-determined permanent strain for the differences between the laboratory and field conditions, including compaction method and loading stresses. This will enable base deformation to be accurately predicted for pavement design.

7. Simplified Arnold rut depth model

7.1 Methodology

As discussed in Section 5.7, the Arnold rut depth model (Arnold 2004) predicts deformations of all pavement layers and subgrade. It also requires a full RLT data set to model deformation behaviour of base and subgrade. However, only base deformation needs to be predicted for practical use in material specifications. Further simplifications in the model could also be made as follows:

- The number of stress stages in the RLT test could be reduced to four so that they can be performed on one specimen. This would reduce the effort in laboratory RLT permanent strain testing.
- Incremental permanent deformation for the period 25-50 k-cycles of a granular base can be calculated and used as criteria for ranking of base performance.

To validate this simplified Arnold rut depth model, the following steps were carried out utilising the laboratory RLT test results at Nottingham University (Section 5.2) and field pavement test results at CAPTIF (Chapter 4):

- Step 1: Select a reduced set of RLT test data (i.e. 4 stress stages) using existing full RLT data set for the CAPTIF aggregates (i.e. CAPTIF 1, 2, 3, and 4).
- Step 2: Use the reduced RLT data set in the Arnold rut depth model (Arnold 2004) to predict incremental base deformation for the period 25-50 k-cycles for the CAPTIF pavement trials.
- Step 3: Compare the predicted incremental base deformation with measured pavement rut depths in the CAPTIF trials for validation and to aid in determining appropriate base deformation limits for the simplified approach.

Details of these three steps are described below.

7.2 Step 1: Selection of reduced set of RLT test data

In principle, the four stress stages were selected such that the incremental permanent strain data between 25k and 50k load cycles produced by these four stress stages could be used fitted with the same relationships of incremental permanent strain and stresses (see Equation 7.1) that fitted to the full data set.

$$\Delta\varepsilon_{p(25\text{-}50k)} = e^{(A2)}\, e^{(B2\ p)}\, (e^{(C2\ q)} - 1) \qquad \text{(Equation 7.1)}$$

(See p.26 for symbols)

Table 7.1 shows typical results of the reduced data set (as highlighted in bold) that were selected from a full RLT data set. In the curve-fitting process the parameter B2 had to be fixed at a value of −15 because of the difficulty in determining three parameters (i.e. A2, B2, and C2) on only four data points. The value of −15 was chosen as an average value of all trialled values, which were found to produce the smallest fitted errors (i.e. using full

data set) for all materials, with the exception of CAPTIF 4 material. Generally, a relationship of permanent strain rate and stresses determined from this curve-fitting procedure produced higher fitting errors than that fitted to the full data set. Table 7.1 also shows typical fitting errors produced by the two cases.

Table 7.1 Comparison of predicted strains for the period 25-50 k-cycles using a full and reduced RLT data set (material CAPTIF 1).

Stage	p (kPa)	q (kPa)	Measured RLT strain (%)	Predicted strains using full data set		Predicted strains using reduced data set	
				Strain (%)	% Error	Strain (%)	% Error
1	76	43	0.067	0.052	−22.4%	0.037	−44.8%
2	77	91	0.165	0.163	−1.2%	0.116	−29.7%
3	77	139	0.429	0.387	−9.8%	0.275	−35.9%
4	**77**	**183**	**0.784**	**0.808**	**3.1%**	**0.570**	**−27.3%**
5	149	135	0.107	0.107	0.0%	0.089	−16.8%
6	154	183	0.230	0.217	−5.7%	0.180	−21.7%
7	151	229	0.387	0.470	21.4%	0.387	0.0%
8	**150**	**274**	**0.449**	**0.941**	**109.6%**	**0.770**	**71.5%**
9	152	319	3.874	1.771	−54.3%	1.450	−62.6%
10	**247**	**324**	**0.335**	**0.372**	**11.0%**	**0.374**	**11.6%**
11	247	376	1.178	0.813	−31.0%	0.812	−31.1%
12	**250**	**419**	**1.493**	**1.493**	**0.0%**	**1.493**	**0.0%**
13	243	465	3.303	3.303	0.0%	3.242	−1.8%
				Mean Error	**1.6%**		**−14.5%**

Note: Stress conditions used for reduced data set are highlighted in bold

Table 7.2 compares the values of parameters (A2, B2, and C2) of the relationships of permanent strain rate and stresses fitted with the reduced and full data sets for all materials CAPTIF 1, CAPTIF 2 , CAPTIF 3, and CAPTIF 4. The results indicated that CAPTIF 1, 2, and 3 materials produced relatively consistent values of model parameters for both cases of reduced and full data set. However, CAPTIF 4 material produced different values of model parameters for the two cases and, hence, the use of reduced data set resulted in poor predictions of permanent strain rate.

Table 7.2 Comparison of predicted incremental strains for the period 25-50 k-cycles using a full and reduced RLT data set (material CAPTIF 1).

Parameters of Equation 3.12	CAPTIF 1		CAPTIF 2		CAPTIF 3		CAPTIF 4	
	Full Set	Reduced Set	Full Set	Reduced Set	Full Set	Reduced Set	Full Set	Reduced Set
A2	−1.5	−2.0	−1.8E-07	−8.2E-07	−1.8	−1.6	1.6	1.5
B2	−17.1	**−15.0**	−8.4	**−15.0**	−22.5	**−15.0**	−32.4	**−15.0**
C2	14.8	14.7	9.3	13.1	15.5	10.7	13.4	4.7

Note: Fixed values are highlighted in bold

7.3 Step 2: Predicted incremental base deformation using reduced data set

The base incremental permanent deformations for the period 25-50 k-cycles were predicted using stresses (in terms of mean principle stress, *p*, and deviator stress, *q,* at the single wheel centre line for all the CAPTIF tests. As discussed in Section 5.4, the stresses were predicted with the simple FEM model DEFPAV.

Table 7.3 summarises the incremental base deformations for the period 25-50 k-cycles predicted from both full and reduced data set for all CAPTIF pavement tests with a thin asphalt surfacing layer of 25 mm. The predicted incremental base deformations were expressed in terms of deformation per 1 M cycles (mm/10^6 cycles). The measured deformation rates, extrapolated from the measured deformation between 25-50 k-cycles were also included in Table 7.3 for comparison. The results indicated that:

- Significant differences were observed in the predicted base deformations of all pavement test sections (viz. in the range of 2–110 mm). However, the measured rut depths were in a smaller range of 0.65–6.1 mm.
- No direct correlation was observed between rankings based on incremental base deformations predicted from either the full or the reduced data set for all pavement cases and rankings based on measured incremental pavement rut depths.
- The poor predictions of stresses using the simple DEFPAV FEM was a probable cause of the errors as later shown using analysis using the ARRB/Austroads FEM.

7.4 Step 3: Comparison of predicted incremental base deformation with measured pavement rut depth

Table 7.4 compares the predicted average incremental base deformations for all CAPTIF test sections with the same aggregate type with the measured average incremental pavement rut depth for the period 25–50 k-cycles. The results in Table 7.4 indicated that the rankings based on the average performance of materials were more consistent with the rankings based on measured pavement rut depths.

Table 7.3 Comparison of predicted incremental base deformation and measured incremental base rut depth for the period 25-50 k-cycles for all CAPTIF tests.

Test	Predicted base deformation using a full set		Predicted base deformation using a reduced set		Measured surface deformation	
	Deformation	Ranking	Deformation	Ranking	Deformation	Ranking
	mm/10^6 cycles		mm/10^6 cycles		mm/10^6 cycles	
1: 40kN	21	8	17	9	3.2	9
1: 50kN	22	10	17	9	6.1	15
1a: 40kN	21	8	17	9	2.7	5
1a: 60kN	20	7	15	8	5	14
1b: 40kN	31	13	24	13	3.4	11
1b: 60kN	29	12	22	12	4.8	13
2: 40kN	45	14	110	15	3.3	10
2: 50kN	46	15	98	14	4.6	12
3: 40kN	3.9	1	2.1	1	3.1	7
3: 50kN	6.0	3	2.7	3	3.1	7
3a: 40kN	3.9	1	2.1	1	2.9	6
3a: 60kN	8.6	4	3.4	5	0.65	1
3b: 40kN	9.2	5	3.2	4	2.2	4
3b: 60kN	24	11	5.9	7	0.77	3

Table 7.4 Comparison of predicted average incremental base deformation and measured average incremental pavement rut depth for different aggregates.

Aggregate	Predicted base deformation using a full data set		Predicted base deformation using a reduced data set		Measured surface deformation	
	Deformation	Ranking	Deformation	Ranking	Deformation	Ranking
	mm/10^6 cycles		mm/10^6 cycles		mm/10^6 cycles	
CAPTIF 3	9.3	1	3.2	1	2.1	1
CAPTIF 1	24	3	19	3	4.2	3
CAPTIF 2	45	4	104	4	4.0	2

The non-linear correlation between predicted base deformations from the reduced data set correlated against those predicted with the full data set is also given Figure 7.1. The correlation between the results produced by the two methods was strong. This indicates that this simplified analysis with the reduced RLT data set can produce results as good as the full data set.

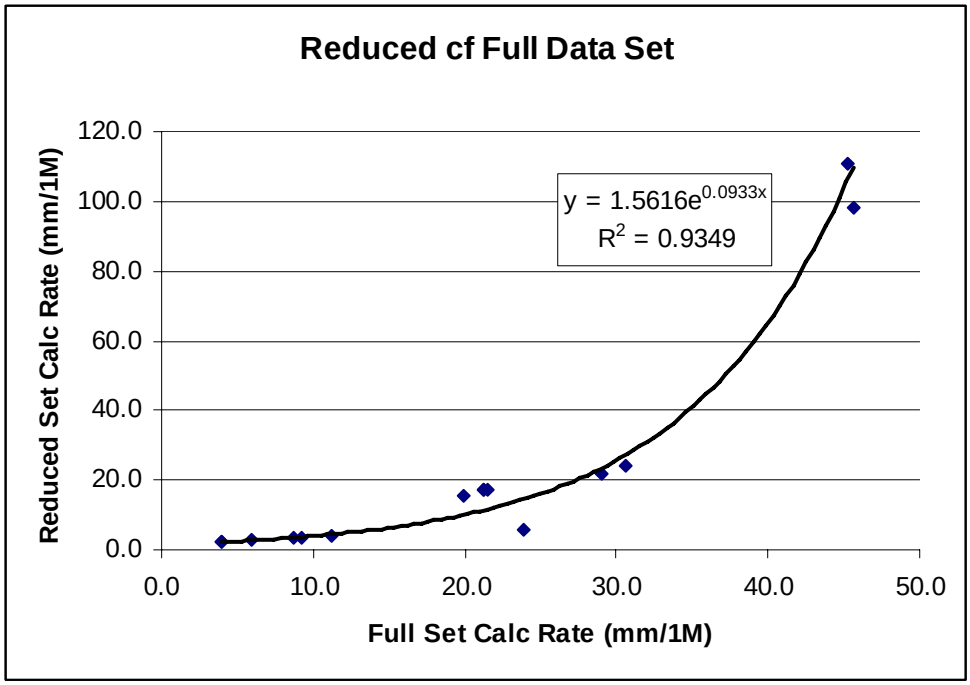

Figure 7.1 Comparison of rate of rutting between predictions from a full and reduced RLT data set.

7.5 Summary

The proposal was to simplify the Arnold rut depth model (Arnold 2004) to predict base deformation for the purpose of base selection. Simplifications were made in the selection of a reduced RLT data set and in the prediction of incremental deformation for the period 20–50 k-cycles.

However, in the validation of the reduced of RLT data set (viz. 4 stress stages) using full RLT data sets obtained for various base materials, it was found that there were some difficulties in determining 3 parameters of the permanent strain model using only four data points. In this case, it was necessary to fix one of the three parameters in the curve-fitting procedure. However, such curve-fitting procedure may not consistently produce the same relationships as those derived from full data sets. Therefore, the curve-fitting procedure (with a fixed parameter) for the reduced data set should be used with caution.

In the validation of predicted base deformation using measured surfaced deformations from all CAPTIF trials, significant differences were also found between the predicted base deformations of all pavement test sections (viz. in the range of 2–110 mm) and the measured rut depths (in the range of 0.65–6.1 mm). Therefore, the simplified Arnold rut depth model may not closely predict the field incremental base deformation for the period 20–50 k-cycles. However, this was likely caused by the poor predictions of stresses using the DEFPAV FEM.

Given that the reduced RLT data set can produce results as good as the full data set for most pavement cases studied, it was suspected that the poor predictions of rut depth at CAPTIF were a result of:

- an over-simplification of the RLT data by considering only the slope of permanent strain between 25k and 50k loading cycles,
- errors in the predicted pavement stresses produced by the FEM model DEFPAV.

Therefore, further investigations in these areas are required to improve the simplified Arnold rut depth model before it can be used to predict base deformation of various base thicknesses. A discussion on the effects of errors in the predicted pavement stresses is given in Chapter 8.

8. Effects of predicted pavement stresses on base deformation prediction

As discussed above, two 2-dimensional FEM models were used to predict pavement stresses: the FEM model VMOD-PAVE (Vuong 1985a, 2005a) as used to develop the Austroads test method, and the simple FEM model DEFPAV (Snaith et al. 1980) as used in the Arnold rut depth model. They produced different pavement stresses as described in Chapters 5 and 6. This also resulted in selecting different RLT test stresses that are applied in the routine Austroads RLT multi-stage permanent strain testing methods for base material ranking and simplified Arnold rut depth model for predicting base deformation.

Recently, the FEM model VMOD-PAVE has been improved by ARRB and has shown the ability to accurately predict strains and stresses for the pavement tests with the Accelerated Loading Facility (ALF) (Vuong 2005a). In principle, the improved FEM model VMOD-PAVE used improved non-linear material models to take into account the effects of residual horizontal stress from compaction, mean stress, shear stress, and stress limits for failure and no-tension. Therefore, it is likely to produce fewer errors in the predicted stresses than those predicted with DEFPAV, which can take into account only the effects of total stress on granular and subgrade modulus.

In this chapter, the improved model VMOD-PAVE (Vuong 2005a) was used to predict stresses in some standard pavement cross sections to assist in the selection of appropriate RLT test stresses. The RLT incremental permanent strains results obtained in Section 7.3 were also used to predict incremental base deformations and compared with the predicted values using Arnold's method.

8.1 Predicted pavement stresses for standard pavement cross sections

Details of FEM analyses with VMOD-PAVE for standard pavement cross sections are given in Vuong (2005b). In principle, they were based on the structural analysis of two-layered granular pavements subject to a circular load of 20 kN with different contact stresses in the range of 500–1000 kPa. However, only results of pavement stresses at the axis through the loading centre for the average contact stress of 750 kPa are extracted and reported below.

Table 8.1 summarises nine trial pavements which were selected for the FEM analyses.

- The granular base has a thickness in the range of 200–400 mm.
- Three different subgrade types: soft, medium, and stiff, were selected.

Table 8.1 Selected trial pavements (with design traffic) for FEM analysis.

Design Granular Base Thickness (mm)	Subgrade type		
	Soft (CBR 5)	Medium (CBR 10)	Stiff (CBR 20)
200	Pavement 1 (Failed)	Pavement 2 (10^5 ESA)	Pavement 3 ($7x10^6$ ESA)
300	Pavement 4 (10^5 ESA)	Pavement 5 ($5x10^6$ ESA)	Pavement 6 ($>10^8$ ESA)
400	Pavement 7 ($1.2x10^6$ ESA)	Pavement 8 (10^8 ESA)	Pavement 9 ($>10^8$ ESA)

Details of models of resilient modulus of the granular base and subgrade and the values of model parameters are given in Vuong (2005a, 2005b). Figures 8.1a and 8.1b show the results of predicted resilient moduli of the base and subgrade, respectively, at various thicknesses on the axis through the loading centre. Note that Pavement 1 failed under the circular load of 20 kN with contact stress of 750 kPa and therefore, was not considered a typical granular pavement. The results of Pavement 1 are not included in Figures 8.1a and 8.1b.

The top 500 mm of the three subgrade types (soft, medium and stiff) had average moduli of about 55–74 MPa (soft), 99–138 MPa (medium), and 181–262 MPa (stiff). Therefore, based on the Austroads relationship of modulus = 10 CBR, the soft, medium, and stiff subgrade types may be assumed to have a equivalent CBR values of 5, 10, and 20 respectively.

According to Fig 8.4 of the Austroads *Pavement design guide* (2004), the pavements would have design estimates of traffic in the range of 10^5-10^8 ESA as given in Table 8.1. Therefore, they cover different pavement classes as listed below:

- Low traffic volumes ($<10^6$ ESA): Pavements 2 and 4
- Medium traffic volumes (10^6 – 10^7 ESA): Pavements 3, 5, and 7.
- High traffic volumes ($>10^7$ ESA): Pavements 6, 8, and 9.

Figures 8.2a and 8.2b show the predicted mean stresses and deviator stresses in the granular bases, respectively. The results in these figures indicate that the stresses can vary with depths and subgrade types.

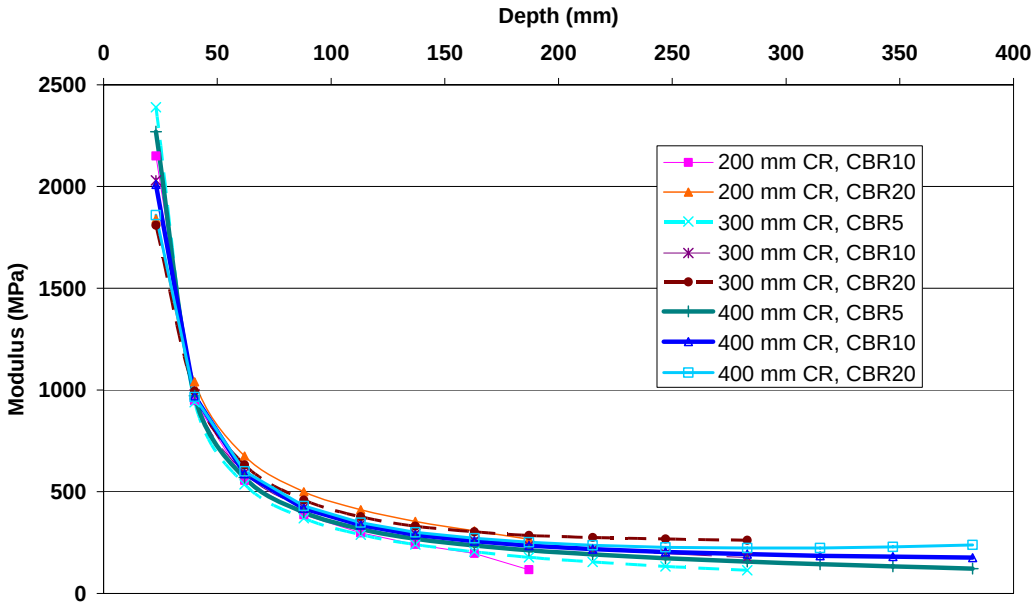

(a) Granular base moduli

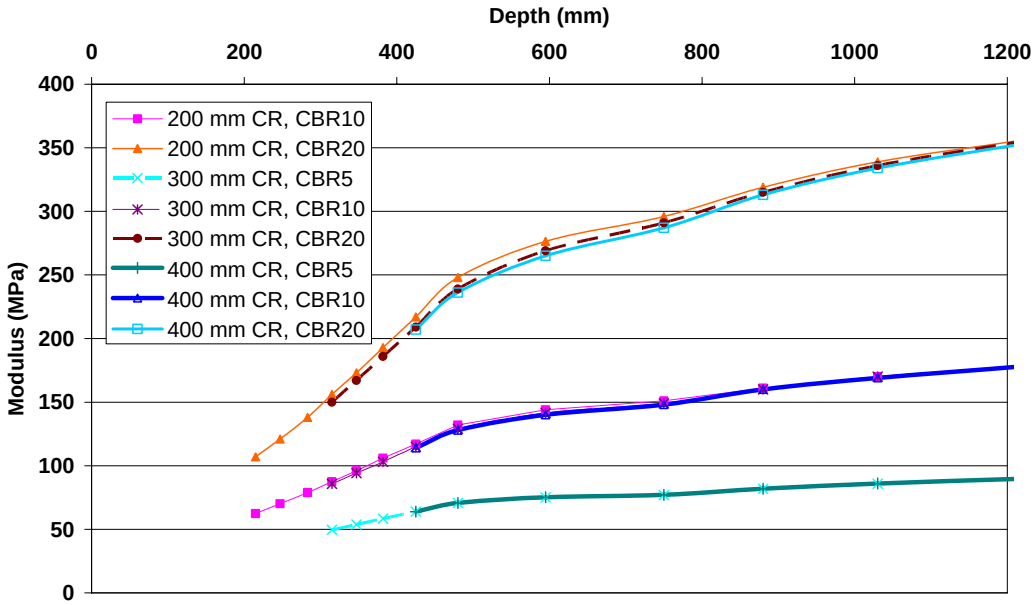

(b) Subgrade moduli

Figure 8.1 Moduli in the granular pavements caused by a circular load of 20 kN with contact tyre stress of 750 kPa (CR = crushed rock, 200mm CBR5 failed).

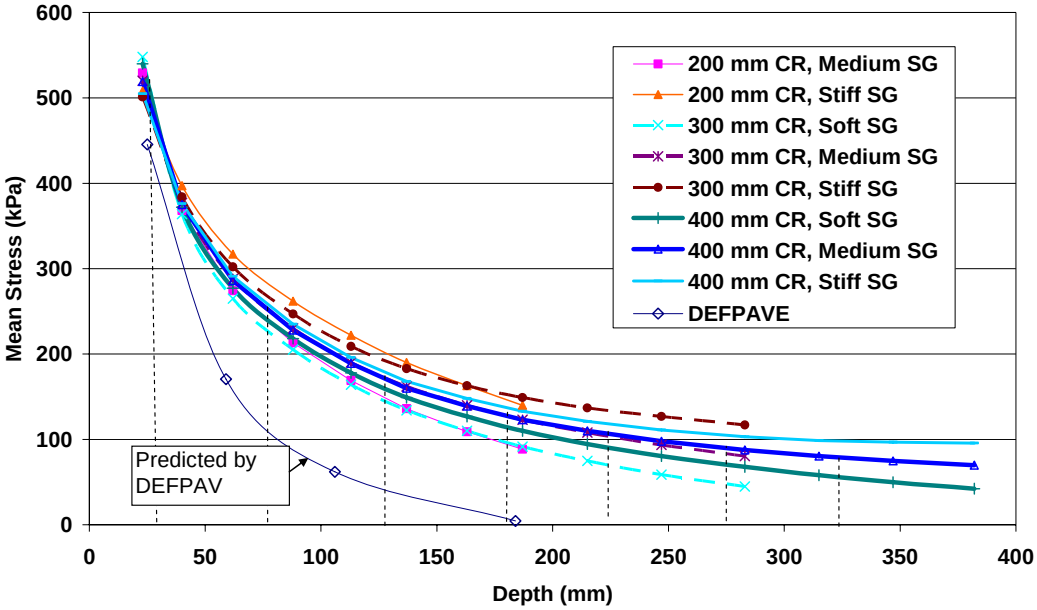

(a) Mean Stress

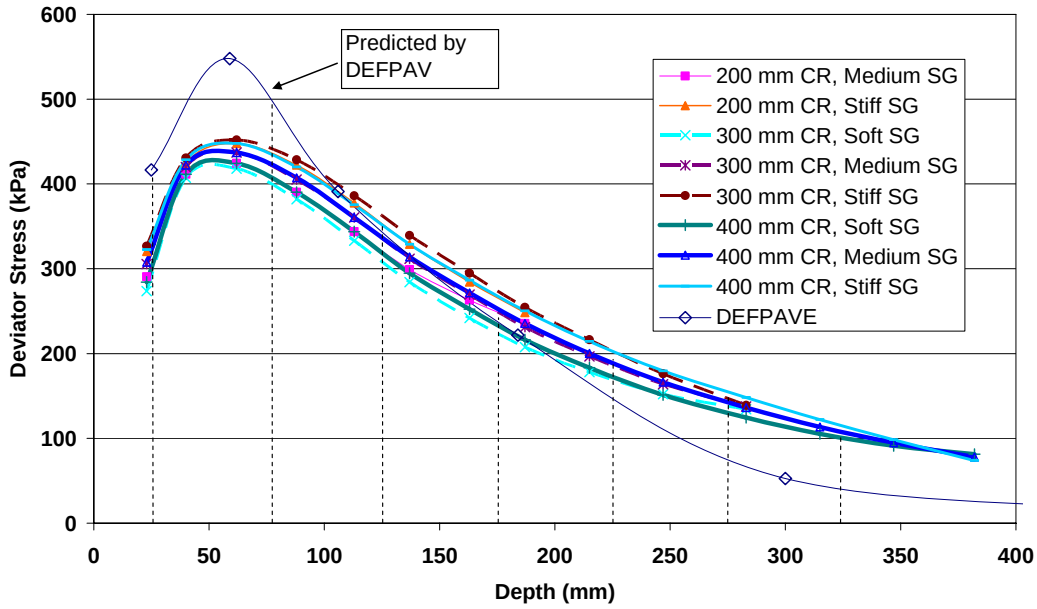

(b) Deviator Stress

Figure 8.2 Stresses in the granular material covered with 25 mm chipseal caused by 40 kN axle load on a single tyre with a contact tyre stress of 750 kPa.

8.2 Comparison of predicted pavement stresses produced by various FEM models

Typical results of stresses predicted by DEFPAV (see Table 5.1) was also included in Figure 8.2a and 8.2b for comparison. DEFPAV was found to produce lower mean stresses at all depths, higher deviator stresses in the top 100 mm base, and lower deviator stresses in the bottom 100 mm base.

8.3 Comparison of predicted base deformation

Arnold's permanent strain rate models for the period between 25 k and 50 k load cycles for all the CAPTIF materials obtained in Section 7.3 were also used to predict incremental base deformations for all pavements and the results are summarised in Table 8.2.

Table 8.2 Incremental base deformation for the period 25–50 k-cycles for a range of pavement cross sections using Arnold's model (Equation 3.12).

Material	RLT Data Set	Base Deformation (mm/10^6 cycles)								
		Pave. 1	Pave. 2	Pave. 3	Pave. 4	Pave. 5	Pave. 6	Pave. 7	Pave. 8	Pave. 9
CAPTIF 1	Full	3.1	2.4	1.5	2.8	2.4	2.3	2.6	2.7	2.8
	Reduced	2.5	2.1	1.4	2.3	2.1	2.1	2.2	2.3	2.4
CAPTIF 2	Full	8.3	7.9	6.7	9.0	8.9	9.2	9.4	9.9	10.4
	Reduced	11.5	9.3	6.2	10.8	9.5	9.2	10.5	10.6	11.0
CAPTIF 3	Full	1.4	1.0	0.4	1.2	0.9	0.7	1.1	1.0	1.0
	Reduced	1.1	0.8	0.5	1.1	0.9	0.8	1.1	1.0	1.0
CAPTIF 4	Full	10.1	4.8	1.2	8.9	4.1	2.3	7.6	5.2	4.1
	Reduced	3.8	2.5	1.3	4.4	3.1	2.4	4.7	4.0	3.6

The values of predicted base incremental deformation (which are for pavements having thicknesses in the range of 200–400 mm) ranged from 0.7–11.5 mm/10^6 cycles. They are much smaller than the predicted base incremental deformation values of all pavement test sections (having thicknesses in the range of 200–275 mm) using Arnold's method varied in the range of 2–110 mm/10^6 cycles) as given in Table 7.3. They are also closer to the measured surface incremental rut depths (in the range of 0.6–6.1 mm/10^6 cycles). Therefore, the effects of predicted pavement stresses on the predicted pavement deformation is very significant.

Note that the predicted ranking of the materials, in order of lowest to highest base incremental deformation between 25–50 k-cycles (see Table 8.3) shows CAPTIF 3 material having consistently the best performance. CAPTIF 2 material was always the worst performing material. CAPTIF 1 and 4 materials tended to swap positions between CAPTIF 3 and 2 materials. These rankings in performances were similar to those found at CAPTIF tests and appeared to be independent of the chosen cross section. This result is promising as a standard cross section with stresses computed can be used to predict the relative performance of granular materials from RLT tests.

Table 8.3 Ranking of material performance from incremental base deformation for the period 25–50 k-cycles.

Deformation Ranking	Ranking of pavements in order of lowest to highest deformation rate								
	P. 1	P. 2	P. 3	P. 4	P. 5	P. 6	P. 7	P. 8	P. 9
Lowest	3r	3r	3f	3r	3f	3f	3f	3f	3f
	3f	3f	3r	3f	3r	3r	3r	3r	3r
	1r	1r	4f	1r	1r	1r	1r	1r	1r
	1f	1f	4r	1f	1f	4f	1f	1f	1f
	4r	4r	1r	4r	4r	1f	4r	4r	4r
	2f	4f	1f	4f	4f	4r	4f	4f	4f
	4f	2f	2r	2f	2f	2r	2f	2f	2f
Highest	2r	2r	2f	2r	2r	2f	2r	2r	2r

f = predictions from full RLT data set
r = predictions from reduced RLT data set
1, 2, 3, 4 are CAPTIF materials 1, 2, 3 and 4

Validation of the predicted pavement responses (stresses, strains and deflection) produced by VMOD-PAVE has been undertaken. The recommendation is that this FEM model be used to predict pavement stresses for selecting RLT test stresses.

8.4 Comparison of predicted deformation life

Pavement life was computed by assuming:

- an initial rut depth for the first period 0-25 k-cycles of 5 mm,
- the rate of deformation after 25 k-cycles was constant and the same as that predicted for the period 25-50 k-cycles,
- a terminal end-of-life rut depth of 15 mm occurring within the granular pavement layers only.

The results of predicted pavement life are summarised in Table 8.4. The field pavement lives estimated from the Austroads *Pavement design guide* (Figure 8.4 in Austroads 2004) are also included in Table 8.4 for comparison. The results indicate that predicted pavement lives do not vary much for all pavement configurations; whereas the field pavement showed a much large range from 10^5 – 3 x 10^{11} ESA. Therefore, this simplified method may not accurately predict field pavement life.

Table 8.4 Pavement life estimated from the predicted deformation of the granular layer.

Material	RLT Data Set	Pavement life estimated for each pavement (10^6 ESA)								
		P. 1	P. 2	P. 3	P. 4	P. 5	P. 6	P. 7	P. 8	P.9
CAPTIF 1	Full	3.2	4.1	6.6	3.6	4.2	4.4	3.8	3.8	3.6
	Reduced	4.1	4.8	6.9	4.4	4.8	4.7	4.6	4.4	4.1
CAPTIF 2	Full	1.2	1.3	1.5	1.1	1.1	1.1	1.1	1.0	1.0
	Reduced	0.9	1.1	1.6	0.9	1.1	1.1	1.0	0.9	0.9
CAPTIF 3	Full	7.0	10.4	22.3	8.4	11.6	13.8	9.4	10.1	10.3
	Reduced	9.1	11.9	19.3	9.3	11.3	12.5	9.4	9.7	9.8
CAPTIF 4	Full	1.0	2.1	8.5	1.1	2.5	4.4	1.3	1.9	2.4
	Reduced	2.6	4.0	7.4	2.3	3.2	4.1	2.1	2.5	2.8
Pavement life estimated by Austroads		**0.01**	**0.13**	**5.8**	**0.12**	**4.2**	**1292**	**1.2**	**138**	**285,000**

Pavement life calculated from the deformation of the granular layer, assuming an initial 5 mm deformation caused by compaction and the end of life criteria of a 15 mm deformation.

8.5 Summary

Comparison of two FEM stress prediction models: DEFPAV (used in the Arnold rut depth model), and VMOD-PAVE (used in the ARRB/Austroads simple performance prediction models) indicated that DEFPAV is too simple and is likely to produce large errors in the predicted stresses.

Comparison of pavement stresses predicted with the two models DEFPAV and VMOD-PAVE also indicated that DEFPAV predicted higher deviator (or shear) stresses at the top of the base and lower mean stress (or confining stress) than those predicted with VMOD-PAVE.

Comparisons of predicted incremental base deformations for the period 20–50 k-cycles using the same RLT data set but different pavement stresses predicted with DEFPAV and VMOD-PAVE indicated that the effects of predicted stresses on the base deformation prediction were very significant, i.e. deformation rates in the ranges of 0.7–11.5 mm/10^6 cycles for VMOD-PAVE, and 2–110 mm/10^6 cycles for DEFPAV.

The use of pavement stresses predicted with VMOD-PAVE appeared to produce base incremental deformations closer to field values. Therefore, the recommendation is to use VMOD-PAVE to predict stresses in base layers for the selection of RLT test stresses for prediction of base deformation.

9. Effects of RLT testing equipment and methods on base deformation prediction

Chapters 5 and 6 have presented two RLT multi-stage permanent strain testing methods, namely routine Austroads and research Nottingham RLT test methods. Given the many differences between the two methods (see Table 2.1), it was difficult to compare the minimum RLT permanent strain data set obtained with the Austroads method (in Chapter 8) with the full RLT data set obtained at University of Nottingham (in Chapter 7) to quantify the effects of these differences.

However, based on experience gained in the development of both routine and research RLT test methods at ARRB, some comments on the effects of the differences are given in the following sections. They enable selection of an RLT test method for deformation prediction which meets the requirements in New Zealand.

9.1 Effects of test parameters on permanent strain data

9.1.1 Effects of material size

For practical reasons, the ratio of sample size over the maximum grain size was selected as 5 to allow specimens of 100 mm diameter for maximum particle size of up to 19 mm. Insufficient information exists to support the use of 100 mm diameter × 200 mm high specimens for maximum particle size of up to 40 mm. Testing experience at ARRB indicates that, if the sample contains more than 5% by mass of material retained on the 19 mm aperture sieve, the test result might not be representative of that obtained from testing the bulk material. Therefore, the recommendation in the 2000 Austroads RLT test method was that where oversize material is included in a compacted test specimen, the percentage of that oversize material contained within the specimen shall be reported.

Therefore, the recommendation here is that specimens of 150 mm diameter × 300 mm high are used for maximum particle size of up to 40 mm.

9.1.2 Effects of sample preparation

Vuong (1998) has demonstrated that different compaction methods (static, dynamic, vibratory and gyratory) produce different results of resilient modulus and permanent deformation. In the absence of field moduli and permanent strain data, it was decided that only one sample preparation procedure, namely the dynamic compaction method, be used in the 2000 Austroads RLT test method, with the possibility of including other methods when more reliable field data became available.

Note that vibratory compaction tends to produce lower permanent strain than dynamic compaction for non-plasticity granular materials (Vuong 1998). Comparison of standard granular base materials used in New Zealand and Australia indicates that the proportion passing the 75 micron sieve as specified by *TNZ M/4* (TNZ 1995) is much lower than permitted by Australian member authorities. This indicates that non-plastic granular materials are more common in New Zealand. Therefore, it may be desirable to use

vibratory compaction for New Zealand granular materials, provided that the RLT results are only used for material ranking rather than for predicting base deformation and layer moduli.

9.1.3 Effects of target density and moisture content

Given that the vibratory compaction test is currently not used by Australian Member Authorities (AMAs), Transit NZ's compaction specification could not be compared with AMA compaction specifications.

Note that most AMAs use standard and modified compaction to specify field compaction of base materials (say in the range of 98–100% Modified Maximum Dry Density) and moisture content at sealing (say in the range of 60–80% Modified Optimum Moisture Content). Therefore, the dynamic compaction is conveniently used by various AMAs to prepare the triaxial sample to the target density and moisture conditions very close to specified field compaction and moisture content at sealing. RLT testing for permanent strain and resilient modulus is then performed on the unsaturated specimen under drained conditions. However, testing of an unsaturated specimen under undrained conditions, without pore pressure measurement, is also permitted.

The same principle can be applied for New Zealand conditions, i.e. the target density and moisture content could be very close to specified field compaction and moisture content at sealing.

9.1.4 Effects of drainage condition

The saturated and undrained condition is considered to be the most critical condition in RLT testing as the material has the lowest effective strength because of high pore pressures. However, this condition may not be the same as long-term moisture conditions in conventional bases (with protection against moisture penetration), unless the bases were specifically designed to soak up moisture in very wet conditions. Further, because of the severe pore pressure effects on deformation at undrained saturated conditions the use of this condition is not recommended when the objective is to accurately model permanent deformation in the pavement.

Given the difficulties in accurately measuring pore pressure in partially saturated granular materials in both field and laboratory conditions, assessing the differences in pore pressure between field and laboratory conditions and quantifying the effects of pore pressure are difficult for various material types. No inter-laboratory study has been done on undrained RLT testing to standardise the test equipment and testing procedures. Therefore, a need exists to improve the method for pore pressure measurement in partially saturated material as well as to standardise the test equipment and test procedures of the undrained RLT before this test method can be introduced for practical use.

9.1.5 Effects of vertical loading pulses

Insufficient information is available to compare permanent strains produced by the two different vertical loading pulses applied in the Nottingham and Austroads RLT test

methods. However, the effects of loading rate were assumed to be not significant and, therefore, the recommendation of the 2000 Austroads RLT test method was that a longer loading pulse be used to eliminate potential errors associated with the collection and interpretation of stresses and strains.

Using a higher loading speed may be desirable to reduce the testing time, if 50,000 loading cycles per stress stage is required in permanent strain testing, provided that the loading equipment, control software and measuring equipment are capable of producing acceptable errors associated with the collection and interpretation of stresses and strains. An inter-laboratory study would also be needed to standardise these features.

9.2 Effects of strain measurement methods

Different strain measurement methods may produce different results of permanent strain, depending on the accuracy and reliability of the measurement devices.

As discussed in Vuong & Kinder (1984), frictionless end caps are preferred to produce more uniform stress and strain distribution in the specimen. An on-sample strain measurement device (which includes two rigid rings mounted on the specimen, each having four clamped points around the specimen) should also be used to measure the average resilient and permanent strains of the middle half of the specimen, which is also the average strain of the whole specimen. The off-sample strain measurement method (using external LVDTs mounted on the loading piston) should not be used to measure the average resilient and permanent strains of the specimen, as they are influenced by the deflections and/or deformations of the loading piston, the frictionless end caps, and flexible loading piston-end cap connection.

However, for practical reasons, friction end caps are recommended in most RLT testing procedures. Because of the influence of the friction end caps, the stress and strain distributions along the sample length can be non-uniform and substantially different along the sample length. As a result, the sample can develop a barrel shape or 45 degree shear plane. Therefore, the average resilient and permanent strain for the specimen is more difficult to determine. Testing at ARRB using various strain measurement methods (Vuong 1985a) also indicated that:

- The on-sample strain measurement device can be used to measure the average resilient and permanent strains of the middle half of the specimen.
- The off-sample strain measurement method using LVDTs mounted between sample end caps can also be used to measure the average resilient and permanent strains of the specimen, provided that bedding errors at sample ends can be reduced and discounted (if not eliminated) with the use of smooth end surfaces and some initial pre-conditioning loading cycles (say 100–1000 loading cycles).

Currently, the ARRB RLT equipment uses two LVDTs mounted on the sample end caps to measure the average permanent strain for the whole sample, whereas the Nottingham RLT equipment uses studs mounted on the sample to measure local strains at two locations on the specimen.

The ARRB RLT equipment conforms with the 2000 Austroads RLT test method and has been subjected to inter-laboratory studies to check its reliability. However, the Nottingham RLT equipment may require further modifications to measure local strains at four locations on the specimen to increase the reliability. It does not conform with the 2000 Austroads method and has not been subjected to inter-laboratory studies to check its reliability and accuracy. Therefore, the recommendation is that two LVDTs, mounted on the sample end caps to measure the average permanent strain for the whole sample, be used for practical reasons.

9.3 Effects of multi-stage loading procedure

Most RLT testing standards recommend that a virgin or new specimen be used for each stress stage of RLT permanent strain tests. Given most of the cost in RLT testing is in the sample preparation, both the Arnold (2004) and Austroads RLT test methods utilise multi-stage tests to undertake RLT permanent strain tests to cover a range of stress conditions to reduce testing costs.

However, Arnold (2004) ignores the effects of loading history or permanent strain developed in the previous stages and starts the deformation curve for each stress stage from zero cycles and zero deformation. Through validation of the Arnold (2004) rut depth models against available CAPTIF testing data (see Section 5.6) it was shown that the rut depth model could underestimate the initial rutting at 25 k-cycles by around 3 mm for the CAPTIF tests. However, the differences between the predicted and measured deformation in the first 25 k-cycles may be confined to the effect of multi-stage loading in the laboratory permanent strain results or may arise from other assumptions made in the rut depth model as discussed in Section 3.3 (such as 1-dimensional laboratory testing condition, models for resilient modulus, etc.). Although this method is simple and the validation with CAPTIF data is encouraging, quantifying errors produced by this assumption for different material types is needed.

On the other hand, the ARBB interpretation method (Vuong 2000) takes into account permanent strain developed in the previous stages and starts the loading stage with an equivalent number of cycles that produced the previous permanent strain (see Appendix 2, Section A2.8). This method is more theoretically correct than the Arnold method and, therefore, can be applied for all material types (including quality base materials, marginal materials for sub-base and subgrade). Through comparisons of predicted base deformation with the measured surface deformation measured in the CAPTIF tests (see Section 6.8), the predicted base deformations were shown to be slightly lower than the measured rut depth and produced a similar long-term rate of rutting (slope) after that.

For the purpose of predicting permanent deformation, the number of loading cycles per stress stage should be as high as practical. The Austroads RLT test method requires only 10,000 cycles per stress stage, thus enabling a 3-stage permanent strain test to be completed in 11 hours testing time (at the loading rate of 2 seconds per cycle using low-cost pneumatic RLT testing facilities). However, to complete a 3-stage permanent strain

test with 50,000 cycles per stress stage, as suggested in the 1995 RLT test method and the Nottingham test method, would require up to 55 hours testing time in using low-cost pneumatic RLT testing facilities. Alternatively, high-cost hydraulic RLT testing facilities can be used to increase the loading rate (say 1 second per cycle), thus reducing the testing time by half.

9.4 Summary

Comparison of RLT testing equipment and test methods used by ARRB and Nottingham University indicated that they had different requirements such as RLT testing equipment (triaxial cell, measurement devices, software), sample preparation methods (e.g. dynamic and vibratory compaction), and testing procedures (load pulse, stress levels, number of loading cycles, drained or undrained). Quantifying the effects of testing equipment, sample compaction method and testing procedure was difficult at this stage. However, based on experience gained in the development of both routine and research RLT test methods at ARRB, it was possible to select a practical RLT test method for deformation prediction which meets the material requirements in New Zealand. The recommendation is that :

- Specimens of 150 mm diameter × 300 mm high are used for maximum particle size of up to 40 mm.
- Vibratory compaction is used to prepare New Zealand materials
- Two LVDTs mounted on the sample end caps to measure the average permanent strain for the whole sample be used for practical reasons.

Higher loading speed can be used to reduce the testing time (say maximum 5 cycles per second) for long-term permanent strain testing (> 50,000 loading cycle per stress stage). However, no study has been done to assess the reliability and reproducibility of test results produced by RLT testing equipment at such high loading speed. Therefore, the recommendation is that an inter-laboratory study is conducted to check the performance of the loading equipment, control software and measuring equipment for the high speed RLT testing equipment for standardisation purposes.

.

10. Proposed material assessment methods for alternative materials

10.1 Modified Austroads/ARRB RLT test method

Based on the results of the validation of available methods of performance assessment for granular materials (see Chapters 5, 6 and 7) and further discussions on the effects of predicted pavement stresses and RLT test methods on base deformation prediction (see Chapters 8 and 9), the proposal is to incorporate the modified Austroads/ARRB RLT test method (see Appendix 2 and Table 10.1) for ranking materials and prediction of field base deformation into *TNZ M/22* (2000) *Notes for the evaluation of unbound road base and sub-base aggregates*.

This test method (with the use of dynamic compaction to prepare laboratory specimens) has already been subjected to inter-laboratory precision studies (Vuong et al. 1998) for the purpose of standardisation of testing equipment and test procedures for 20 mm maximum particle size base materials. Vuong & Yeo (2004) demonstrated that the predicted ranking of base materials were similar to the rankings observed from ALF testing.

Also demonstrated in this report is that the methods can be extended to 40 mm maximum particle size base materials (with the use of a larger sample size of 150 mm diameter and 300 mm high and vibratory compaction to prepare laboratory specimens) to select base materials (at their operating conditions of density and moisture content) for the different pavement categories of low, medium, and high traffic.

Table 10.1 Proposed material assessment methods using 1-D RLT testing for New Zealand condition.

Feature	Modified Austroads/ARRB method	Simplified Arnold rut depth model
Material type	Maximum particle size of 20–40 mm	Maximum particle size of 20-40 mm
Sample size	150 mm diameter and 300 mm length	150 mm diameter and 300 mm length
Sample preparation	Vibratory Hammer Compaction test in NZS 4402:1986	Vibratory Hammer Compaction test in NZS 4402:1986
Target density-	95% Vibratory MDD (TNZ B/2:1997) or Specified field dry density	Specified field dry density
Moisture condition	Fully saturated condition or optimum moisture content (OMC) or Specified field operating moisture content	Specified field-operating moisture content

Table 10.1 (continued)

Features	Modified Austroads/ARRB method	Simplified Arnold rut depth Model
1-D RLT test apparatus (vertical loading pulse)	Austroads specifications for loading pulse (trapezoidal pulse with 0.2 s load and 1.8 s rest) and software to control the load and record the data are recommended for both pneumatic and hydraulic loading facilities	To suit available RLT hydraulic equipment and control software in New Zealand* Sinusoidal pulse at 5 times a second (5 Hz) using hydraulic equipment*
Triaxial Cell and instrumentation	Austroads specifications of loafing friction and loading piston-top cap connections when using external load cell and 2 LVDTs mounted between loading caps to measure whole-sample strain	Austroads specifications of loading friction and loading piston-top cap connections when using external load cell and 2 LVDTs mounted between loading caps to measure whole-sample strain On-sample measurement method*
Drainage condition	Drained	Drained condition (no pore pressure measurement) Undrained condition (with pore pressure measurement)*
Stress conditions for permanent strain testing	Austroads requirements of 3 stages on one specimen with constant confining stress of 50 kPa and deviator stresses of 350 kPa, 450 kPa and 550 kPa	4 stages on one specimen (see Table 2.1)
Number of specimens required	1 specimen per target density and moisture condition	1 specimen per 4 stress stages per target density and moisture condition
Number of loading cycles	10,000 cycles per stress stage	50,000 cycles per stress stage
Interpretation of test results	Behaviour rating based on trend of permanent strain with loading cycles for simple material ranking method, or ARRB total permanent strain model using a load equivalency rule to take into account permanent strain developed in previous loading stages	Still undecided between ARRB permanent strain model and Arnold (2004) incremental permanent strain model. The former is accurate, but more complex; whereas the latter method is simpler, but requires further validation using RLT test results and field performance
Assessment methods	Compare permanent strain and resilient modulus with values of standard materials which have known field performance	Compare predicted base deformation with design limits of base deformation**

* Still require interlaboratory precision study to standardise test equipment and testing procedures.

** Still require laboratory and field results to define the limits of base deformation for different pavement classes

10.2 Proposed RLT material test method and simplified rut depth model based on Arnold (2004)

Requirements of RLT testing equipment and test procedures that are suitable for base deformation prediction are given in Table 10.1. Based on the results of predicted base deformation for standard pavements in Chapter 8, it is also proposed to select the cross section of 400 mm granular material over a subgrade CBR of 5 for predicting performance as the most typical for a new pavement in New Zealand. The pavement stresses in this pavement are to be used as a basis for selecting a reduced set of RLT stresses as given in Table 10.2. They are also be used to calculate permanent strain at different depths in the pavement as given in Table 10.3.

Thus the following steps are proposed to evaluate the suitability of a material for use in the top 200 mm of the pavement:

- **Step 1:** Conduct multi-stage RLT permanent strain test as specified in Table 10.2.

Table 10.2 Proposed RLT permanent strain testing for base deformation prediction.

RLT Testing Stress Stage	1	2	3	4
Deviator stress - q (MPa)	0.180	0.270	0.330	0.420
Mean stress - p (MPa)	0.150	0.150	0.250	0.250
Cell Pressure - σ_3 (MPa)	0.090	0.060	0.140	0.110
Cyclic Vertical Loading Speed	Sinusoidal at 5 Hz	Sinusoidal at 5 Hz	Sinusoidal at 5 Hz	Sinusoidal at 5 Hz
Number of Loads (*N*)	50,000	50,000	50,000	50,000
[1]Calculate Permanent Strain Rate from 25k to 50k load cycles (*treat each stage separately*)	$(\varepsilon_{p50k} - \varepsilon_{p25k})$ /(25,000)	$(\varepsilon_{p50k} - \varepsilon_{p25k})$ /(25,000)	$(\varepsilon_{p50k} - \varepsilon_{p25k})$ /(25,000)	$(\varepsilon_{p50k} - \varepsilon_{p25k})$ /(25,000)

[1] Multiply permanent strain rate by 100 and then by 10^6 to obtain units of % per 1 M load cycles.

- **Step 2:** Determine model parameters to compute permanent strain rate using Microsoft Excel Solver or similar to determine parameters *a*, *b* and *c* for Equation 10.1 using data obtained in the RLT tests in Step 1. Parameter *b* is assumed to equal 15.0 for ease of analysis as determined in Section 7.2 for the reduced data set. Units of stresses *q* and *p* are in MPa

$$\varepsilon_{p(rate)} = e^{(a)}\, e^{(bp)}\, e^{(cq)} - e^{(a)}\, e^{(bp)} \quad - \qquad \text{(Equation 10.1)}$$

- **Step 3:** Determine rutting rate for standard cross section using pavement stresses as given in Table 10.3.

Table 10.3 Proposed pavement stresses for calculation of base deformation.

Depth (mm)	Thickness T (mm)	p (MPa)	q (MPa)	$\varepsilon_{p(rate)} = e^{(a)} e^{(bp)} e^{(cq)} - e^{(a)} e^{(bp)}$	$T * \varepsilon_{p(rate)}/100^*$
23	31.5	0.540	0.284		
40	19.5	0.372	0.412		
62	24.0	0.277	0.424		
88	25.5	0.218	0.390		
113	24.5	0.178	0.344		
137	25.0	0.149	0.295		
163	25.0	0.127	0.252		
187	26.0	0.110	0.216		
215	30.0	0.095	0.183		
247	34.0	0.081	0.151		
283	34.0	0.068	0.125		
315	32.0	0.058	0.105		
347	33.5	0.050	0.091		
382	39.0	0.042	0.081		
				Rutting Rate Σ	

* divide by 100 if $\varepsilon_{p(rate)}$ is in %

- **Step 4:** From rutting rate determine number of load cycles to 15 mm rut depth using Equation 10.2.

$$N = (15 - C)/Rate \qquad \text{(Equation 10.2)}$$

where:

N = load cycles in units of millions if *Rate* is in mm per 1 million

C = 5 mm being the initial rutting that occurs in a new pavement caused by consolidation, compaction and conditioning by traffic

Rate = rutting rate determined from step 2, usually in mm per 1M load cycles

Currently, the simplified Arnold rut depth model for base incremental deformation prediction has the potential to provide estimates of deformation of a base layer of various thicknesses (at its operating conditions of density and moisture content), which can be used to justify the material selection for use in the pavement categories of low, medium, and high traffic. However, a number of issues need to be addressed, particularly in the quantification in the quantification of errors produced by:

- different pavement stress prediction models,
- different interpretation methods of test data obtained with the multi-stage permanent strain test,
- different laboratory compaction methods, which may arise in the use of different material types, different pavement configurations, different loading configurations and different moisture environments.

11. Summary and recommendations

The work used available field performance data in New Zealand to calibrate and validate the following selected material assessment methods based on laboratory RLT testing:

- a simple performance assessment method developed at ARRB (Vuong 2000) to predict field performance (in terms of terminal deformation behaviour, deformation life and layer deformation) from a reduced set of permanent strain results obtained from the existing Austroads RLT test method for material specifications,
- a rut depth model developed in 2004 by Arnold at the University of Nottingham to predict field performance (in terms of incremental deformations of unbound granular pavements for various loading periods) using a full set of RLT permanent strain results at 12 different stress levels,
- a simplified Arnold rut depth model (by considering only the rate of deformation between 25–50 k-cycles and a reduced RLT data set representing only four different stress levels) to rank materials for use in material specifications.

11.1 Austroads/ARRB simple performance assessment method

In the Austroads/ARRB simple performance assessment method, a range of pavement cross sections were analysed using a two-dimensional Finite Element Model (FEM) (VMOD-PAVE) under a design vehicle load of 40 kN on a single tyre to select representative pavement stresses at different depths (base, upper sub-base and lower sub-base). These representative stresses were applied in the Austroads RLT permanent strain test to determine permanent strains, which were then converted into simple indices such as terminal deformation behaviour, deformation life and layer deformation. In the validation of the Austroads/ARRB material assessment methods using pavements tested with CAPTIF 40 kN axle load in New Zealand, laboratory material rankings were found to be consistent with the rankings based on field performance. However, different laboratory compaction methods also produced different predictions of deformation life and base deformation. Therefore, in the current form, the simple Austroads/ARRB method can only be used to rank the performance of granular bases. Further research on the effects of laboratory compaction is required to enable field deformation life and layer deformation to be accurately predicted for pavement design.

11.2 Arnold rut depth method

The Arnold rut depth model required a large RLT testing programme (full data set) to obtain permanent strain data at various stress levels in the pavement. The RLT testing equipment and test procedures used in this method were different from those adopted in the Austroads RLT test method. However, this method used a simple two-dimensional FEM model (DEFPAV) to predict pavement stresses and a simple procedure to estimate incremental permanent strains for various loading periods from the RLT multi-stage permanent strain testing. In the calibration/validation of the Arnold rut depth model using

17 actual pavements (15 pavements tested with CAPTIF in New Zealand and 2 in-service pavements in Ireland), the model could not consistently and accurately predict field deformations, particularly for pavements with thick asphalt surfacing layers (> 40 mm). However, trends in rut depth progression (i.e. slope after 500 k-cycles) between the predicted and measured rut depth curves were similar for some 11 pavements out of the 17 pavements studied.

11.3 Simplified Arnold rut depth model

To simplify the Arnold rut depth model, the total number of RLT stages (12 stages) as required by this model was reduced to four. Some difficulties were encountered in fitting the 3-parameter incremental permanent strain model (as adopted in the Arnold rut depth model) using only four data points, but these was overcome by fixing one of the variables. Comparison of predicted incremental base deformations for the period 20–50 k-cycles and the field values measured in the above 17 actual pavements also indicated that they were significantly different (i.e. the predicted incremental deformations in the range of 2 to 110 mm/10^6 cycles as compared with field values in the range of 0.6 to 6.0 mm/10^6 cycles).

11.4 Comparison of stress prediction models

Comparison of two FEM stress prediction models DEFPAV (used in the Arnold rut depth model) and VMOD-PAVE (used in the ARRB/Austroads simple performance prediction models) indicated that DEFPAV is too simple and is likely to produce large errors in the predicted stresses. Comparisons of predicted incremental base deformations for the period 20–50 k-cycles using the same RLT data set but different pavement stresses predicted with DEFPAV and VMOD-PAVE indicated that the effects of predicted stresses on the base deformation prediction were very significant. The use of pavement stresses predicted with VMOD-PAVE appeared to produce base incremental deformations closer to field values. By using the pavement stresses calculated with VMOD-PAVE, the simplified Arnold rut depth model was found to rank the material performance in the same order as found in the CAPTIF tests. Therefore, the recommendation is to use VMOD-PAVE to predict stresses in base layers for the selection of RLT test stresses for prediction of base deformation.

11.5 Comparison of equipment and methods

Comparison of RLT testing equipment and test methods used by ARRB and Nottingham University indicated that they had different requirements such as RLT testing equipment (triaxial cell, measurement devices, software), sample preparation methods (e.g. dynamic and vibratory compaction), and testing procedures (load pulse, stress levels, number of loading cycles, drained or undrained). Quantifying the effects of testing equipment, sample compaction method and testing procedure was difficult at this stage. However, based on experience gained in the development of both routine and research RLT test methods at ARRB, selecting a practical RLT test method for deformation prediction which meets the material requirements in New Zealand was possible. The recommendation is that :

- specimens of 150 mm diameter × 300 mm high are used for maximum particle size of up to 40 mm,
- vibratory compaction is used to prepare New Zealand materials,
- two LVDTs are mounted on the sample end caps to measure the average permanent strain for the whole sample, for practical reasons,
- higher loading speed can be used to reduce the testing time (say maximum 5 cycles per second) for long-term permanent strain testing (> 50,000 loading cycle per stress stage). However, no study has been done to assess the reliability and reproducibility of test results produced by RLT testing equipment at such high loading speeds. Therefore, an inter-laboratory study should be conducted to check the performance of the loading equipment, control software and measuring equipment for the high speed RLT testing equipment for standardisation purposes.

11.6 Recommendations

1. Based on the results of the validation of available methods of performance assessment for granular materials and further discussions on the effects of predicted pavement stresses and RLT testing equipment and test methods on deformation prediction, the recommendation is that the Austroads/ARRB RLT test method for material specifications is tentatively incorporated into *TNZ M/22* (2000) *Notes for the evaluation of unbound road base and sub-base aggregates* with the following modifications:
    - A large triaxial specimen size of 150 mm diameter and 300 mm high should be used for 40 mm maximum particle size base materials.
    - The triaxial specimen should be prepared using vibratory compaction to suit the material types used in New Zealand.

2. This test method was already subjected to inter-laboratory precision studies (Vuong et al. 1998) for the purpose of standardisation of testing equipment and test procedures for 20 mm maximum particle size base materials. Results in this report have also demonstrated that the methods can be extended to 40 mm maximum particle size base materials. However, further research is required to determine the acceptance parameters for New Zealand pavement conditions.

3. No RLT test has been conducted using the simplified Arnold rut depth model. Therefore, further research should be conducted to evaluate it against the Austroads/ARRB RLT test method. This test method should also be subjected to a precision study for standardisation purposes to ensure that the testing equipment and test procedure can produce repeatable and accurate test results.

4. Density and moisture conditions for RLT testing should be similar to field conditions and RLT testing should be conducted in a drained condition to enable field performance to be correctly predicted. The undrained condition may not be the same as long-term moisture conditions in conventional bases (with protection against moisture penetration), unless the bases were specifically designed to soak up moisture in very wet conditions. Further, because of the severe pore pressure effects on deformation

under undrained saturated conditions, the use of this condition is not recommended when the objective is to accurately model permanent deformation in the pavement.

5. Given the difficulties in measuring pore pressure accurately in partially-saturated granular materials in both field and laboratory conditions, assessing the differences between field and laboratory conditions and quantifying the effects of pore pressure for various material types is difficult. No inter-laboratory study has been done on undrained RLT testing to standardise the test equipment and testing procedures. Therefore, a need exists to improve the method for pore pressure measurement in partially saturated material and to standardise the test equipment and test procedures of the undrained RLT before the introduction of this test method for practical use.

6. Further research should also be undertaken to improve deformation prediction models. A number of research issues need to be addressed in this area, particularly the quantification of errors produced by:

    - different pavement stresses prediction models,
    - different interpretation methods of test data obtained with the multi-stage permanent strain test,
    - different laboratory compaction methods, which may arise in the use of different material types, different pavement configurations, different loading configurations and different moisture environments.

12. References

Alabaster, D., de Pont, J., Steven, B. 2002. The fourth power law and thin surfaced flexible pavements. *International Conference on Asphalt Pavements 5:* 1-4. Copenhagen, Denmark.

Arnold, G. 2004. *Rutting of granular pavements*. PhD thesis. University of Nottingham: England, UK.

Arnold, G., Alabaster, D., Steven, B. 2001. Prediction of pavement performance from repeat load triaxial tests on granular materials. *Transfund New Zealand Research Report No. 214.* Transfund New Zealand: Wellington, New Zealand.

Arnold, G., Steven, B., Alabaster, D., Fussell, A. 2005a. Effect on pavement wear of an increased mass limits for heavy vehicles – Stage 3. *Land Transport New Zealand Research Report 279*. Land Transport New Zealand: Wellington, New Zealand.

Arnold, G., Steven, B., Alabaster, D., Fussell, A. 2005b. Effect on pavement wear of an increase in mass limits for heavy vehicles – concluding report. *Land Transport New Zealand Research Report 281*. Land Transport New Zealand: Wellington, New Zealand.

Austroads. 1992. *Pavement design - A guide to the structural design of road pavements*. Austroads: Sydney, Australia.

Austroads. 2004. *Austroads Pavement Design Guide*. Austroads: Sydney, Australia.

BSI (British Standards Institution). 1990. *BS 1377-4:1990. Methods of tests for soils for civil engineering purposes. Compaction related tests*. British Standards Institution: London, UK.

Chiu, H.K. 1982. Program VMOD4 for finite element nonlinear elastic analysis of foundation. *Research Report 82-02-G*. Department of Civil Engineering, Monash University: Melbourne, Australia.

de Pont, J.J. 1997. OECD DIVINE Project - Element 1. Longitudinal Pavement Profiles. *Research Report 708.* Industrial Research Limited: Auckland.

de Pont, J.J., Pidwerbesky, B.D. 1995. The impact of vehicle dynamics on pavement performance. *Fourth International Symposium on Heavy Vehicle Weights and Dimensions: 323-332*. University of Michigan Transportation Research Institute: Ann Arbor, Michigan, USA.

de Pont, J.J., Pidwerbesky, B.D., Steven, B.D. 1996. The influence of vehicle dynamics on pavement life. *Fourth Engineering Foundation Conference on Vehicle-Infrastructure Interaction*. San Diego, California, USA.

de Pont, J., Steven, B., Alabaster, D., Fussell, A. 2001. Effect on pavement wear of an increase in mass limits for heavy vehicles. *Transfund New Zealand Research Report No. 207*. Transfund New Zealand: Wellington, New Zealand. 55pp.

de Pont, J., Steven, B., Alabaster, D., Fussell, A. 2002. Increase in mass limits effect on pavement wear – Stage 2. *Transfund New Zealand Research Report No. 231*. Transfund New Zealand: Wellington, New Zealand. 50pp.

Dodds A., Logan T., McLachlan, M., Patrick, J. 1999. Dynamic load properties of New Zealand basecourse*. Transfund New Zealand Research Report No. 151*. Transfund New Zealand: Wellington, New Zealand.

Guezouli, S., Elhannani, M., Jouve, P. 1993. NOEL: a non linear finite element code for road pavement analysis. Flexible pavements. Ed. A. Gomes Correia. Technical University of Lisbon. *Proceedings of the European Symposium Euroflex*: *20-22.* Lisbon, Portugal.

Hicks, R.G. 1970. *Factors influencing the resilient properties of granular materials*. PhD thesis. University of California, Berkeley: Berkeley, California, USA.

Kenis, W.J. 1978. Predictive design procedures. VESYS users manual: an interim design method for flexible pavements using VESYS structural subsystem. *Final report No. FHWA-RD-77-154*. United States Federal Highway Administration: Washington DC, USA.

Snaith, M.S., McMullen, D., Freer-Hewish, R.J., Shein, A. 1980. *Flexible pavement analysis.* Contracted Report to Sponsors, European Research Office of the US Army.

Standards Australia. 1995. *AS 1289.6.8.1 – Methods of testing soils for engineering purposes. Soil strength and consolidation tests – determination of the resilient modulus and permanent deformation of granular unbound pavement materials.* Standards Australia: Sydney, Australia.

Standards New Zealand. 1986. *NZS 4402. 4.1.3:1986. Soil compaction tests – Determination of the dry density/water content relationship – Test 4.1.3 New Zealand vibrating hammer compaction test*. Standards New Zealand: Wellington, New Zealand.

Steven, B. 2005. Repeated load triaxial testing of CAPTIF materials conducted at Transportation Laboratory of the University of Canterbury. Contract Report for ARRB Group (unpublished).

TNZ (Transit New Zealand). 1997. *TNZ B/2 – Specification for construction of unbound granular pavement layers.* (Since replaced by B/02:2005.) Transit New Zealand: Wellington, New Zealand.

TNZ (Transit New Zealand). 1995. *TNZ M/4 – Specification for crushed basecourse aggregate*. Transit New Zealand: Wellington, New Zealand.

TNZ (Transit New Zealand). 2000. *TNZ M/22 (provision Notes 1 and 2) – Notes for the evaluation of unbound road base and sub-base aggregates*. Transit New Zealand: Wellington, New Zealand.

Transport South Australia. 2000. *Standard specification for supply and delivery of pavement materials. Revision 1.0, TSA 2000/02428.*

University of Nottingham. 2003. Laboratory operating procedures. 11.18: Tiaxial testing. Unpublished internal document of Nottingham Centre for Pavement Engineering, University of Nottingham: Nottingham, UK.

Vuong, B.T. 1985a. Non-linear finite element analysis of road pavements. *Australian Road Research Board (ARRB) Internal Report, AIR 403-5*.

Vuong, B.T. 1985b. Permanent deformation and resilient behaviour of a Victorian crushed rock using the repeated load triaxial test. *Internal Report No. AIR 403-6, 1985-04.* Australian Road Research Board: Vermont South, Victoria, Australia

Vuong, B.T. 1986. Non-linear finite element analysis of road pavements. *Australian Road Research Board (ARRB) Report No. ARR 138.*

Vuong, B.T. 1987. Mechanical response properties of road materials obtained from the ALF pavement test section at Benalla, Victoria. *AIR 403-10*. Australian Road Research Board: Vernont South, Victoria, Australia.

Vuong, B.T. 1992. Influence of density and moisture content on dynamic stress-strain behaviour of a low plasticity crushed rock. *Road and Transport Research 1(2):* 88-100.

Vuong, B.T. 1998. Effects of anisotropy and stress on repeated load triaxial test results. *Proceedings of the Fifth International Conference on the Bearing Capacity of Roads and Airfields 3:* 1301-1313. July 1998. Trondheim, Norway

Vuong. B.T. 2000. *Technical basis in the development of the Austroads repeated load triaxial test method (APRG 00/33) and assessment method of granular materials*. ARRB Transport Research Ltd. Working Document (unpublished).

Vuong, B.T. 2001a. Improved characterisation of unbound pavement materials– development, validation and implementation. *20th ARRB Conference*.

Vuong, B.T. 2001b. *Improved performance-based material specifications and performance prediction models for granular pavements*. PhD thesis. Department of Civil and Geological Engineering, Faculty of Engineering, RMIT University: Melbourne, Australia.

Vuong, B.T. 2003a. Development of performance-based specifications for unbound granular materials – Part A: Issues and Recommendation. *Austroads AP-T29*. Austroads: Sydney, Australia.

Vuong, B.T. 2003b. Development of performance-based specifications for unbound granular materials – Part B: Use of RLT test to predict performance. *Austroads AP-T30*. Austroads: Sydney, Australia.

Vuong, B.T. 2004. Incorporation of laboratory performance tests into performance-based specifications for unbound granular materials. *Road and Transport Research 13(3):* 3-24.

Vuong, B.T. 2005a. Initial development of models to predict pavement wear under heavy vehicles. Report for Austroads Project No: T+E.P.N.537 (unpublished).

Vuong, B.T. 2005b. Effects of axle loads on single tyre and tyre-surface contact pressures on the prediction of pavement stresses, strains and deflections using VMOD-PAVE. Working document (Unpublished).

Vuong. B.T., Brimble, R. 2000. Austroads Repeated Load Triaxial Test Method – Determination of permanent deformation and resilient modulus characteristics of unbound granular materials under drained conditions. *APRG 00/33 (MA)* June.

Vuong, B.T., Brimble, R., Yeo, R., Sinadinos, C. 1998. Some aspects in the development of the standard repeated load triaxial testing equipment and test procedures for characterisation of unbound granular materials. *ARRB Transport Research Ltd Conference, 19th, 1998, Sydney, New South Wales, Australia:* 178-204 (Session C).

Vuong, B.T., Hazell, D. 2003. Development of performance-based specifications for unbound granular materials: issues and recommendations. *Road and Transport Research 12(4):* 13-25.

Vuong, B.T., Kinder, D.F. 1984. A deformation measurement device for use in repeated load triaxial tests. *Australian Road Research Board (ARRB). Internal Report No. AIR 403-2.* 14pp.

Vuong, B.T., Yeo, R. 2004. *Performance of granular pavements with thin surface seals – measured versus prediction.* Presentation at the UNBAR Conference, Nottingham, UK.

Wardle, L.J. 1980. *Program CIRCLY user's manual*. CSIRO Div. Applied Geomechanics: Melboune, Australia.

Appendix 1 TNZ laboratory RLT test method for performance-based specifications

A1.1 Methodology

Transit New Zealand specification *TNZ M/22 – Provisional Notes 1. Notes for the evaluation of unbound road bases and sub-base aggregates* (TNZ 2000) allows the use of RLT testing in the evaluation of unbound road base aggregates to relax the compliance of grading, sand equivalent and broken face.

In principle, *TNZ M/22* specifies that:

- the laboratory triaxial specimen shall be prepared using the Vibratory Hammer Compaction test in NZS 4402 to a target design density of 95% Vibratory MDD as specified in Transit New Zealand Specification TNZ B/2:1997.
- RLT testing shall be performed on the compacted specimen at an undrained, fully saturated condition (or at optimum moisture content if it can be demonstrated through the design of within-pavement drainage that full saturation of the pavement materials will not occur over the life of the pavement).

A granular material is accepted for base construction if it shows shakedown deformation behaviour.

The RLT testing method and criteria for material assessment adopted in *TNZ M/22* are briefly described below. Problems associated with the use of this specification for alternative materials are also identified and discussed.

A1.2 Description of the TNZ RLT test method

TNZ M/22 specifies that RLT testing be carried out to standards as specified in the 1995 Australian Standard *AS 1289.6.8.1 –1995 Methods of testing soils for engineering purpose: soil strength and consolidation tests – determination of the resilient modulus and permanent deformation of granular unbound pavement materials* (Standards Australia 1995), with some special conditions as described below.

A1.2.1 Sample size

TNZ M/22 specifies that the specimen size shall be 150 mm diameter, 300 mm length for all materials with maximum particle size in the range of 20–40 mm, and when using 40 mm top size aggregate the material shall not be scalped.

A1.2.2 Sample preparation and target density-moisture conditions

The specifications are quoted in Section A1.1. In both cases, the pore pressure at rest shall be measured and reported.

A1.2.3 Specifications of testing equipment and software

Similar to the 1995 Australian Standard RLT test method, *TNZ M/22* permits the use of one-dimensional RLT test apparatus (with repeated vertical stress and static confining

pressure and only axial strain measurement) to eliminate the difficulties in the design and operating of testing equipment for complex 3-D repeated loading condition (with both repeated vertical stress and confining pressure and axial and radial strains measurement). However, the equipment specifications are loosely defined, viz. the allowance of :

- various repeated loading facilities to apply vertical loading pulses,
- various triaxial cells with different loading frictions,
- simple measurement devices such as external load cells and external LVDTs (mounted on the loading rod) to measure applied load and sample displacement, respectively.

Stricter equipment specifications were required in the new 2000 Austroads RLT test method (Vuong & Brimble 2000) to provide more reliable test results.*TNZ M/22* also requires measurement of pore pressure. However, no guideline is available on the effects of pore pressure on RLT test results.

A1.2.4 Testing procedures

Permanent strain testing

Similar to the 1995 Australian Standard RLT test method, *TNZ M/22* specifies 50,000 cycles of a specified stress level (that is typical in the base or upper sub-base or lower sub-base) per test specimen in the testing of permanent deformation.

The stress condition for the permanent deformation test shall be the same as or more severe than a deviator stress of 425 kPa and a confining stress of 125 kPa. The sample shall be unconsolidated.

Multi-stage resilient modulus testing

No multi-stage testing for resilient modulus was specified in *TNZ M/22*.

A1.3 Material assessment method

Typical test results for a standard base material obtained with the *TNZ M/22* RLT test method are given in Figure A1.1.

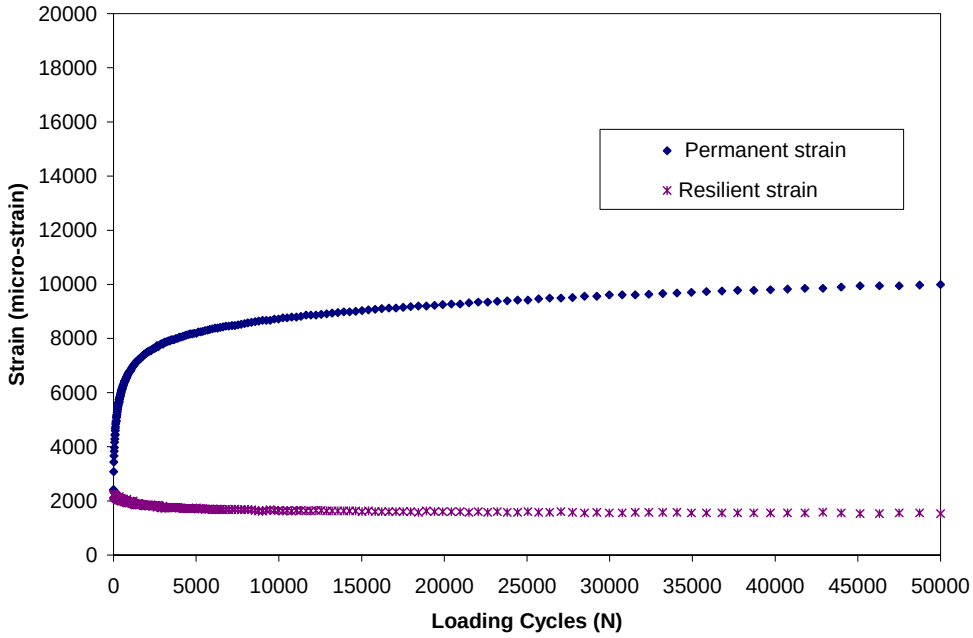

Figure A1.1 Typical results obtained from permanent deformation testing.

The basecourse is considered to have passed if:

- the results of permanent strain RLT test shows the basecourse material exhibits stable behaviour. Stable behaviour is defined as a decreasing rate of permanent strain accumulation on a permanent strain v number of cycles graph,
- it satisfies a minimum soaked CBR requirement of 80%.

A1.4 Discussion

Effectively, the adoption of the RLT testing in the current TNZ performance-base specifications (TNZ 2000) is based on the assumption that the minimum design requirement of pavement performance will be achieved if the basecourse material exhibits stable deformational behaviour under a cyclic vertical deviator loading of 425 kPa and a constant confining stress of 125 kPa on a sample compacted to 95% vibratory compaction and a maximum moisture condition of 100% saturation under undrained conditions.

The above assumption was derived by testing aggregates that are routinely used in New Zealand pavements as complying with Transit New Zealands specification for basecourse aggregate (*TNZ M/4*) along with an aggregate being deliberately contaminated with 10% silty clay fines and thus not complying with *TNZ M/4* specification for basecourse aggregate. Results are in Dodds et al. (1999) which showed that 100% saturation with undrained conditions resulted in early failure of the contaminated sample while the complying aggregates passed. In this study there was no attempt to determine the magnitude of rutting; the triaxial test was simply used as a pass-fail test.

Studies by both Vuong (2004) and Arnold (2004) found it is necessary to determine the deformation performance in the triaxial apparatus for a range of stress conditions to cover

combinations of vertical and horizontal stresses present in a pavement under a wheel load. For example, Arnold (2004) found that the stress conditions at a depth of 150-200 mm where the vertical loading is less than 250 kPa but the horizontal confining stress is nearly nil caused the largest amount of deformation within the pavement. This is because a granular material has very little tensile strength and requires horizontal confinement to have the necessary strength to support the load. Thus the loading in the current *TNZ M/22* specification may not be the most severe loading in the pavement. However, the most severe loading is material-dependent and it can only be determined by multi-stages RLT tests at a range of stress conditions by modelling and interpretation of extrapolation. This research will aim to develop the most appropriate set of test stress conditions to ensure confidence in the method of material assessment.

Note that *TNZ M/22 – Provisional Notes 1* also allows the contractor to change all of the conditions of the RLT test if it can be demonstrated that the test conditions chosen are more accurate and more representative of the in-service conditions. However, no guidance is available for determination of in-service conditions (in terms of moisture content, density and stress levels).

Other concerns are associated with:

- uncertainty as to whether the materials selected based on the current specifications (RLT test result and minimum soaked CBR requirement of 80%) may have the capacity to withstand the higher stresses placed by new heavy vehicles,
- loosely defined specifications of loading equipment that may produce unreliable test results.

Appendix 2 2000 Austroads laboratory RLT test method for performance-based specifications (Vuong 2000)

This appendix reproduces in full (with modified numbering) an unpublished working document (Vuong 2000). Sections A2.4 and A2.5 are used in Sections 3.2 and 3.2.5.1 of this report.

A2.1 Methodology

The 2000 Austroads repeated load triaxial (RLT) test method for the determination of permanent deformation and resilient modulus characteristics of unbound granular materials (Vuong & Brimble 2000) has been developed as part of an Austroads funded project: *Development of performance-based specifications of unbound granular materials*. The RLT test results are considered to predict field performance, if laboratory conditions of dry density, moisture content and loading stresses are similar to field conditions. A brief description follows of the test method and procedures for assessment of material performance using the results obtained from the test method.

A2.2 Description of the 2000 Austroads RLT test method

The equipment specifications, sample preparation and testing procedures are briefly described below.

A2.2.1 Equipment specifications

Figure A2.1 shows the standard 1-D repeated load triaxial test apparatus, which is used to test standard specimens of 100 mm diameter and 200 mm length for unbound pavement materials with a maximum particle size not exceeding 19 mm.

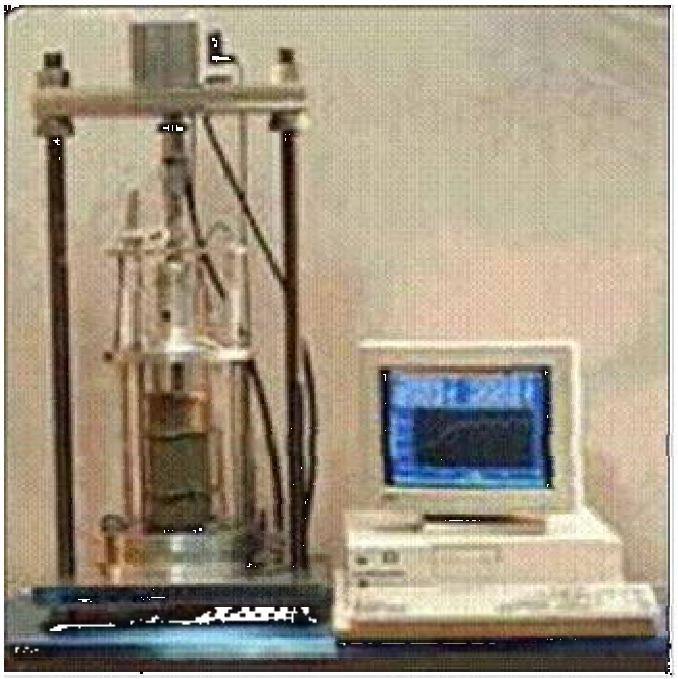

Figure A2.1 Standard repeated load triaxial testing apparatus.

The following modifications to the 1995 Australian Standard RLT testing equipment (Standards Australia 1995) were made to improve the repeatability and reproducibility of the test results:

- Loading friction in the triaxial cell is reduced so that no correction is necessary for the effects of loading friction on the measured resilient modulus.
- Sample resilient strain and permanent deformation are measured with two 5 mm internal displacement transducers mounted between the top and bottom loading caps to reduce errors caused by noise, system deflection and sample bending. Large sample permanent deformation (>5 mm) can be measured with a 20 mm displacement transducer mounted externally on the loading shaft.
- The loading system is improved to effectively control dynamic vertical stress (by reducing static seating stress to <2 kPa) and static confining stress (by reducing the dynamic stress to <1 kPa with the use of an air–water interface).
- Software is improved to control dynamic vertical stress and static confining stress, and record and report their loading characteristics (static seating stress, noise level, etc.) during resilient modulus and permanent strain testing. The 10 points running average filtering technique (rather than the 2 points running average) was incorporated into the software to further reduce noise levels and hence increase the allowable ranges of applied stress and sample stiffness.

A2.2.2 Sample size

As in the 1995 Australian Standard RLT test method, specimen size of 100 mm diameter and 200 mm length is used to determine permanent deformation and resilient modulus of unbound pavement materials with a maximum particle size not exceeding 19 mm.

Oversize materials can be used, provided that the weight of particles exceeding 19 mm shall be less than 5% total weight and replaced by 19 mm top size aggregate to maintain a similar grading.

A2.2.3 Sample preparation and target density-moisture conditions

The 1995 Australian Standard RLT test method permits various laboratory sample preparation methods using different compaction methods (static, dynamic and vibratory) to prepare the triaxial specimen to target design density and moisture conditions. However, Vuong (1998) has demonstrated that different compaction methods (static, dynamic, vibratory and gyratory) produce different results of resilient modulus and permanent deformation. In the absence of field moduli and permanent strain data, it was decided that only one sample preparation procedure, the dynamic compaction method, would be used in the 2000 Austroads RLT test method, with the possibility of including other methods when more reliable field data became available.

As both permanent deformation and resilient modulus test results are significantly dependent on the density and moisture condition of the specimen (Vuong 1992), it is important that the specimen should have the target moisture and density ratios. It has been found that experienced operators can prepare specimens within the tolerances of 0.5% for density ratio and 0.5% for moisture ratio using the dynamic compaction method. Nevertheless, such differences in density and moisture ratios can significantly

affect the test results of permanent strain and resilient modulus. Therefore, it is recommended that:

- If the test is performed at a single density and moisture combination, at least two specimens prepared to the target density and moisture ratios shall be tested to check the repeatability of the test results. The average values and the maximum differences of density ratio, moisture ratio, permanent strain and resilient modulus between tested specimens shall be reported.
- If multiple tests are performed at different density and moisture conditions to obtain a full characterisation of the material for the purpose of material ranking and specifications, one specimen per density and moisture combination is required. (For material characterisation, it is recommended that testing is conducted at a minimum of three (3) moisture and three (3) density conditions.) However, in the New Zealand context this level of testing is not practical nor realistic given limited budgets for testing.

As RLT tests are expensive, generally the ranges of moisture content and compaction levels is limited and sometimes only one moisture content and compaction test is used. Therefore, in New Zealand, the compaction level for RLT testing in *TNZ M/22* was set as the minimum allowable level in compaction of unbound granular bases (*TNZ B/2*) and a fully saturated condition specified. However, it is recommended that at least one RLT test is repeated at a moisture level less than saturated but typical of in-service conditions to determine the influence of moisture of permanent deformation.

A2.2.4 Testing procedures

The 1995 Australian Standard RLT test method specifies 50,000 cycles of a specified stress level (that is typical in the base or upper sub-base or lower sub-base) per test specimen in the testing of permanent deformation. However, multi-stage testing procedures are used in this test method to determine permanent strains and resilient modulus under different loading regimes for the assessment of their stress-dependent characteristics. This allows better performance assessment procedures to be developed for selecting material types to be used at different depths in the pavement.

Multi-stage permanent strain testing procedure

A multi-stage loading procedure is used to determine permanent strain at different stress levels. In this procedure, the specimen is to be loaded with three stress stages, each involving 10,000 cycles at a stress condition of specified dynamic deviator stress and static confining stress.

Table A2.1 suggests the required values of the dynamic deviator stress and static confining stress for the stress stages 1, 2, and 3 are obtained from for the following types of materials:

- base materials (0 to 150 mm below the pavement surface),
- upper sub-base materials (150 to 250 mm below the pavement surface),
- lower sub-base materials (>250 mm below the pavement surface).

These stress levels cover ranges of deviator stress, stress ratio and mean stress for the purpose of examining the stress-dependent permanent strain characteristics of the material to be tested.

Table A2.1 Stress levels for permanent strain testing (material ranking and specifications).

Permanent deformation stress levels						
Stress stage number	**Base**		**Upper sub-base**		**Lower sub-base**	
	σ_3 (kPa)	**σ_d (kPa)**	**σ_3 (kPa)**	**σ_d (kPa)**	**σ_3 (kPa)**	**σ_d (kPa)**
1	50	350	50	250	50	150
2*	50	450	50	350	50	250
3	50	550	50	450	50	350

σ_3 = confining stress or cell pressure
σ_d = deviatoric stress or cyclic vertical load
* Design stress level

Each of the three stress stages selected is tested as follows:

(i) For the first stress stage:

a. Apply the static confining pressure to the specimen for 30 minutes to allow for pre-consolidation.

b. While holding the static confining pressure apply cycles of loading and unloading of the respective dynamic vertical stress for 10,000 cycles.

c. Record at least 13 reading sets of applied stresses, vertical resilient displacements and vertical permanent displacements at approximately 1, 5, 10, 20, 50, 100, 200, 250, 500, 1000, 2000, 5000, and 10 000 cycles.

(ii) For the second stress stage, apply cycles of loading and unloading of the respective dynamic vertical stress for 10,000 cycles and record at least 10 reading sets of applied stresses, vertical resilient displacements and vertical permanent displacements at approximately 10 500, 11 000, 12 500, 13 500, 14 500, 15 500, 16 500, 17 500, 18 500 and 20 000 cycles.

(iii) For the third stress stage, apply cycles of loading and unloading of the respective dynamic vertical stress for 10,000 cycles and record at least 10 reading sets of applied stresses, vertical resilient displacements and vertical permanent displacements at approximately 21 000, 22 000, 23 000, 24 000, 25 000, 26 000, 27 000, 28 000, 29 000 and 30 000 cycles.

It should be noted that the RLT stress level in Stage 2 for each layer represents typical in-service stress conditions under a 40 kN axle load on a single wheel that are expected to produce similar permanent strain in the layer concerned; whereas the RLT stress levels in Stages 1 and 3 are used to assess permanent strain for underloading and overloading conditions. The method for selecting these stress levels is discussed in details in Technical Note 1 (Appendix 2, Section A2.7 of this report).

Resilient modulus testing

In addition to the values of resilient modulus determined in the multi-stage permanent strain testing, a multi-stage loading procedure is also used to determine resilient moduli at 66 different stress levels. In this procedure, provided that the specimen is still in elastic condition, it can be loaded with a series of selected stress stages, each involving at least 50 cycles at the stress condition of specified dynamic deviator stress and static confining stress.

The following criteria are used to check the elastic condition of the specimen before each resilient modulus testing stage:

(a) When using the same specimen as used for determination of permanent strain testing, the following conditions shall be met before any resilient modulus testing stage:

(i) The specimen shall have a total permanent strain of less than 80% of failure strain (or 1% strain).

(ii) The resilient strain shall not substantially increase with increasing loading cycles during any previous permanent strain testing stages, i.e. the difference between the final and initial resilient strains for each permanent stage shall not be higher than 10% of the initial resilient strain for the stage concerned.

The specimen that does not meet these tolerances must be discarded and a new specimen must be prepared for resilient modulus testing. Do not re-use material from a previously compacted and tested specimen.

(b) During the multiple stress-stage resilient modulus tests, the resilient modulus determined for a repeated stress stage shall not be more than 15% lower than those determined at any previous permanent strain and resilient modulus testing stages with the same stress conditions. The stress stage that does not meet these tolerances must be reported separately and noted as a failure condition. All subsequent stress stages that follow a failure stress stage shall be reported in the same manner.

Table A2.2 suggests the required values of the dynamic deviator stress and static confining stress for 66 stress stages selected for base materials. These stress levels cover ranges of deviator stress, stress ratio and mean stress for the purpose of examining the stress-dependent resilient modulus characteristics of the material to be tested. Included within the 66 stress stages are several duplicate stress states for the purpose of checking the elastic condition of the test specimen throughout the multiple loading stress stages. The loading stages shall be applied in sequential order as shown in Table A2.2 to reduce the rate of early failure that could occur during the 66-stage testing.

For upper and lower sub-base materials, which may have a low strength, the number of stress stages may be reduced to those that have a stress ratio of (σ_d/σ_3) below the failure stress ratio. Other stress levels may be specified for fine-grain subgrade, of which modulus is not sensitive to confining pressure, if required.

Table A2.2 Stress levels for resilient modulus (material ranking and specifications).

Resilient modulus stress levels					
Stress stage number	**σ_3 (kPa)**	**σ_d (kPa)**	**Stress level number**	**σ_3 (kPa)**	**σ_d (kPa)**
0	50	100	33	40	250
1	75	150	34	30	210
2	100	200	35	40	280
3	125	250	36	50	350
4	150	300	37	75	525
5	100	200	38	40	280
6	50	150	39	20	150
7	75	225	40	30	245
8	100	300	41	40	325
9	125	375	42	50	400
10	150	450	43	30	245
11	75	225	44	20	185
12	40	125	45	30	275
13	30	100	46	40	370
14	40	150	47	50	450
15	50	200	48	30	275
16	75	300	49	20	225
17	100	400	50	30	335
18	125	500	51	40	450
19	75	300	52	50	550
20	30	125	53	20	250
21	20	100	54	30	375
22	30	150	55	40	500
23	40	200	56	20	300
24	50	250	57	30	450
25	75	375	58	40	600
26	100	500	59	30	500
27	50	250	60	20	350
28	30	180	61	30	550
29	50	300	62	20	375
30	75	450	63	30	575
31	50	300	64	20	400
32	30	180	65	20	500

For each of the 66 stress stages selected, apply and hold the static confining pressure to the specimen, then apply cycles of loading and unloading of the respective deviator stress for pre-conditioning before resilient modulus determination as specified below.

Pre-conditioning is to be performed for each resilient modulus test to allow the end caps to bed into the specimen and/or to allow the applied stresses and resilient strains to stabilise under the imposed stress condition before the measurements of the stresses and

strains for the determination of resilient modulus at the stress condition concerned. The number of loading cycles for pre-conditioning to be used for each stress condition will depend on the previous stress history applied to the specimen and the elastic condition of the specimen.

(i) 1000 cycles of pre-conditioning shall be used for the first stress stage applied to a new specimen that has no previous pre-conditioning (permanent strain testing).

(ii) At least 50 cycles pre-conditioning shall be used for any subsequent loading stage after that first stress stage or after the permanent strain testing.

For each cycle after the pre-conditioning stage, record the applied stresses, vertical resilient displacements and vertical permanent displacements for the calculation of resilient modulus. Continue the application of the loading/unloading cycles until the resilient modulus values determined from the last six results change by less than 5% of the mean value of those six results or until 200 cycles at each stress level have been completed.

Report the last mean values of stresses, vertical resilient strains and vertical permanent strain and resilient modulus.

A2.3 Typical results

A2.3.1 Permanent strain

Figure A2.2 shows typical results obtained from permanent strain testing using the standard RLT test method *APRG 00/33*.

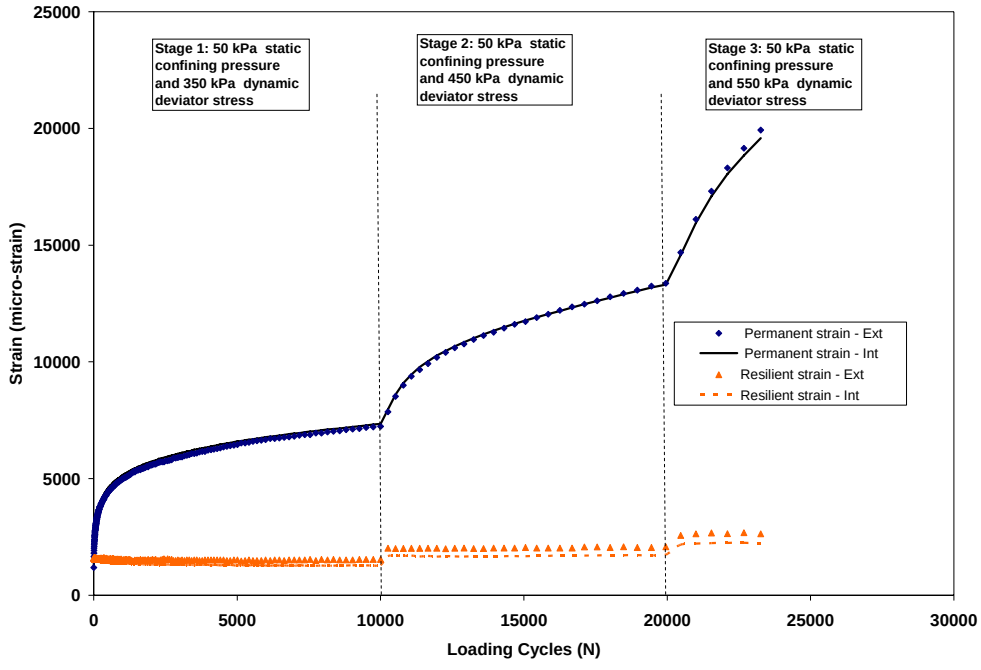

Figure A2.2 Typical results obtained from permanent deformation testing (for base material to be used at depth of 0–150 mm below the surface).

Based on the test results, permanent strain values at the end of each stress condition can be extracted for the assessment of relative performance between various materials, i.e. comparing with typical permanent strain values for traditional materials that have known field performance.

In addition, three simple methods for performance assessment based on observed behaviour, deformation life and estimated base deformation are given in Sections A2.4.1, A2.4.2, and A2.4.3.

A2.3.2 Resilient modulus

Figure A2.3 shows typical results obtained from resilient modulus testing.

From the test results, test values at representative stress conditions in the base, upper sub-base and lower sub-base can be extracted for the assessment of relative performance between various materials, i.e. comparing with typical resilient modulus values for traditional materials that have known field performance.

Alternatively, models of resilient modulus can be derived from the resilient modulus test results (Vuong 1985a, 2001a, 2004) and then used as input into pavement models, such as linear elastic layered model NONCIRL (CIRCLY-based) and FEM model VMOD-PAVE (Vuong 2001a, 2004), to predict the critical stresses and strains in bound (surface) layers and subgrade, which can be used to assess the pavement performance, in terms of design file based on the Austroads semi-empirical performance models (Austroads 1992, 2004).

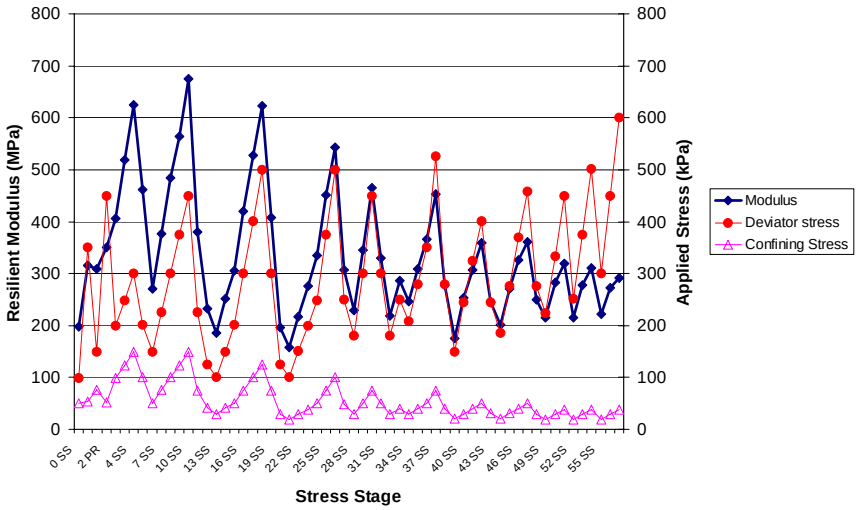

Figure A2.3 Typical results obtained from resilient modulus testing (for granular materials to be used in base, upper sub-base and lower sub-base).

A2.4 Performance assessment procedures

Three procedures have been developed to assess the material performance using the results of the 3-stage permanent strain test as shown in Figure A2.2. They are based on different methods of interpretation of the multi-stage permanent strain test results, namely basic material behaviour, deformation life and estimated base deformation as briefly described below.

A2.4.1 Performance assessment based on material behaviour

In principle, the material performance can be judged based on three basic material behaviour modes that can exhibit at a given loading stress as follows:

- Stable behaviour is defined as a decreasing permanent strain rate and decreasing to constant resilient strain with increasing loading cycles.
- Unstable behaviour is defined as a deceasing to constant permanent strain rate and constant to increasing resilient strain with increasing loading cycles.
- Failure behaviour is defined as a constant to increasing rate of permanent strain and increasing resilient strain with increasing loading cycles or when the total permanent strain reach a nominal failure strain observed in static triaxial shear test (say in the range of 15 000 – 20 000 microstrain).

Table A2.3 summarises the proposed requirements of material behaviour exhibiting in the 3-stage permanent strain test, which can be used to select a base material for use in different pavement classes subjected to light, medium and heavy traffic.

- For pavements subjected to light traffic ($<10^6$ ESA), it is considered appropriate to allow a constant deformation rate in the base layer at the design stress level in the base layer under a 40 kN wheel load (Stage 2). In this case, the basecourse is considered to have passed if the results of permanent strain RLT test show that the basecourse material exhibits stable behaviour in Stage 1 and unstable behaviour in Stage 2.
- For pavements subjected to medium traffic (10^6–10^7 ESA), where potential occurs for higher traffic loads, it is considered appropriate to allow a decreasing deformation rate in the base layer at the critical stress level in the base layer under a 40 kN wheel load (Stage 2). In this case, the basecourse is considered to have passed if the results of permanent strain RLT test show that the basecourse material exhibits stable behaviour in Stage 2, and may exhibit failure in Stage 3.
- For pavements subjected to heavy traffic, where potential occurs for stresses in the pavement to reach the stresses in Stage 3, it is considered appropriate to allow a decreasing deformation rate in the base layer at the stress level in Stage 3. In this case, the basecourse is considered to have passed if the results of permanent strain RLT test show that the basecourse material exhibits stable behaviour in Stage 2 and unstable behaviour in Stage 3.

Table A2.3 Requirements of material behaviour in the 3-stage permanent strain for different pavement classes (for base materials at depth 0-150 mm below the surface).

Stage	Loading stress (kPa)		Behaviour requirement to pass		
	Static confining	Dynamic deviator	$<10^6$ ESA	10^6-10^7 ESA	$>10^7$ ESA
Stage 1	50	350	Stable	Stable	Stable
Stage 2*	50	450	Unstable	Stable	Stable
Stage 3	50	550	Failure	Unstable to failure	Stable to unstable

*Design stress level

A similar procedure is used for the assessment of upper sub-base and lower sub-base materials. In addition, comparison of resilient modulus is also made for material ranking (on the basis of subgrade deformation protection).

This assessment procedure is very simple and is suitable for material specifications.

A2.4.2 Performance assessment based on deformation life

In principle, the material performance can be judged based on number of loading cycles at a given loading stress to reach failure condition or deformation life.

In this case, a curve fitting procedure is required (see Technical Note 2, Section A2.8 of this report) to determine the relationships between permanent strain and loading cycle for different stress levels applied in the 3-stage loading test. From the relationship for each stage, the number of loading cycles to reach a nominal failure strain (say 15,000 microstrain) can be calculated and plotted against the applied stress as shown in Figure A2.4. The loading cycles to failure at the design stress in Stage 2 (or design deformation life) and deformation lives for other stress levels outside the tested stress range (e.g. strength or stress that causes failure in one cycle) can be determined by means of extrapolation for material performance assessment.

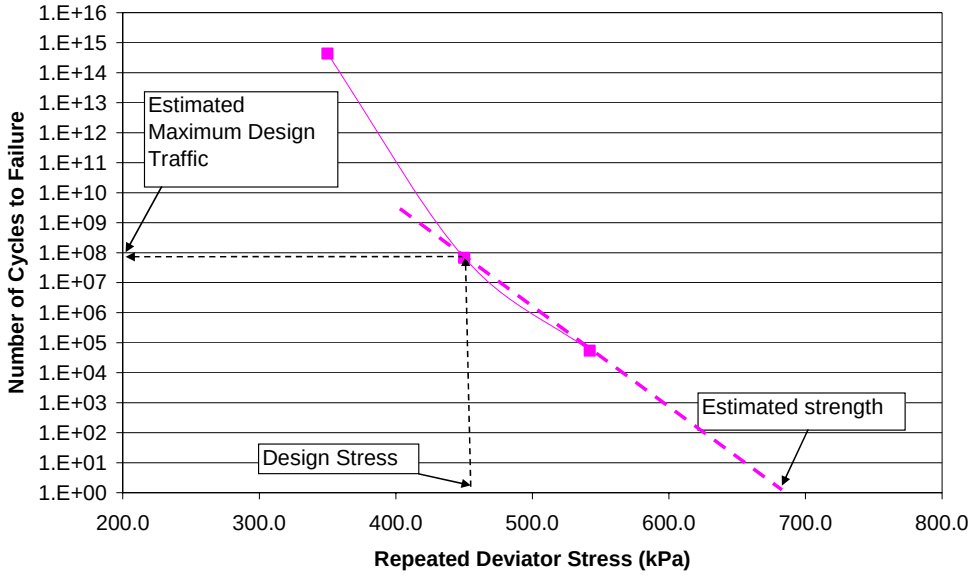

Figure A2.4 Material deformation lives determined at different stress levels (for base material to be used at depth of 0-150 mm below the surface).

Figure A2.5 also shows the proposed the requirements of deformation life for base materials to be used in different pavement classes (which are subjected to different design lives). Each curve is defined by:

- the minimum design deformation life at the critical design stress in Stage 2 and strength limits (stress that cause failure in one cycle),

- the design deformation life at the design stress, which is the same as the design traffic life,
- the material strength, which is selected based on current practice in material selection for different pavement classes, using low quality materials with low strength (say < 600 kPa) in low-traffic local roads (<10^5 ESA) and high quality materials with high strength (say >800 kPa) in high class heavy-duty roads (>10^7 ESA).

In this case, the basecourse is considered to have passed for a specific pavement design life if the results of permanent strain RLT test show that the basecourse material shows greater deformation lives for the 3 loading stages than the required minimum deformation lives (i.e. on the right hand side of each curve to be selected for design life concerned).

Examples of two materials A and B are also shown in Figure A2.5. Material A is considered to have a better performance than material B as the results of permanent strain RLT test show that material A produces higher deformation lives for all stress levels. In addition, based on the proposed requirements of deformation life, material A is considered suitable for pavements with a design traffic of <10^7 ESA; whereas material B is be suitable for pavements with a design traffic of <10^6 ESA.

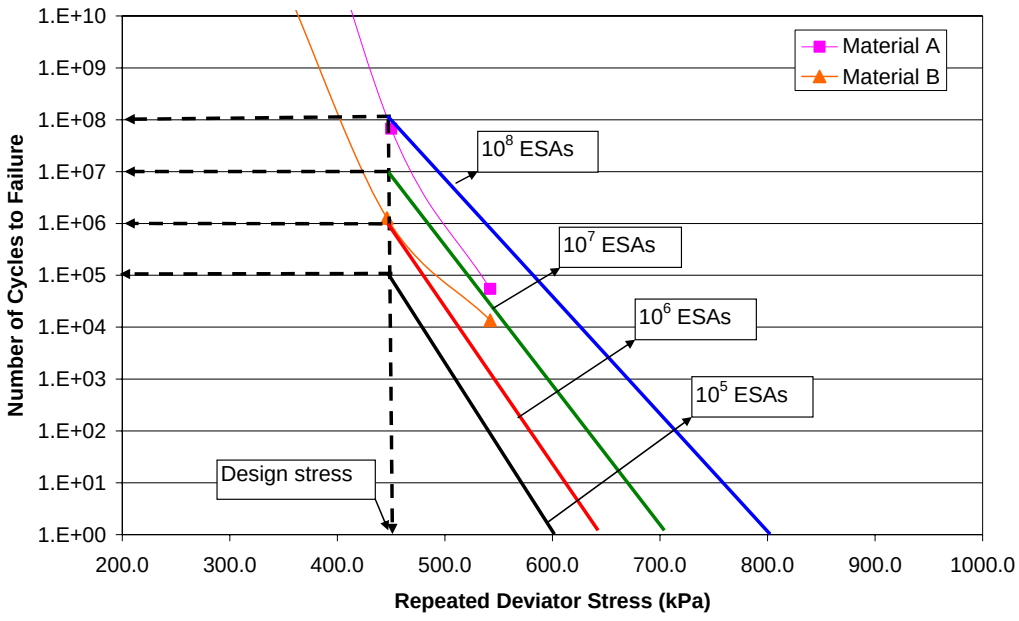

Figure A2.5 Requirements of design deformation life and strength for different pavement classes (for base material to be used at depth of 0-150 mm below the surface).

This method is more versatile than the assessment method based on material behaviour (see Section A2.4.1) as it can be used for a designated pavement design life.

A2.4.3 Performance assessment based on estimated base deformation

Alternatively, the relationships between permanent strain and loading cycle for each stress level derived from the 3-stage permanent strain test (see Section A2.4.2) can be used to predict deformations of a granular layer with sprayed seal at a given design traffic life (expressed in terms of loading cycles of standard axle loads, N) using a simple rule, i.e. deformation of each base (or upper sub-base or lower sub-base) layer being the product of permanent strain at the design stress level ($\varepsilon_{p(Stage2)}$) and the thickness of the layer (ΔH) concerned.

$$\Delta d_{Base} = \varepsilon_{p(Stage2)Base} \times \Delta H_{Base} \quad \text{(Equation A2.1)}$$

$$\Delta d_{Upper\ Sub\text{-}base} = \varepsilon_{p(Stage2)Upper\ Sub\text{-}base} \times \Delta H_{Upper\ Sub\text{-}base} \quad \text{(Equation A2.2)}$$

$$\Delta d_{Lower\ Sub\text{-}base} = \varepsilon_{p(Stage2)Lower\ Sub\text{-}base} \times \Delta H_{Lower\ Sub\text{-}base} \quad \text{(Equation A2.3)}$$

Note that the RLT test stresses selected for each material at a given depth (see Table A2.1) include a design stress (Stage 2), and two stress levels for the layers below and above this depth (Stage 1 and Stage 3). Therefore, they can also be used to calculate deformation of a thicker layer than the specified thickness by sub-layering the layer and summing the deformation of the sub-layers; e.g.

$$\Delta d_{Basetotal} = [\varepsilon_{p(Stage2)Base} \times \Delta H_{Base}] + [\varepsilon_{p(Stage1)Base} \times \Delta H_{Upper\ Sub\text{-}base}] \quad \text{(Equation A2.4)}$$

This method is more suitable for pavement design, where different requirements of base (or sub-base) deformation are specified for different design traffic lives (or different pavement classes.

A2.5 Standardisation and validation

Inter-laboratory studies have been conducted using the simplified RLT test method to standardise the testing equipment and test procedures (Vuong et al. 1998).

A preliminary evaluation of the above ARRB assessment methods has been made using field performance obtained from limited accelerated pavement testing trials at ARRB (Vuong & Yeo 2004). The comparisons of laboratory and field performance in these ALF trials indicated that the three assessment methods can be used to rank material based on relative comparison of deformations rather than absolute deformations. However, a concern was that stress conditions in actual granular pavement layers under rolling wheel loads are different from those in laboratory RLT testing conditions. Therefore, it may be desirable that the laboratory-determined permanent strain be corrected for the differences between the laboratory and field loading condition, if the predicted performance is shown to be different from field performance.

It was also proposed (Vuong 2003b) that the above ARRB assessment methods should be validated using:

- interim specification limits derived based on results of a testing programme of typical traditional base materials with known field conditions and performance,

- field performance obtained for various field conditions of density and moisture content.

A2.6 Discussion

As discussed in Vuong (2003b), the proposed laboratory RLT tests for shear strength, permanent deformation and resilient modulus do not address all required material attributes (such as material durability, desired finish surface characteristics for traffic, suitability for sprayed seal surfacing, suitability for a given construction process, product variability, etc.). They are only used to determine the above material performance measures for the design of granular mixes before production. Therefore, other index tests and test limits, as currently adopted for traditional materials in the 'recipe-based' material specifications, will be retained.

Also as discussed in Vuong (2003b), it is considered necessary to conduct RLT performance tests for shear strength, permanent deformation and resilient modulus at different combinations of density-moisture and different load levels to take into account:

- different field conditions of density and moisture contents for various material types, construction standards and drainage designs,
- different levels of performance assessment in terms of performance at construction stages and during the service life,
- limitations of the candidate performance test simulating actual field loading conditions,
- stress-dependent characteristics of unbound materials.

However, it is also imperative to reduce testing and analysing efforts in those procedures to make the performance test acceptable for material specifications as well as for pavement design.

Within the above context, the simplified RLT test method and simple material assessment procedures were developed to select materials to used at different depths (base, upper sub-base and lower sub-base) in sprayed seal surfacing granular pavements.

Inter-laboratory studies have been conducted using the simplified RLT test method to standardise the testing equipment and test procedures (Vuong & Brimble 2000). Evaluation of the ARRB assessment methods has recently been made using field performance obtained from limited accelerated pavement testing trials at ARRB (Vuong & Yeo 2004). The comparisons of laboratory and field performance in these ALF trials indicated that the three assessment methods can be used to rank material performance.

However, no work has been done to validate the ARRB simple assessment methods for materials and pavement conditions in New Zealand. It may be desirable that the test method be modified for larger material size used in New Zealand (40 mm nominal size) and a different compaction method (say vibratory compaction) to suit these materials. It should be noted that stress conditions in actual granular pavement layers under rolling

wheel loads are very complicated. Therefore, it may also be desirable that the laboratory-determined permanent strain and modulus be corrected for the differences between the laboratory and field compaction and loading conditions, if the predicted performance is shown to be different from field performance. The recommendation is that the ARRB simple performance model be validated with recent CAPTIF field trials as a precursor to a more extensive investigation on its suitability for practical use.

Note that, as part of the current Austroads research programme, ARRB has also developed a general response and deformation prediction model (Vuong 2005a) to predict pavement response (stresses, strains and deflections) and surface/subsurface deformations under actual vehicle loading configurations with or without wander.

In principle, the general Pavement Deformation Prediction model uses the same approach, i.e. conducting a pavement analysis using a FEM computer program to predict recoverable (elastic) strains and stresses in the pavement under the specified load. The predicted vertical strains (and/or stresses) are then used to calculate the vertical permanent strains using relationships between vertical permanent strain and vertical strains (and/or stresses), which were determined from RLT testing. The vertical permanent strains are integrated and summed to obtain a surface deformation. However, they are more accurate with the use of:

- more comprehensive 2-D and 3-D FEM models (namely VMOD-PAVE and Strand7) that have been developed to take into account the effects of residual horizontal stress from compaction, mean stress, shear stress, and stress limits for failure and no-tension (Vuong 2005a). These FEM models require material data from various laboratory testing methods, including K_o triaxial compression test, triaxial shear test and RLT resilient modulus test.
- general relationships between vertical permanent strain and vertical strains (and/or stresses) that have also been developed for all material types (Vuong 2005a). They also requires a large amount of data from the RLT permanent strain testing.

Currently, validation of these models has been undertaken utilising field trials tested with ALF (Vuong 2005a). Given that insufficient laboratory data exist for the use of these FEM and permanent strain models to predict field performance obtained from CAPTIF trials, the ARRB general Response and Deformation Prediction models will not be validated against field performance obtained from CAPTIF trials in this study.

A2.7 Technical note 1: Method for selection of RLT stresses

This technical note describes the method for selecting the RLT test stresses for different material types to be used as base (at depth of 0–150 mm below the surface), upper sub-base (at depth of 150–250 mm below the surface) and lower sub-base (at depth below 250 mm) in sprayed seal surfacing granular pavements.

A2.7.1 Methodology

Pavement stresses in sprayed seal surfacing pavements were estimated using non-linear 2-D axis-symmetrical Finite Element Models VMOD-PAVE (Vuong 1985a, 2000). In the

FEM analysis, typical granular pavements with thin sprayed seals were loaded with two loading cases:

- a 20 kN single wheel, with radius of loading area of 95.4 mm and tyre pressure of 700 kPa), which is a quarter of the standard axle load of 80 kN,
- a 40 kN single wheel (with radius of loading area of 135.6 mm and tyre pressure of 700 kPa).

It is expected that the stresses and strains in the granular base layer under the 40 kN standard dual-wheels would be very close to those produced by the above loading conditions.

To reduce the efforts in both laboratory RLT permanent strain testing and pavement analysis, three stress conditions, which are representative of pavement stresses at different depths, are selected for RLT permanent strain testing so that the permanent strain data determined from this minimum data set can be directly used to assess the base performance in the field without performing a pavement analysis.

A2.7.2 VMOD-PAVE (Version 1999)

VMOD-PAVE was developed at ARRB for pavement analysis (Vuong 1986) using the FEM computer program VMOD4 developed at Monash University (Chiu 1982). More details of VMOD-PAVE are given in Vuong (1986).

In this study, VMOD-PAVE (Version 1999) was modified to incorporate the non-linear material model of resilient modulus of the crushed rock base (see Equations A2.5 and A2.6), which was determined using the Austroads laboratory RLT testing method.

$$E = K_1 \times \left(\frac{\sigma_m}{Pa}\right)^{K_2} \times \left(\frac{\tau}{Pa}\right)^{K_3} \qquad \text{(Equation A2.5)}$$

$$E = K_1 \times \left(\frac{\sigma_m}{Pa} + 1\right)^{K_2} \times \left(\frac{\tau}{Pa} + 1\right)^{K_3} \qquad \text{(Equation A2.6)}$$

where:

E	=	resilient modulus (MPa),
σ_m	=	mean normal stress (MPa)
	=	$(\sigma_1 + \sigma_2 + \sigma_3)/3$
τ	=	octahedral shear stress
	=	$[(\sigma_1 - \sigma_2)^2 + (\sigma_1 - \sigma_3)^2 + (\sigma_2 - \sigma_3)^2]^{0.5}/3$
Pa	=	reference stress (atmospheric pressure 0.100 MPa)
K_1, K_2, K_3		experimental test constants

A2.7.3 Typical results of modulus, stress and strain

Figures A2.6, A2.7 and A2.8 show typical results of modulus, stresses and strains determined from an FEM pavement analysis for a granular pavement with 200 mm crushed rock base and 30 mm sprayed seal.

It was noted from analyses of various pavement configurations and material types using the VMOD-PAVE (Version 1999) that predicted vertical stresses in the base layer did not vary much with changes in base thickness (in the range of 200-700 mm). However, horizontal stresses can be significantly influenced by base thicknesses, base materials and subgrade types.

Therefore, it was considered that:

- the FEM-predicted vertical stresses (Figure A2.7a) were more reliable than the horizontal stresses (Figure A2.7b),
- the predicted pavement stresses should be considered as indicative values, but not absolute values for all pavement cases.

It was also noted that maximum vertical strains in the granular base often occur at about 70–130 mm depth (see Figure A2.8a). This influences the selection of representative stress levels that cause damage in the base layer (at depth of 0–150 mm below the surface) as discussed below.

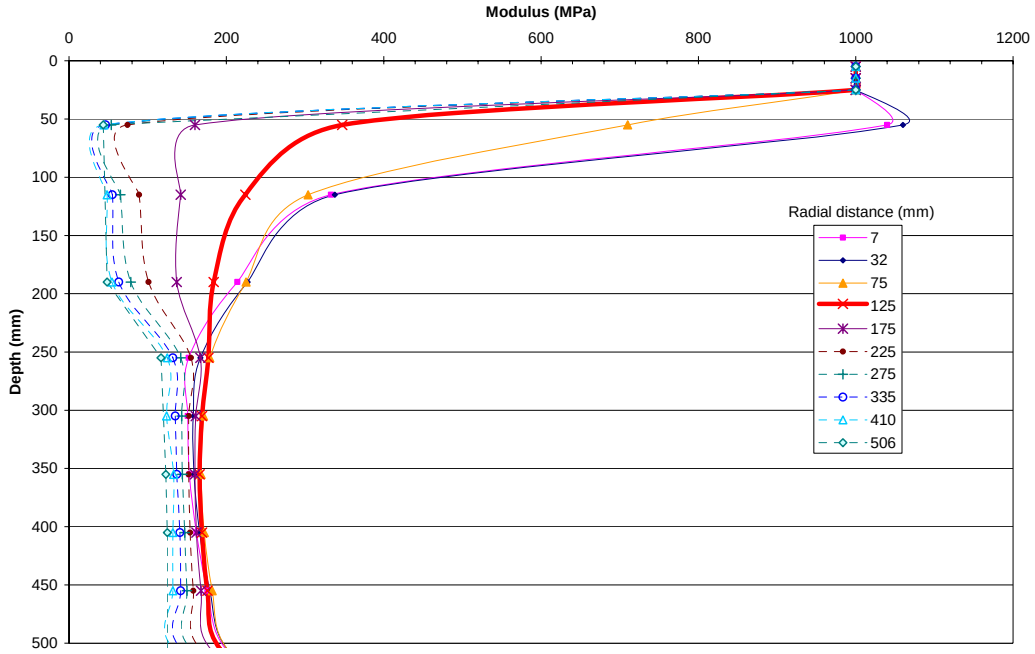

Figure A2.6 Variation of modulus in the crushed rock base under a single wheel with 700 kPa (predicted with FEM).

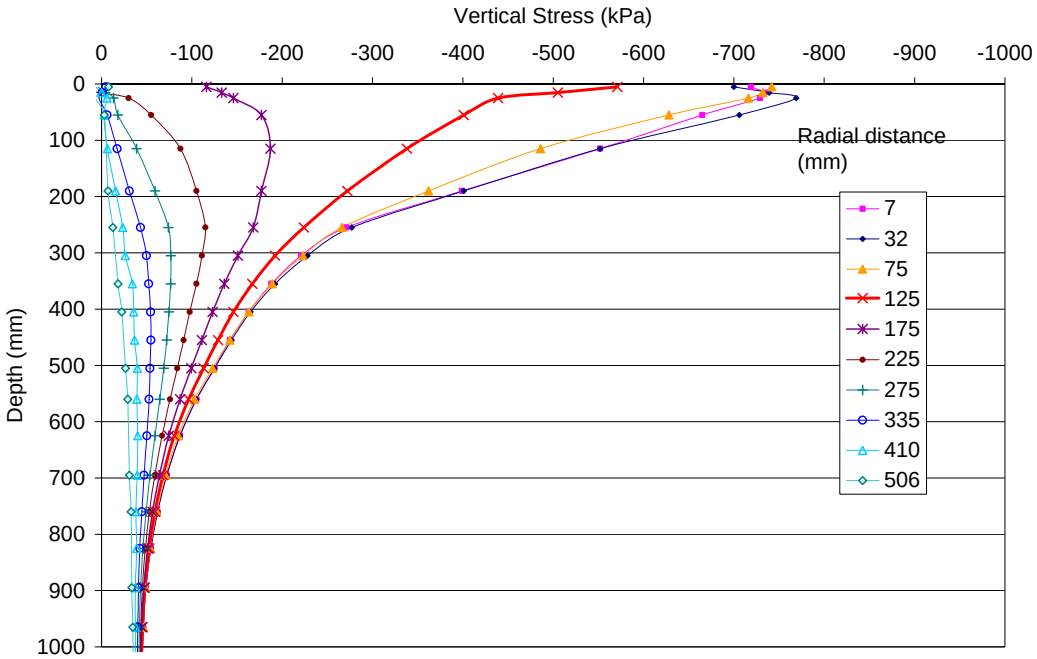

(a) Vertical stresses.

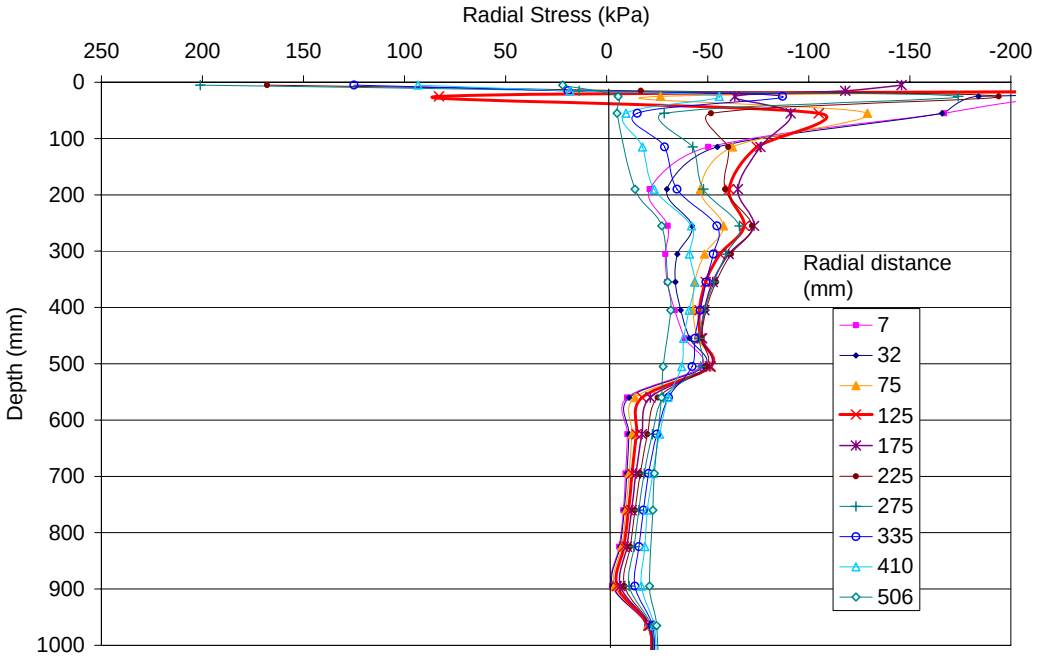

(b) Horizontal stresses.

Figure A2.7 Variation of stresses in the crushed rock base (predicted with FEM, -ve = compression).

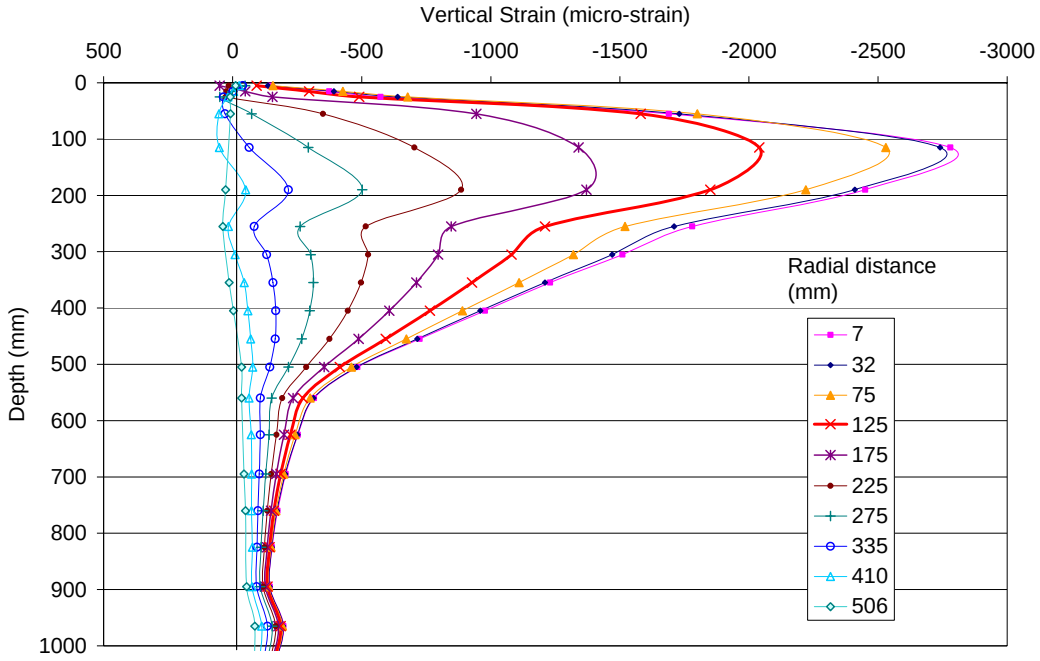

(a) Vertical strains.

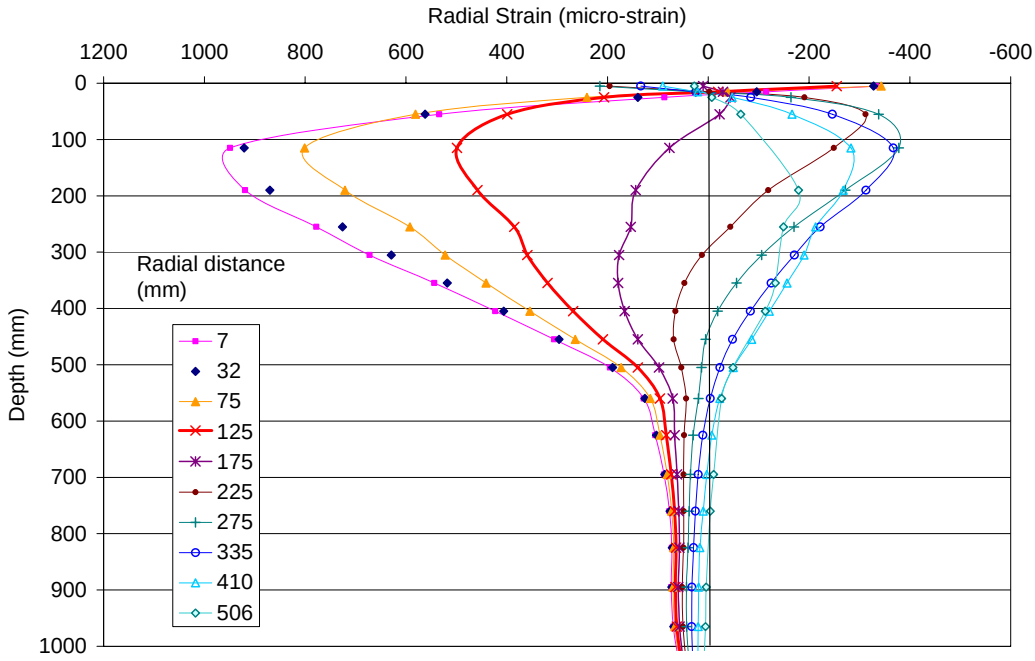

(a) Radial strains.

Figure A2.8 Variation of strains in the crushed rock base (predicted with FEM, -ve = compression).

A2.7.4 Selected RLT test stresses for performance assessment

As discussed previously, for each of the material types to be used at different depths in the pavement (i.e. base, upper sub-base, and lower sub-base), the RLT stress level in Stage 2 represents typical in-service stress conditions under a 40 kN axle load on a single

wheel that are expected to produce similar permanent strain in the layer concerned, whereas the RLT stress levels in Stages 1 and 3 are used to assess permanent strain for underloading and overloading conditions.

In view of the selection of representative stresses for assessment of base, upper sub-base and lower materials to be used at different depths under the design 40 kN axle load, it was considered appropriate to use the maximum vertical strains in the layer as criteria to assess the deformation life of the layer concerned. This approach has been used by Austroads, i.e. the current Austroads subgrade strain criterion is used to assess the pavement deformation life (Austroads 2004). Therefore, the design vertical and horizontal stresses were selected at the location that produces maximum vertical strain.

- For base layer (at depth 0–150 mm below the surface), maximum vertical strain occurs at a depth of 70–130 mm depth and under the centre of the loading area (Figure A2.8a). At this location, the vertical stresses are in the range of 350–450 kPa (Figure A2.7a) and horizontal stresses are in the range of 50-75 kPa (Figure A2.7b).
- For lower sub-base materials (at depth > 250 mm below the surface), maximum vertical strain occurs at the top of the layer and under the centre of the loading area (Figure A2.8a). At this location, the vertical stresses are in the range of 350–450 kPa (Figure A2.7a) and horizontal stresses are in the range of 25–50 kPa (Figure A2.7b).
- For the upper sub-base materials (at depth 150–250 mm below the surface), it was considered that the maximum vertical strains at the middle of the layer can be used as criteria to assess the deformation life of this layer. Figure A2.8a shows that maximum vertical strains at middle of the layer occurred under the centre of the loading area. At this location, the vertical stresses are in the range of 450–550 kPa (Figure A2.7a) and horizontal stresses are in the range of 50–75 kPa (Figure A2.7b).

For simplicity, it was decided to select the design vertical stresses for base, upper sub-base, and lower sub-base as average values of 500 kPa, 400 kPa, and 300 kPa, respectively. An average horizontal stress of 50 kPa was also selected for all base, upper sub-base, and lower sub-base so that they can be applied in a multi-stage permanent strain testing without introducing complications in testing procedure and interpretation of the permanent strain results.

In view of the selection of the RLT stress levels in Stages 1 and 3, which are used to assess permanent strain for underloading and overloading conditions, it was decided that:

- The design stresses selected for the layer directly below the layer concerned be used as the stress level in Stage 1. This would enable assessment of this material if it is to be used in a lower layer.
- The design stresses selected for the layer directly above the layer concerned be used as the stress level in Stage 3. This would enable assessment of this material if it is to be used in an upper layer.

- For the base layer, the vertical stress for Stage 3 was arbitrarily selected as 600 kPa, which produces the same increment of vertical stress between stages. In addition, it reflects an overloading of 20% from the standard loading stress of 700 kPa to 840 kPa that could occur in reality.

The selected RLT test stresses (in terms of static confining stress or cell pressure and deviatoric stress or cyclic vertical load) were summarised in Table A2.1.

Note that further development and validation of VMOD-PAVE has been carried out (Vuong 2005a). This has improved the prediction of pavement stresses and hence, more accurate RLT test stresses. This will be discussed in a later report.

A2.8 Technical note 2: Curve-fitting procedures for permanent strain-loading cycle relationship

This technical note describes a curve-fitting procedure for determining the relationships of permanent strain-loading cycles for different stresses applied in the Austroads RLT three-stage permanent strain test.

A2.8.1 General curve-fitting procedures

Permanent strain-loading cycle relationship for stress level in Stage 1

In the case single stage repeated loading, a simple permanent strain-loading cycle relationship as expressed in Equation A2.7 is used to fit the vertical permanent strain (ε_p) data.

$$\varepsilon_p = \frac{\mu.\varepsilon_r}{\alpha}.N^{\alpha} \qquad \text{(Equation A2.7)}$$

where:

N = number of loading cycles

ε_r = vertical recoverable (resilient) strain predicted with FEM

α, μ = are material parameters, which can vary depending on material type and applied stresses

This empirical law is universally found in both 1-D and 3-D repeated load triaxial testing of unbound granular materials and subgrade (Vuong 1985b, 1986, 1987, 2001a, 2001b) and asphalt (Kenis 1978).

Figure A2.9 shows a typical plot of log(permanent strain) – log(loading cycle) obtained in the first loading stage of the 3-stage permanent strain testing for the crushed rock base. In this case, the model parameters μ and α can be derived by curve fitting with the measured data.

Loading Stage 1: $\varepsilon_p\ (1) = [\mu(1)\times\varepsilon_r(1)/\alpha(1)].\times N^{\alpha(1)}$ (Equation A2.8)

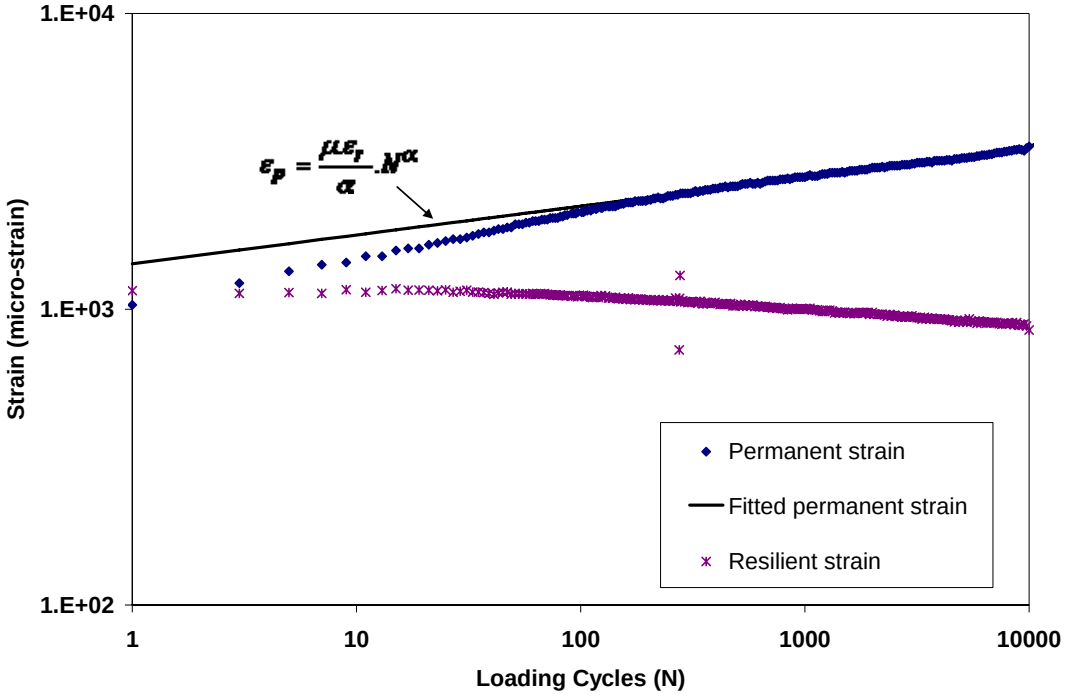

Figure A2.9 Comparison of predicted and measured permanent strain for single-stage loading test (using Equation A2.7).

Permanent strain-loading cycle relationships for stress levels in Stages 2 & 3

The relationships for stresses applied in Stages 2 and 3 are also in forms of:

Loading Stage 2: $$\varepsilon_p\ (2) = [\mu(2) \times \varepsilon_r(2)/\alpha(2)]. \times N^{\alpha(2)}$$ (Equation A2.9)

Loading Stage 3: $$\varepsilon_p\ (3) = [\mu(3) \times \varepsilon_r(3)/\alpha(3)]. \times N^{\alpha(3)}$$ (Equation A2.10)

However, for the stress level applied in Stages 2 or 3 of the 3-stage permanent strain testing, a rule was required to convert the permanent strain occurring at the start of the loading stage to an 'equivalent' number of loading cycles so that the permanent strain-loading cycle curve under constant repeated loading stress can be established and used to derive the model parameters μ and α for the stress level concerned.

In this study, the strain hardening rule loading as illustrated in Figure A2.10 was used to calculate the equivalent number of loading cycles for the second or third loading stage of the 3-stage permanent strain testing.

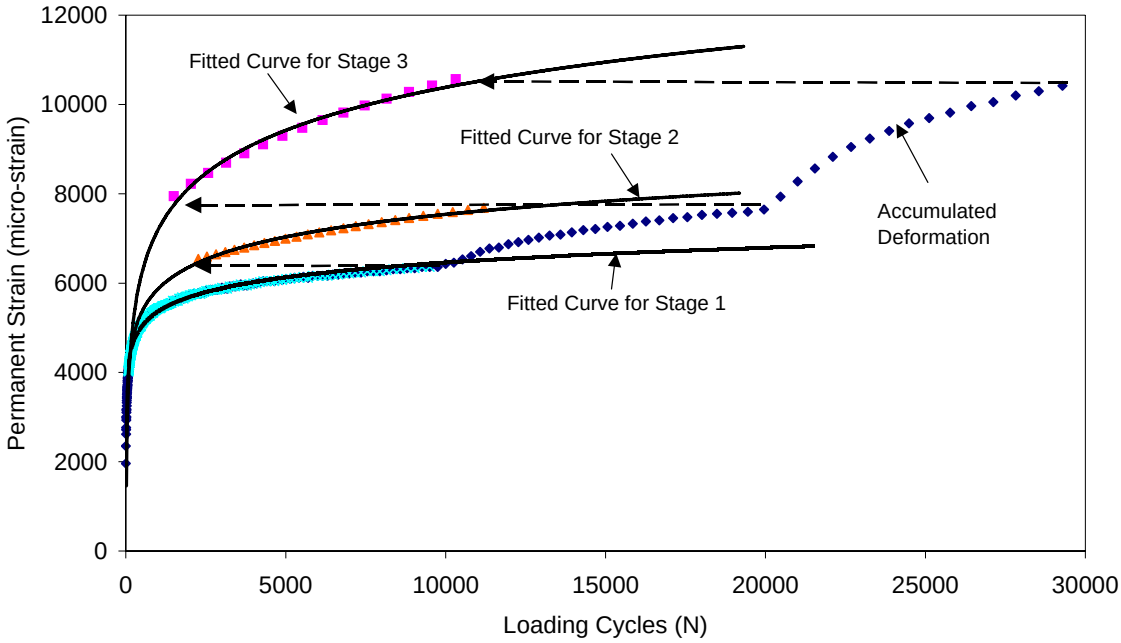

Figure A2.10 Strain hardening rule for calculation of cumulative permanent strain under variable repeated loading stresses.

The permanent strain-loading cycle relationship under constant repeated loading stress for the current stress stage (I) is written as.

$$\varepsilon_{p,Neq}(I) = A(I).Neq(I)^{\alpha(I)} \qquad \text{(Equation A2.11)}$$

where:

I = 1, 2, 3

A(I) = material constant for each stage as defined by Equation A2.12

Neq(I) = equivalent number of loading cycles for each stage (*I*)as defined by Equation A2.14

$$A(I) = \frac{\mu(I)\varepsilon_r}{\alpha(I)} \qquad \text{(Equation A2.12)}$$

By setting the permanent strain at the end of the previous stress stage, $\varepsilon_{p,f}(I\text{-}1)$, equal to the pre-conditioned permanent strain at the start of the current stress stage, $\varepsilon_{p,o}(I)$, the equivalent number of loading cycle at the start of the current stress stage, $Neq_o(I)$, can be calculated using Equation A2.13 as:

$$Neq_o(I) = [\varepsilon_{p,f}(I-1)/A(I)]^{1/\alpha(I)} \qquad \text{(Equation A2.13)}$$

Therefore, the total permanent strain after the application of additional loading cycles in the current stress stage, say *N(I),* can be calculated using Equation A2.11, with the total equivalent loading cycles, *Neq(I)*, being calculated as:

$$Neq(I) = Neq_o(I) + N(I) \qquad \text{(Equation A2.14)}$$

Generally, the transformation process requires an iterative technique to back-calculate all the parameters in these equations. With each set of estimated model parameters (α and μ or A), the resultant permanent strains for all combined loading stages is then calculated using the strain hardening rule and then compared with the measured permanent strains. New values for the parameters $\mu(I)$, and $\alpha(I)$ for each loading stage are then generated by an algorithm within the model until a best fit between the predicted and measured cumulative deformation for all stress stages can be achieved.

The above procedure can be incorporated in Microsoft Excel, which provides a special function SOLVER to enable selection of the final values of $\alpha(I)$ and $\alpha(I)$ for minimum fitted errors for each Stage (I).

A2.8.2 Simplified curve-fitting procedures for stress levels in Stages 2 and 3

However, for crushed rocks, small variation in μ. could be found in the Austroads multi-stage permanent strain test with a constant confining stress. In this case, as the first guess, a similar value for μ could be applied for all stress stages. This allows estimation of $\mu(2)$ and $\mu(3)$ or $A(2)$ and $A(3)$ using:

$$\mu(2) = \mu(3) = \mu(1) \qquad \text{(Equation A2.15)}$$

$$A(2).\alpha(2)/\varepsilon_r(2) = A(3).\alpha(3)/\varepsilon_r(3)\ A(1).= \alpha(1)/\varepsilon_r(1) = \qquad \text{(Equation A2.16)}$$

In this case, the following steps were used to back-calculate the three independent permanent strain-loading cycle relationships from the test results obtained with the Austroads RLT test method.

- **Step 1:** Determine the values of $A(1)$, $\alpha(1)$, $\varepsilon_r(1)$ for stress level 1 by fitting Equation A2.8 to permanent strain data obtained for Stage 1.

$$\varepsilon_p(1) = A(1).N(1)^{\alpha(1)} \qquad \text{(Equation A2.17)}$$

- **Step 2:** An iterative technique was used to then calculate $\alpha(2)$ and $A(2)$ for Stage 2:
  1. Assume a seed value for $\alpha(2)$.
  2. Use Equation A2.6 to calculate $A(2)$ from $A(1)$, $\alpha(1)$, $\varepsilon_r(1)$, $\varepsilon_r(2)$, and $\alpha(2)$.
  3. Use the permanent strain at the end of the previous stress stage, $\varepsilon_{p,f}(1)$ to calculate the equivalent number of loading cycle at the start of the stress stage, $Neq_o(2)$, using:

$$Neq_o(2) = [\varepsilon_{p,f}(1)/A(2)]^{1/\alpha(2)} \qquad \text{(Equation A2.18)}$$

  4. Convert the loading cycles applied in the stress stage (2) to the total equivalent loading cycles using:

$$Neq(2) = Neq_o(2) + N(2) \qquad \text{(Equation A2.19)}$$

5. Determine the fitted errors by fitting Equation A2.20 to data obtained for Stage 2:

$$\varepsilon_{p,Neq}(2) = A(2).Neq(2)^{\alpha(2)} \quad \text{(Equation A2.20)}$$

6. Add a small increment to the current value $\alpha(2)$ and repeat steps 1 to 5 until a minimum fitted error is achieved.

- **Step 3:** Repeat step 2 to calculate $\alpha(3)$ and $A(3)$ for stage 3:
  1. Assume a seed value for $\alpha(3)$.
  2. Use Equation A2.6 to calculate $A(3)$ from $A(2)$, $\alpha(1)$, $\varepsilon_r(1)$, $\varepsilon_r(2)$ and $\alpha(3)$.
  3. Use the permanent strain at the end of the previous stress stage, $\varepsilon_{p,f}(2)$ to calculate the equivalent number of loading cycle at the start of the stress stage, $Neq_o(3)$, using:

$$Neq_o(3) = [\varepsilon_{p,f}(2) / A(3)]^{1/\alpha(3)} \quad \text{(Equation A2.21)}$$

  4. Convert the loading cycles applied in the stress stage (3) to the total equivalent loading cycles using:

$$Neq(3) = Neq_o(3) + N(3) \quad \text{(Equation A2.22)}$$

  5. Determine the fitted errors by fitting Equation A2.23 to data obtained for Stage 3.

$$\varepsilon_{p,Neq}(3) = A(3).Neq(3)^{\alpha(3)} \quad \text{(Equation A2.23)}$$

  6. Add a small increment to the current value $\alpha(3)$ and repeat steps 1 to 5 until a minimum fitted error is achieved.

The above procedure can be easily incorporated in Microsoft Excel, which provides a special function SOLVER to determine the final values of $\alpha(2)$ and $\alpha(3)$ for minimum fitted errors.

Note that as α can increase with increasing applied repeated deviator stress and repeated deviator stresses are monotonically increased in the three loading stages in the Austroads Simplified Test Method, the following condition should also be found in the back-calculated solution.

$$\alpha(1) \leq \alpha(2) \leq \alpha(3) \quad \text{(Equation A2.24)}$$

Appendix 3 Description of Arnold 2004 rut depth model

A general performance model to predict pavement rutting developed by Arnold at the University of Nottingham was trialled during the mass limits study at CAPTIF (Arnold 2004). This model showed promising results for the limited number of CAPTIF tests where rut depth was predicted. As part of his PhD studies, Arnold validated the model to a larger data set of CAPTIF pavement trials and the results are reported here. The methodology used by Arnold to predict rut depth is briefly described below. However, in its present state the method to predict rut depth is impractical because of its complexity, non-linear finite element analysis and large number of Repeated Load Triaxial (RLT) tests required. Hence, this research aims to simplify the rut depth model to develop a practical test and analysis procedure for routine use in specifications for determining a traffic loading limits for saturated and non-saturated moisture conditions.

A3.1 Methodology

Figure A3.1 shows the methodology for calculation of rut depth as proposed by Arnold (2004). The following major steps were used to predict the surface rut depth of a granular pavement:

- Step 1: Conduct permanent strain testing using the Nottingham RLT test method to collect permanent strain and resilient modulus data.
- Step 2: Develop material models of resilient modulus and permanent strain for pavement analysis.
- Step 3: Conduct pavement analysis to predict pavement stress and surface rut depth.
- Step 4: Validate with field performance and make adjustments to assumptions of residual stress and initial rut depth, if required.

Generally, numerous assumptions are applied in the first three steps, which are associated with the use of simple laboratory testing and pavement analysis methods selected in this study. These assumptions can significantly affect the magnitude of measured laboratory permanent strains and calculated pavement stresses and, hence, the predicted rut depth. Therefore, it is necessary to validate the predicted rut depth using field performance. In the validation process (Step 4), actual results of rut depth obtained from accelerated pavement testing are compared to the rut depth calculated and, if required, adjustments of predicted stresses and rut depths can be made to generate predicted results closer to field performance. The validation process (Step 4) utilised pavement test results at CAPTIF for the past 6 years.

Details of these above steps (including assumptions and associated errors) are summarised in Figure A3.1.

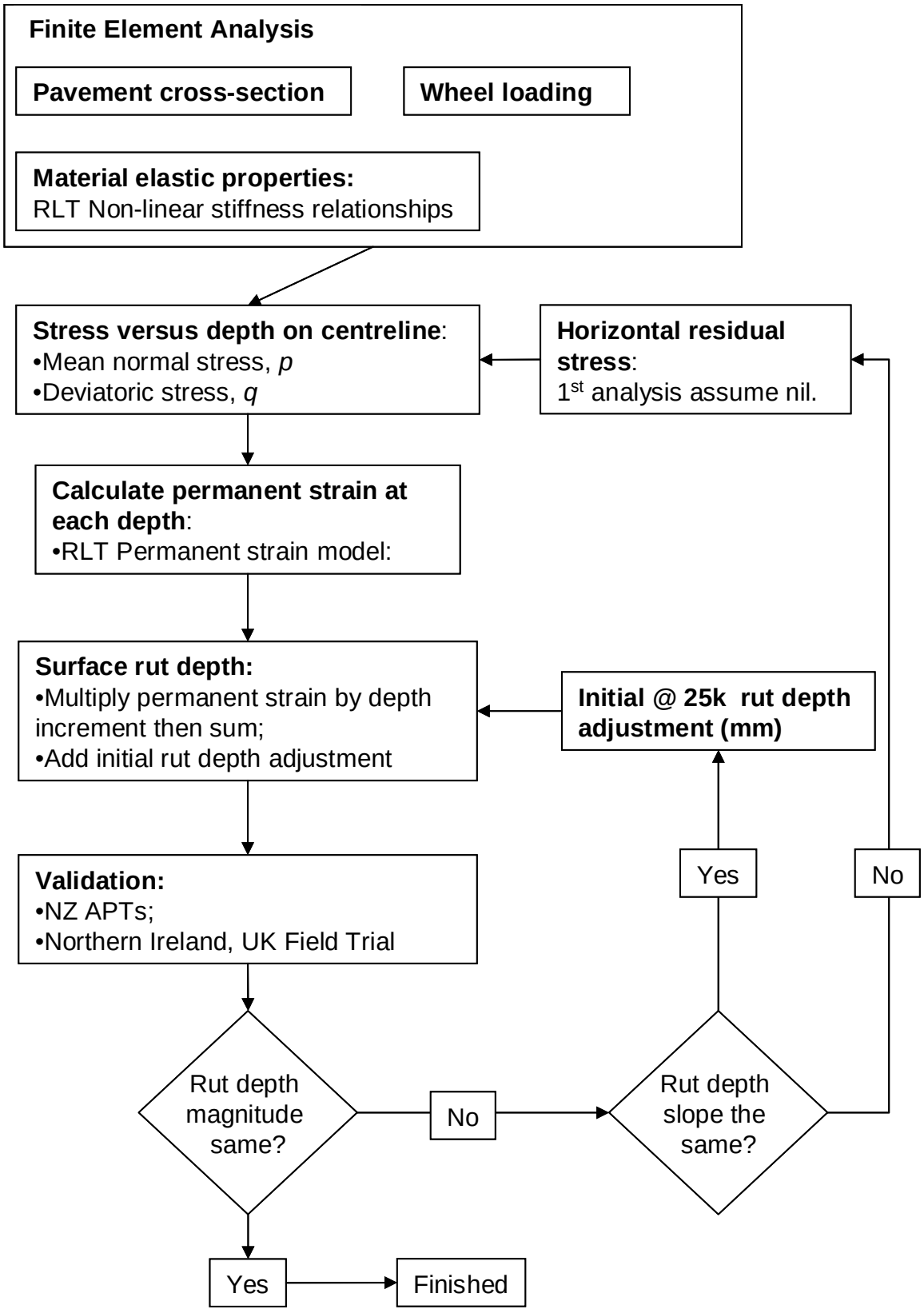

Figure A3.1 Methodology for calculation of rut depth and validation (Arnold 2004).

A3.2 Description of the Nottingham RLT Test Method

A3.2.1 Objective

The objective of the laboratory RLT testing programme is to obtain permanent strain data at various stress states so that the behaviour of an unbound granular material can be described using a model to calculate permanent strain for any given stress value. In the testing programme, only testing stresses are varied to cover the full spectra of stresses expected in the pavement while the particle size distribution, compacted density and moisture content are constant for each material.

A3.2.2 Sample size

Specimen size of 150 mm diameter and 300 mm length is used to determine permanent deformation and resilient modulus for all materials with maximum particle size in the range of 20–40 mm, and when using 40-mm top size aggregate the material shall not be scalped.

A3.2.3 Sample preparation and target density-moisture conditions

As these materials were granular and constructed in the field trials using vibrating steel rollers, it was decided to use vibrating hammer compaction to prepare laboratory triaxial specimens. Details of procedures for sample preparation using the vibrating hammer compaction method are given in the laboratory operating procedures of the Nottingham Centre of Pavement Engineering (University of Nottingham 2003).

The New Zealand specification for field compaction of pavements (TNZ B/2: 1997) requires a target compacted density of 97% of maximum dry density (MDD) and before sealing a moisture content 70% of optimum moisture content (OMC). These targets were also used for the construction of the Northern Ireland and New Zealand pavement tests. Therefore, it was decided to use the same targets used in New Zealand for the construction of pavements (i.e. 97% MDD and 70% OMC) for the compacted RLT samples.

The vibrating compaction test method (BSI 1990) was used to determine laboratory MDD and OMC values for establishing the target dry density and moisture content for materials tested in the RLT apparatus. For oversize materials, particles greater than 20 mm diameter were removed, as required for the 100 mm diameter mould. The effect of removing the particles greater than 20 mm was considered minor for the small sample quantity (approximately 2 kg) as it generally meant replacing one stone of greater than 20 mm with approximately two stones 14 to 20 mm. It was also considered that the MDD and OMC determined from a New Zealand Standard compaction test would be almost identical to *BS 1377-4:1990 - 3.7* (BSI 1990).

A3.2.4 Repeated load triaxial apparatus

The University of Nottingham's RLT apparatus was used in the testing programme. The features of the University of Nottingham's 150 mm diameter RLT apparatus for testing

granular materials with particle sizes up to 40 mm are illustrated in Figure A3.2 and are described as follows:

- use of closed loop servo-hydraulic loading systems for cycling both deviator and confining stresses,
- accurate measurement of axial and radial deformations directly on the test specimen using LVDTs and by cast epoxy strain hoops fitted with foil strain gauges respectively,
- measurement of axial load on the top platen,
- measurement of pore pressure,
- computer control and data acquisition.

(a) Photo of testing apparatus

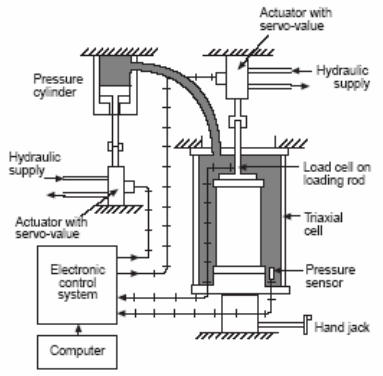

(b) Schematic diagram

Figure A3.2 University of Nottingham RLT apparatus.

For reasons of simplicity, the 1-D RLT apparatus (with static confining pressure and repeated axial load) was used in this research testing programme. However, the 1-D RLT apparatus only approximates actual cyclic stresses that occur in-service. For example, principal stress rotation and cyclic confining pressure/stresses are not replicated in the RLT tests. Thus errors are expected with the RLT tests, although their magnitude is unknown. As the effect of principal stress rotation and cyclic confining stresses increase the severity of the loading, the expectation was that the RLT tests would under-estimate the magnitude of permanent strain.

A3.2.5 Permanent strain testing

(a) Testing procedure

The normal permanent testing procedure specifies that a new specimen is used for each stress level. However, to reduce testing time multi-stage tests were conducted. These tests involved testing a range of stress conditions on one sample, and after at least 50,000 load cycles if the sample had not failed new stress conditions were applied and loading applied for another 50,000 cycles. These new stress conditions were always slightly more severe (i.e. closer to the yield line) than the previous stress conditions.

Vertical loading was a sinusoidal pulse at 5 times a second (5 hertz) applied for 50,000 loading cycles for each new loading stress.

For multi-stage testing it seemed sensible to simply increase the vertical cyclic stress each time, while keeping the cell pressure constant. However, stress invariants *p* (mean principal stress) and *q* (deviatoric stress) are a convenient way of describing 3-D stress states and are commonly used in relationships for permanent strain. Therefore, in this multi-stage testing procedure, testing stresses were chosen by keeping *p* (average of principal stresses) constant while increasing *q* (deviator stress) for each new stress level up to and occasionally above the yield line. The results of the static shear failure tests plotted in *p*-*q* stress space (Figure A3.3) were used as an approximate upper limit for testing stresses.

(b) Testing programme

The testing programme aimed to cover the full spectra of stresses that are expected to occur in-service.

Figure A3.3 shows the full spectra of stresses expected in a pavement. The bulk of the stresses calculated show the mean principal stress (*p*) varies from 50–300 kPa and the deviatoric stress (*q*) from 50–700 kPa. These ranges of stresses were confirmed with some pavement analysis using the CIRCLY linear elastic programme (Wardle 1980). At the base of the granular layers negative values of mean principal stress *p* were calculated, but as a granular material has limited tensile strength, negative values of mean principal stress were discounted.

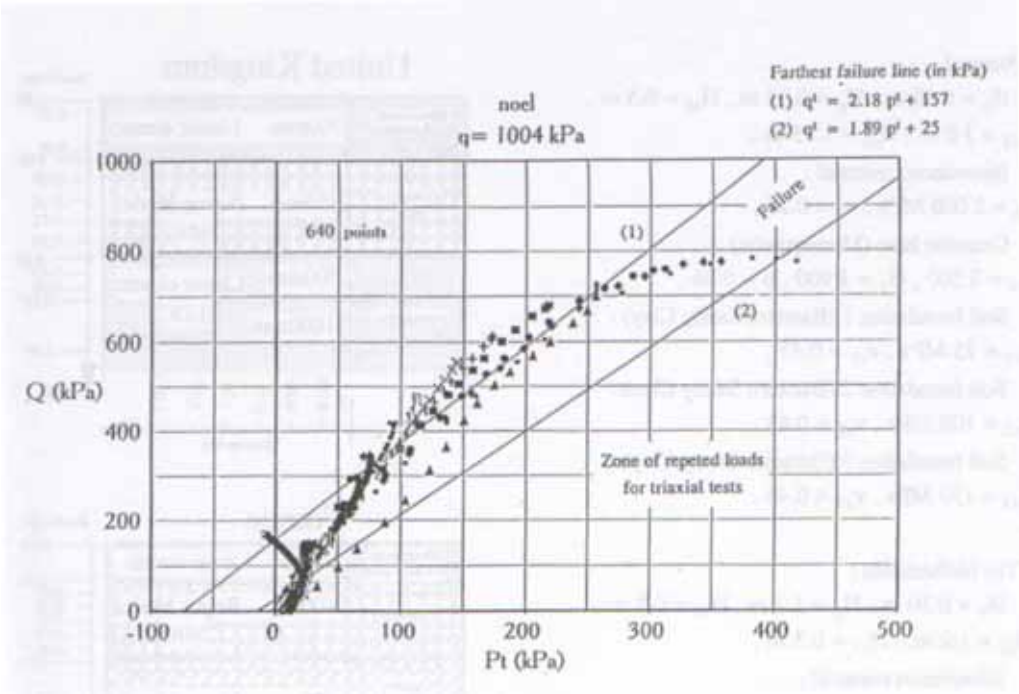

Figure A3.3 Stresses expected in a pavement (after Guezouli et al. 1993).

Table A3.1 summarises the proposed permanent strain testing programme for a typical crushed rock, which has a Mohr-coulomb yield strength of c = 55 kPa and ϕ = 44 degrees.

- RLT permanent strain tests are undertaken at a range of testing stresses (viz. normal stress in the range of 75–250 kPa and shear stress in the range of 37–562 MPa).
- Three samples for each material were tested at three different values of maximum mean principal stress p (75, 150, and 250 kPa). This covered the full spectra of stresses in *p*-*q* stress space for later interpolation of permanent strain behaviour in relation to stress level.

An example of the testing stresses chosen along with the monotonic shear failure line is shown in Figure A3.4 for the CAPTIF 1 aggregate (see Arnold 2004 for description of the material).

Table A3.1 Chosen RLT testing programme to determine permanent strain for a material with a given shear strength (for 50 000 cycles).

Specimen No.	Test No.	σ_1 (kPa)		σ_3 (kPa)	*p* (MPa)		*q* (MPa)	
		from	to	constant				
1	1A	69	112	58	62	76	0	43
	1B	55	145	43	47	77	0	91
	1C	40	179	27	31	77	0	139
	1D	26	209	11	16	77	0	183
	1E	17	220	0	6	73	0	203
2	2A	111	247	100	104	149	0	135
	2B	101	284	88	93	154	0	183
	2C	83	313	70	74	151	0	229
	2D	69	343	54	59	150	0	274
	2E	58	376	40	46	152	0	319
	2F	42	409	22	29	151	0	367
3	3A	149	473	134	139	247	0	324
	3B	130	506	118	122	247	0	376
	3C	119	538	105	110	250	0	419
	3D	98	563	83	88	243	0	465
	3E	90	604	72	78	249	0	515

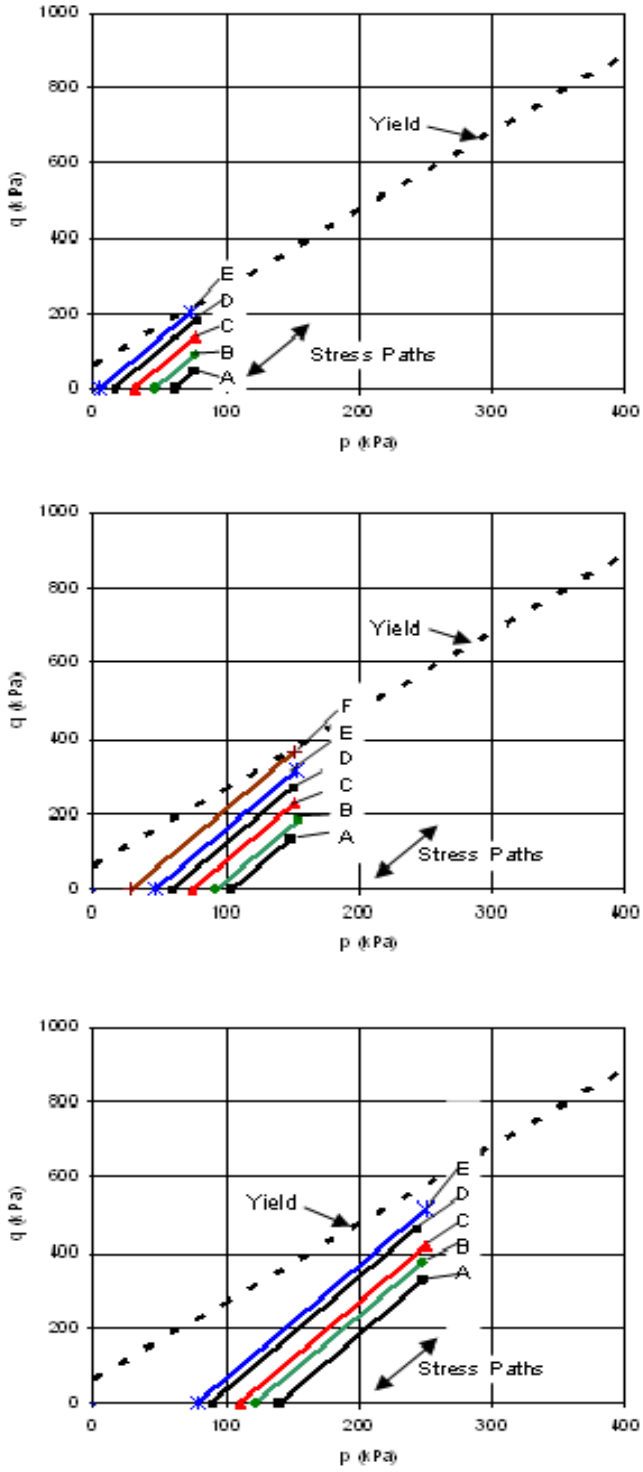

Figure A3.4 Chosen RLT testing programme to determine permanent strain for a material with a given yield strength.

A3.2.6 Typical testing results

Figure A3.5 shows typical results of total cumulative permanent strain versus number of loading cycles for a multi-stage permanent strain test.

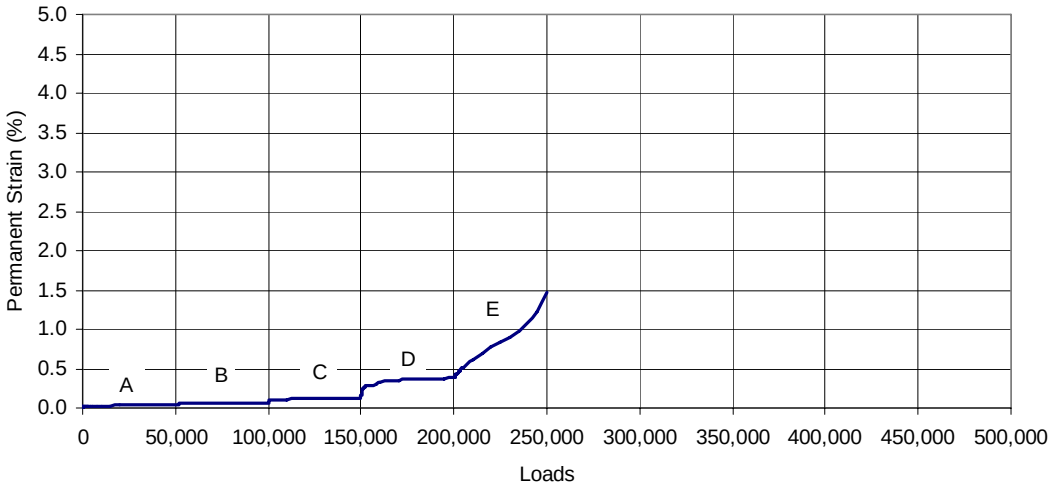

Figure A3.5 Typical results of RLT permanent strain result (CAPTIF 1 material, Test 1 - p=75 kPa).

Results of these tests were also reported in terms of average resilient strain and incremental permanent strain for each set of testing stresses (usually 50k). They are then fitted with selected material models of resilient modulus and permanent strain, which are required as inputs into the Arnold (2004) permanent strain model for predicting pavement rut depth. The material models are briefly described below. The Arnold (2004) permanent strain model is described in Section 5.3.1.

A3.3 Material models adopted in the rut depth model

A3.3.1 Resilient modulus model

A 2-D axi-symmetrical Finite Element Model, namely DEFPAV (Snaith et al. 1980), was selected for pavement analysis to predict stresses in the tested pavements. This FEM model requires modulus input in terms of the k-θ model (Hicks 1970) (Equation A3.1). Therefore, resilient properties of the materials were deduced in terms of the K-θ model in this study.

$$E = K_1 \times \theta^{K_2} \qquad \text{(Equation A3.1)}$$

where:

E = resilient modulus (MPa),

θ = total stress (MPa) = $(\sigma_1 + \sigma_2 + \sigma_3)$

K_1, K_2 experimental test constants.

Typical results of curve fitting using this model are given in Figure A3.6.

The K-θ model may not fit the test data well for different granular materials and subgrades as tested by Arnold (2004). Therefore, by applying this model in FEM analysis, it was expected that the FEM-predicted stresses and strains may involve some errors. However, it was not possible to quantify the errors at this stage.

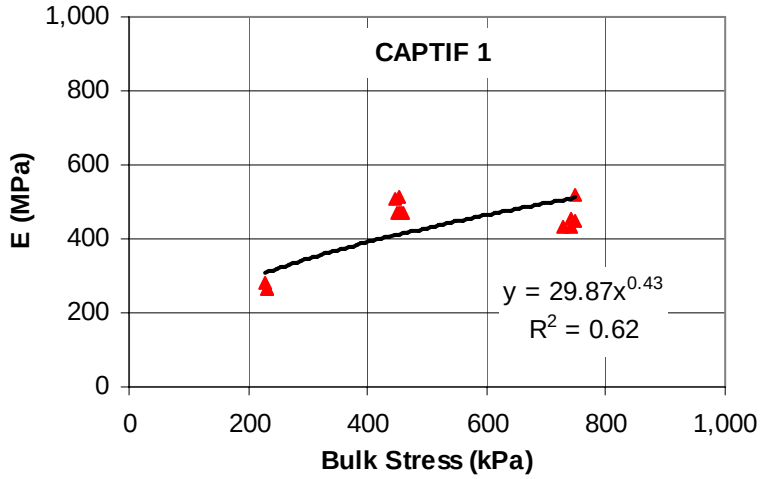

Figure A3.6 Typical curve fitting of RLT resilient modulus using the K-θ model.

A3.3.2 Permanent strain models

A simple procedure was also used to calculate incremental surface deformation based on the FEM-predicted pavement stresses (see Section A3.3.1). This procedure is used to predict incremental surface deformation at four loading periods, namely:

1. early behaviour (compaction important): 0–25k loads,
2. mid-term behaviour: 25–100k loads,
3. late behaviour: 100k–1M loads,
4. long-term behaviour: > 1M loads.

This procedure requires relationships of permanent strain rates as functions of stresses for the above four periods. Therefore, permanent strain data obtained from the RLT testing were also deduced in terms of permanent strain rates and stresses for the calculation of incremental surface deformation at each of these four stages.

Figure A3.7 summarises the procedure used in this study to model permanent strain rates with respect to stresses.

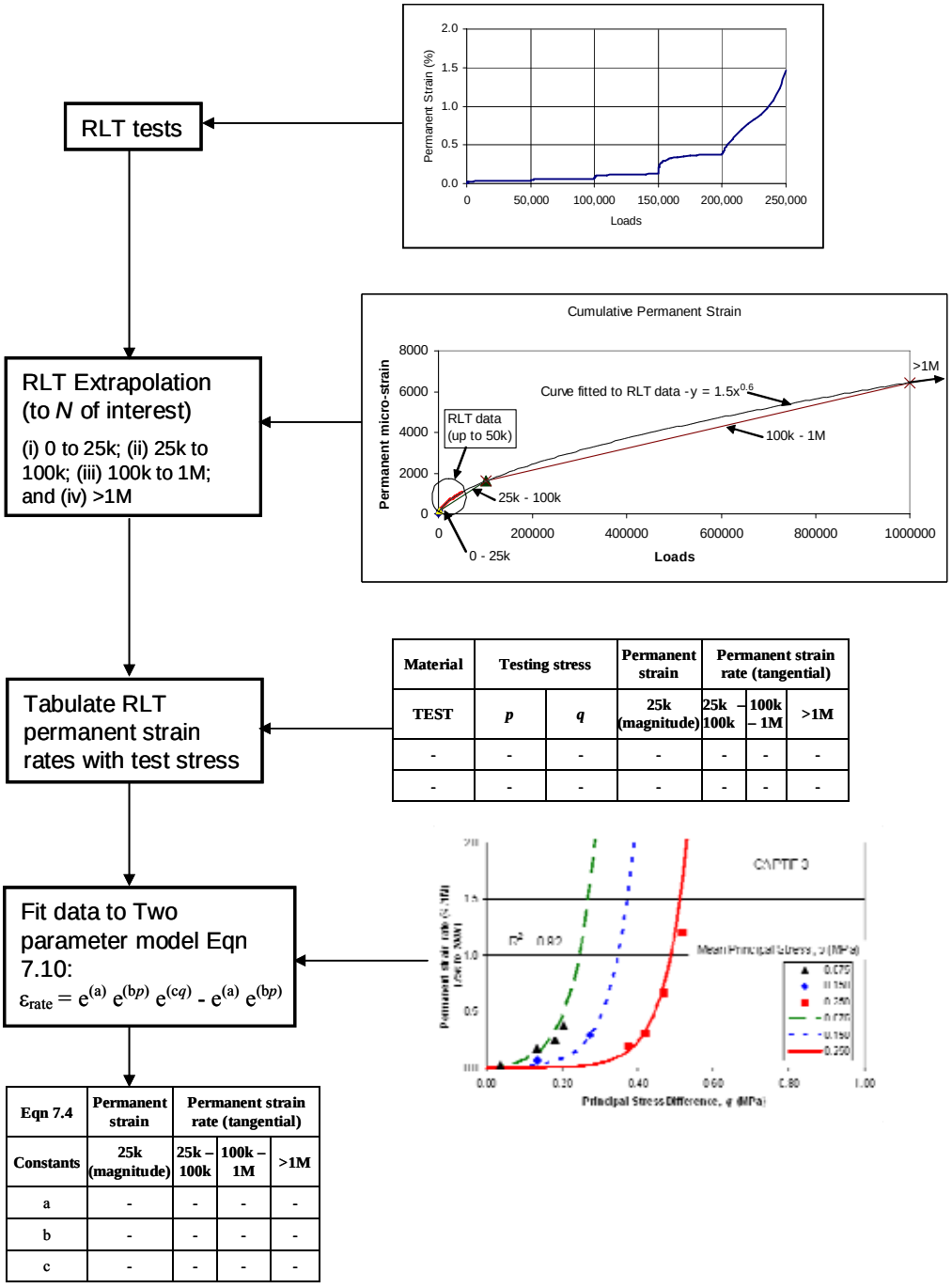

Figure A3.7 Interpretation of RLT permanent strain tests.

The following steps are used:

- Step 1: Individualisation of permanent strain data for each stress level.

  To individualise the permanent strain data for each stress level tested in the multi-stage permanent strain test, after each new stress level is applied, both the loading count and permanent strain returned to zero, and the permanent strain plots for 50 k-cycles applied in each stage were produced.

- Step 2: Estimation of incremental permanent strains and average permanent strain rates for each loading period.

i. From the new plots for 50 k-cycles applied in each stage, the magnitude of incremental permanent strain between 0–25k loads is determined.

ii. The permanent strain plots for 50 k-cycles applied in each stress stage were then fitted with a power model ($y = ax^b$) and for some of the higher testing stresses a linear model as these provided the best fit to the measured data. These models were then used to estimate incremental permanent strains for the other three loading periods of 25k to 100k (mid-term), 100k to 1M (late), and 1M to 2M (long-term).

iii. The average permanent strain rate for each period was then determined by dividing incremental permanent strain by the applied number of loading cycles.

- Step 3: Tabulation of average permanent strain rates and stresses for curve fitting.

  Average permanent strain rates and stresses for each loading stage (early, mid-term, late and long-term) were tabulated separately for curve fitting. It is anticipated that the permanent strain rate-stress relationships for these loading stages will be different.

- Step 4: Determination of the permanent strain rate-stress relationships for each loading period.

  It was decided to describe permanent strain rate as a function of mean stress (p) and deviator stress (q). It was also found that Equation A3.2 can be used to fit the data of permanent strain rate at any loading cycle (or incremental permanent strain at any loading period):

$$\delta\varepsilon_p = e^{(A)}\, e^{(Bp)}\, (e^{(Cq)} - 1) \qquad \text{(Equation A3.2)}$$

  where:

e	=	2.718282
$\delta\varepsilon_{p(rate\ or\ magn)}$	=	permanent strain rate
A, B, C	=	constants obtained by regression analysis fitted to the measured RLT data
p	=	mean principal stress (MPa)
q	=	deviator stress (MPa)

  Thus, the average permanent rate and incremental permanent strain for the four loading stages can be described as:

$$\delta\varepsilon_{p(0\text{-}25k)} = e^{(A1)}\, e^{(B1\ p)}\, (e^{(C1\ q)} - 1) \qquad \text{(Equation A3.3)}$$

$$\delta\varepsilon_{p(25\text{-}100k)} = e^{(A2)}\, e^{(B2\ p)}\, (e^{(C2\ q)} - 1) \qquad \text{(Equation A3.4)}$$

$$\delta\varepsilon_{p(100k\text{-}1M)} = e^{(A3)}\, e^{(B3\ p)}\, (e^{(C3\ q)} - 1) \qquad \text{(Equation A3.5)}$$

$$\delta\varepsilon_{p(1M\text{-}2M)} = e^{(A4)}\, e^{(B4\ p)}\, (e^{(C4\ q)} - 1) \qquad \text{(Equation A3.6)}$$

$$\Delta\varepsilon_{p(0\text{-}25k)} = e^{(A1)}\, e^{(B1\ p)}\, (e^{(C1\ q)} - 1) \times 25k \qquad \text{(Equation A3.7)}$$

$$\Delta\varepsilon_{p(25\text{-}100k)} = e^{(A2)}\, e^{(B2\ p)}\, (e^{(C2\ q)} - 1) \times 75k \qquad \text{(Equation A3.8)}$$

$$\Delta\varepsilon_{p(100k\text{-}1M)} = e^{(A3)}\, e^{(B3\ p)}\, (e^{(C3\ q)} - 1) \times 900k \quad \text{(Equation A3.9)}$$

$$\Delta\varepsilon_{p(1M\_2M)} = e^{(A4)}\, e^{(B4\ p)}\, (e^{(C4\ q)} - 1) \times 1000k \quad \text{(Equation A3.10)}$$

where:

$\delta\varepsilon_{p(0\text{-}25k)}$ & $\Delta\varepsilon_{p(0\text{-}25k)}$	are the average permanent strain rate and incremental permanent strain that occur in the first 25k wheel loads, respectively
$\delta\ \varepsilon_{p(25k\text{-}100k)}$ & $\Delta\ \varepsilon_{p(25k\text{-}100k)}$	are the average permanent strain rate and incremental permanent strain from 25-100k wheel loads, respectively
$\delta\ \varepsilon_{p(100k\text{-}1M)}$ & $\Delta\ \varepsilon_{p(100k\text{-}1M)}$	are the average permanent strain rate and incremental permanent strain that occurs from 100k-1M wheel loads, respectively
$\delta\ \varepsilon_{p(1M\text{-}N\ )}$ & $\Delta\ \varepsilon_{p(1M\text{-}N\ )}$	are the average permanent strain rate and incremental permanent strain that occurs from *1M-N* wheel loads (*N > 1M*) , respectively
N =	number of wheel loads
A1, B1, C1	are constants found by fitting data at 0-25k loads
A2, B2, C2	are constants found by fitting data at 25-100k loads
A3, B3, C3	are constants found by fitting data at 100k-1M loads
A4, B4, C4	are constants found by fitting data at 1M-2M loads

Note: the following major assumptions made in interpretation of permanent strain rates obtained from the RLT multi-stage permanent tests would produce some errors in the predicted permanent strains.

- The permanent strain test for each stress stage in the multi-stage permanent strain test can be treated as individual test on the virgin specimen (Step 1). This assumption may not be valid as changes occur in both sample density and shear deformation in the specimen over the course of testing. Therefore, it was expected that there would be significant errors associated with this assumption, particularly in the estimation of permanent strain rates for first period of 0-25 k-cycles (Step 2 (i)).
- Given that test data for each stress level were limited to 50 k-cycles, extrapolation was required to estimate strain rates in the loading periods between 50 k-cycles and 2M cycles. Therefore, further errors exist in the estimations of permanent strain rates for loading periods after 50 k-cycles, if curve fittings are not perfect (Step 2 (ii)).

This will be discussed further in Section A3.5.

A3.4 Rut depth model (Arnold 2004)

A3.4.1 Methodology

A pavement analysis using an FEM model was conducted to predict stresses in the pavement under the centre of a single wheel. These stresses were used in a spreadsheet to calculate the permanent strain at incremental points under the centre of the load using the model determined from RLT testing (Section 5.3 of this report). Permanent strains were integrated and summed to obtain a surface rut depth.

The FEM method used to predict pavement stresses and the rut depth model used to calculate maximum surface deformation are briefly described below.

A3.4.2 FEM analysis to predict pavement stresses

A simple 2-D axi-symmetrical non-linear finite element model, DEFPAV (Snaith 1980), was used to predict stresses within the pavement. DEFPAV was chosen because of its availability and ease of use in terms of obtaining the outputs and utilising the non-linear resilient characteristics of the granular and subgrade materials.

The following assumptions were considered in a pavement analysis using this FEM model:

- A single circular load of uniform stress is used to approximate actual dual-tyre wheel load.
- Modulus of unbound material is expressed in terms of K-θ model and Poisson's ratio is constant.
- Material is weightless.
- Zero horizontal residual confining stresses resulted after compaction of the pavement layers.
- Tensile stresses are allowed to be developed in granular elements.

Given that the above assumptions only approximated the non-linear characteristics of the granular and subgrade materials, it was expected that there could be errors in the calculation of stresses from DEFPAV. Currently, the errors associated with these assumptions are unknown.

It was proposed that the horizontal residual stress could be arbitrarily adjusted to improve rut depth predictions, if they are found to be different from the field results. These adjustments will be made during validation with field performance obtained from actual field trials.

From the pavement stress analysis, the mean principal stress (p) and deviatoric stress (q) under the centre of the load are calculated for input into a spreadsheet along with depth for the calculation of rut depth.

A3.4.3 Calculation of maximum surface deformation

Average permanent strain rate for a specified stress can be predicted using Equations A3.11 - A3.14 as shown in Section 3.3of this report. Those equations are used to predict incremental surface deformation at four loading periods, namely:

- Early behaviour (compaction important): 0 – 25 k loads.
- Mid term behaviour: 25 k – 100 k loads.
- Late behaviour: 100 k – 1 M loads.
- Long term behaviour: > 1 M loads.

Equations A3.11 – A3.14 are used to calculate incremental surface permanent deformation at the centre of the single circular load for each loading period.

$$\Delta d_{(0\text{-}25k)} = \sum \delta\varepsilon_{p(0\text{-}25k)}(I) \times \Delta H(I) \times \Delta N_{(0\text{-}25k)} \quad \text{(Equation A3.11)}$$

$$\Delta d_{(25\text{-}100k)} = \sum \delta\varepsilon_{p(25\text{-}100k)}(I) \times \Delta H(I) \times \Delta N_{(25\text{-}100k)} \quad \text{(Equation A3.12)}$$

$$\Delta d_{(100k\text{-}1M)} = \sum \delta\varepsilon_{p(100k\text{-}1M)}(I) \times \Delta H(I) \times \Delta N_{(100k\text{-}1M)} \quad \text{(Equation A3.13)}$$

$$\Delta d_{(1M\text{-}2M)} = \sum \delta\varepsilon_{p(1M\text{-}2M)}(I) \times \Delta H(I) \times \Delta N_{(1M\text{-}2M)} \quad \text{(Equation A3.14)}$$

where:

Δd = incremental surface deformation

$\Delta\varepsilon_p(I)$ = incremental permanent strain for the stresses at depth I (or depth to middle of the sub-layer I)

$\Delta H(I)$ = associated depth increment (or thickness of the sub-layer I)

ΔN = applied number of loading cycles for the loading period concerned

The total surface permanent deformation at the centre of the single circular load at a specified loading cycle is the sum (Σ) of incremental deformation (Δd) in all previous loading periods:

$$d = \sum \Delta d \quad \text{(Equation A3.15)}$$

In this study, it was assumed that the predicted surface permanent deformation (d) at the centre of the single circular load is similar to the rut depth (RD) developed in actual pavements trafficked with actual heavy vehicles.

$$RD = d \quad \text{(Equation A3.16)}$$

In this case, the following assumptions were also applied:

- A single circular load of uniform stress is used to approximate actual dual-tyre wheel load.
- No transverse loading distribution existed.
- No heave resulted from shallow shearing.

The expectation was that these assumptions would result in some errors in the calculation of rut depth. However, the errors associated with these assumptions are currently unknown. Therefore, it was proposed that the predicted rut depth be compared to the measured rut depth in the pavement trials. Based on comparison with actual pavement

test results an initial rut depth was added (or subtracted) to account for all the errors involved.

A3.5 Adjustments of predicted rut depths (Validation)

As discussed previously, many assumptions are applied in the laboratory RLT testing method (Section 5.2 of this report), interpretation of permanent strain data (Section 5.3), and calculation of pavement stresses and rut depths (Sections 5.4 and 5.5). These assumptions can significantly affect the magnitude of predicted material permanent strains and pavement stresses and, hence, predicted rut depth.

The calculated surface rut depth with number of wheel loads was therefore compared with actual rut depth measured from full-scale pavements tested with accelerated pavement testing at CAPTIF. Based on the comparisons, it may be necessary to apply correction factors to the predicted of rut depths if they were found to be different from the measured values.

The following methods were also considered appropriate for the adjustment of predicted rut depths:

- For rut depth at 25 k, adjustment is directly based on the differences between measured and predicted rut depth. This is because the differences are caused by sample preparation and compaction which is very difficult to quantify because of the use of RLT multi-stage tests where prior loading effected the initial deformation that occurs at the start of a new loading stress.
- For rut depth increments at greater than 25 k-cycles, adjustment is made in terms of the magnitude of horizontal stress added. This parameter was found to significantly influence the predicted rut depth. In this case, an iterative process is required to determine the initial rut depth adjustment and the amount of horizontal residual stress to add so that the calculated surface rut depth matches the measured values.

Appendix 4 Results of calibration of the Arnold (2004) rut depth model

A4.1 Models for permanent strain at 25 k-cycles

Parameters for Equation 3.7 which is used to calculate the amount of permanent strain in the first 25k load cycles are listed in Table A4.1. These parameters were determined from incremental permanent strains at 25k determined from the multi-stage RLT permanent strain tests.

The predicted strain at 25 k-cycles are plotted against measured RLT values as shown in Figure A4.1.

Table A4.1 Model parameters for calculation of permanent strain for the first 25 k-cycles from Equation 3.7.

Material	Model Parameters (Equation 3.7) $\varepsilon_{p(25k)} = e^{(a)}\, e^{(bp)}\, e^{(cq)} - e^{(a)}\, e^{(bp)}$			Mean error
	a	b	c	ε_p (%)
NI* Good	−3.474	−25.732	16.745	0.04
NI Poor	−4.290	−73.977	48.286	0.03
CAPTIF** 1	−4.369	−13.052	14.410	0.03
CAPTIF 2	−0.616	−14.472	8.026	0.08
CAPTIF 3	−8.763	−13.166	18.360	0.04
CAPTIF 4	5.262	−166.979	60.888	0.07
CAPTIF Subgrade	0.401	−20.243	4.479	0.01

Mean error = (∑error at each individual data point) /Total number of data points

* NI = Northern Ireland in-service pavement sample

** CAPTIF = Canterbury Accelerated Pavement Testing Indoor Facility

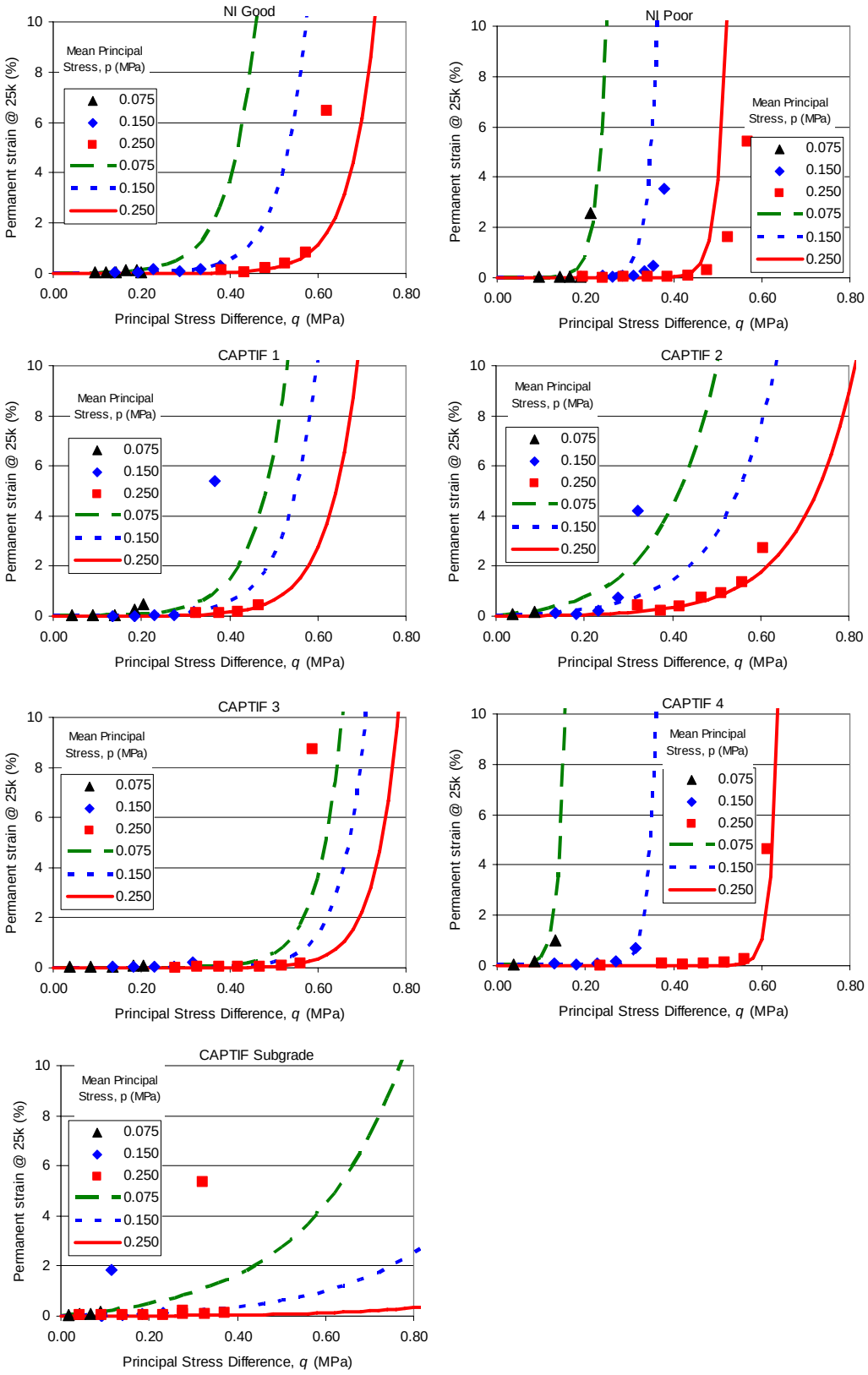

Figure A4.1 Comparison of measured permanent strains at 25 k-cycles and fitted curves using Equation 3.7.

A4.2 Models for permanent strain rates after 25 k-cycles

Parameters for Equations 3.8, 3.9 and 3.10, which are used to calculate the amount of permanent strain in the three periods of 25–50 k-cycles, 100–1000 k-cycles and 1000–2000 k-cycles are listed in Table A4.2. These parameters were determined by fitting these equations with average permanent strain rates for the three periods as determined from the multi-stage RLT permanent strain tests. The mean errors produced by the fitted curves are listed in Table A4.2.

Excluded from the fit were the tests that failed before 50k load cycles, which was the last/highest stress level in each multi-stage test. Results where failure occurs do not follow the same trend as the other results because of significantly larger deformations and shear failure that is occurring which is a different mechanism of accumulation of permanent strain from the other test results.

It should be noted that in the curve fitting of CAPTIF Subgrade test results, all test results with a mean principal stress of 0.250 MPa were excluded as they could not be fitted to the model. The exclusion of these test results was justified as they were much higher than the maximum mean principal stress of 0.150 MPa required in the subgrade.

Table A4.2 Parameters of permanent strain rate model.

Material	ε_{rate}	Model Parameters (Equation 3.6) $\varepsilon_{rate} = e^{(a)}\, e^{(bp)}\, e^{(cq)} - e^{(a)}\, e^{(bp)}$			Mean error
		a	b	c	ε_{rate} (%/1M)
NI Good	$\varepsilon_{rate(25k-50k)}$	−0.772	−21.409	14.485	0.21
	$\varepsilon_{rate(50k-100k)}$	−1.085	−23.331	15.277	0.20
	$\varepsilon_{rate(100k-1M)}$	−4.142	−3.192	9.807	0.14
NI Poor	$\varepsilon_{rate(25k-50k)}$	−3.359	−51.175	38.679	0.21
	$\varepsilon_{rate(50k-100k)}$	−2.484	−51.971	37.363	0.58
	$\varepsilon_{rate(100k-1M)}$	−1.867	−63.175	19.965	0.39
CAPTIF 1	$\varepsilon_{rate(25k-100k)}$	−1.548	−18.937	14.993	0.22
	$\varepsilon_{rate(100k-1M)}$	−3.100	−13.578	12.203	0.10
CAPTIF 2	$\varepsilon_{rate(25k-100k)}$	−0.345	−9.732	10.548	0.77
	$\varepsilon_{rate(100k-1M)}$	−5.372	−12.507	20.768	0.47
CAPTIF 3	$\varepsilon_{rate(25k-100k)}$	−2.460	−19.956	15.197	0.13
	$\varepsilon_{rate(100k-1M)}$	−7.141	−12.761	19.283	0.09
CAPTIF 4	$\varepsilon_{rate(25k-100k)}$	−28.868	−27.061	70.421	0.03
	$\varepsilon_{rate(100k-1M)}$	−26.047	−17.251	60.272	0.03
CAPTIF Subgrade	$\varepsilon_{rate(25k-100k)}$	2.260	−22.602	9.036	0.04
	$\varepsilon_{rate(100k-1M)}$	0.842	−17.372	9.783	0.09

Comparison between measured permanent strain rates and those calculated with the constants listed in Table A4.2 are plotted in Figures A4.2, A4.3 and A4.4. Visually the model fits the data well, where the correct trend is shown being an increasing permanent strain rate with increasing deviatoric stress (q). Mean errors were generally less than

1%/1M which when applied to rut prediction is equivalent to an error of 1 mm per 100 mm thickness every 1 million wheel passes.

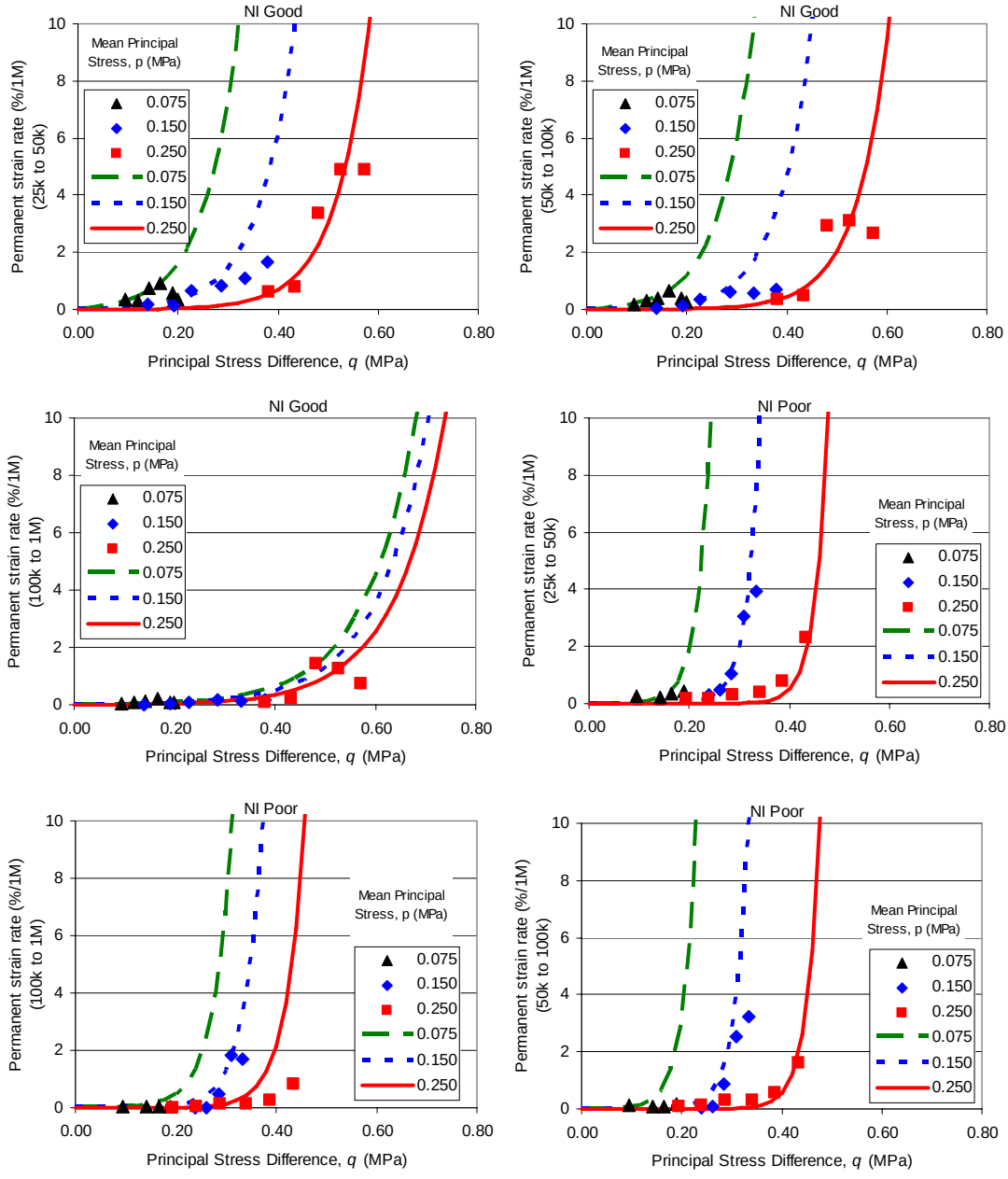

Figure A4.2 Comparison of measured incremental permanent strains for loading periods after 25 k-cycles and fitted curves using Equation 3.8 and 3.9 for NI Good and NI Poor materials.

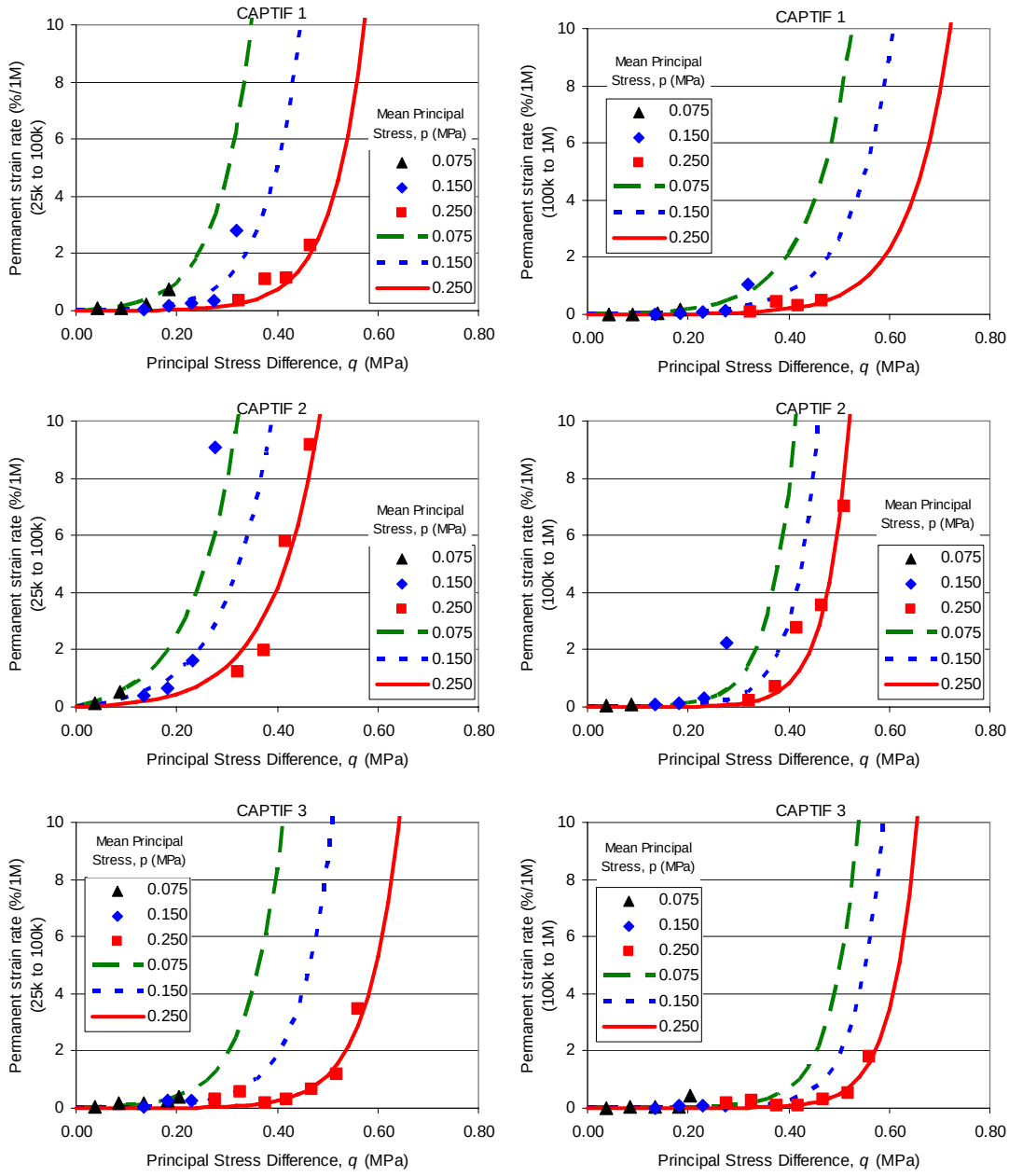

Figure A4.3 Comparison of measured incremental permanent strains for loading periods after 25 k-cycles and fitted curves using Equation 3.8 and 3.9 for CAPTIF 1, CAPTIF 2, and CAPTIF 3 materials.

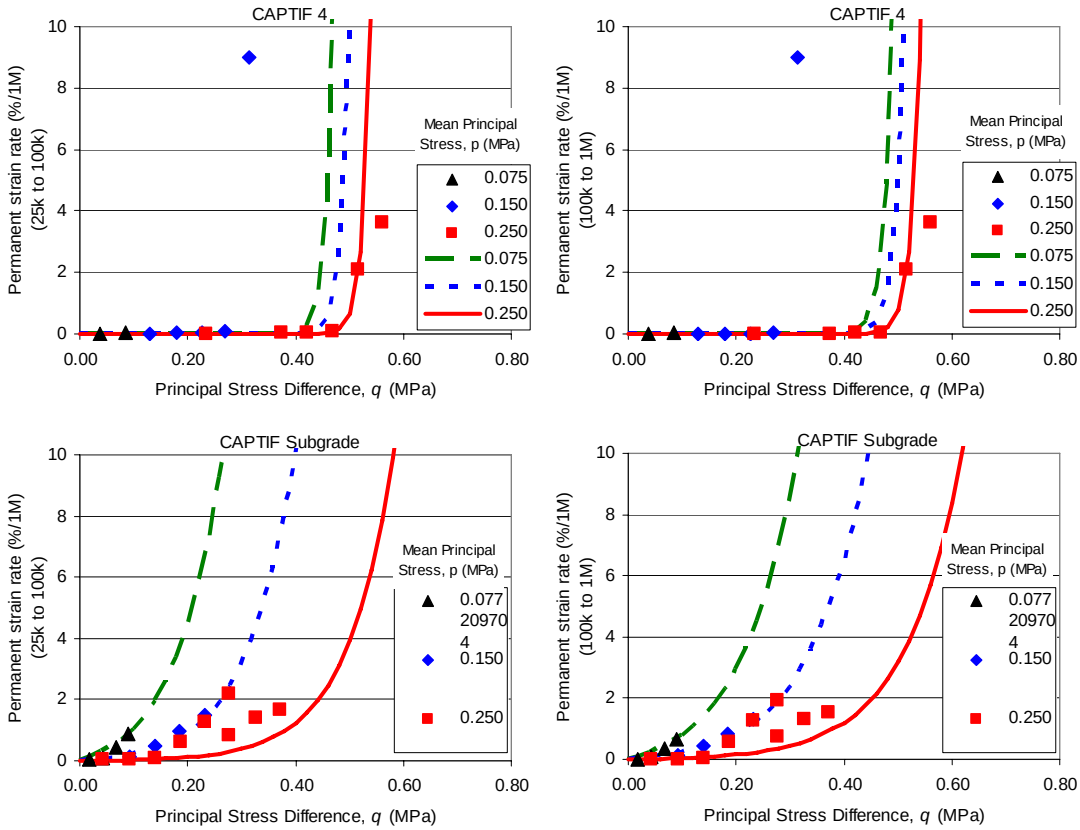

Figure A4.4 Comparison of measured incremental permanent strains for loading periods after 25 k-cycles and fitted curves using Equation 3.8 and 3.9 for CAPTIF 4 and CAPTIF Subgrade materials.

A4.3 Predicted model of resilient modulus (from RLT data)

Figure A4.5 shows the results of resilient modulus for various materials, which were fitted with the k-θ model (Equation 3.5). The fitted R^2 values produced by the fitted curves are in the range of 0.03–0.96, indicating that the k-θ model may not be best suited to describing resilient modulus for various material types (including granular materials and subgrade). Errors in modulus could be up to ±40%, although, as the rut depth model utilises stress values, the effect of errors in modulus values is less compared with strains which are directly related to modulus values.

Table A4.3 sumarises the values of resilient modulus, which were calculated from the k-θ model and parameters from Figure A4.5, for a range of bulk stresses/mean stresses for input into DEFPAV.

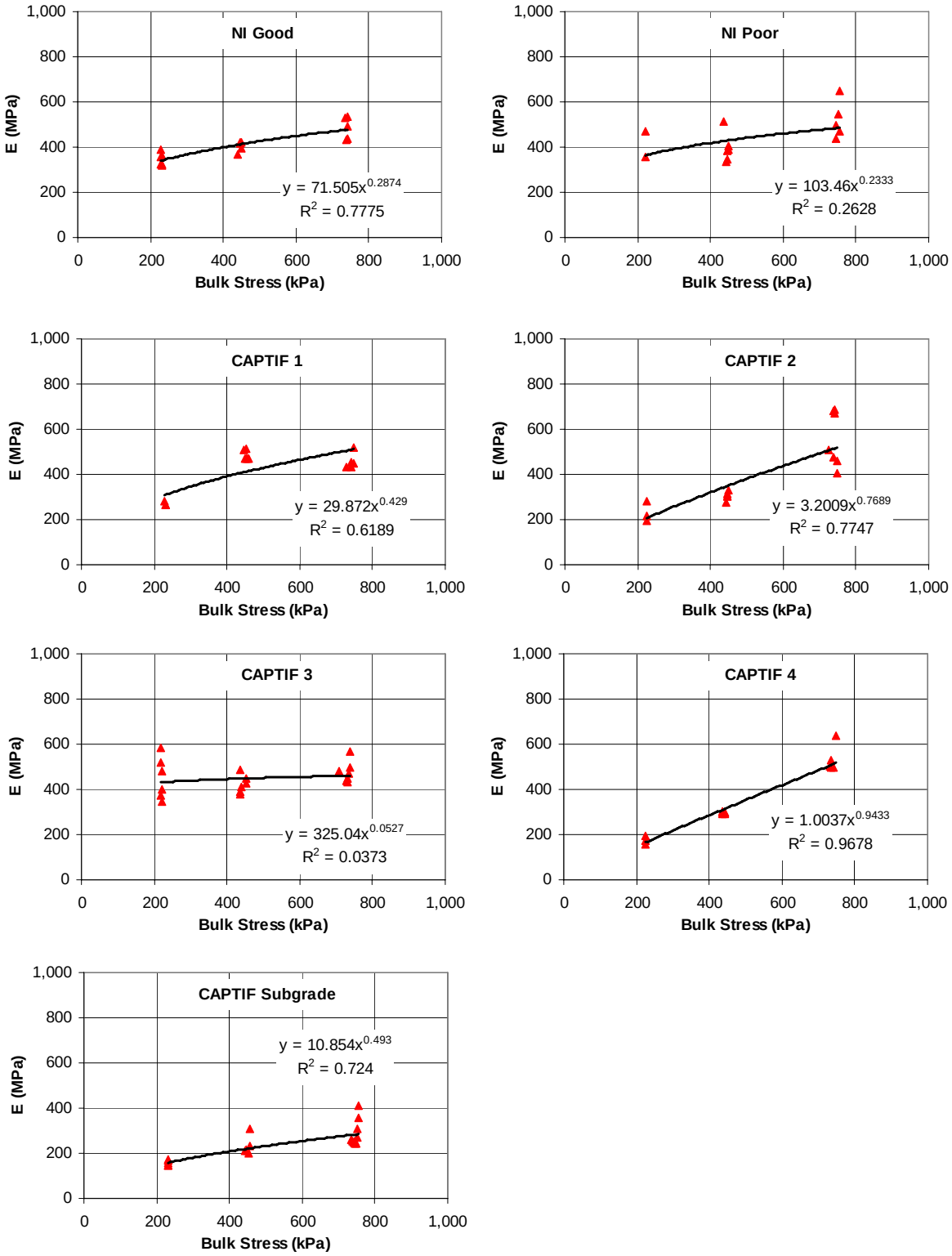

Figure A4.5 Elastic modulus versus bulk stress for the different materials.

Table A4.3 Resilient properties for input into DEFPAV finite element model.

Mean Stress (kPa)	Resilient Moduli (MPa)						
	NI Good	NI Poor	CAPTIF 1	CAPTIF 2	CAPTIF 3	CAPTIF 4	CAPTIF Subgrade
25	247	283	190	89	408	59	91
50	302	333	256	151	423	113	128
100	368	391	345	257	439	218	181
150	414	430	411	351	448	319	221
250	479	485	511	520	461	517	284

A4.4 Predicted pavement stresses from FEM pavement analysis

Table A4.4 summarises the cross sections and load of ten New Zealand accelerated pavement tests (NZ apts) (cross sections 1, 1a, 1b, 2, 2a, 2b, 3, 3a, 3b, and 4) and two Northern Ireland pavement tests (cross sections 5 & 6) to be modelled in DEFPAV.

Table A4.4 Cross section and loading identification for pavement analysis.

ID	Granular Material	Granular Thickness (mm)	Load = 40 kN	Load = 50 kN	Load = 60 kN
1	CAPTIF 1	275	1: 40kN	1: 50kN	
1a		275	1a: 40kN		1a: 60kN
1b		200	1b: 40kN		1b: 60kN
2	CAPTIF 2	275	2: 40kN	2: 50kN	
3	CAPTIF 3	275	3: 40kN	3: 50kN	
3a		275	3a: 40kN		3a: 60kN
3b		200	3b: 40kN		3b: 60kN
4	CAPTIF 4	200		4: 50kN	
5	NI Good	650	5: 45kN[1]		
6	NI Poor	650	6: 45kN[1]		

[1] 45kN is the most common weight passing over the Northern Ireland field trial

It should be noted that the two-wheel loads were modelled in DEFPAV as single-wheel loads. Tyre contact stress was assumed equal to 750 kPa.

Properties for the asphalt layer were assumed as linear elastic with a resilient modulus of 3000 MPa and a Poisson's ratio of 0.35 which are considered typical values (Austroads 1992).

For the granular and subgrade materials, inputs of resilient modulus are given in Table A4.4. Poisson ratios for the granular and subgrade materials were assumed as 0.35 and 0.45 respectively as recommended in the Austroads pavement design guide (Austroads 1992).

Tables A4.5, A4.6 , A4.7, and A4.8 summarise mean principal stresses, *p,* and deviator stresses, *q*, under the centre of the load at depth increments of 25 mm computed using DEFPAV for all loading and cross section combinations (Table A4.4). It was assumed in this first analysis that the horizontal stress from compaction is nil.

Table A4.5 Stresses in the pavement at various depth increments under a single wheel calculated with DEFPAV.

ID	Stress	Depth (mm)							
		25	***59***	***106***	***184***	***300***	***483***	***1102***	***2569***
1: 40kN	***p***	445.6	170.5	62.1	4.6	26.1	0.7	−2.5	0.2
	q	723.2	535.7	322.9	152.4	61.2	11.4	−0.7	0.2
1a: 40kN	***p***	445.6	170.5	62.1	4.6	26.1	0.7	−2.5	0.2
	q	723.2	535.7	322.9	152.4	61.2	11.4	−0.7	0.2
2: 40kN	***p***	387.4	191.1	139.9	51.8	48.4	1.4	−3.6	0.2
	q	710.0	609.1	440.5	242.7	99.5	15.6	−1.3	0.2
3: 40kN	***p***	446.7	263.4	106.6	−45.4	17.9	1.5	−1.9	0.0
	q	638.5	488.0	300.1	128.3	43.1	9.6	−0.4	0.0
3a: 40kN	***p***	446.7	263.4	106.6	−45.4	17.9	1.5	−1.9	0.0
	q	638.5	488.0	300.1	128.3	43.1	9.6	−0.4	0.0
1: 50kN	***p***	471.1	181.5	75.2	7.3	34.3	1.6	−3.3	0.2
	q	715.0	540.8	349.8	183.5	79.9	15.2	−0.9	0.2
2: 50kN	***p***	421.2	248.3	179.0	75.8	59.0	3.5	−4.9	0.2
	q	625.1	630.8	519.7	310.6	131.9	21.8	−1.7	0.2
3: 50kN	***p***	478.4	291.4	120.2	−53.4	23.3	2.5	−2.4	0.0
	q	656.7	518.5	330.5	148.8	53.5	12.5	−0.4	0.1
1a: 60kN	***p***	476.8	195.7	90.1	12.0	40.3	3.2	−4.1	0.2
	q	676.5	533.9	374.7	214.3	98.5	19.3	−1.2	0.2
3a: 60kN	***p***	502.6	312.8	130.8	−60.2	28.4	3.5	−2.8	0.0
	q	669.3	539.3	354.0	165.8	62.8	15.3	−0.4	0.1

Table A4.6 Stresses in the pavement at various depth increments under a single wheel calculated with DEFPAV.

ID	Stress	Depth (mm)							
		25	***50***	***84***	***141***	***225***	***358***	***808***	***1875***
1b: 40kN	***p***	443.2	167.0	97.5	9.6	46.3	8.4	−5.1	0.1
	q	729.6	576.1	401.3	237.6	117.4	28.8	−0.8	0.2
3b: 40kN	***p***	461.9	293.5	121.9	−69.2	34.5	6.8	−3.3	−0.3
	q	648.6	525.8	354.0	178.6	77.7	21.9	0.2	−0.1
1b: 60kN	***p***	490.2	237.7	141.4	12.5	60.1	16.6	−7.5	−0.2
	q	687.3	590.4	468.8	314.6	167.8	45.9	−0.6	0.1
3b: 60kN	***p***	517.4	340.7	145.5	−77.7	46.3	12.8	−4.4	−0.5
	q	676.6	570.1	409.9	230.2	112.4	34.2	0.9	−0.1

Table A4.7 Stresses in the pavement at various depth increments under a single wheel calculated with DEFPAV.

ID	stress	Depth (mm)							
		90	***115***	***149***	***206***	***290***	***423***	***873***	***1940***
4: 50kN	***p***	104.8	91.5	75.7	61.1	51.4	18.8	−2.2	−1.2
	q	312.6	267.1	213.2	154.3	98.5	39.1	4.7	−0.2

Table A4.8 Stresses in the pavement at various depth increments under a single wheel calculated with DEFPAV.

ID	stress	Depth (mm)									
		100	***125***	***159***	***216***	***300***	***331***	***374***	***445***	***575***	***666***
5: 45kN	***p***	92.5	72.9	52.7	36.2	28.5	25.9	22.2	18.9	18.7	22.3
	q	269.3	218.9	163.1	111.0	84.5	73.4	61.0	48.4	39.5	32.2
6: 45kN	***p***	100.1	78.5	56.4	37.6	29.1	26.3	22.4	18.9	18.7	22.2
	q	282.5	230.1	171.5	116.3	88.0	76.2	63.1	49.8	40.3	32.6

A4.5 Required adjustments (from comparison with measured rut depth)

A4.5.1 Adjusted rut depths for the first 25 k-cycles

As discussed in Section 5.4, it was expected the value of permanent strain after the first 25 k wheel loads will be inaccurate because the value is being derived from RLT multi-stage tests (see Figure A4.6). Therefore, for the first analysis, the predicted rut depths were adjusted to the measured rut depth after the first 25k, while the residual horizontal stresses were assumed to be nil.

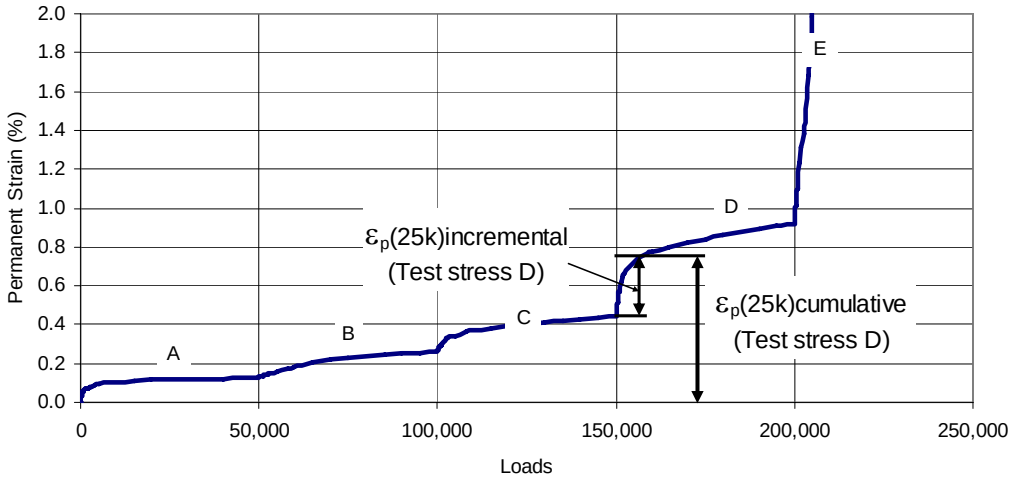

Figure A4.6 The difference between incremental and cumulative permanent strain at 25,000 load cycles for each testing stress.

About 11 out of 17 pavement sections produced the predicted rut depth (after an adjustment to rut depth after an initial 25 k) that can be reasonably fitted with the measured rut depths. Values of the adjusted rut depths are given in Table A4.9.

Table A4.9 Adjustments required to obtain best fit of calculated to measured rut depth.

Pavement Test Section ID and loading	Adjustments to obtain fit to measured rut depth.		Figure
	Rut depth added @ 25k (mm)	Horizontal residual stress (kPa)	
1: 40kN	−1.4	17	5.6
1: 50kN	0.6	0	
1a: 40kN	−1.6	17	
1a: 60kN	0.0	0	
1b: 40kN	−3.5	17	
1b: 60kN	−3.3	0	
2: 40kN	−2.6	250	5.7
2: 50kN	−1.1	200	
3: 40kN	1.1	0	5.8
3: 50kN	0.9	0	
3a: 40kN	2.2	0	
3a: 60kN	4.3	0	
3b: 40kN	1.3	0	
3b: 60kN	5.9	0	
4: 50kN	6.3	50	5.9
5: 45kN	1.9	0	5.10
6: 45kN	0.9	0	5.11

The predicted rut depth at 25 k for most pavement sections required an additional value in the range between 0 mm and +6 mm to obtain an accurate prediction of rut depth, with the exception of pavement section 1b: 60kN that required an adjustment of −3.3 mm. However, the trend in rut depth progression (i.e. slope of graph) predicted was generally nearly the same as that measured. The accuracy in the prediction of rut depth progression is because it is related to the longer term steady state response in the RLT permanent strain tests and not caused by the initial response being affected by sample preparation (e.g. compaction).

A4.5.2 Adjusted residual horizontal stresses

For the six remaining pavement sections, it was necessary to add horizontal residual stress in order to obtain a near-perfect match between predicted and measured rut depth. Values of both adjusted rut depths and residual stresses are given in Table A4.9.

It was found that pavement sections 1: 40 kN, 1a: 40 kN and 1b: 40 kN required reasonable adjustment of residual horizontal stress (in the order of 17 kPa). However, pavement sections 2: 40kN, 2: 50kN and 4: 50kN required very high adjusted values of residual horizontal stress in the range of 50–250 kPa, which were not expected to occur in the granular bases. Sections 2: 40 and 50kN both utilised the CAPTIF 2 granular material which consists of good quality aggregate with 10% by mass of silty clay fines added to weaken the material. This weakening of the aggregate was evident in the RLT tests showing the highest deformations and thus the rut depth model without horizontal confining stress added predicted rutting of the order of 90 mm. However, in the CAPTIF accelerated pavement test the section with the CAPTIF 2 aggregate showed adequate performance, probably because of the indoor dry environment. The ability of the RLT apparatus and associated rut depth model to identify the CAPTIF 2 material as a poor material is a good result showing its ability to be used for material assessment.

Table A4.10 shows the rut depths attributable to aggregate and subgrade for the New Zealand accelerated pavement test sections at CAPTIF. This was not necessary for the Northern Ireland trials (ID 5 and 6) as the subgrade was solid rock material and so was not modelled plastically, a characteristic of the site.

- For pavement test sections 1, 1a, and 1b, 40–50% of the predicted rut depth was attributable to the granular material (CAPTIF 1).
- For pavement test section 2, most of the rutting could be attributed to the CAPTIF 2 base (90–94%).
- For pavement test sections 3, 3a, and 3b, only 12–16% of the rutting could be attributed to the granular material (CAPTIF 3, Table 3.1 in this report).
- For pavement test section 4, most of the rutting could be attributed to the subgrade (96%). Another point with this pavement test section is that, after 100 k loads, no additional rutting was predicted to occur in the granular material (CAPTIF 4) because the rut progression was a result of subgrade rutting only.

Based on the predicted contributions of base and subgrade deformations, it was likely that error in the predicted rut depth for pavement test section 2 resulted from error in the RLT

permanent strain tests for the CAPTIF 2 material. It was considered that the moisture content in the pavement test could have been less than that tested in the RLT apparatus and therefore the CAPTIF 2 material was stronger in-situ.

Table A4.10 Rut depths attributable to aggregate and subgrade in NZ accelerated pavement tests as predicted from Arnold (2004) rut depth model.

Pavement Test Section ID and loading	Rut Depth @ 100 k				Rut Depth @ 1 M			
	A (mm)	S (mm)	A %	S %	A (mm)	S (mm)	A %	S %
1: 40kN	3.2	1.5	69	31	6.1	5.2	54	46
1: 50kN	3.3	1.8	64	36	6.2	6.6	48	52
1a: 40kN	3.2	1.5	69	31	6.1	5.2	54	46
1a: 60kN	3.0	2.2	58	42	5.8	8.2	41	59
1b: 40kN	4.6	2.0	70	30	8.3	7.6	52	48
1b: 60kN	4.3	2.7	61	39	8.0	11.2	42	58
2: 40kN	8.6	1.8	82	18	105	7.0	94	6
2: 50kN	8.1	2.3	78	22	85	9.3	90	10
3: 40kN	0.2	1.2	14	86	0.6	4.1	12	88
3: 50kN	0.3	1.4	16	84	0.7	5.0	13	87
3a: 40kN	0.2	1.2	14	86	0.6	4.1	12	88
3a: 60kN	0.4	1.6	18	82	0.9	5.8	13	87
3b: 40kN	0.4	1.5	20	80	0.8	5.4	13	87
3b: 60kN	0.8	2.0	29	71	1.5	7.8	16	84
4: 50kN	0.4	2.3	14	86	0.4	10.0	4	96

A= aggregate
S= sub-grade

Appendix 5 Laboratory permanent strain results obtained with the Austroads RLT test method

A5.1 Laboratory results of permanent strain

Table A5.1 summarises the results of dry density and moisture contents for six specimens of two base materials CAPTIF 1 and CAPTIF 3 tested with the Austroads RLT test methods by ARRB and the Transportation Laboratory at the University of Canterbury.

Table A5.1 Densities and moisture contents of RLT specimens.

Material	Maximum grain size (mm)	Sample diameter (mm)	Compaction method	Sample No.	Laboratory Dry Density (t/m^3)	Laboratory Moisture Content (%)
CAPTIF 1	20	100	Dynamic	NZ9726	2.172	2.7
CAPTIF 3				MO39546	2.168	4.6
CAPTIF 1	40	150	Vibratory	CANT1	2.070	1.8
CAPTIF 2				CANT2	2.158	2.7
CAPTIF 4				CANT3	2.151	2.5

Figures A5.1 to A5.5 show the results of permanent strain obtained for the RLT specimens.

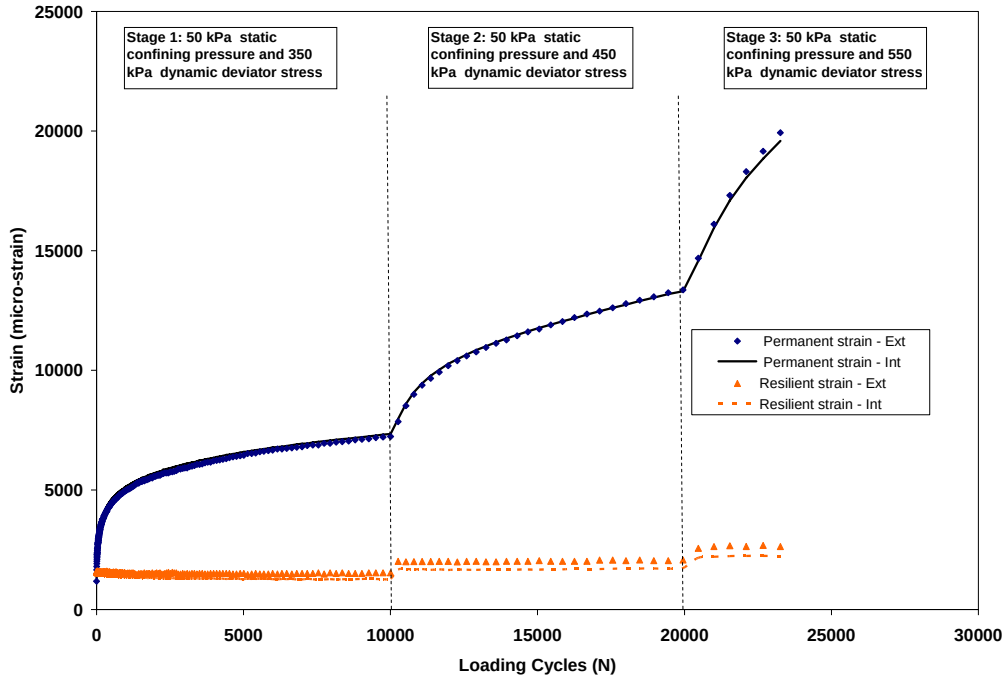

Figure A5.1 Permanent strain results for CAPTIF 1 (NZ9726, 2.172 t/m^3 DD 2.7% MC).

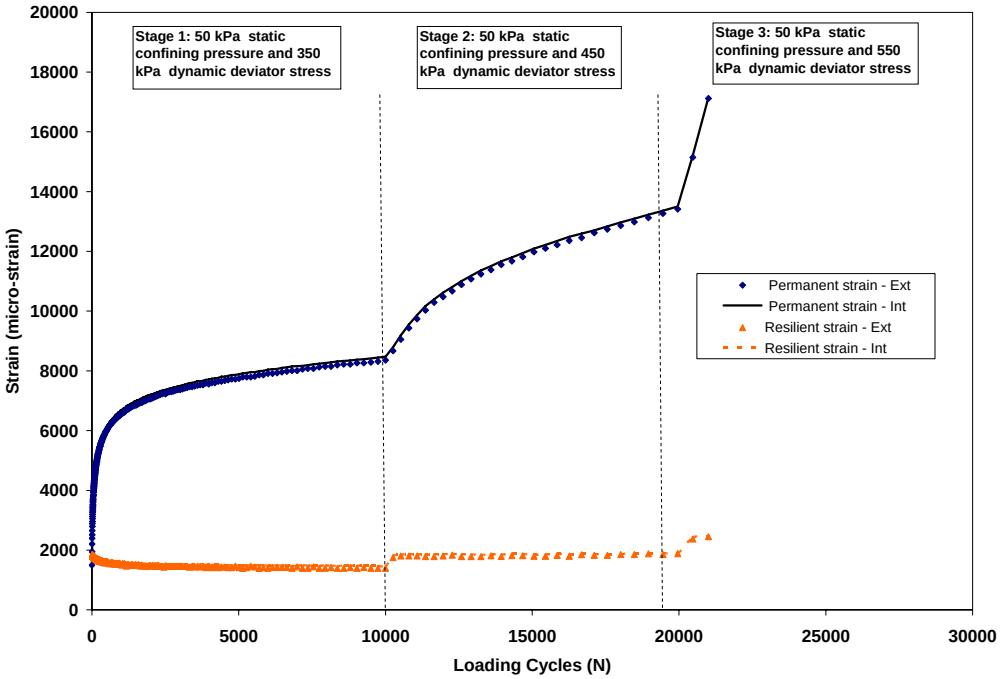

Figure A5.2 Permanent strain results for CAPTIF 3 (MO39546, 2.168 t/m^3 DD, 4.6% MC).

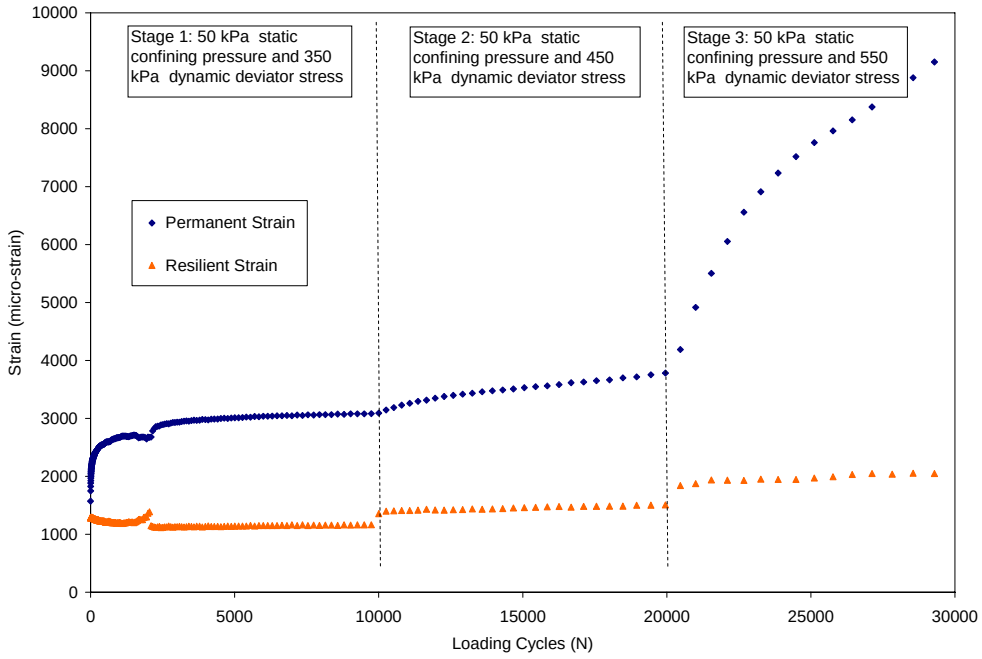

Figure A5.3 Permanent strain results for CAPTIF 1 (CANT1, 2.070 t/m^3 DD, 1.8% MC).

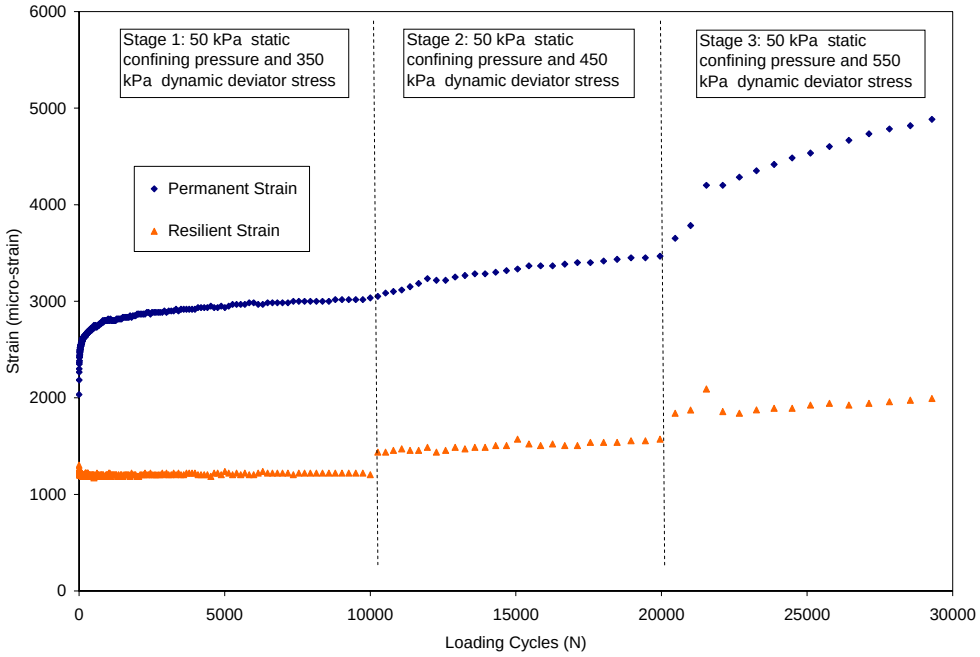

Figure A5.4 Permanent strain results for CAPTIF 2 (CANT2, 2.158 t/m^3, 2.7%).

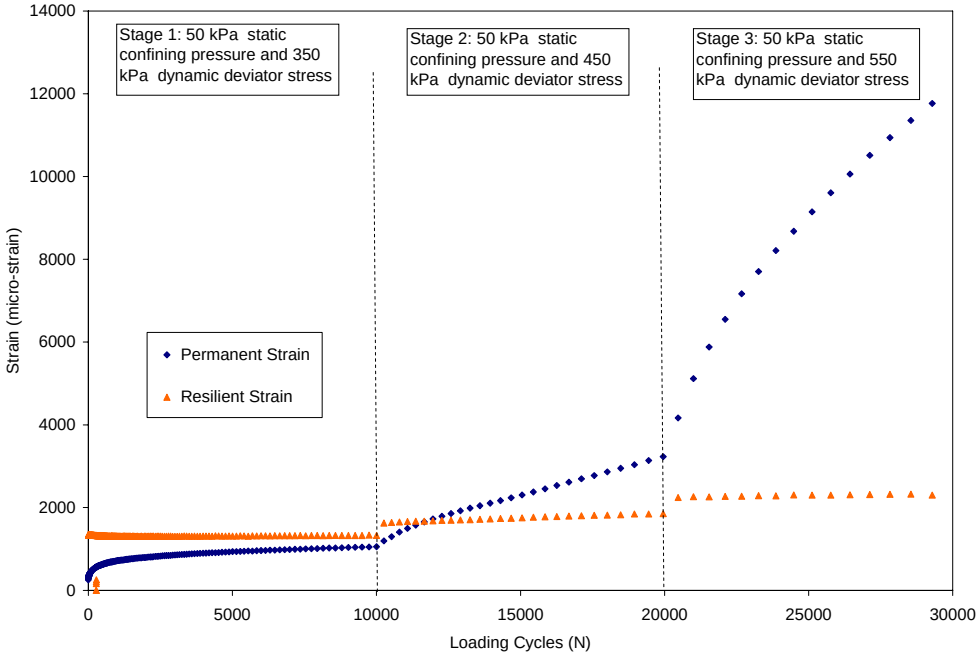

Figure A5.5 Permanent strain results for CAPTIF 4 (CANT3, 2.151 t/m^3, 2.5%).

A5.2 Permanent strain-loading cycle relationships

The relationship between permanent strain and loading cycle for each stress stage can be expressed using a simple power law as given in Equation A2.7:

$$\varepsilon_p = [\mu.\varepsilon_r/\alpha].\ N^{\alpha} \qquad \text{(Equation A2.7)}$$

where:

ε_r = resilient strain for the stress level applied.

α, μ = material constants

The procedures for back-calculation of permanent strain data as described in Technical Note 2 (Appendix 2, Section A2.8) was used to determine the values of parameters α and μ for each stress stage in the multi-stage permanent strain test.

Figures A5.6 to A5.10 show the curves fitted closely with the test data and the variation of the model parameters with repeated deviator stresses for all specimen tested.

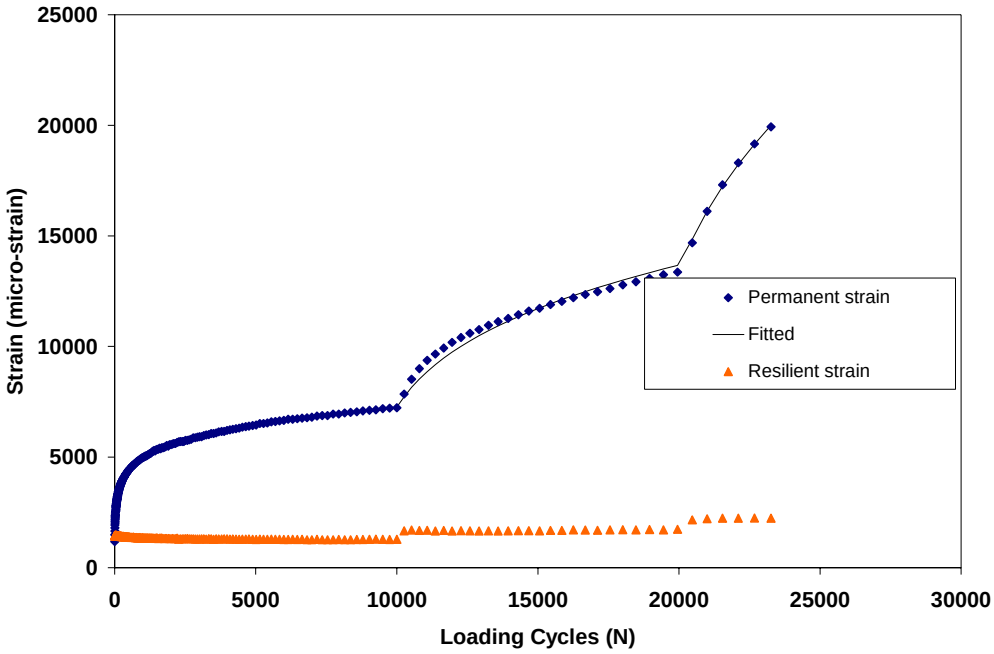

(a) Fitted curve

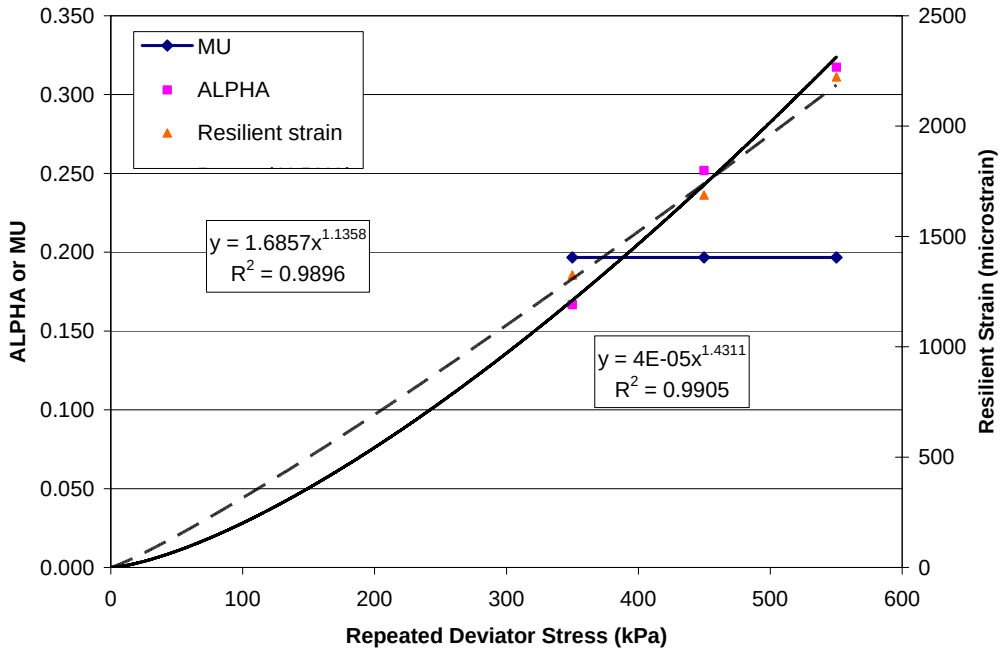

(b) Model parameters

Figure A5.6 Permanent strain model for CAPTIF 1 (NZ9726, 2.172 t/m^3, 2.7%).

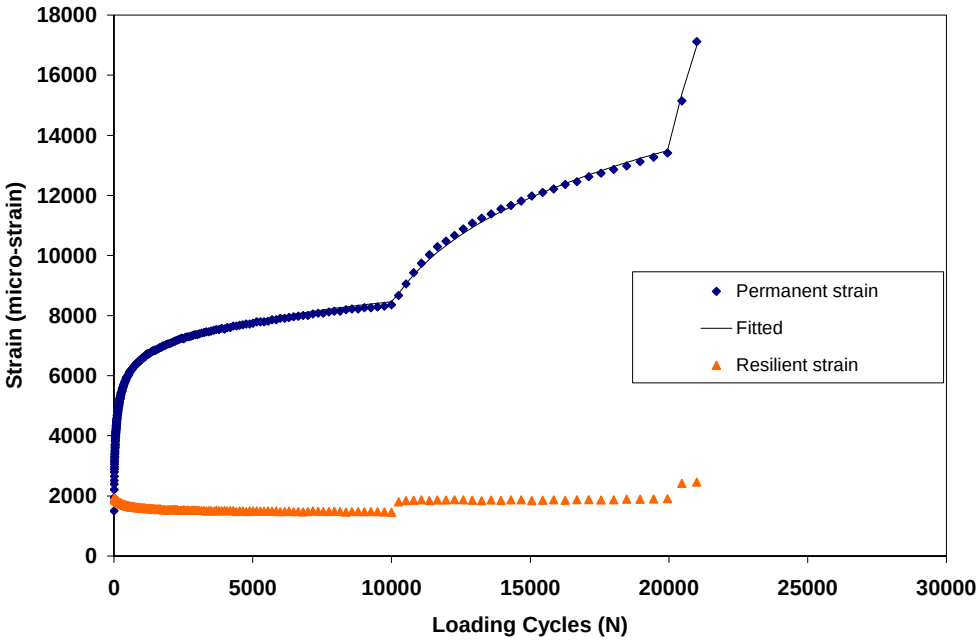

(a) Fitted curve

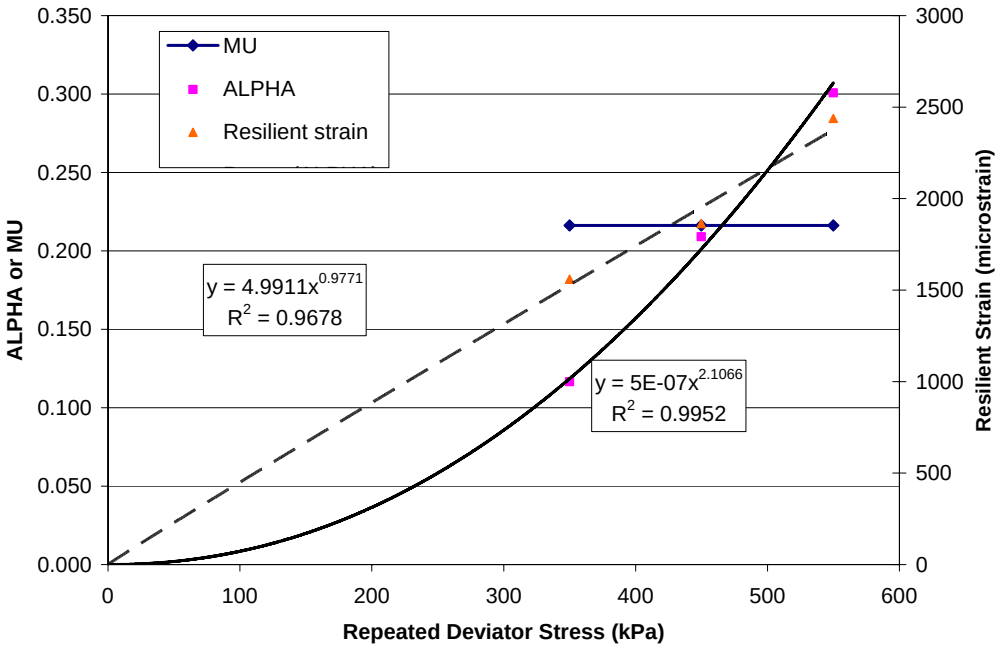

(b) Model parameters

Figure A5.7 Permanent strain model for CAPTIF 3 (MO39546, 2.168 t/m^3, 4.6%).

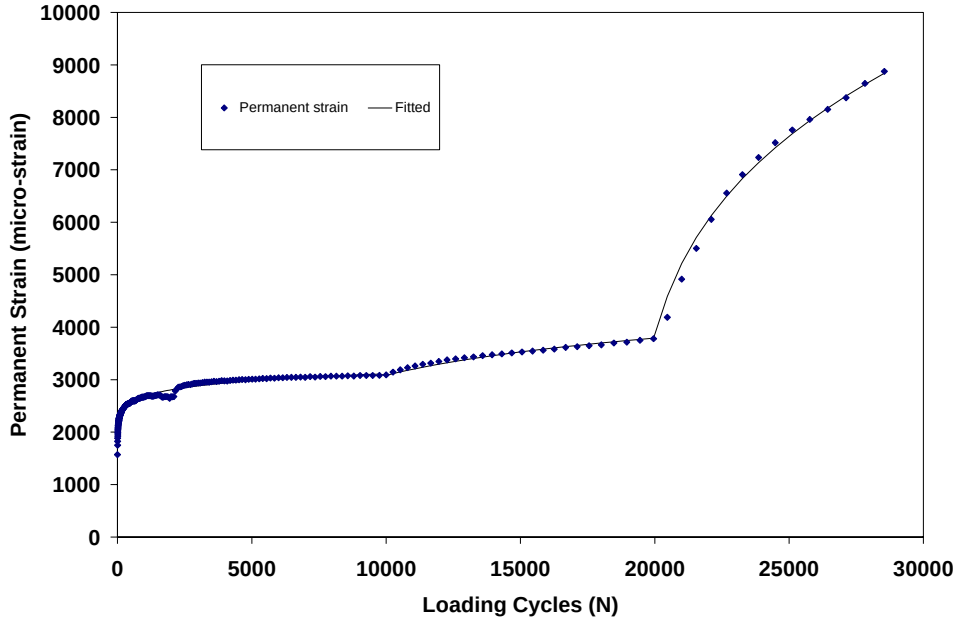

(a) Fitted curve

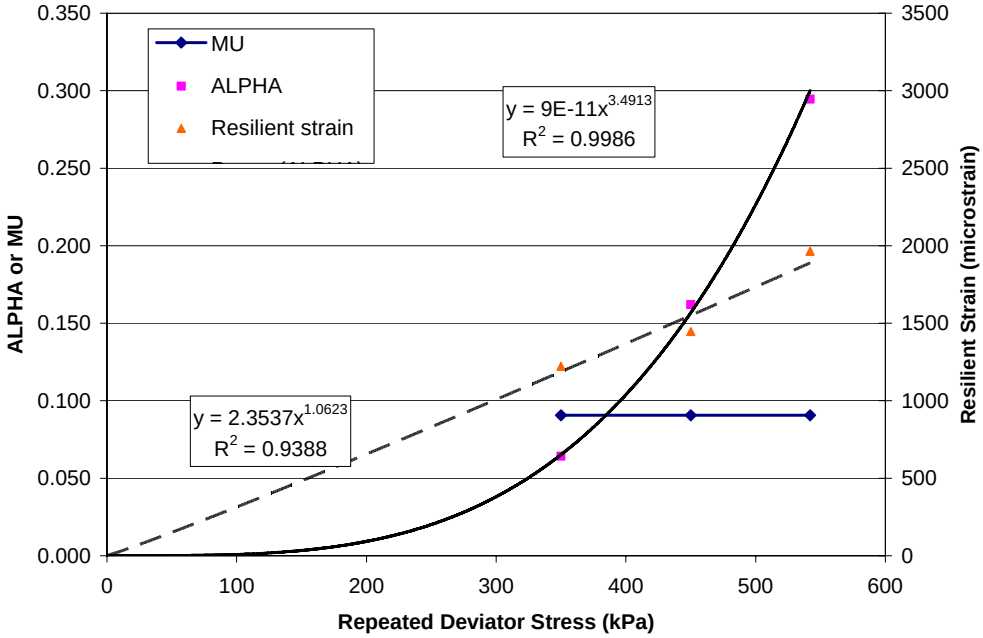

(b) Model parameters

Figure A5.8 Permanent strain model for CAPTIF 1 (CANT1, 2.070 t/m^3, 1.8%).

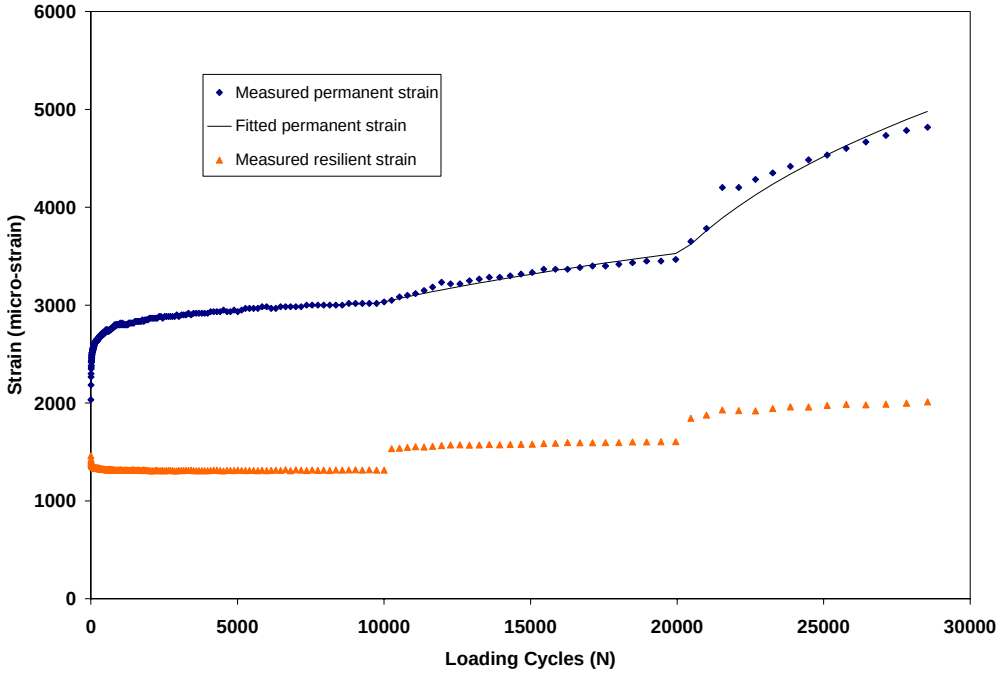

(a) Fitted curve

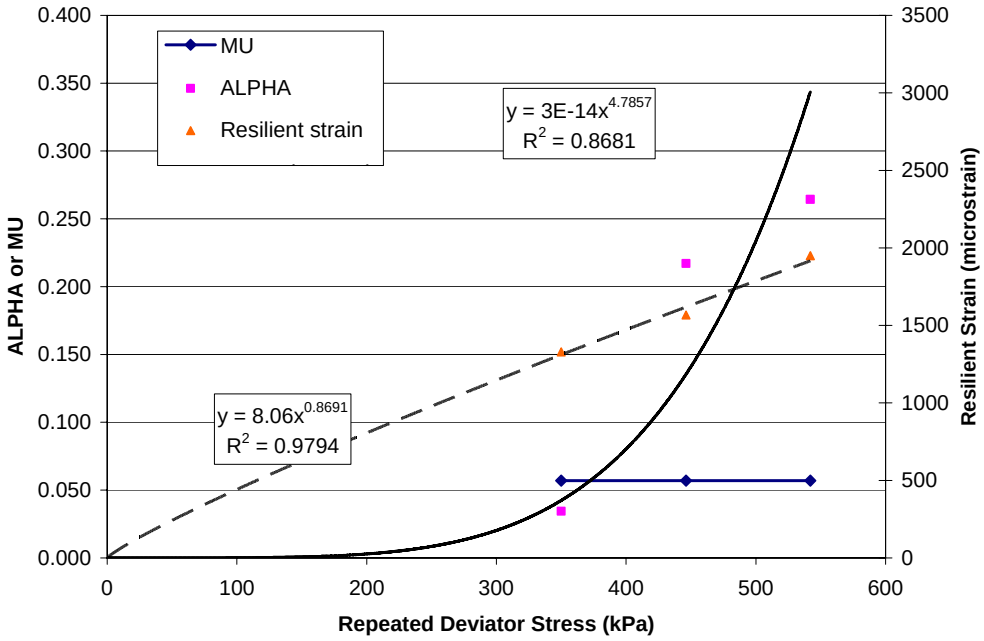

(b) Model Parameters

Figure A5.9 Permanent strain model for CAPTIF 2 (CANT2, 2.158 t/m^3, 2.7%).

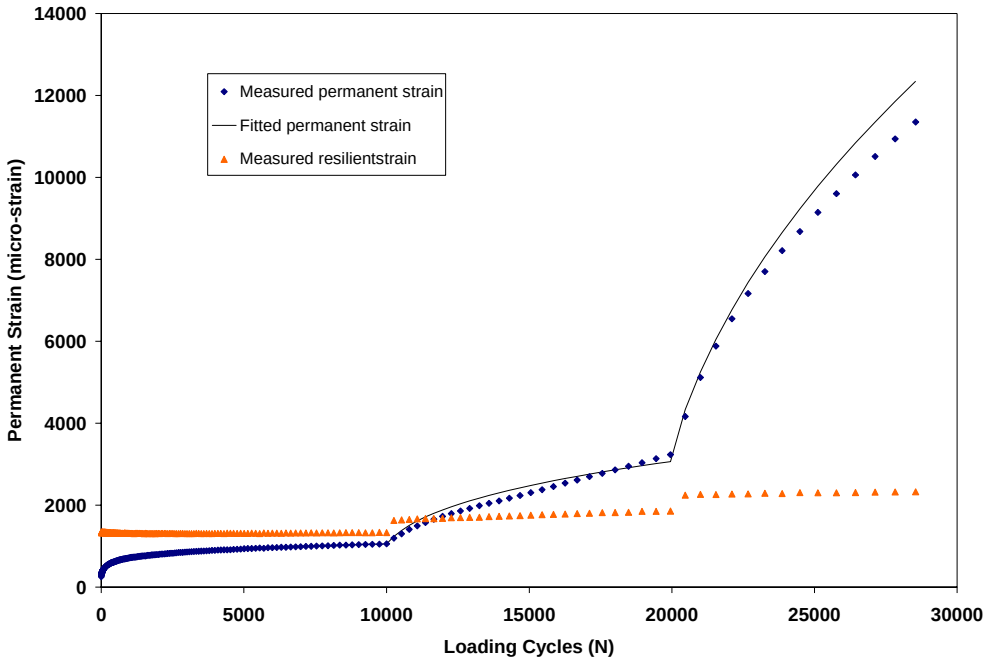

(a) Fitted curve

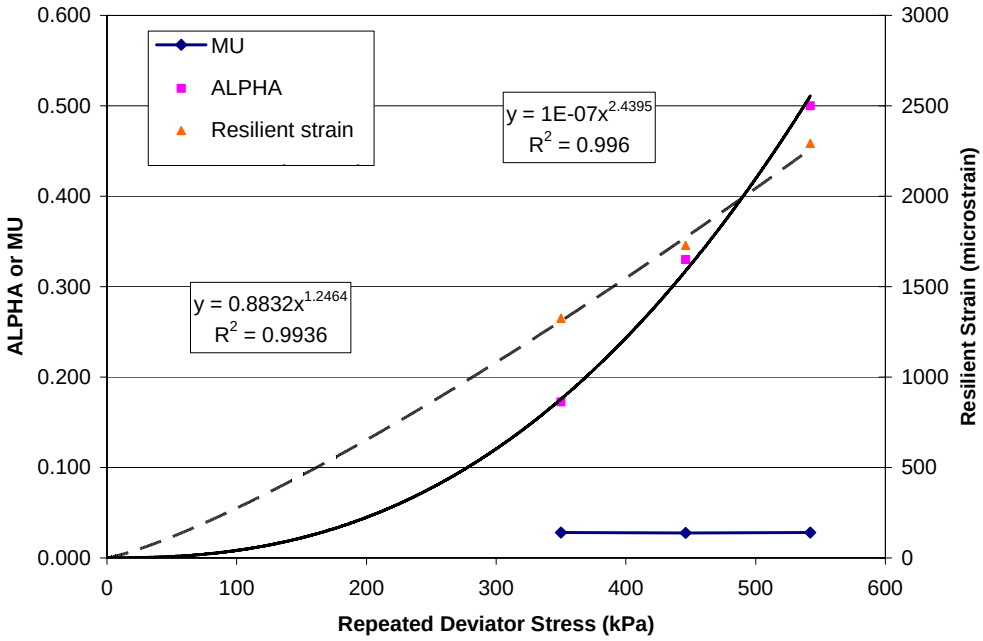

(b) Model parameters

Figure A5.10 Permanent strain model for CAPTIF 4 (CANT3, 2.151 t/m^3, 2.5%).

A5.3 Assessment of deformation life

The procedure for determination of deformation lives as described in Section A2.8, Appendix 2 was used to determine the design deformation life and shear strength for the material tested and the results are given in Figures A5.11 to A5.15.

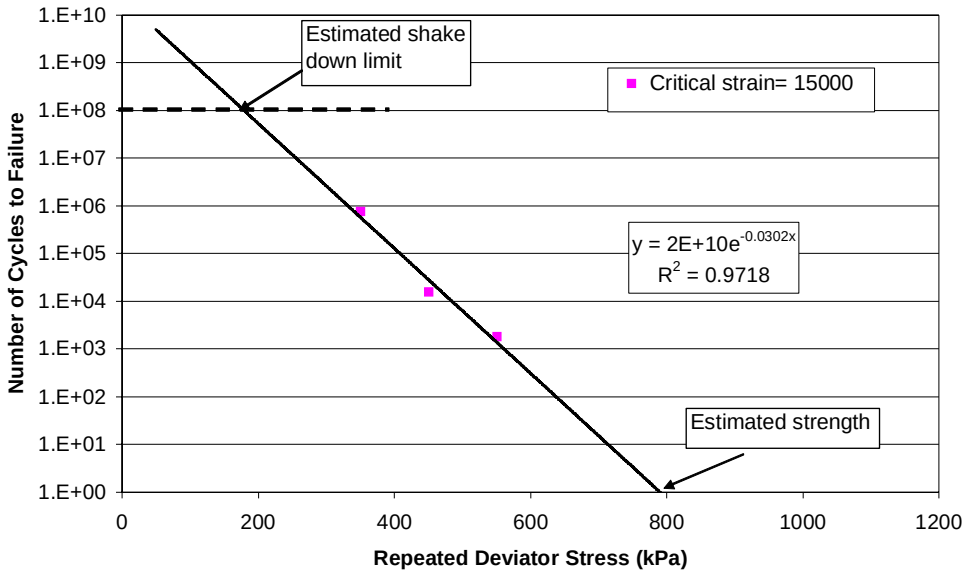

Figure A5.11 Deformation lives and strength limit for CAPTIF 1 (NZ9726, 2.172 t/m^3, 2.7%).

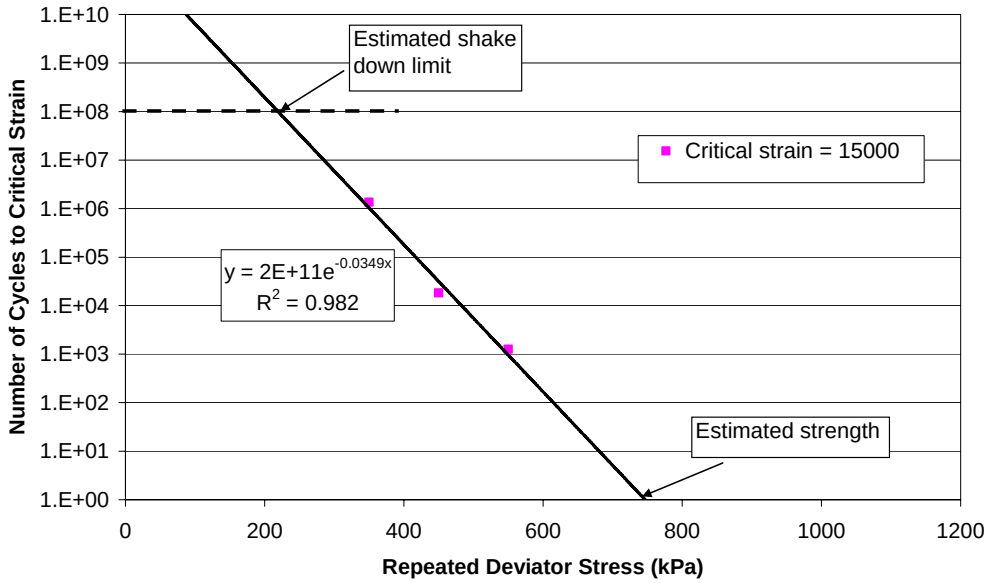

Figure A5.12 Deformation lives and strength limit for CAPTIF 3 (MO39546, 2.168 t/m^3, 4.6%).

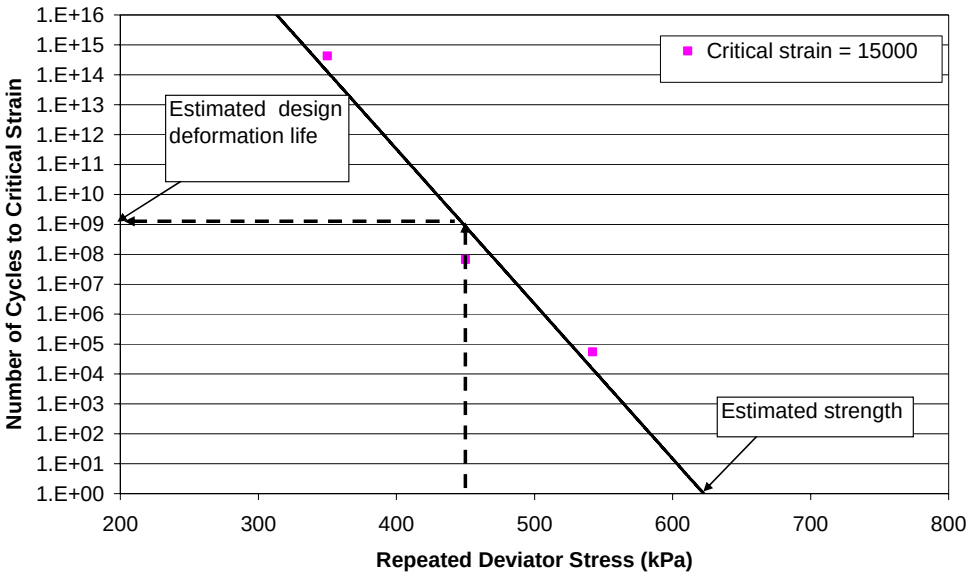

Figure A5.13 Deformation lives and strength limit for CAPTIF 1 (CANT1, 2.070 t/m^3, 1.8%).

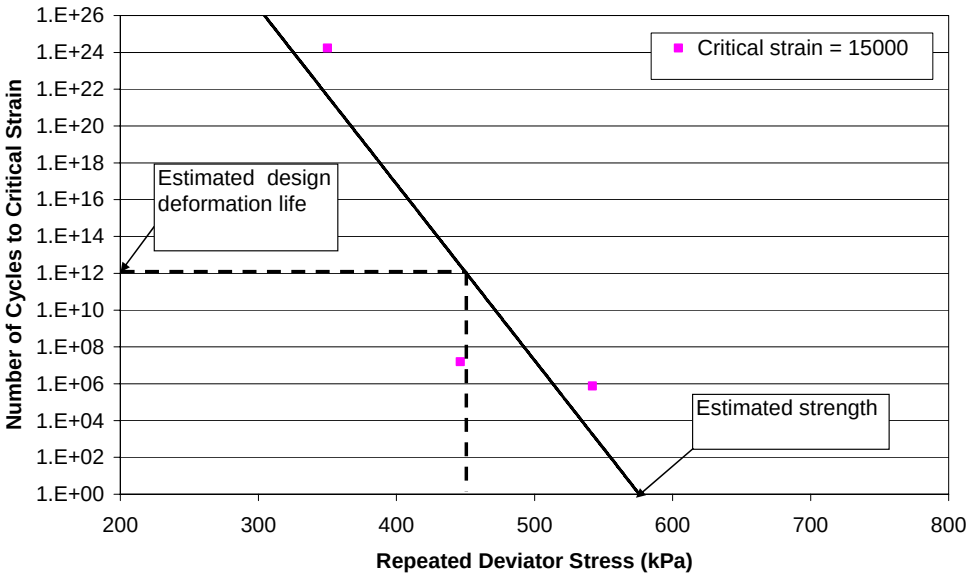

Figure A5.14 Deformation lives and strength limit for CAPTIF 2 (CANT2, 2.158 t/m^3, 2.7%).

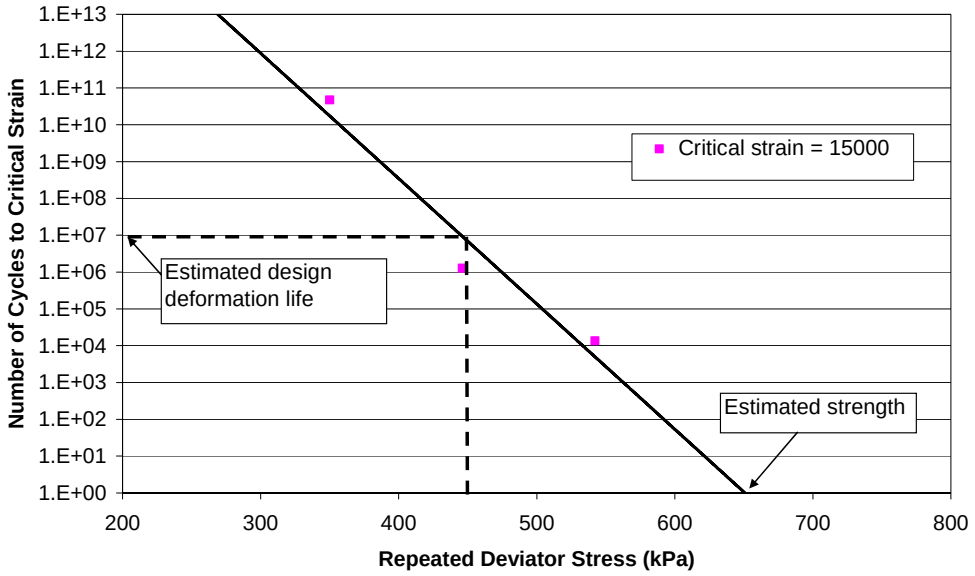

Figure A5.15 Deformation lives and strength limit for CAPTIF 4 (CANT3, 2.151 t/m^3, 2.5%).

Appendix 6 Results of validation of simplified rut depth model based on Arnold (2004)

A6.1 RLT test data – Reduced set

The first step in simplifying the rut depth model proposed by Arnold (2004) is to reduce the number of stages in the RLT test. Using existing RLT data a total of 4 testing stresses were selected for the CAPTIF aggregates (i.e. CAPTIF 1, 2, 3, and 4). Also, the only data from these testing stresses required was the rate of permanent deformation or slope between 25 k and 50 k load cycles as the aim is to determine a ranking of performance. Tables A6.1 to A6.4 details the effect on the prediction of permanent strain rate using a reduced RLT data set as highlighted in bold.

Table A6.1 Effect of obtaining equation parameters (a, b. and c – Equation 3.6) from reduced RLT data set for CAPTIF 1 material.

Material	p (MPa)	q (MPa)	$\varepsilon_{p(rate)}$ – 25k to 50k (% per 1M) $\varepsilon_{p(rate)} = e^{(a)} e^{(bp)} e^{(cq)} - e^{(a)} e^{(bp)}$			Eq. 3.6 Parameters (a, b, c)		
			Measured	Calculated (Equation)				
			RLT	Full set	Reduced set		Full set	Reduced set
CAPTIF 1	0.076	0.043	0.067	0.052	0.037	a	−1.545	−2.040
CAPTIF 1	0.077	0.091	0.165	0.163	0.116	b	−17.153	−15.000
CAPTIF 1	0.077	0.139	0.429	0.387	0.275	c	14.856	14.757
[1]CAPTIF 1	**0.077**	**0.183**	**0.784**	**0.808**	**0.570**			
CAPTIF 1	0.149	0.135	0.107	0.107	0.089			
CAPTIF 1	0.154	0.183	0.230	0.217	0.180			
CAPTIF 1	0.151	0.229	0.387	0.470	0.387			
[1]CAPTIF 1	**0.150**	**0.274**	**0.449**	**0.941**	**0.770**			
CAPTIF 1	0.152	0.319	3.874	1.771	1.450			
[1]CAPTIF 1	**0.247**	**0.324**	**0.335**	**0.372**	**0.374**			
CAPTIF 1	0.247	0.376	1.178	0.813	0.812			
[1]CAPTIF 1	**0.250**	**0.419**	**1.493**	**1.493**	**1.493**			
CAPTIF 1	0.243	0.465	3.303	3.303	3.242			
			Mean Error	**0.24**	**0.29**			

[1] Note: Stress conditions used for reduced data set are highlighted in bold

Table A6.2 Effect of obtaining equation parameters (a, b and c – Equation 3.6) from reduced RLT data set for CAPTIF 2 material.

Material	p (MPa)	q (MPa)	$\varepsilon_{p(rate)}$ – 25k to 50k (% per 1M) $\varepsilon_{p(rate)} = e^{(a)} e^{(bp)} e^{(cq)} - e^{(a)} e^{(bp)}$			Eq. 3.6 Parameters (a, b, c)		
			Measured	Calculated (Equation)				
			RLT	Full set	Reduced set		Full set	Reduced set
[1]**CAPTIF 2**	**0.075**	**0.037**	**0.146**	**0.217**	**0.202**	**a**	**−1.8E−07**	**−8.2E−07**
CAPTIF 2	**0.075**	**0.086**	**0.703**	**0.656**	**0.685**	**b**	**−8.47**	**−15.00**
CAPTIF 2	**0.150**	**0.135**	**0.536**	**0.706**	**0.514**	**c**	**9.34**	**13.15**
CAPTIF 2	0.150	0.183	1.059	1.267	1.064			
CAPTIF 2	**0.151**	**0.231**	**2.461**	**2.123**	**2.060**			
CAPTIF 2	0.151	0.276	16.305	3.391	3.832			
CAPTIF 2	0.249	0.321	1.815	2.308	1.603			
CAPTIF 2	**0.250**	**0.374**	**2.035**	**3.820**	**3.189**			
CAPTIF 2	0.246	0.416	5.948	5.940	5.948			
CAPTIF 2	**0.242**	**0.465**	**12.331**	**9.790**	**12.064**			
CAPTIF 2	**0.247**	**0.510**	**16.740**	**14.291**	**20.145**			
CAPTIF 2	**0.246**	**0.559**	**22.809**	**22.827**	**38.935**			
			Mean Error	**1.75**	**2.85**			

[1] Note: Stress conditions used for reduced data set are highlighted in bold

Table A6.3 Effect of obtaining equation parameters (a, b, and c – Equation 3.6) from reduced RLT data set for CAPTIF 3 material.

Material	p (MPa)	q (MPa)	$\varepsilon_{p(rate)}$ – 25k to 50k (% per 1M) $\varepsilon_{p(rate)} = e^{(a)} e^{(bp)} e^{(cq)} - e^{(a)} e^{(bp)}$			Eq. 3.6 Parameters (a, b, c)		
			Measured	Calculated (Equation)				
			RLT	Full Set	Reduced Set		Full Set	Reduced Set
[1]CAPTIF 3	**0.072**	**0.037**	**0.072**	**0.023**	**0.032**	**a**	**−1.870**	**−1.603**
CAPTIF 3	**0.072**	**0.086**	**0.349**	**0.084**	**0.102**	**b**	**−22.592**	**−15.000**
CAPTIF 3	**0.074**	**0.135**	**0.249**	**0.206**	**0.213**	**c**	**15.588**	**10.711**
CAPTIF 3	**0.074**	**0.181**	**0.469**	**0.459**	**0.396**			
CAPTIF 3	**0.151**	**0.135**	**0.102**	**0.06**	**0.068**			
CAPTIF 3	0.151	0.183	0.329	0.082	0.127			
CAPTIF 3	**0.147**	**0.230**	**0.281**	**0.197**	**0.240**			
CAPTIF 3	0.146	0.274	0.403	0.404	0.403			
CAPTIF 3	**0.246**	**0.278**	**0.330**	**0.045**	**0.094**			
CAPTIF 3	0.246	0.327	0.756	0.096	0.161			
CAPTIF 3	**0.246**	**0.375**	**0.239**	**0.206**	**0.275**			
CAPTIF 3	0.244	0.420	0.455	0.425	0.455			
CAPTIF 3	**0.244**	**0.469**	**0.801**	**0.928**	**0.781**			
CAPTIF 3	**0.244**	**0.517**	**1.367**	**1.963**	**1.309**			
CAPTIF 3	**0.243**	**0.562**	**4.042**	**4.042**	**2.152**			
			Mean Error	**0.17**	**0.23**			

[1] Note: Stress conditions used for reduced data set are highlighted in bold

Table A6.4 Effect of obtaining equation parameters (a, b, and c – Equation 3.6) from reduced RLT data set for CAPTIF 4 material.

Material	p (MPa)	q (MPa)	$\varepsilon_{p(rate)}$ – 25k to 50k (% per 1M) $\varepsilon_{p(rate)} = e^{(a)} e^{(bp)} e^{(cq)} - e^{(a)} e^{(bp)}$			Eq. 3.6 Parameters (a, b, c)		
			Measured	Calculated (Equation)				
			RLT	Full Set	Reduced Set		Full set	Reduced set
CAPTIF 4	0.077	0.036	0.213	0.271	0.281	a	1.65	1.55
CAPTIF 4	0.077	0.085	0.615	0.909	0.739	b	−32.42	−15.00
CAPTIF 4	0.150	0.130	0.134	0.190	0.426	c	13.48	4.76
CAPTIF 4	0.151	0.179	0.531	0.397	0.661			
[1]CAPTIF 4	**0.150**	**0.227**	**0.816**	**0.816**	**0.969**			
CAPTIF 4	0.148	0.270	1.341	1.585	1.341			
CAPTIF 4	**0.148**	**0.314**	**8.769**	**2.912**	**1.775**			
CAPTIF 4	**0.250**	**0.235**	**0.127**	**0.036**	**0.230**			
CAPTIF 4	0.247	0.374	0.482	0.266	0.573			
CAPTIF 4	0.246	0.421	0.758	0.520	0.758			
CAPTIF 4	**0.246**	**0.469**	**1.092**	**1.002**	**0.986**			
CAPTIF 4	**0.245**	**0.515**	**2.022**	**1.914**	**1.272**			
CAPTIF 4	**0.244**	**0.562**	**3.521**	**3.686**	**1.637**			
			Mean Error	**0.58**	**0.82**			

[1] Note: Stress conditions used for reduced data set are highlighted in bold

The reduced data set of four RLT test stresses was devised to cover a range of stresses and was developed by trialling other data sets until the data set which gave the least error between measured and predicted permanent strain rate was chosen. During this process it was found that the parameter b was required to be fixed at a value of −15 because of the difficulty in determining three parameters on only four data points. The value of −15 was an estimated value and a range of values were trialled with little difference in the mean error with the exception of CAPTIF 4 material.

It was found that the reduced data set for CAPTIF 1, 2, and 3 materials was adequate to model deformation behaviour of the materials as detailed in Figure A6.1 for CAPTIF 3 However, the use of the reduced data set for CAPTIF 4 resulted in poor predictions of permanent strain rate as shown in Figure A6.2. The poor prediction of CAPTIF 4 material was primarily a result of parameter b being fixed at −15 where a value of −30 was considered more appropriate and closer to the −32 found with the full data set.

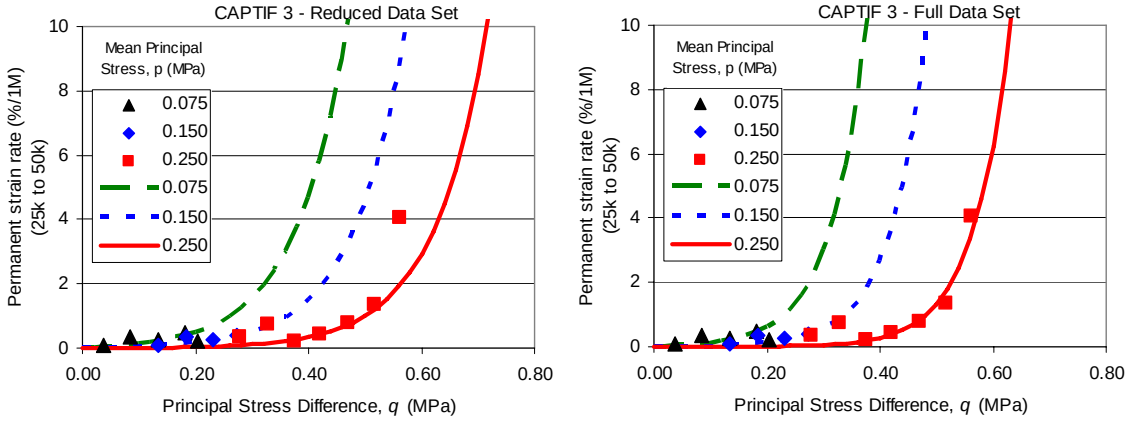

Figure A6.1 Effect of obtaining equation parameters (a, b, and c – Eq. 3.6) from reduced RLT data set for CAPTIF 3 material.

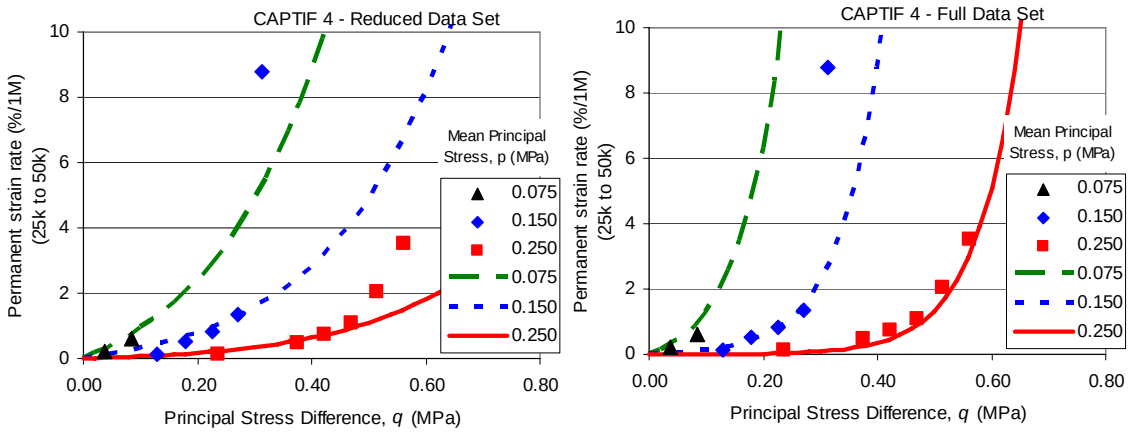

Figure A6.2 Effect of obtaining Equation parameters (a, b and c – Equation 3.6) from reduced RLT data set for CAPTIF 4 material.

A6.2 Rate of rutting prediction with reduced data set

The permanent strain rate model requires stresses *p* (mean principle stress) and *q* (deviatoric stress) as inputs. As part of Arnold's research at the University of Nottingham, an axisymmetric finite element model DEFPAV was used to calculate the centre line stresses for all the CAPTIF tests (Table A6.5). These stresses were used to calculate the rate of rutting using Equation 3.6 with the parameters found with the full and reduced data set. Results are shown in Tables A6.6 to A6.13.

Table A6.5 Pavement test sections at CAPTIF used for predicting centre-line stresses (see Table 6.2)

ID	Granular material	Granular thickness (mm)	Load = 40 kN	Load = 50 kN	Load = 60 kN
1	CAPTIF 1	275	1: 40kN	1: 50kN	
1a		275	1a: 40kN		1a: 60kN
1b		200	1b: 40kN		1b: 60kN
2	CAPTIF 2	275	2: 40kN	2: 50kN	
3	CAPTIF 3	275	3: 40kN	3: 50kN	
3a		275	3a: 40kN		3a: 60kN
3b		200	3b: 40kN		3b: 60kN
4	CAPTIF 4	200		4: 50kN	
5	NI Good	650	5: 45kN[1]		
6	NI Poor	650	6: 45kN[1]		

Table A6.6 Rate of rutting predictions for CAPTIF test section 1.

Layer thickness	Wheel load 40 kN			Full set		Reduced set	
	Depth	p (MPa)	q (MPa)	Rate	mm/10^6 cycles	Rate	mm/10^6 cycles
17	−25	0.446	0.723	4.738	0.8	7.013	1.2
40.5	−59	0.171	0.536	32.728	13.3	27.293	11.1
62.5	−106	0.062	0.323	8.838	5.5	5.959	3.7
97	−184	0.005	0.152	1.699	1.6	1.028	1.0
	−300			**TOTAL**	21.2		17.0
Layer thickness	**Wheel load 50 kN**			**Full set**		**Reduced set**	
	Depth	**p (MPa)**	**q (MPa)**	**Rate**	**mm/10^6 cycles**	**Rate**	**mm/10^6 cycles**
17	−25	0.471	0.715	2.709	0.5	4.239	0.7
40.5	−59	0.181	0.541	29.266	11.9	24.975	10.1
62.5	−106	0.075	0.350	10.553	6.6	7.300	4.6
97	−184	0.007	0.184	2.689	2.6	1.632	1.6
	−300			**TOTAL**	21.5		17.0

Table A6.7 Rate of rutting predictions for CAPTIF test section 1a.

Layer thickness	Wheel load 40 kN			Full set		Reduced set	
	Depth	p	q	Rate	mm/10^6 cycles	Rate	mm/10^6 cycles
17	−25	0.446	0.723	4.738	0.8	7.013	1.2
40.5	−59	0.171	0.536	32.728	13.3	27.293	11.1
62.5	−106	0.062	0.323	8.838	5.5	5.959	3.7
97	−184	0.005	0.152	1.699	1.6	1.028	1.0
	−300			**TOTAL**	21.2		17.0
Layer thickness	**Wheel load 60 kN**			**Full set**		**Reduced Set**	
	Depth	**p**	**q**	**Rate**	**mm/10^6 cycles**	**Rate**	**mm/10^6 cycles**
17	−25	0.477	0.676	1.385	0.2	2.203	0.4
40.5	−59	0.196	0.534	20.705	8.4	18.231	7.4
62.5	−106	0.090	0.375	11.852	7.4	8.446	5.3
97	−184	0.012	0.214	4.015	3.9	2.455	2.4
	−300			**TOTAL**	19.9		15.4

Table A6.8 Rate of rutting predictions for CAPTIF test section 1b.

Layer Thickness	Wheel Load 40 kN			Full Set		Reduced Set	
	Depth	p	q	Rate	mm/10^6 cycles	Rate	mm/10^6 cycles
12.5	−25	0.443	0.730	5.427	0.7	7.986	1.0
29.5	−50	0.167	0.576	63.370	18.7	52.236	15.4
45.5	−84	0.098	0.401	15.501	7.1	11.195	5.1
70.5	−141	0.010	0.238	5.991	4.2	3.637	2.6
	−225			**TOTAL**	30.6		24.1
Layer Thickness	**Wheel Load 60 kN**			**Full Set**		**Reduced Set**	
	Depth	**p**	**q**	**Rate**	**mm/10^6 cycles**	**Rate**	**mm/10^6 cycles**
12.5	−25	0.490	0.687	1.294	0.2	2.116	0.3
29.5	−50	0.238	0.590	23.320	6.9	22.351	6.6
45.5	−84	0.141	0.469	19.951	9.1	15.730	7.2
70.5	−141	0.013	0.315	18.266	12.9	11.079	7.8
	−225			**TOTAL**	29.0		21.8

Table A6.9 Rate of rutting predictions for CAPTIF test section 2.

Layer thickness	Wheel load 40 kN			Full set		Reduced set	
	Depth	p	q	Rate	mm/10^6 cycles	Rate	mm/10^6 cycles
17.0	−25	0.387	0.710	28.340	4.8	34.046	5.8
40.5	−59	0.191	0.609	58.161	23.6	171.433	69.4
62.5	−106	0.140	0.441	18.360	11.5	40.125	25.1
97.0	−184	0.052	0.243	5.568	5.4	10.729	10.4
	−300			**TOTAL**	45.2		110.7
Layer thickness	**Wheel load 50 kN**			**Full set**		**Reduced set**	
	Depth	**p**	**q**	**Rate**	**mm/10^6 cycles**	**Rate**	**mm/10^6 cycles**
17.0	−25	0.421	0.625	9.615	1.6	6.710	1.1
40.5	−59	0.248	0.631	43.907	17.8	96.750	39.2
62.5	−106	0.179	0.520	27.852	17.4	63.391	39.6
97.0	−184	0.076	0.311	9.036	8.8	18.769	18.2
	−300			**TOTAL**	45.6		98.1

Table A6.10 Rate of rutting predictions for CAPTIF test section 3.

Layer thickness	Wheel load 40 kN			Full set		Reduced set	
	Depth	p	q	Rate	mm/10^6 cycles	Rate	mm/10^6 cycles
17.0	−25	0.447	0.639	0.134	0.0	0.231	0.0
40.5	−59	0.263	0.488	0.808	0.3	0.718	0.3
62.5	−106	0.107	0.300	1.477	0.9	0.972	0.6
97.0	−184	−0.045	0.128	2.747	2.7	1.174	1.1
	−300			**TOTAL**	3.9		2.1
Layer thickness	**Wheel load 50 kN**			**Full set**		**Reduced set**	
	Depth	**p**	**q**	**Rate**	**mm/10^6 cycles**	**Rate**	**mm/10^6 cycles**
17.0	−25	0.478	0.657	0.087	0.0	0.175	0.0
40.5	−59	0.291	0.518	0.689	0.3	0.654	0.3
62.5	−106	0.120	0.331	1.750	1.1	1.109	0.7
97.0	−184	−0.053	0.149	4.724	4.6	1.759	1.7
	−300			**TOTAL**	6.0		2.7

Table A6.11 Rate of rutting predictions for CAPTIF test section 3a.

Layer thickness	Wheel load 40 kN			Full set		Reduced set	
	Depth	p	q	Rate	mm/10^6 cycles	Rate	mm/10^6 cycles
17.0	−25	0.447	0.639	0.134	0.0	0.231	0.0
40.5	−59	0.263	0.488	0.808	0.3	0.718	0.3
62.5	−106	0.107	0.300	1.477	0.9	0.972	0.6
97.0	−184	−0.045	0.128	2.747	2.7	1.174	1.1
	−300			**TOTAL**	3.9		2.1
Layer thickness	**Wheel load 60 kN**			**Full set**		**Reduced set**	
	Depth	**p**	**q**	**Rate**	**mm/10^6 cycles**	**Rate**	**mm/10^6 cycles**
17.0	−25	0.503	0.669	0.061	0.0	0.139	0.0
40.5	−59	0.313	0.539	0.589	0.2	0.594	0.2
62.5	−106	0.131	0.354	1.992	1.2	1.226	0.8
97.0	−184	−0.060	0.166	7.370	7.1	2.438	2.4
	−300			**TOTAL**	8.6		3.4

Table A6.12 Rate of rutting predictions for CAPTIF test section 3b

Layer thickness	Wheel load 40 kN			Full set		Reduced set	
	Depth	p	q	Rate	mm/10^6 cycles	Rate	mm/10^6 cycles
12.5	−25	0.462	0.649	0.111	0.0	0.205	0.0
29.5	−50	0.294	0.526	0.737	0.2	0.685	0.2
45.5	−84	0.122	0.354	2.437	1.1	1.402	0.6
70.5	−141	−0.069	0.179	11.178	7.9	3.282	2.3
	−225			**TOTAL**	9.2		3.2
Layer thickness	**Wheel load 60 kN**			**Full set**		**Reduced set**	
	Depth	**p**	**q**	**Rate**	**mm/10^6 cycles**	**Rate**	**mm/10^6 cycles**
12.5	−25	0.517	0.677	0.049	0.0	0.120	0.0
29.5	−50	0.341	0.570	0.507	0.1	0.544	0.2
45.5	−84	0.145	0.410	3.424	1.6	1.808	0.8
70.5	−141	−0.078	0.230	31.399	22.1	6.959	4.9
	−225			**TOTAL**	23.8		5.9

Table A6.13 Rate of rutting predictions for CAPTIF test section ID 4.

Layer thickness	Wheel load 50 kN			Full set		Reduced set	
	Depth	p	q	Rate	mm/10^6 cycles	Rate	mm/10^6 cycles
12.5	−90	0.105	0.313	11.558	1.4	3.361	0.4
29.5	−115	0.092	0.267	9.520	2.8	3.072	0.9
45.5	−149	0.076	0.213	7.451	3.4	2.669	1.2
70.5	−206	0.061	0.154	5.029	3.5	2.052	1.4
	−290			**TOTAL**	11.2		4.0

The total rate of rutting per 1 M wheel loads is summarised and compared with the actual rut depth and rutting rate after 1 M wheel loads at CAPTIF. These results are shown in Table A6.14. A correlation between CAPTIF rut depth or CAPTIF rate of rutting could not be obtained with the predictions from either the full or the reduced data set although the rankings of materials' average performance were similar to the CAPTIF rankings as shown in Table A6.15.

Table A6.14 Predicted rate of rutting compared with actual measured rut depth during CAPTIF tests.

Test	Rate	Rate	Total	Rate	ESA
	Full set	Reduced set	CAPTIF	CAPTIF	Life (Nx10^6)
	mm/10^6 cycles	mm/10^6 cycles	mm	mm/10^6 cycles	CAPTIF
1: 40kN	21.2	17.0	6.0	3.2	2.5
1: 50kN	21.5	17.0	11.2	6.1	2.5
1a: 40kN	21.2	17.0	5.9	2.7	2.6
1a: 60kN	19.9	15.4	10.8	5.0	2.6
1b: 40kN	30.6	24.1	6.5	3.4	2.4
1b: 60kN	29.0	21.8	11.5	4.8	2.4
2: 40kN	45.2	110.7	6.7	3.3	2.4
2: 50kN	45.6	98.1	9.6	4.6	2.4
3: 40kN	3.9	2.1	5.2	3.1	4.5
3: 50kN	6.0	2.7	6.2	3.1	4.5
3a: 40kN	3.9	2.1	6.0	2.9	2.4
3a: 60kN	8.6	3.4	9.4	0.65	2.4
3b: 40kN	9.2	3.2	6.0	2.2	2.8
3b: 60kN	23.8	5.9	11.4	0.77	2.8
4: 50kN	11.2	4.0	9.7	0.66	5.0

Table A6.15 Predicted rate of rutting compared with actual measured rut depth during CAPTIF tests averaged per aggregate type.

Aggregate	mm/10^6 cycles	mm/10^6 cycles	Total	Rate	Life (Nx10^6)
	Full Set	Reduced Set	CAPTIF	CAPTIF	CAPTIF
CAPTIF 3	9.3	3.2	7.4	2.1	3.2
CAPTIF 4	11.2	4.0	9.7	0.7	5.0
CAPTIF 1	23.9	18.7	8.7	4.2	2.5
CAPTIF 2	45.4	104.4	8.2	4.0	2.4

As an aside, the predicted rut depths from the reduced data set were correlated against those predicted with the full data set (Figure A6.3). It appears both the full and reduced RLT data sets can be used to predict differences in performance of various aggregates. Rut depths measured at CAPTIF were similar for all test sections and showed all materials are suitable as basecourse aggregate. If 20 mm is chosen as a maximum acceptable rate of rutting then the RLT tests would predict the CAPTIF 2 aggregate is not suitable as a basecourse material. This is a reasonable result as CAPTIF 2 is an aggregate deliberately contaminated with 10% by mass of plastic clay fines and is considered unsuitable as a basecourse material. The CAPTIF 2 material test section survived at CAPTIF because of the dry indoor conditions of the test track.

Results also show for this simplified analysis the reduced RLT data set produced results as good as the full data set. The poor predictions of rut depth at CAPTIF were a result of an over simplification of the RLT data by only considering the slope of permanent strain between 25k and 50k loading cycles. Arnold (2004) showed that the CAPTIF rut depth can be predicted accurately by considering all aspects of the permanent strain plot from the RLT tests.

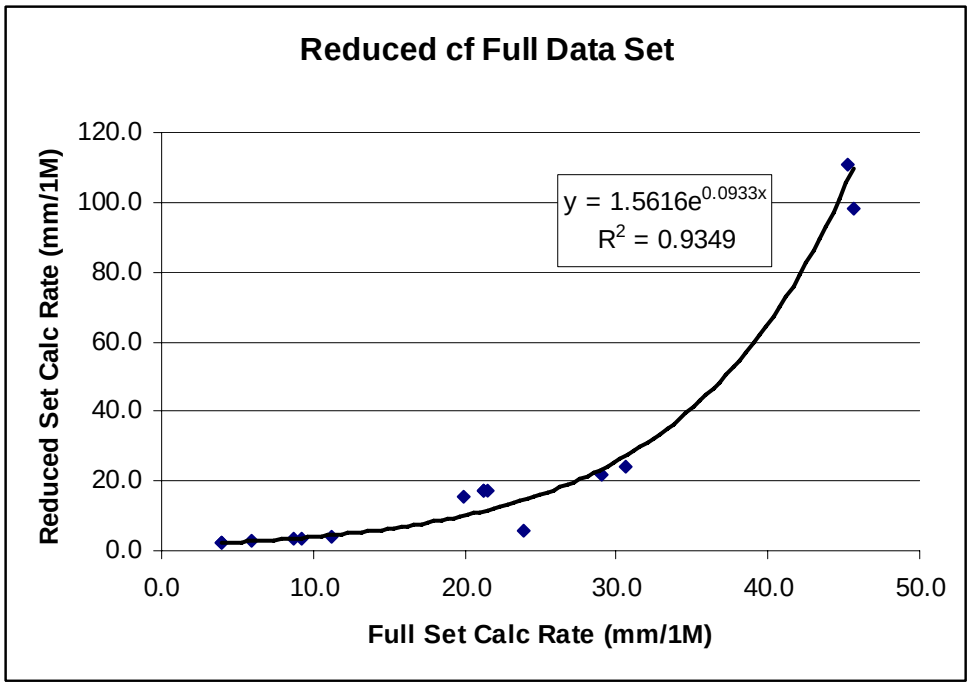

Figure A6.3 Comparison of rate of rutting between predictions from a full and reduced RLT data set.

Predicting in-service performance of alternative pavement materials for New Zealand conditions

Land Transport New Zealand
Research Report 304